A REGIONAL TERRESTRIAL HEAT-FLOW STUDY IN ARIZONA

by

Charles R. Shearer

Submitted in Partial Fulfillment
of the Requirements for the Degree of
Doctor of Philosophy
in Geoscience

NEW MEXICO INSTITUTE OF MINING AND TECHNOLOGY

Socorro, New Mexico

October, 1979

TABLE OF CONTENTS

LIST OF FIGURES

LIST OF TABLES

ACKNOWLEDGEMENTS

I wish to thank Dr. Marshall Reiter, my advisor, for inspiration, suggestions, and constructive criticism during the course of my research and the writing of this manuscript. Thanks are also due to the other members of the advisory committee, Dr. Charles Chapin, Dr. Kent Condie, Dr. Alan Gutjahr, and Dr. Allan Sanford.

The following organizations and individuals gave permission to make the new heat-flow measurements: AMAX Exploration Inc, American Selco, Anaconda, L. Clark Arnold, Bear Creek Mining Co., Cities Service Mineral Corp., Continental Oil Co. Minerals Dept., R. H. Dewitt, Dresser Minerals, Duval Corporation, Freeport Exploration Co., Paul A. Handverger, Kerr-McGee Corp., Mrs. Floy Morton, Newmont Exploration Ltd., Nuclear Dynamics, Occidental Minerals Corp., Phelps Dodge Corp., Phillips Uranium Corp., Rosario Exploration Co., Superior Oil Co. Minerals Div., Town Mines, U.S. Air Force, U.S. Bureau of Reclamation, U.S. Forest Service, Utah International Inc. The Arizona Oil and Gas Conservation Commission provided lithologic samples. The Atomic Energy of Canada Ltd. made the uranium, thorium and potassium analyses.

This work was supported by Department of Energy contract ET-76-S-04-3721 and by National Science Foundation grant GI-32482.

ABSTRACT

New heat-flow data in Arizona suggest that the southern Basin and Range has perhaps recently undergone less extension than other areas of the Basin and Range province. The role of ground-water movement as a major factor in the variation of heat-flow data in the Arizona Basin and Range is demonstrated at two locations where an increase of the surface heat-flow by a factor of 2 or more over a lateral distance of several tens of km is attributed to ground-water circulation. Heat flow-heat production data suggest that crustal and upper mantle magmatic and thermal sources, such as are reported beneath the Rio Grande rift, are much less abundant in the crust and upper mantle beneath southern Arizona and northwestern Mexico. A heat-flow transition between the Basin and Range and the Colorado Plateau occurs within a lateral distance of 80 km in Arizona where predicted steady-state temperatures indicate that the M-discontinuity is nearly coincident with an isotherm. The deep new heat-flow data suggest that the mean value for the Arizona Basin and Range is 1.9 to 2.0 HFU, indicating that there may be as little as 0.3 HFU difference between the Colorado Plateau and the Arizona Basin and Range. This difference could be due primarily to magmatic intrusion in the Arizona Basin and Range.

INTRODUCTION

Regional studies of terrestrial heat flow provide data which are important boundary conditions for lithospheric thermal models. Heat-flow data combined with measurements of radiogenic heat production in the upper crust can provide information about thermal processes in the crust and upper mantle.

The present study has resulted in 43 new heat-flow values in Arizona and 4 new heat-flow values in southwestern New Mexico. Radiogenic heat production data and reduced heat-flow values are presented for 12 of the data sites in Arizona. The heat-flow values are given in HFU (1 HFU = 1 $\mu cal/cm^2$-sec = 41.8 mW/m^2). Heat production data are in HGU (1 HGU = 1 x 10^{-13} cal/cm^3-sec = 0.418 $\mu W/m^3$).

REGIONAL GEOLOGY AND GEOPHYSICS

The area of study is almost entirely in Arizona and includes major parts of two physiographic provinces, the southern Basin and Range and the Colorado Plateau. These provinces are separated in Arizona by a northwest-trending Transition Zone (Wilson and Moore, 1959).

The southwestern half of Arizona lies within the southern Basin and Range, a region of late Cenozoic extensional faulting that occurs from southern Nevada into northern Mexico. Eaton et al. (1978), on the basis of regional gravity data, consider the southern Basin and Range and the Great Basin as two areas having contrasting crustal structure. Eaton (1979) further notes that the southern Basin and Range is relatively inactive tectonically at present and has an elevation much lower than that of the Great Basin. The southern Basin and Range region was relatively quiescent from the end of the Laramide orogeny until Oligocene time when the region entered a period of intermediate to silicic volcanism, granitic pluton emplacement, and the development of cauldron complexes (Shafiqullah et al., 1978). The transition from predominantly calc-alkalic volcanism to basaltic volcanism and the beginning of regional extension occurred 37 to 23 m.y. BP (Oligocene to early Miocene) (Christensen and Lipman, Figure 5, 1972). Crowe (1978) dates the beginning of block faulting in the

southeasternmost Chocolate Mountains in extreme southeastern California at pre-26 m.y. BP and probably pre-32 m.y. BP, but dates the transition to basaltic volcanism in the area at 13 m.y. BP.

Shafiqullah et al. (1978) consider the southern Basin and Range region to have a history of three stages of tectonism since the beginning of the Oligocene. Stage 1 was characterized by intrusion of granitic plutons, crustal melting, and widespread intermediate to silicic volcanics. The $^{87}Sr/^{86}Sr$ ratios of these volcanics are probably too high for the rocks to have been derived solely from primitive mantle material. Stage 2 (24 to 12 m.y. BP) represents a transition from silicic to basaltic volcanism. Stage 3 encompasses the last 12 m.y., characterized by rifting of thin, brittle crust and by basaltic volcanism. The Stage 3 basalts have primitive mantle $^{87}Sr/^{86}Sr$ ratios and apparently came from the mantle without significant contamination.

Atwater (1970) has suggested that the Basin and Range province is a wide, structurally weak boundary between the Pacific and North American plates and has developed as an oblique shear zone related to the growth of the San Andreas transform fault system. Throughout the southern Basin and Range of Arizona, the predominant orientation of the late-Tertiary structure is north-northwest (Eardley, 1962; Rehrig and Heidrick, 1976). Opening of the Gulf of California 4 m.y. BP (Larson et al., 1968) may have caused renewed strike-slip

offset along the range-bounding faults of southwestern Arizona (Sumner and Thompson, 1974). A notable feature of this part of the Basin and Range is the Pinacate volcanic field located just south of the international border, between 113° and 114° west longitude. Sumner (1972) describes the Sierra del Pinacate as a Quaternary shield volcano of olivine basalt. Although eruptive activity peaked in Pleistocene time (Jahns, 1959), some small activity has been reported as recently as January, 1935 (Ives, 1935).

About 17 m.y. BP, a fundamental change in the character of volcanism occurred in the Great Basin (Stewart and Carlson, 1978); a similar change occurred at about 13 m.y. in the southern Basin and Range of Arizona (Shafiqullah et al., 1970). Volcanic rocks younger than 17 or 13 m.y. respectively, are predominantly basalt or bimodal basalt and rhyolite while volcanic rocks older than 17 or 13 m.y. are predominantly calc-alkalic (Christensen and Lipman, 1972). There is a rather geographically uniform distribution of andesitic volcanic rocks 65 to 17 m.y. BP across southern Arizona with some rhyolitic volcanics of this time period reported in central and southeastern Arizona (Stewart and Carlson, Plate 11-1, 1978). Volcanic rocks younger than 17 m.y. in Arizona are almost all basaltic and are located in the Basin and Range of western Arizona along the Colorado Plateau-Basin and Range boundary that trends northwest to southeast across Arizona (Stewart and Carlson, Plate 11-2, 1978).

The crust of the southern Basin and Range is generally 20 to 35 km thick, as compared to 35 to 50 km under the Colorado Plateau and the Rocky Mountains (Pakiser, 1963; Thompson and Burke, 1974; Stewart, 1978). Warren (1969) reports that the M-discontinuity is about 22 km below the surface at Gila Bend, Arizona, and dips downward to the northeast to reach a depth of about 35 km beneath the Mogollon Rim in central Arizona. Warren (1969) further notes that in central Arizona the Basin and Range and the Colorado Plateau province are in approximate isostatic equilibrium, as is most of the United States from the west coast to the eastern edge of the Basin and Range province (Thompson and Burke, 1974; Stewart, 1978). Upper-mantle velocities in the southern Basin and Range are generally lower than 7.9 km/sec (Stewart, 1978). Warren (1969) reports 7.85 km/sec in central Arizona. However, Toppozada (1974) reports an upper-mantle velocity greater than 8.0 km/sec in the Basin and Range of southeastern Arizona.

The Basin and Range province is generally characterized by an average heat-flow value of 2.0 HFU or greater, although there is considerable variation in reported values (Warren et al., 1969; Sass et al., 1971a; Roy et al., 1972; Reiter and Shearer, in press). Notable examples of this variation are the Battle Mountain high (>2.5 HFU) and the Eureka low (0.7 to 1.5 HFU) where at least part of this variation is due to hydrothermal activity (Sass et al., 1971a).

The northeastern half of Arizona lies within the Colorado Plateau province, an uplifted crustal block having relatively horizontal and undeformed strata as compared to the Basin and Range provinces. The principal structural elements of the Colorado Plateau are Laramide (Kelley, 1955; Eardley, 1962). Uplift of the Plateau as a block has occurred since Eocene time (Eardley, 1962). Chapin and Seager (1975) report the initial uplift of the eastern edge of the Colorado Plateau in early Miocene time, concurrent with early rift basin formation in central New Mexico at about 26 to 20 m.y. BP. Luchitta (1972) dates the structural and topographic differentiation between the Colorado Plateau and the southern Basin and Range in northwestern Arizona between 18 and 10 m.y. BP, about mid-Miocene. A later date, 10 to 5 m.y. BP, has been reported for major relative uplift of the southwestern margin of the Colorado Plateau (McKee and McKee, 1972).

Volcanic activity formed the Pliocene diatremes at Hopi Buttes in the southern Colorado Plateau near the southern edge of the Black Mesa Basin in northeastern Arizona (Williams, 1936). Widespread Quaternary basalt flows occur in Arizona and New Mexico along the Mogollon Slope of the southern Colorado Plateau (Hunt, 1956; Wilson et al., 1960).

Seismic studies show that the Colorado Plateau has a thicker crust than the southern Basin and Range, but that the two provinces have similar P_n velocities. Roller (1965) reports a crustal thickness of 43 km at Chinle, Arizona and 40 km at Hanksville, Utah, and an associated P_n velocity

of 7.8 km/sec. Warren (1969) presents refraction data indicating a flat M-discontinuity at 40 km depth beneath the Mogollon Slope with an associated P_n velocity of 7.85 km/sec. Surface wave dispersion data indicate a crustal thickness of 40 km for the Colorado Plateau (Bucher and Smith, 1971; Keller et al., 1975). Keller et al. (1978) point out that surface wave and seismic refraction data indicate that the crustal structure of the interior of the Colorado Plateau is typical of stable continental areas. Gough (1974) reports that the electrical conductivity under the Colorado Plateau is of Great Plains type or intermediate between the Great Plains and the Basin and Range types.

Reiter et al. (1979a) report that the regional heat flux for the interior of the Colorado Plateau is about 1.5 to 1.6 HFU. Earlier published heat-flow data indicate that the most reliable values for the Colorado Plateau interior are also about 1.5 HFU (Roy et al., 1968a; Decker, 1969; Sass et al., 1971a; Costain and Wright, 1973; Reiter et al., 1975). Two regions within the Colorado Plateau, the San Juan volcanic field and the Mogollon Slope, have heat flows of 2.0 HFU and greater (Reiter et al., 1979b; Reiter and Shearer, in press).

On the basis of structural considerations, Wilson and Moore (1959) suggest a Transition Zone between the Colorado Plateau and the southern Basin and Range in Arizona. This Transition Zone decreases irregularly in width from about

100 km in east-central Arizona to a sharp boundary in northwestern Arizona. Eaton (1979) considers this region to have been a "transform boundary" with distributed oblique shear during the opening of both the southern Basin and Range and the Rio Grande rift. Voluminous masses of basaltic rock, younger than 17 m.y., are located along this Transition Zone (Stewart and Carlson, Plate 11-2, 1978). These include the Oligocene to Pliocene White Mountains volcanic field in east central Arizona (Ratte' et al., 1969; Moore, 1978) and the Pliocene to Holocene San Francisco volcanic field at Flagstaff (Moore and Wolfe, 1976).

PRESENTATION OF HEAT-FLOW DATA

Heat-flow data are summarized in Table 1 for 43 new heat-flow sites in Arizona and for 4 new sites in southwestern New Mexico. Temperature gradient data only are presented for an additional 11 sites in Arizona where rock samples are unavailable to complete the heat-flow calculations. Locations of the heat-flow sites are indicated in Figure 1.

Heat-flow values are calculated by multiplying linear temperature gradients measured in drillholes by the corresponding average measured thermal conductivity values. A best heat-flow value for a site is usually determined by averaging the different heat-flow estimates throughout a drillhole. If, however, the heat-flow estimates in a drillhole vary substantially, a best heat-flow value may be chosen by consideration of such parameters as: the linearity of the temperature gradients, thermal conductivity control, rock properties indicated by drilling problems, the potential for vertical water movement in the drillhole and possible regional ground-water movement.

The heat-flow values presented in Table 1 have been evaluated using the criteria of Reiter et al. (1975). An "A" value is considered accurate to within ±10%, a "B" value is considered accurate to within ±20%, and a "C" value has an uncertainty of greater than 20%.

Figure 1. Heat-flow sites in Arizona and southwestern New Mexico. ○ indicate new heat-flow sites presented in this study; ⌖ are new temperature gradient sites presented in this study. ▣ are data from Reiter et al. (1975), Reiter et al. (1979a), and Reiter and Shearer (in press). ▲ indicate data from Roy et al. (1968a), Decker (1969), Warren et al. (1969), and Sass et al. (1971a). X's indicate sites where temperature data are disturbed by ground-water movement. Data in the San Juan Basin, northwestern New Mexico, are not included on this figure. Profile AA' indicates the location of a heat-flow transition between the Basin and Range and the Colorado Plateau. Dotted patterns indicate areas of Tertiary and Quaternary volcanics. The Transition Zone for Arizona, enclosed by solid lines, is that defined by Wilson and Moore (1959); this zone is undefined in New Mexico. Names of counties are underlined.

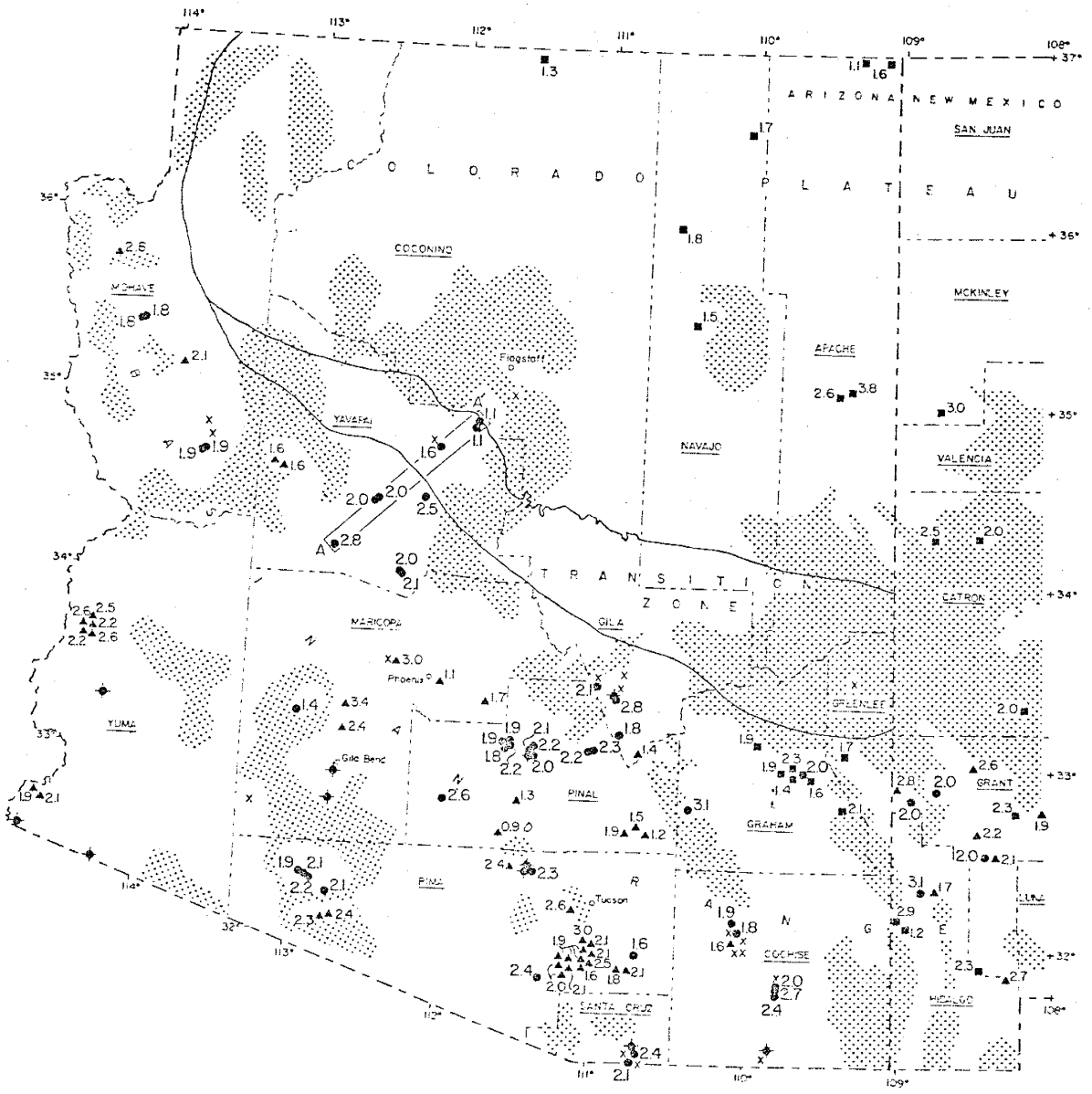

Table 1. Summary of Heat-flow Data

Cochise County

Site Name and Location	Surface Elevation (m)	Depth Interval (m)	Temperature Gradient (Value ± St. Dev. in °C/km)	Thermal Conductivity (Value ± St. Dev. in mcal/cm-sec-°C)	Heat Flow (HFU)	Best Heat-flow Estimate (HFU)	Quality of Heat-flow Estimate
Slaughterhouse Canyon 20-23S-25E 31°25.1'N lat 109°49.6'W long	1400	110-180	19.3±0.18	No Samples			
ST-1 34-19S-25E 31°44.6N lat 109°47.7W long	1414	170-240	27.0±0.19	8.70±0.84 10 fragment samples	2.35 ±0.24	2.35	C
ST-2 27-19S-25E 31°44.9'N lat 109°47.6'W long	1414	160-190	28.6±0.31	9.32±0.53 3 fragments, 1 core	2.67 ±0.18	2.67	C
ST-3 22-19S-25E 31°45.9'N lat 109°44.4'W long	1390	130-160	27.0±0.55	7.23±1.36 4 fragment samples	1.95 ±0.41	1.95	C
#K-21 25-15S-22E 32°06.1N lat 110°03.5'W long	1494	260-340	25.1±0.13	6.99±1.00 4 core samples	1.75 ±0.26	1.77	B
		340-470	28.2±0.12	6.31±0.25 2 core samples	1.78 ±0.08		
#127 14-15S-22E 32°08.1'N lat 110°04.6'W long	1500	230-300	24.1±0.10	7.75±1.27 7 core samples	1.87 ±0.31	1.87	B

Table 1. (cont'd)

Gila County

Site Name and Location	Surface Elevation (m)	Depth Interval (m)	Temperature Gradient (Value ± St. Dev. in °C/km)	Thermal Conductivity (Value ± St. Dev. in mcal/cm-sec-°C)	Heat Flow (HFU)	Best Heat-flow Estimate (HFU)	Quality of Heat-flow Estimate
0-2 17-3S-15E 33°09.9'N lat 110°49.7'W long	945	270-330	28.3±0.24	6.13±0.60 6 fragment samples	1.73 ±0.18	1.76	B
		350-380	22.1±0.44	8.10±0.70 5 fragment samples	1.79 ±0.19		
SH-1 20-1N-14E 33°25.0'N lat 110°57.5'W long	1273	150-190	25.8±0.63	7.94 1 core sample	2.05 ±0.05	2.13	B
		220-240	25.1±0.83	9.04 1 core sample	2.27 ±0.07		
		280-300	25.5±1.17	8.06±0.61 2 core samples	2.06 ±0.25		
VD73-12 30-1N-15E 33°24.1'N lat 110°52.0'W long	1036	190-220	31.5±0.38	No Samples			
		230-300	30.5±0.20	No Samples			
VD-14 30-1N-15E 33°23.9'N lat 110°51.9'W long	1059	190-420	29.5±0.06	No Samples		2.80	B
		420-580	27.9±0.16	10.05±1.19 20 fragment samples	2.80 ±0.35		

Table 1. (cont'd)

Graham County

Site Name and Location	Surface Elevation (m)	Depth Interval (m)	Temperature Gradient (Value ± St. Dev. in °C/km)	Thermal Conductivity (Value ± St. Dev. in mcal/cm-sec-°C)	Heat Flow (HFU)	Best Heat-flow Estimate (HFU)	Quality of Heat-flow Estimate
CBH-1 25-5S-26E 32°57.8'N lat 109°37.5'W long	1631	480-640	31.8±0.15	6.00±0.45 6 core samples	1.91 ±0.45	1.98	A
		640-780	33.0±0.28	5.94±0.45 5 core samples	1.96 ±0.17		
		840-1100	34.9±0.08	5.95±0.58 8 core samples	2.08 ±0.21		
#87 2-8S-19E 32°45.7'N lat 110°22.7'W long	1341	280-340	66.3±0.64	4.56±0.27 3 core samples	3.02 ±0.21	3.11	B
		380-440	63.3±0.06	5.05±0.33 6 core samples	3.20 ±0.21		

Table 1. (cont'd)

Maricopa County

Site Name and Location	Surface Elevation (m)	Depth Interval (m)	Temperature Gradient (Value ± St. Dev. in °C/km)	Thermal Conductivity (Value ± St. Dev. in mcal/cm-sec-°C)	Heat Flow (HFU)	Best Heat-flow Estimate (HFU)	Quality of Heat-flow Estimate
IS-12 21-2S-7W 33°14.8'N lat 112°58.7'W long	333	80-130	27.4±0.14	5.11±0.56 6 core samples	1.40 ±0.16	1.40	C
Lookout Well 2-8S-5W 32°45.5'N lat 112°44.6'W long	335	90-120	39.5±0.22	No Samples			
Well #4 24-6S-5W 32°53.9'N lat 112°43.3'W long	262	30-180	39.8±1.01	No Samples			

Table 1. (cont'd)

Mohave County

Site Name and Location	Surface Elevation (m)	Depth Interval (m)	Temperature Gradient (Value ± St. Dev. in °C/km)	Thermal Conductivity (Value ± St. Dev. in mcal/cm-sec-°C)	Heat Flow (HFU)	Best Heat-flow Estimate (HFU)	Quality of Heat-flow Estimate
R-1 14-15N-14W 34°38.4'N lat 113°41.2'W long	1305	170-330	27.7±0.06	7.02±0.57 7 core samples	1.94 ±0.16	1.94	A
R-2 13-15N-14W 34°38.5'N lat 113°41.0'W long	1292	210-530	28.1±0.11	6.58±0.33 7 core samples	1.85 ±0.10	1.90	A
		600-800	29.9±0.13	6.51±0.26 8 core samples	1.95 ±0.09		
#761 25-23N-18W 35°21.2'N lat 114°08.9'W long	1457	80-150	18.8±0.18	9.73±1.50 5 core samples	1.83 ±0.30	1.79	B
		190-290	21.9±0.10	7.96±1.18 12 core samples	1.74 ±0.27		
#807 19-23N-17W 35°22.1'N lat 114°08.1'W long	1400	300-880	24.7±0.08	7.13±2.10 15 core samples	1.76 ±0.52	1.76	B

Table 1. (cont'd)

Pima County

Site Name and Location	Surface Elevation (m)	Depth Interval (m)	Temperature Gradient (Value ± St. Dev. in °C/km)	Thermal Conductivity (Value ± St. Dev. in mcal/cm-sec-°C)	Heat Flow (HFU)	Best Heat-flow Estimate (HFU)	Quality of Heat-flow Estimate
C-1 22-17S-16E 31°56.3'N lat 110°41.5'W long	1183	320-380	27.0±0.15	6.03±0.19 2 fragment samples	1.63 ±0.06	1.63	C
SWS-18 3-19S-10E 31°48.3'N lat 111°18.3'W long	1067	250-300	48.9±0.16	5.05±0.54 4 fragment samples	2.47 ±0.27	2.36	B
		300-360	55.4±0.11	4.12±1.28 1 fragment, 2 cores	2.28 ±0.71		
WA-5 32-12S-6W 32°20.6'N lat 112°54.8'W long	622	280-360	26.5±0.06	6.81±1.16 8 core samples	1.81 ±0.31	1.89	B
		360-420	28.5±0.36	6.94±0.64 3 core samples	1.98 ±0.21		
WA-7 33-12S-6W 32°19.9'N lat 112°52.9'W long	588	550-690	30.9±0.16	6.68±0.30 4 core samples	2.06 ±0.10	2.06	B
WA-11 10-13S-6W 32°18.7'N lat 112°51.9'W long	561	480-540	24.3±0.05	8.90±0.53 5 core samples	2.16 ±0.13	2.16	B
WG-1 12-14S-5W 32°13.9'N lat 112°43.9'W long	573	110-140	47.8±0.52	4.40±0.06 4 fragment samples	2.10 ±0.05	2.09	B
		200-230	46.1±0.62	4.48±0.33 4 fragment samples	2.07 ±0.18		
#41 11-12S-9E 32°23.8'N lat 111°24.1'W long	652	220-260	46.9±0.87	No Samples			
		260-340	33.7±0.20	No Samples			
		350-390	37.4±0.48	No Samples			
		390-460	36.1±0.12	No Samples			
#42 2-12S-9E 32°25.3'N lat 111°24.4'W long	643	420-460	49.2±0.47	No Samples			
		460-540	32.5±0.18	No Samples			
		550-580	32.9±0.19	No Samples			
		580-610	41.7±0.37	No Samples			

Table 1. (cont'd)

Pima County

Site Name and Location	Surface Elevation (m)	Depth Interval (m)	Temperature Gradient (Value ± St. Dev. in °C/km)	Thermal Conductivity (Value ± St. Dev. in mcal/cm-sec-°C)	Heat Flow (HFU)	Best Heat-flow Estimate (HFU)	Quality of Heat-flow Estimate
#43 11S 12S-9E 32° 23.8'N lat 111° 23.9'W long	658	370-430	36.0±0.19	6.26±0.25 4 fragment samples	2.25 ±0.10	2.25	A
		430-480	40.6±0.32	5.55±0.26 4 fragment samples	2.25 ±0.12		
		600-650	35.4±0.39	6.36±0.39 6 core samples	2.25 ±0.16		

Table 1. (cont'd)

Pinal County

Site Name and Location	Surface Elevation (m)	Depth Interval (m)	Temperature Gradient (Value ± St. Dev. in °C/km)	Thermal Conductivity (Value ± St. Dev. in mcal/cm-sec-°C)	Heat Flow (HFU)	Best Heat-flow Estimate (HFU)	Quality of Heat-flow Estimate
A64 (Q-32) 6-4S-6E 33°06.9'N lat 111°34.5'W long	475	70-190	23.2±0.22	8.15±1.26 9 fragment samples	1.89 ±0.31	1.89	C
Florence #1 26-4S-9E 33°03.4'N lat 111°23.3'W long	488	110-180 190-250	27.7±0.32 28.4±0.20	7.21±0.40 5 fragment samples 6.84±0.27 4 fragment samples	2.00 ±0.13 1.94 ±0.09	1.97	B
Florence #2 26-4S-9E 33°03.4'N lat 111°23.3'W long	488	110-160 170-210 220-260	36.3±0.92 33.4±0.27 39.4±0.26	No Samples No Samples No Samples			
Florence #3 21-4S-9E 33°03.9'N lat 111°25.2'W long	488	170-370	33.2±0.11	6.40±0.60 12 fragment samples	2.12 ±0.21	2.12	B
Florence #4 15-4S-9E 33°05.1'N lat 111°24.1'W long	488	100-160 180-240 270-320 340-360 370-410	31.8±0.37 37.2±0.30 32.6±0.69 21.2±0.09 35.6±0.32	5.94±0.95 4 fragment samples 7.19±1.01 4 fragment samples 7.45±1.57 4 fragment samples 6.63±0.70 3 fragment samples 7.40±0.13 3 fragment samples	1.89 ±0.32 2.67 ±0.40 2.43 ±0.56 1.41 ±0.15 2.63 ±0.07	2.21	B
Kelvin #1 9-4S-13E 33°05.6'N lat 111°01.4'W long	637	50-590	26.7±0.07	8.43±0.63 38 core samples	2.26 ±0.17	2.26	A
Kelvin #2 16-4S-13E 33°05.5'N lat 111°01.5'W long	762	80-110	26.6±0.78	8.43±0.63 (Kelvin #1 value)	2.24 ±0.23	2.24	C

Table 1. (cont'd)

Pinal County

Site Name and Location	Surface Elevation (m)	Depth Interval (m)	Temperature Gradient (Value ± St. Dev. in °C/km)	Thermal Conductivity (Value ± St. Dev. in mcal/cm-sec-°C)	Heat Flow (HFU)	Best Heat-flow Estimate (HFU)	Quality of Heat-flow Estimate
MBX #2 1-4S-7E 33°06.7'N lat 111°35.8'W long	466	80-100	21.5±0.15	8.71±0.99 3 fragment samples	1.87 ±0.22	1.87	C
MBX #6 1-4S-7E 33°06.4'N lat 111°35.9'W long	454	40-240	21.0±0.18	8.34±1.93 12 fragment samples	1.75 ±0.42	1.75	C
MBX #7 1-4S-7E 33°06.7'N lat 111°35.5'W long	466	130-150	25.1±0.60	8.90±0.67 2 fragment samples	2.23 ±0.22	2.23	C
Stanfield 31-7S-4E 32°46.6'N lat 111°59.6'W long	472	570-600	28.4±0.67	9.23±0.33 3 fragment, 2 core	2.62 ±0.16	2.62	C

Table 1. (cont'd)

Santa Cruz County

Site Name and Location	Surface Elevation (m)	Depth Interval (m)	Temperature Gradient (Value ± St. Dev. in °C/km)	Thermal Conductivity (Value ± St. Dev. in mcal/cm-sec-°C)	Heat Flow (HFU)	Best Heat-flow Estimate (HFU)	Quality of Heat-flow Estimate
CQ-40 15-24S-16E 31°20.9'N lat 110°41.8'W long	1679	240-370	33.6±0.08	6.32±0.28 10 core samples	2.12 ±0.10	2.12	B
Washington Camp 34-23S-16E 31°23.2'N lat 110°42.0'W long	1710	70-110 110-150 160-180 180-220	35.4±0.27 32.7±0.18 32.7±0.09 34.9±0.23	No Samples No Samples No Samples No Samples			
#704 3-24S-16E 31°22.7'N lat 110°41.4'W long	1688	300-360 370-410 410-570	26.0±0.28 29.0±0.25 29.9±0.29	9.60±0.97 4 core samples 7.73±0.37 4 core samples 7.98±1.42 9 core samples	2.50 ±0.28 2.24 ±0.13 2.39 ±0.45	2.38	B

Table 1. (cont'd)

Yavapai County

Site Name and Location	Surface Elevation (m)	Depth Interval (m)	Temperature Gradient (Value ± St. Dev. in °C/km)	Thermal Conductivity (Value ± St. Dev. in mcal/cm-sec-°C)	Heat Flow (HFU)	Best Heat-flow Estimate (HFU)	Quality of Heat-flow Estimate
Binghamton Mine 36-13N-1½E 34°27.5'N lat 112°12.0'W lat	1378	60-100	20.7±0.16	12.0±1.2 4 fragments, 2 core	2.49 ±0.3	2.49	C
C-4 32-10N-5W 34°89.9'N lat 112°48.1'W long	945	40- 80	34.1±0.11	8.44 1 fragment sample	2.88 ±0.01	2.82	B
		80-140	36.2±0.20	8.24±0.32 2 fragment samples	2.98 ±0.13		
		150-200	33.8±0.12	7.69±0.02 2 fragment samples	2.60 ±0.02		
DDH75-17 23-16N-2E 34°45.1'N lat 112°04.9'W long	1522	340-470	16.7±0.13	8.96±0.42 7 core samples	1.50 ±0.08	1.58	B
		470-510	20.3±0.32	8.18±0.23 2 core samples	1.66 ±0.07		
H-1 25-12½N-3W 34°26.1'N lat 112°30.2'W long	1573	80-420	29.4±0.04	6.87±0.59 10 fragments, 5 core	2.02 ±0.18	2.02	A
H-2 25-12½N-3W 34°26.3'N lat 112°29.9'W long	1585	250-290	28.8±0.13	7.23±0.16 3 core samples	2.08 ±0.06	2.01	A
		310-360	30.1±0.51	6.62±0.81 3 core samples	1.99 ±0.27		
		440-480	26.1±0.39	7.53±0.76 2 core samples	1.97 ±0.23		
		640-740	28.3±0.14	7.11±0.44 5 core samples	2.01 ±0.13		
Sedona #1 28-18N-5E 34°55.9'N lat 111°49.4'W long	427	290-340	11.1±0.08	9.61±0.27 5 fragment samples	1.07 ±0.04	1.07	B
		340-370	13.6±0.28	7.88±0.29 2 fragment samples	1.07 ±0.06		

Table 1. (cont'd)

Yavapai County

Site Name and Location	Surface Elevation (m)	Depth Interval (m)	Temperature Gradient (Value ± St. Dev. in °C/km)	Thermal Conductivity (Value ± St. Dev. in mcal/cm-sec-°C)	Heat Flow (HFU)	Best Heat-flow Estimate (HFU)	Quality of Heat-flow Estimate
Sedona #2 23-17N-5E 34°53.6'N lat 111°50.3'W long	371	300-350	14.2±2.21	7.72±0.76 6 fragment samples	1.10 ±0.28	1.10	C
#5 15-8N-1W 34°02.5'N lat 112°20.5'W long	799	120-370	49.7±0.13	4.09±0.16 4 core samples from nearby drillhole	2.03 ±0.08	2.03	B
#17 15-8N-1W 34°02.5'N lat 112°21.1'W long	901	220-500	51.6±0.14	4.09±0.16 4 core samples from nearby drillhole	2.11 ±0.09	2.11	B

Table 1. (cont'd)

Yuma County

Site Name and Location	Surface Elevation (m)	Depth Interval (m)	Temperature Gradient (Value ± St. Dev. in °C/km)	Thermal Conductivity (Value ± St. Dev. in mcal/cm-sec-°C)	Heat Flow (HFU)	Best Heat-flow Estimate (HFU)	Quality of Heat-flow Estimate
CH28-YM 2-13S-20W 32°20.1'N lat 114°16.4'W long	183	150-170	41.0±6.62	No Samples			
Stone Cabin 8-2S-19W 33°16.0'N lat 114°14.6'W long	428	130-160 180-230 230-270 270-310	61.2±0.73 53.9±0.41 85.0±0.48 75.1±0.61	No Samples No Samples No Samples No Samples			
Yuma Federal #1 8-11S-24W 32°30.0'N lat 114°44.5'W long	46	590-630 640-820	39.0±0.55 38.7±0.14	No Samples No Samples			

Table 1. (cont'd)

Southwest New Mexico

Site Name and Location	Surface Elevation (m)	Depth Interval (m)	Temperature Gradient (Value ± St. Dev. in °C/km)	Thermal Conductivity (Value ± St. Dev. in mcal/cm-sec-°C)	Heat Flow (HFU)	Best Heat-flow Estimate (HFU)	Quality of Heat-flow Estimate
Alkali Flats 1-23S-20W 32°20.0'N lat 108°51.2'W long	1267	140-260	66.8±0.23	4.73±0.21 11 fragment samples	3.16 ±0.15	3.13	C
		260-300	73.6±0.63	4.20±0.19 2 fragment samples	3.09 ±0.17		
Burro Mts 24-19S-16W 32°38.6'N lat 108°29.8'W long	1848	220-320	30.4±0.13	6.76±0.61 10 core samples	2.06 ±0.19	2.06	B
E-2 8-17S-20W 32°50.6'N lat 108°55.8'W long	1761	120-150	34.7±0.30	5.98±0.62 3 core samples	2.08 ±0.23	2.00	B
		150-170	38.5±1.15	5.30±0.37 4 core samples	2.04 ±0.20		
		180-230	33.4±0.79	5.62±0.37 2 core samples	1.88 ±0.17		
White Signal 26-20S-15W 32°32.1'N lat 108°22.2'W long	1809	410-540	22.8±0.18	8.99±1.43 4 core samples	2.05 ±0.34	2.05	B

Figure 2a is a histogram of the new Arizona heat-flow data presented in Table 1, while Figure 2b is a histogram of the new Arizona data in Table 1 combined with earlier published data for the Basin and Range of Arizona. The new heat-flow data acquired in this study have approximately the same mean value and standard deviation as does the full data set. Lachenbruch and Sass (Figure 9-2, 1978) note that the Basin and Range province has a mean heat-flow value of 2.12 HFU with a standard deviation of 0.75 HFU.

Figure 3 depicts the set of new Arizona heat-flow values in Table 1 as a function of both the maximum depths reached by the temperature logs and the general rock type. The horizontal line is the mean heat-flow value (Figure 2a). The scatter of the data drops off sharply at about 650m depth. There is no apparent uniform trend toward higher or lower heat flow with increasing depth; however, the five values from depths greater than 650m have a mean value of 1.94 HFU as compared to the mean of 2.07 HFU for the full data set. The five deep values were measured in plutonic rock which may be less susceptible to ground-water disturbance than the other rock types represented in Figure 3. It has been suggested that ground-water circulation is a major factor in the variation in heat-flow data (Lachenbruch and Sass 1977; Reiter et al., 1979b). Data in Figure 3 suggest the possibility that ground-water circulation at shallow depths may be preferentially increasing near-surface heat flow.

Figure 2. 2a. Histogram of heat-flow values in Arizona from Table 1. 2b. Histogram of heat-flow values in Arizona from Table 1 and earlier published data for the Basin and Range in Arizona (Roy et al., 1968a; Warren et al., 1969; Sass et al., 1971a; Reiter and Shearer, in press).

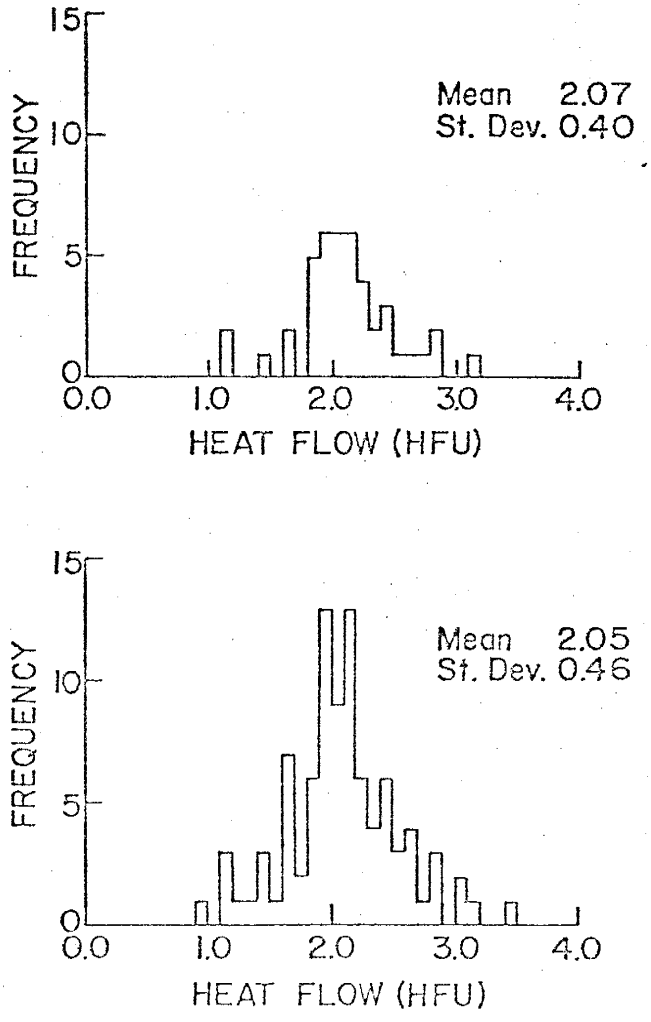

Figure 3. Heat-flow estimate versus maximum depth of temperature log. Data is from Table 1. Horizontal line indicates mean of the heat-flow values. Symbols indicate rock types.

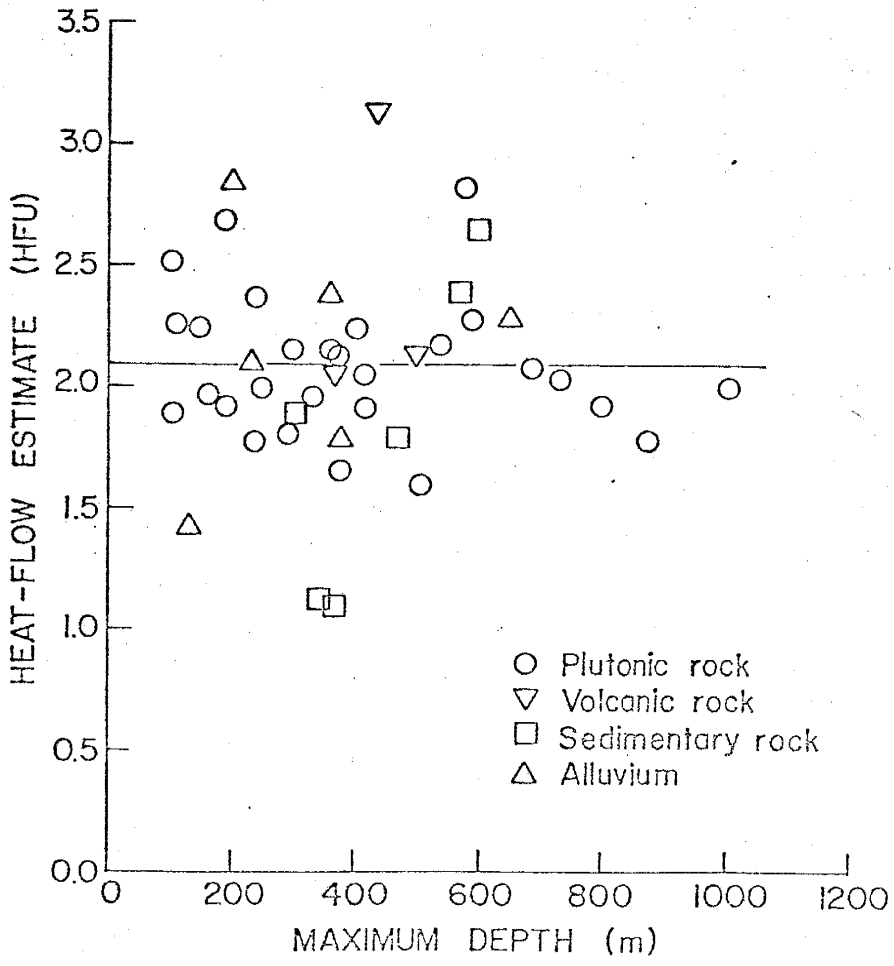

In southeastern Arizona, Cochise County, the new and previously reported heat-flow values vary from 1.58 HFU to 2.67 HFU; however, the average of the six measurements in this region, 2.03± 0.40 HFU, is about the same as the average for the Basin and Range (Table 1, Figure 1). In southwestern New Mexico three new measurements in plutonic rock have very close agreement (2.00 HFU, 2.05 HFU, 2.06 HFU) and are complemented by the 1.98 HFU measured at CBH-1 in Graham County, southeastern Arizona (Table 1, Figure 1). These four heat-flow measurements suggest a uniformity of heat flow along the southern edge of the structural Transition Zone in southeastern Arizona and southwestern New Mexico. Another new measurement in valley fill at Alkali Flats in southwestern New Mexico has a value of 3.13 (Table 1, Figure 1) and is in a region where previously reported data demonstrate large variation suggesting hydrothermal activity.

Twenty-two new heat-flow measurements in the southern Basin and Range are located within a band about 100 km wide, adjacent to the Transition Zone (Figure 1). Values in this band vary from 1.8 to 3.1 HFU. Three sites, #87, VD-14, and C-4, have heat-flow values noticeably above the southern Basin and Range average heat flow. These appear to be local high heat flows because other values within 10 to 40 km of these sites are significantly lower (Figure 1).

Six new heat-flow measurements have been made along a SW-NE transition from the Basin and Range to the Colorado

Plateau (Figure 1, AA'). These data sites are considered to define the heat-flow transition between the Basin and Range and the Colorado Plateau in this region. The heat-flow transition is believed to occur over a lateral distance of 80 km.

Data site IS-12 in western Maricopa County has a heat flow of 1.40 HFU. This value falls in the broad range of values, 1.1 HFU to 3.4 HFU, previously reported for this area (Sass et al., 1971a; Warren et al., 1969). These locations are generally close to the Gila River in a region of heavy agricultural irrigation and the extreme range of heat-flow values probably reflects the ground-water usage patterns.

Three of the new heat-flow sites in south central Arizona have values somewhat above average for the Basin and Range; these are 2.62 HFU in southwestern Pinal County and 2.36 HFU and 2.25 HFU in central Pima County. In western Pima County, two values have been published, 2.3 HFU and 2.4 HFU (Roy et al., 1968a). These values are different from four new values, 1.89 HFU, 2.06 HFU, 2.16 HFU, and 2.09 HFU, in the same area (Figure 1). As yet, there appears to be no apparent trend toward higher heat-flow values moving from the northeast to southwest as one approaches the Pinacate volcanic field or the Gulf of California.

PRESENTATION OF RADIOGENIC HEAT-PRODUCTION DATA

Birch et al. (1968) have noted a linear relation between heat flow measured in igneous plutons and the radiogenic heat production of the plutonic rocks. This relation is expressed by

$$q = q^* + DA(0) \qquad (1)$$

where q is the measured surface heat flow, A(0) is the radiogenic heat production of surface plutonic rocks, and q^* and D are characteristic constants for major geologic provinces. Birch et al. (1968) and Roy et al. (1968b) consider A(z), the vertical distribution of radiogenic heat production, to be constant to depth D, and q^* to be the heat flux into the base of the crustal layer of thickness D. Lachenbruch (1970) proposes a vertical distribution described by

$$A(z) = A(0)e^{-z/D} \qquad (2)$$

whereby q^* is considered the heat flux from the lower crust and mantle and D is the logarithmic decrement by which radiogenic heat production diminishes downward.

Using the parameters q^* and D as criteria, Roy et al. (1968b) define three heat-flow provinces: the Sierra Nevada with $q^* = 0.4$ HFU and $D = 10$ km; the Basin and Range with $q^* = 1.4$ HFU and $D = 9.4$ km; the eastern United States with $q^* = 0.8$ HFU and $D = 7.5$ km. A reduced heat-flow value for a data site, q^*, is calculated from equation (1) transposed to

$$q^* = q - DA(0), \qquad (3)$$

where q and A(0) are the measured surface heat flow and the measured surface heat production, respectively, for that data site. D is assigned a value considered to be applicable to the region. A value of 10 km for D is used by Roy et al. (1968b) for the Basin and Range and is also used in heat production calculations in this study.

In order to estimate crustal heat production, borehole samples have been collected for twelve of the new heat-flow sites in Arizona. At ten sites, the samples come from the boreholes in which the heat-flow measurements have been made. For the other two cases, the samples come from boreholes very near those holes in which the heat-flow measurements have been made. The analysis of the samples has been carried out by a commercial laboratory. The procedure for uranium analysis is a neutron activation/delayed neutron counting technique while that for thorium and potassium is a neutron activation/delayed gamma ray counting method. Table 2 lists the twelve data sites and the heat production data. The locations of the twelve sites are indicated on Figure 1.

Nine of the twelve data sites have reduced heat-flow values greater than the q* reported for the Basin and Range (1.4 HFU) by Roy et al. (1968b). These nine data sites are distributed throughout the southern Basin and Range of Arizona (Table 1, Figure 1). The granite, granodiorite, and gneiss samples are all Precambrian rocks, with the possible

Table 2
Summary of radiogenic heat-production data

Site	Rock Type	Uranium (ppm)	Thorium (ppm)	Potassium (%)		Heat Production (HGU)*	Reduced Heat Flow (HFU)
761	Monzonite	6.1 ± 0.9	1.9 ± 0.4	1.3 ± 0.3		7.1 ± 0.6	1.08
R-1	Monzonite	1.7 ± 0.3	4.4 ± 0.8	2.6 ± 0.5		2.3 ± 0.2	
	Gneiss	2.0 ± 0.4	11.6 ± 1.9	4.1 ± 0.7		4.0 ± 0.4	
					Ave.	3.2 ± 0.2	1.62
R-2	Monzonite	1.5 ± 0.3	3.2 ± 0.7	3.0 ± 0.7		2.1 ± 0.3	
	Gneiss	3.2 ± 0.6	14.4 ± 2.3	3.3 ± 0.7		5.1 ± 0.6	
					Ave.	3.4 ± 0.2	1.56
C-4	Granite	7.0 ± 1.1	12.9 ± 1.1	2.4 ± 0.1		6.9 ± 0.7	2.13
H-1	Monzonite	4.3 ± 0.6	2.0 ± 0.1	2.9 ± 0.1		3.6 ± 0.3	
	Granodiorite	1.6 ± 0.2	4.5 ± 0.3	2.4 ± 0.1		2.3 ± 0.1	
	Granodiorite	2.6 ± 0.4	15.0 ± 0.9	4.1 ± 0.1		5.0 ± 0.4	
					Ave.	3.6 ± 0.2	1.66
H-2	Granodiorite	3.4 ± 0.5	8.0 ± 0.5	3.9 ± 0.1		4.4 ± 0.3	
	Monzonite	6.0 ± 0.6	3.2 ± 0.2	3.4 ± 0.1		5.0 ± 0.5	
	Granodiorite	2.3 ± 0.3	4.0 ± 0.3	2.5 ± 0.1		2.7 ± 0.2	
					Ave.	4.0 ± 0.2	1.61
Sedona	Granodiorite	0.8 ± 0.1	1.3 ± 0.2	1.4 ± 0.2		1.0 ± 0.1	
	Granite	1.7 ± 0.2	3.1 ± 0.3	1.8 ± 0.2		2.0 ± 0.1	
					Ave.	1.5 ± 0.1	0.94
Kelvin #1	Granite	4.7 ± 0.9	22.3 ± 3.2	4.0 ± 0.7		7.5 ± 0.8	
	Granite	6.0 ± 0.5	16.3 ± 1.0	4.1 ± 0.3		7.3 ± 0.4	
					Ave.	7.4 ± 0.4	1.52
CBH-1	Monzonite	1.0 ± 0.2	3.6 ± 0.7	1.1 ± 0.3		1.5 ± 0.2	1.83
WA-5	Gneiss	0.8 ± 0.2	7.9 ± 1.3	1.4 ± 0.4		2.1 ± 0.2	1.68
WA-7	Gneiss	2.3 ± 0.5	12.0 ± 1.9	2.1 ± 0.5		3.9 ± 0.4	1.68
SD-704	Granodiorite	12.4 ± 1.9	25.5 ± 3.6	3.1 ± 0.6		12.8 ± 1.3	
	Granodiorite	16.4 ± 2.5	31.0 ± 4.4	2.4 ± 0.5		16.1 ± 1.8	
					Ave.	14.5 ± 1.1	0.93

* 1 HGU = 1 x 10^{-13} cal/cm^3-sec = 0.418 $\mu W/m^3$

exception of the granite sample for C-4. The monzonite samples are all from Laramide intrusives.

Figure 4 shows a plot of the heat-flow versus heat-production data for the twelve new sites in Arizona. R-1 and R-2 data are averaged and plotted as a single data point, as are the H-1 and H-2 data. The solid line represents the linear regression fit to the new data points; the dashed line is the linear regression fit presented by Roy et al. (1968b) for the Basin and Range province. The solid line has an intercept of 1.71 ± 0.17 HFU and a slope which indicates a value of 6.2 ± 2.9 km for D. The dashed line has an intercept of 1.4 ± 0.09 HFU and a value of 9.4 ± 1.3 km for D (Roy et al. 1968b; the standard deviations are calculated from data presented by Roy et al. (1968b)). Interestingly, a linear regression fit for the full heat flow-heat production data set presented for the Basin and Range by Roy et al. (1968b) yields an intercept of 1.63 ± 0.16 HFU and a value of 6.2 ± 2.4 km for D. Note that the linear regression fit for the new data in Figure 4 can also be changed by deleting selected points, e.g. deletion of SD-704 yields an intercept of 1.53 ± 0.23 HFU and a value for D of 11.2 ± 5.0 km. Lachenbruch and Sass (1977) have noted that the linear heat flow-heat production relation does not apply in the Basin and Range province as it does in the Sierra Nevada and eastern United States provinces. If the linear heat flow-heat production relation reflects regional heat-flow conditions, then one may suggest that points

Figure 4. Heat flow versus heat production for the new data sites in Arizona. Solid line is fitted to these new data. Dashed line is that presented for the Basin and Range province by Roy et al. (1968b). a is site 761; b is sites R-1 and R-2 averaged; c is site C-4; d is sites H-1 and H-2 averaged; e is the Sedona site; f is the Kelvin #1 site; g is the CBH-1 site; h and i are the WA-5 and WA-7 sites respectively; j is the SD-704 site. The error bars indicate the standard deviation of the heat-flow values (Table 1) and the analytical errors of the heat-production estimates (Table 2).

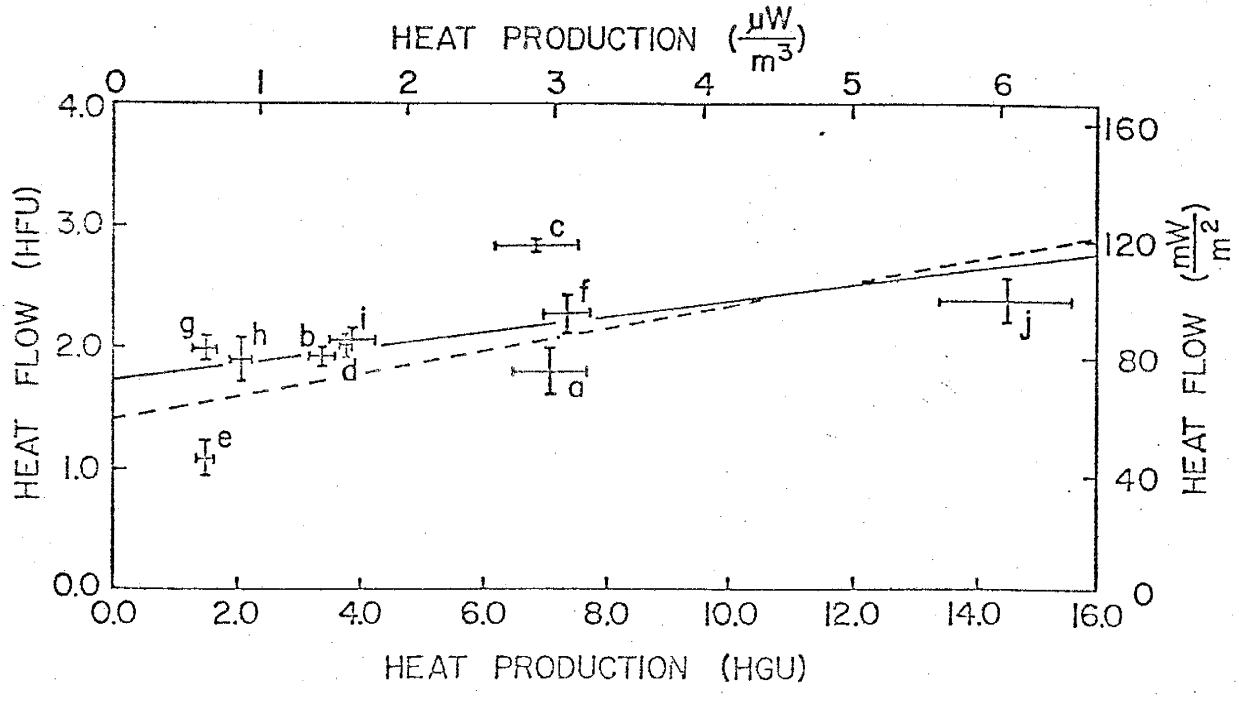

Figure 5. Heat flow versus heat production for sites in Arizona, southern New Mexico, and northern Mexico. Solid line is regression fit of new data. Dashed line from Roy et al. (1968b). + are data from Roy et al. (1968b); * from Warren et al. (1969); ▽ from Sass et al. (1971a); ◇ from Decker and Smithson (1975); □ from Edwards et al. (1978); △ from Smith et al. (1979); ○ from this study.

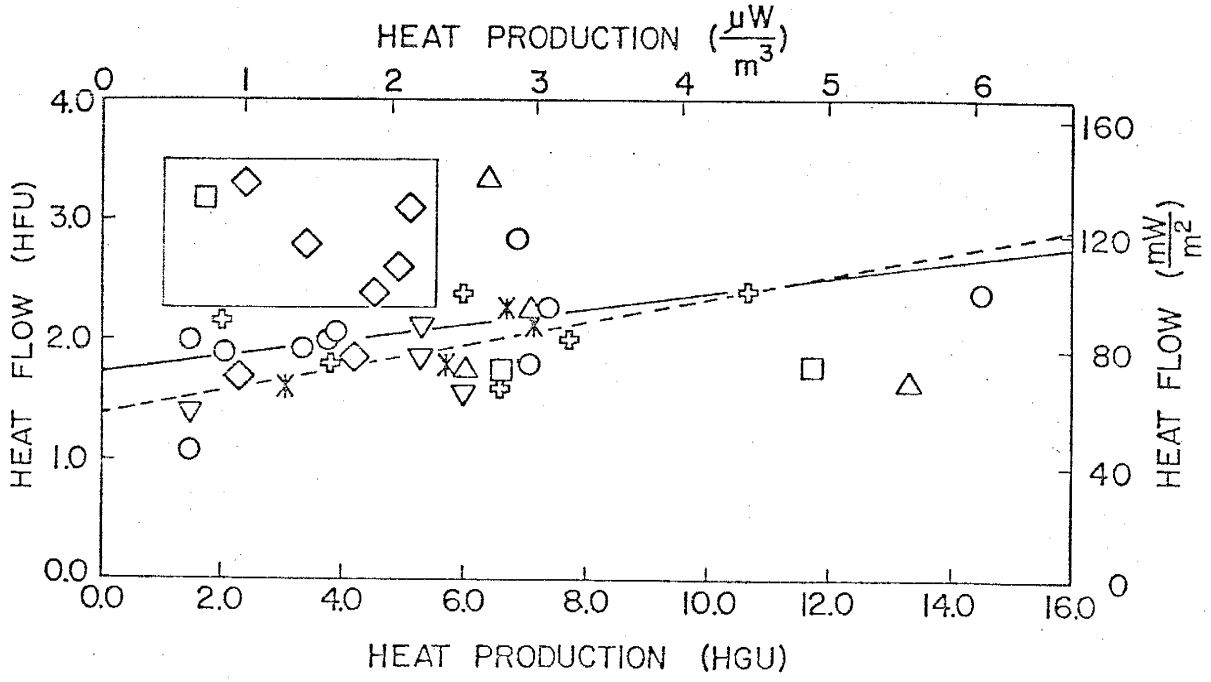

falling far from the linear regression line are being perturbed by hydrothermal phenomena or by unrepresentative crustal radioactivity estimates. Deletion of points falling far from the regression line in order to obtain a better statistical fit may be interpreted as regionally smoothing the data.

The heat flow from the lower crust and upper mantle can also be estimated using a model based on constraints from density, seismic velocity and inferred crustal composition (Allis, 1979). The model implies lateral variations in surface heat production that decrease exponentially with depth to a value of 1.7 HGU at the base of the upper crust. Heat production in the lower crust is considered to be laterally uniform and relatively low. Crustal velocity data reported for central Arizona (Warren, 1969) can be used with this model to obtain an estimate of 1.4 HFU for the heat flow from the lower crust and mantle for an assumed surface heat flow of 2.1 HFU. This estimate is in agreement with the value for q* reported for the Basin and Range by Roy et al. (1968b) and supports the suggestion that about 1.5 HFU come from the lower crust and mantle in the Arizona Basin and Range.

Figure 5 shows heat flow versus heat production for Arizona, southern New Mexico, and northern Mexico. The data points enclosed in the box in the upper left corner of the plot are within or very near the Rio Grande rift in southern

New Mexico. The location of the southern Rio Grande rift data points on this plot demonstrates the sensitivity of the heat flow-heat generation relation to the dynamic crustal and upper mantle conditions likely to exist in tectonically active regions. The Rio Grande rift is believed to be an area of intensive thermal and hydrothermal activity, thus causing measured heat-flow values to be in a data group appreciably above the best linear fit of heat-flow versus heat-production data for the Basin and Range (Edwards et al., 1978; Reiter et al., 1978).

A BASIN AND RANGE-COLORADO PLATEAU HEAT-FLOW TRANSITION

A series of four new data locations in Yavapai county are along a profile trending northeastward across the Transition Zone between the Basin and Range and the Colorado Plateau provinces. The profile is indicated on Figure 1 as AA'. The data sites along AA' are, from northeast to southwest, Sedona #1 and #2, DDH75-17, H-1 and H-2, and C-4 (Table 1). Sedona #1 and #2 are considered as a single data location for the profile because their heat-flow values agree and because of their proximity to each other. H-1 and H-2 are considered to be a single data location for the same reasons.

The Sedona #1 and #2 drillholes penetrate Paleozoic lithologies; Precambrian granite is 28 m below the maximum depth of the Sedona #1 temperature log. Radiogenic measurements have been made on cuttings samples from a drillhole located about 8 km from Sedona #1 and #2 and penetrating some 600 m into Precambrian rocks.

The temperature log for DDH75-17 represents a depth interval of volcanic rocks, adjacent to a large Precambrian quartz porphyry body. Anderson and Creasey (1958) present a chemical analysis for a sample of the quartz porphyry taken in the vicinity of the DDH75-17 drillsite. The chemical analysis shows the quartz porphyry sample to be 2.38% K_2O. Data presented by Tilling and Gottfried (1969) for quartz

monzonite and granite in western United States batholiths yield Th/K = 5.1×10^{-4} and U/K = 1.1×10^{-4}. Using these ratios with a K_2O percentage of 2.38%, the estimated heat production of the quartz porphyry is 3.3 HGU. (1 HGU = 1×10^{-13} $\mu cal/cm^3$-sec).

The drillholes at the H-1 and H-2 data location penetrate a number of Laramide quartz monzonite units which intrude Precambrian granodiorite. Radiogenic measurements have been made on drillhole samples of both rock types.

The temperature log for C-4 stops about 5 m short of a granite unit. The heat production value for C-4 is based on radiogenic measurements made on a single granite core sample from C-4.

Table 3 summarizes the heat-flow and heat-production data for the four locations along the profile. This data has been employed to construct a temperature profile for each of the four locations.

Table 3

Data Location	Heat Flow (HFU)	Heat Production (HGU)
Sedona #1 and #2 (averaged)	1.09 ± 0.14	1.5 ± 0.07
DDH75-17	1.58 ± 0.05	3.3 (estimated)
H-1 and H-2 (averaged)	2.02 ± 0.10	3.8 ± 0.1
C-4	2.82 ± 0.04	6.9 ± 0.7

The temperature profiles are calculated using

$$T = T_o + \frac{A(0)D^2}{K}(1-e^{-z/D}) + \frac{q^*z}{K}, \qquad (4)$$

a solution for the differential equation for one-dimensional, steady-state heat conduction with heat sources in the medium. T_o is the surface temperature and is taken as zero in the calculations. K is the thermal conductivity and is assigned a value of 6 mcal/cm-sec-^oC. A(0) is the radiogenic heat production of surface plutonic rocks and q* and D are characteristic constants from the linear heat flow-heat production relation. This linear relation,

$$q = q^* + DA(0), \qquad (5)$$

where q is the measured surface heat flow, can be used to solve for q*, the reduced heat flow. D is assigned a value of 10 km and q and A(0) are assigned from Table 3.

Figure 6 shows the temperature profiles for the four locations. Each profile is a band because the standard deviations given in Table 3 are incorporated in the calculations. Profiles a, b, c, and d refer to Sedona, DDH75-17, H-1 and H-2, and C-4 locations, respectively. The temperature profile band for the C-4 location is quite narrow because of the relative accuracy of the measured heat flow. The standard deviation for the C-4 heat-flow value is only about 1% of the heat-flow value.

Figure 6 indicates a generally steady increase of temperature at a given depth from the northeast to the southwest

Figure 6. Steady-state temperature profiles for the four locations along the heat-flow transition. a, b, c, d refer to Sedona, DDH75-17, H-1 and H-2, and C-4 locations, respectively. Dashed lines are solidus curves in the presence of excess water after Yoder and Tilley (1962) and Wyllie (1971). GA is gabbro-H_2O, OT is olivine tholeiite, and P is peridotite.

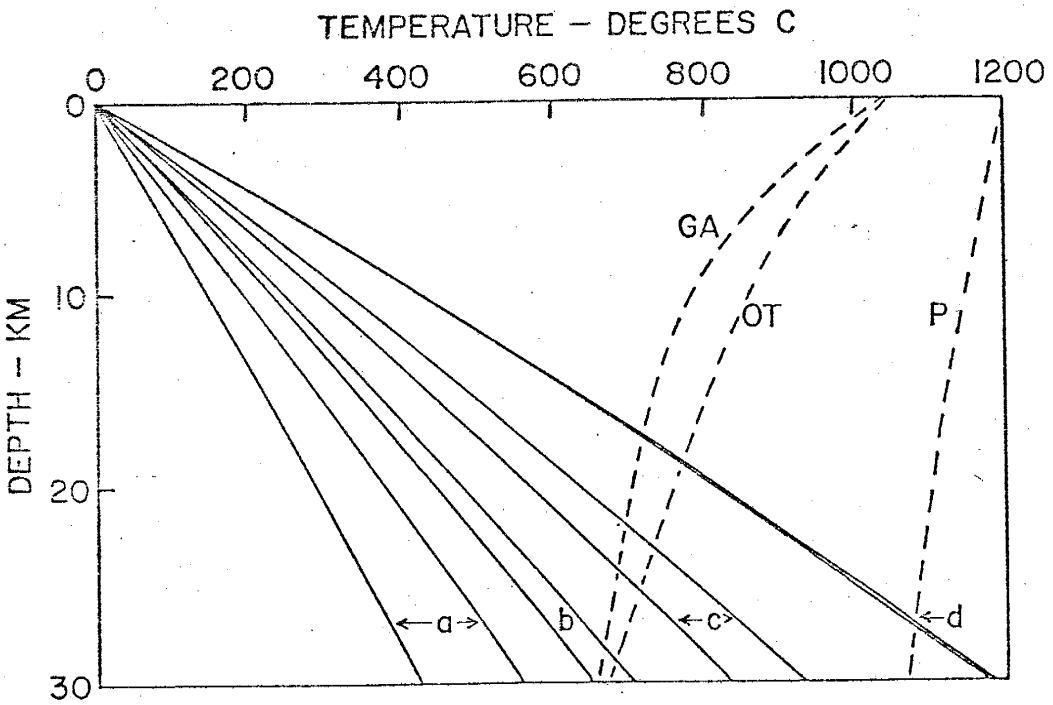

along the heat-flow transition. Also indicated is the possibility of crustal partial melting below the C-4 location and, perhaps, possible partial melting below the H-1 and H-2 location. Chapman and Pollack (1977) estimate depths to partial melting (mixed-volatile solidus) for a continental region having Basin and Range heat flow to be about 60 km and for a region having a Colorado Plateau heat flow to be about 100 km.

The temperature profiles for the four locations have been used to construct a vertical temperature distribution for the heat-flow transition (Figure 7). Points a, b, c, d refer to the Sedona, DDH75-17, H-1 and H-2, and C-4 locations, respectively. The indicated depth to the Moho is based on seismic data presented by Warren (1969). Reiter et al. (1979a) report that the heat flow for the Colorado Plateau is 1.5 to 1.6 HFU. The temperature profile for the Sedona location has been re-calculated with an assigned surface heat flow of 1.5 HFU. The dashed lines in Figure 7 demonstrate how the isotherms would be moved upward below the Sedona location for a surface heat flow of 1.5 HFU. While the temperature logs from Sedona #1 and Sedona #2 do not indicate ground-water movement, this does not preclude the possibility of ground-water movement occurring below the depths reached by the temperature logs and lowering the apparent surface heat flow by about 0.5 HFU. The low heat-flow value at Sedona may also be partly due to the low heat-production value measured for that location (Table 3).

Figure 7. Vertical temperature distribution for the heat-flow transition. a, b, c, d refer to the Sedona, DDH75-17, H-1 and H-2, and C-4 locations, respectively. Moho is constructed from seismic data presented by Warren (1969). Dashed lines represent isotherms for a Sedona heat-flow value of 1.5 HFU. The solid circles are surface heat flows from Table 3. The open circles are reduced heat flows calculated using D = 10 km.

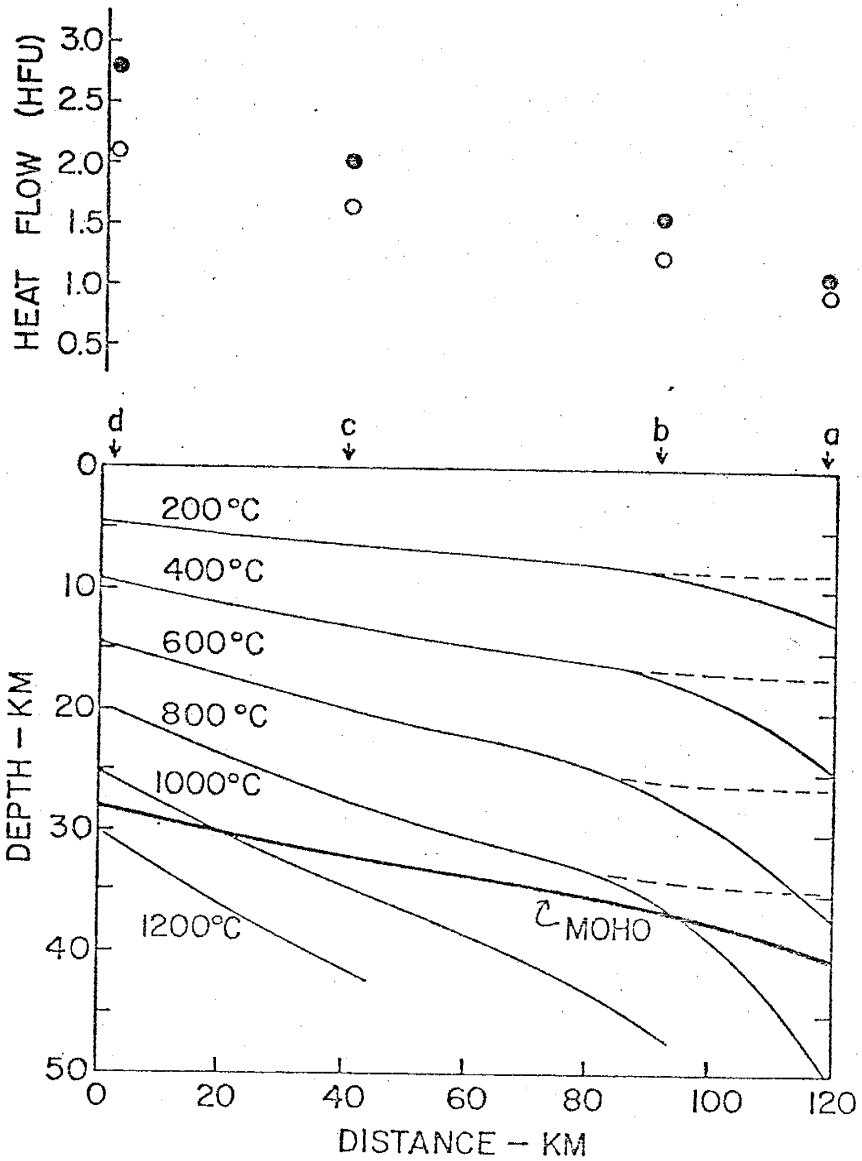

The heat-flow value for the C-4 location is 2.8 HFU, considerably higher than the average southern Basin and Range value of 2.1 HFU. The heat production for C-4, 6.9 HGU, is somewhat greater than the average value of 5.47 HGU for granitic rocks in the Basin and Range (Lachenbruch and Sass, Figure 9-4C, 1978). For a heat-flow of 2.8 HFU, steady-state curves presented by Chapman and Pollack (1977) would indicate partial melting at about 40 km. Other data suggest the high heat-flow observed at C-4 may not extend laterally a great distance. Heat flows of 2.0 HFU and 2.1 HFU are observed to the southeast (#5 and #17, Table 1) while to the northwest values of 1.6 HFU (Roy et al., 1968b) and 1.9 HFU (R1 and R2, Table 1) are observed. To the northeast, the H-1 and H-2 data location indicates a heat flow of 2.0 HFU. The southwest extent of the high heat-flow anomaly suggested by the C-4 data is uncertain due to a lack of data. However, data reported for Quartzite, about 150 km southwest of the C-4 location, indicate a heat flow of 2.4 HFU with a sufficiently high crustal heat production, 10.7 HGU, to yield an estimated mantle (reduced) heat flow characteristic of the Basin and Range (Roy et al., 1968b).

The H-1 and H-2 data location with 2.0 HFU is considered more representative of the southern Basin and Range than the C-4 location. This would indicate that the transition from Basin and Range heat flow to Colorado Plateau heat flow occurs between the H-1 and H-2 location and the Sedona

location, a distance of about 80 km. The heat-flow transition from 1.5 HFU to 2.0 HFU over a lateral distance of 80 km would seem to indicate a lateral temperature difference in the upper mantle.

The depth to the M-discontinuity is about 32 km at the H-1 and H-2 location and is about 40 km at the Sedona location, estimated from seismic data presented by Warren (1969). Calculations used to construct the temperature profile in Figure 6 indicate a temperature of 935°C at 32 km depth below the H-1 and H-2 location and a temperature of 925°C at 40 km depth below the Sedona location (assuming a heat-flow value of 1.5 HFU for the Sedona location). These predicted temperatures suggest that the M-discontinuity is nearly coincident with an isotherm.

CONVECTIVE HEAT TRANSPORT IN BASINS IN ARIZONA

A fundamental characteristic of measured heat flow in the Basin and Range province is the variability in the heat-flow data. Lachenbruch and Sass (Figure 9-2, 1978) note that reported Basin and Range heat-flow data averages 2.12 ± 0.75 HFU. Exclusion of the Battle Mountain high and the Eureka low changes this only slightly to 2.10 ± 0.71 HFU. The appreciable standard deviation of about 0.7 HFU may be due largely to convective heat transfer by ground-water circulation.

Conditions under which temperature gradients, and thus apparent surface heat flow, can be disturbed by ground-water movement have been considered by several investigators including Donaldson (1962), Stallman (1963), Lubimova et al. (1965), Bredehoeft and Papadopulos (1965), Negi and Singh (1967), and Mansure and Reiter (1979).

A mathematical approach similar to that of Lachenbruch and Sass (1977) can be considered. For a homogeneous, isotropic, permeable medium with both conductive heat flux and convective heat transport by fluid flow and with no heat sources, the steady-state, one-dimensional differential equation can be written

$$K \frac{d^2T}{dz^2} - \rho c u \frac{dT}{dz} = 0 \quad . \qquad (6)$$

K is the thermal conductivity of the saturated medium, ρ is the density of the fluid, c is the thermal capacity of the fluid, u is the component of the seepage velocity in the z-

direction, and z is positive downward. Recalling that, in one dimension, the heat conduction equation is

$$q = -K \frac{dT}{dz} , \tag{7}$$

where q is heat flux, equation (6) can be rewritten as

$$\frac{dq}{dz} = -\rho cu \frac{q}{K} . \tag{8}$$

If convection occurs in a layer of thickness $\Delta z = z_2 - z_1$, integration of equation (8) over this depth interval yields

$$\ln \frac{q(z_1)}{q(z_2)} = \frac{\rho cu}{K} \Delta z \tag{9a}$$

or

$$\frac{q(z_1)}{q(z_2)} = e^{\frac{\rho cu}{K} \Delta z} . \tag{9b}$$

Equation (9) can be used to make an approximate calculation of the rate of vertical ground-water movement necessary to produce an observed high heat flow in the Big Sandy Valley in Mohave County. Data from two sites in the Big Sandy Valley and from two sites in the adjoining Hualpai Mountains indicate that convective heat transport may be occurring in the sediments of the Big Sandy Valley. The use of equation (9) requires several assumptions which can be made by considering the hydro-geology of the area as well as the heat-flow data.

The Big Sandy Valley, located in southern Mohave County, is an inter-mountain trough, trending a few degrees west of north (Morrison, 1940). This structural trough is bounded on

the west by the Hualpai Mountains and the Peacock Mountains, blocks of predominantly Precambrian rocks, and on the east by the Cottonwood Cliffs, the Aquarius Cliffs, and the Aquarius Mountains. In the Aquarius Mountains, volcanic rocks of two different episodes of eruption (24.7 ± 3.5 m.y. BP and 18.2 ± 1.5 m.y. BP) rest on eroded Precambrian rocks (Young and McKee, 1978). These volcanic rocks predate the widespread Peach Springs Tuff (~17 m.y. BP) which outcrops along the northern end and the eastern edge of the Big Sandy Valley (Young and McKee, 1978).

Morrison (1940) describes the sediments in the Big Sandy Valley in a general manner. Overlying the basement rocks, which are principally gneiss, schist, and gneissic granite, are the older valley-fill deposits, composed chiefly of a fanglomerate-breccia which grades laterally toward the interior of the valley to finer material and into lake beds. A well-sorted sand overlies the older fill, varying in thickness from a thin layer to possibly as much as 300 m. Above this intermediate sand is a terrace gravel and then the younger alluvium which consists of moderately sorted silt, sand, and gravel.

Ground-water in the intermediate sand is under a small artesian pressure (Morrison, 1940). Minor seeps and springs occur in the valley, but the largest springs occur along the river in the central basin of the valley. One of these is Coffers Hot Spring, a moderate-sized, artesian spring

(Morrison, 1940). Swanberg et al. (1977) report a silica geothermometer temperature of 110°C for the Coffers Hot Spring. Average annual precipitation in the highlands surrounding the Big Sandy Valley is more than 50 cm in the Hualpai Mountains and about 40 cm in the Aquarius Mountains (Gillespie and Bentley, Figure 3, 1971).

Heat-flow data obtained in this study for two sites, R-1 and R-2 (about 400 m apart), in the southern Hualpai Mountains in Mohave County (Figure 1) have heat flows of 1.94 HFU and 1.90 HFU, respectively (Table 1). These heat-flow values support a value of 2.1 HFU reported in the northern Hualpai Mountains (Roy et al., 1968a), and is similar to the Basin and Range average of 2.1 HFU (Lachenbruch and Sass, Figure 9-2, 1978). It may therefore be reasonable to assume that the conductive heat flow for the area represented by the Hualpai Mountains is about 2.0 HFU.

Heat-flow measurements are presented (Table 4) for two drillsites, W-1 and W-2, in the Big Sandy Valley about 20 km and 10 km, respectively, from the R-1 and R-2 location in the Hualpai Mountains. The temperature log for W-1 (Table 4, Figure 8) reaches a depth of 340 m and has a curvature characteristic of upward ground-water movement (Bredehoeft and Papadopulos, 1965). Analysis of the temperature data indicate that the curvature is smooth and continuous from 100 m to 300 m. Heat-flow values decrease with depth from 4.9 HFU to 4.2 HFU (Table 4). The temperature log for W-2 (Table 4,

Figure 8. Temperature log for drillhole W-1.

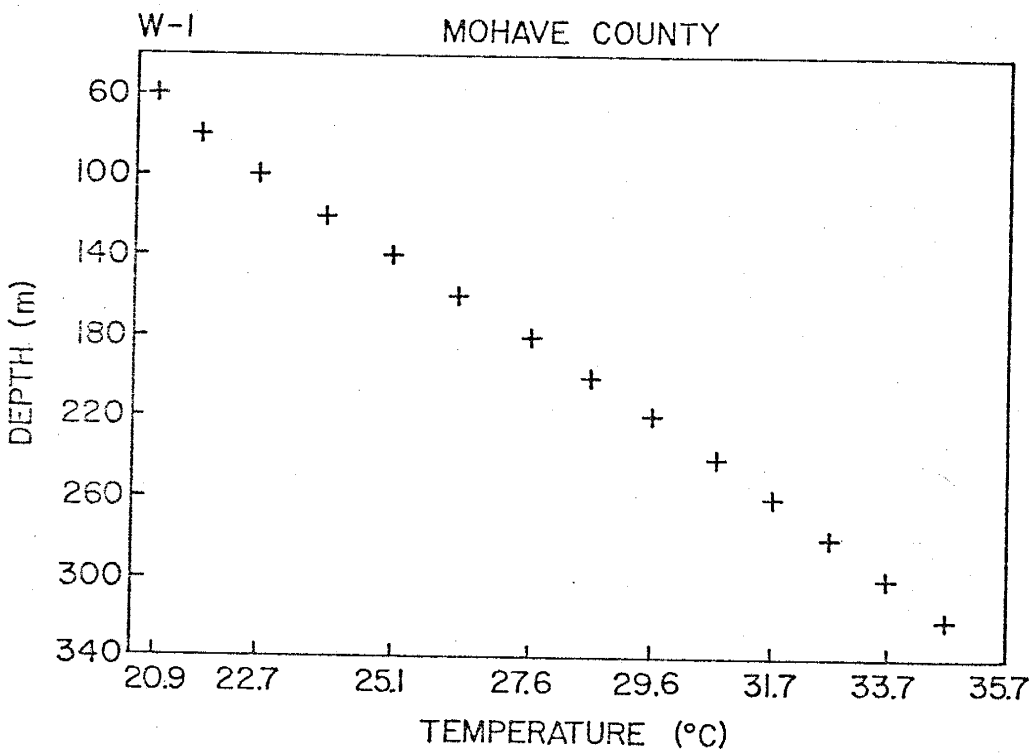

Figure 9. Temperature log for drillhole W-2.

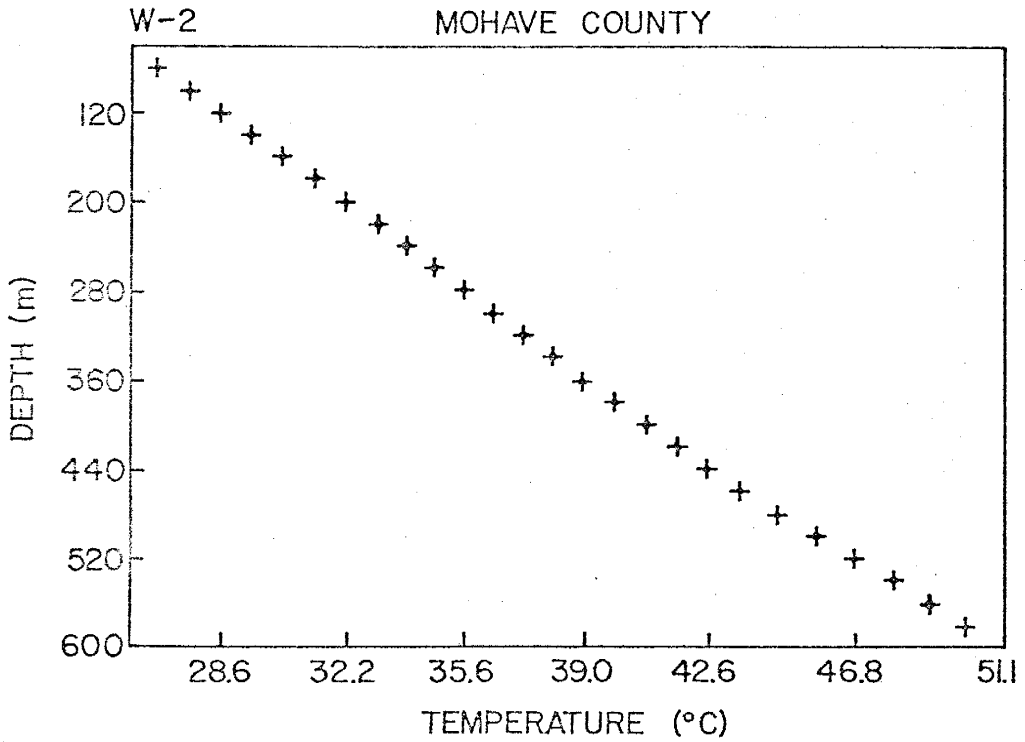

Table 4. Summary of Heat-flow Data for the W-1 and W-2 Drillholes.

Mohave County

Site Name and Location	Surface Elevation (m)	Depth Interval (m)	Temperature Gradient (Value ± St. Dev. in °C/km)	Thermal Conductivity (Value ± St. Dev. in mcal/cm-sec-°C)	Heat Flow (HFU)
W-1 31-17N-13W 34°48.6'N lat 113°40.9'W long	823	100-180	58.9±0.52	8.29±0.83 6 fragment samples	4.88 ±0.53
		180-240	54.0±0.56	8.07±0.76 5 fragment samples	4.35 ±0.46
		240-340	50.6±0.21	8.31±0.74 9 fragment samples	4.20 ±0.39
W-2 17-16N-13W 34°43.3'N lat 113°38.5'W long	716	300-460	44.5±0.18	7.20±0.50 5 fragment samples	3.20 ±0.23
		460-600	54.3±0.19	6.09±0.22 6 fragment samples	3.31 ±0.13

Figure 9) reaches a depth of 600 m, but does not exhibit the temperature gradient variations seen in W-1. The heat-flow values for W-2 are 3.2 HFU and 3.3 HFU going downhole, indicating a possible slight increase of heat flow with depth.

With a few assumptions based on available data, equation (9) can be used to estimate the ground-water movement needed to yield the apparent high heat flow in the Big Sandy Valley. Drillhole W-2 samples indicate that the sediments are at least 600 m thick. It is assumed that 600 m of sediments exist at drillhole W-1, which is less than 5 km from W-2. Because the heat-flow value of 4.9 HFU is observed at 100 m depth in W-1, we wish to consider the convective heat transport between 100 m and 600 m at the W-1 location. Assuming that 2.0 HFU is the conductive heat flow for the region, $q(z_2)$, assigning unit value to ρc for the groundwater and putting $q(z_1)$ = 4.9 HFU, equation (9) can be solved for u, the vertical volume flow over a depth interval, Δz, of 500 m. The value used for K, the thermal conductivity, is 7.59 mcal/cm-sec-^{o}C, the average value measured for samples from both drillholes. The resulting estimated u is about 4 cm/yr, the necessary upward ground-water flow to yield the apparent heat-flow value of 4.9 HFU at site W-1. If Δz, the vertical thickness of the layer where convection occurs, is greater than 500 m, then u will be less than 4 cm/yr.

Similarly, a vertical ground-water velocity can be estimated for the depth interval represented by the temper-

ature log for W-1. Setting $q(z_2)$ = 4.2 HFU, $q(z_1)$ = 4.9 HFU, and Δz = 340 m - 100 m = 240 m, yields a value for u of about 1.5 cm/yr.

The apparent heat flow at W-2 is 3.3 HFU. The character of the temperature data indicates that the ground-water movement producing this increased heat-flow value must be occurring below 600 m. If the upward volume flux at this site is 4 cm/yr as at the W-1 site and the other assumptions for the W-1 calculation are used, a layer of about 280 m thickness in which convection is occurring must be located below the 600 m depth to increase the heat flow from 2.0 HFU to 3.3 HFU.

Evidence for similar hydrothermal phenomena occurring in the Safford Valley of Graham County in southeastern Arizona is presented by Reiter and Shearer (in press). The Safford Valley, like the Big Sandy Valley, is a structural trough within the southern Basin and Range. Temperature data for a drillhole in the Safford Valley alluvial deposits indicate convective heat transport with an apparent heat flow of 5.0 HFU above 500 m depth. Heat-flow data (Reiter and Shearer, in press) in the adjacent mountain block indicate a value of 1.9 HFU for the area, a value about that of the Basin and Range average. A new heat-flow value for this same mountain block is presented in this study. The CBH-1 temperature data reach 1100 m depth and yield a heat flow of 2.0 HFU, agreeing well with the earlier data average of 1.9 HFU. It appears possible, therefore, that ground-water

movement may be increasing the near-surface heat flow in the Safford Valley to a value about 2½ times the heat-flow value measured in the adjacent mountains. Interestingly, this amount of increase is similar to that observed in the Big Sandy Valley.

It is possible that ground-water movement is affecting near-surface heat flow in other basins in Arizona. Published heat-flow values for the general area south of Phoenix range from 3.42 HFU (Warren et al., 1969) to 0.85 HFU (Sass et al., 1971a). Eberly and Stanley (1978) report as much as several km of late-Cenozoic deposits beneath some of the valleys of this area. Circulation of groundwater in these deposits could result in the wide range of observed heat-flow values.

SUMMARY

Although the new heat-flow data in the Arizona Basin and Range reflect variability noted in the heat-flow data of the Basin and Range province as a whole, it may be of importance to note that the magnitude of data variability in Arizona appears to be less. The standard deviation in the Arizona heat-flow data is ±0.46 HFU compared to ±0.75 HFU for all Basin and Range province heat-flow data (Lachenbruch and Sass, 1978, Figure 9-2). It has been suggested that ground-water circulation is a major factor in the variation in heat-flow data (Lachenbruch and Sass, 1977; Reiter et al., 1979b). If the variation in heat-flow data is due in part to deep ground-water circulation along extensional faults, then perhaps the Basin and Range in Arizona has recently undergone less extension than other regions of the Basin and Range province (Eaton, 1979).

The variation in the new Arizona heat-flow data decreases sharply as gradient measurements become deeper than 650 m (Figure 3). The five new heat-flow values from temperature logs reaching depths greater than 650 m have a mean of 1.94 ± 0.12 HFU, about 0.13 HFU less than the mean of the full heat-flow data set. These five values have been measured in plutonic rock. A previously published value of 1.54 HFU, measured in plutonic rock to a depth of 1372 m (Sass et al., 1971a), may qualitatively agree with this

trend. The observation that both the variation and the mean value of the data decrease below 650 m in plutonic rock supports the concepts of ground-water circulation causing a major part of the variation of heat-flow values in the Basin and Range and that the ground-water circulation is preferentially increasing the near-surface heat-flow. In addition to forced convection along vertical faults, free convection in deeply filled grabens can contribute to elevating near-surface temperature gradients, e.g. in the Big Sandy Valley and in the Safford Valley.

Twelve previously reported heat-flow values in the Great Basin from temperature measurements deeper than 650 m have a mean value of 1.89 ± 0.95 HFU (Roy et al., 1968a; Sass et al., 1971a). Only one of the twelve measurements has been made in plutonic rock; the remainder have been made in sedimentary and volcanic rocks. The similarity of the mean of these twelve values to the mean of 1.94 HFU for the deep new Arizona heat-flow data, although interesting, may be inconclusive because of the increased potential for ground-water disturbance of the measurements made in sedimentary and volcanic rocks, as suggested by the greater variation of the deep data in the Great Basin. If one chooses to ignore these differences in rock types, it is possible that the deeper data also suggest less extension in the upper crust in the southern Basin and Range (less variable heat

flow), but similar thermal conditions below the upper crust throughout the Basin and Range province (similar average heat flows).

The magnitude of potential ground-water disturbance to near-surface heat flow has been considered. Analysis of new heat-flow data in western Arizona indicates the possibility for heat flow to change by a factor of 2 or more over a lateral distance of 20 km due to vertical ground-water movement at a specific discharge rate of only a few cm per year. The same phenomenon is observed in southeastern Arizona in the Safford Valley (this study; Reiter and Shearer, in press).

Heat-flow data in southwestern Arizona is of regional geophysical interest because of the area's proximity to the spreading center in the northern Gulf of California and to the strike-slip fault system of the Salton Trough. The heat-flow data in southern Arizona do not seem to indicate an east-west trend toward higher or lower heat flow. South of 32^{o} 30' north latitude, combined new and previously reported heat flow data in Arizona have a mean of 2.0 HFU between 109^{o} and 111^{o} west longitude and a mean of 2.1 HFU between 111^{o} and 113^{o} west longitude. The heat-flow values in western Pima County do not suggest an increased heat flux that might be associated with the Pinacate volcanic field about 80 km to the south-southwest in Sonora, Mexico.

Radiogenic heat production data presented in this paper yield twelve reduced heat-flow values. A linear fit of the heat flow-heat production data from these twelve sites yields an intercept, or q*, of 1.71 HFU and a slope of 6.2 km, compared to values of 1.4 HFU and 9.4 km reported by Roy et al. (1968b) for the Basin and Range province. Available heat flow-heat production data indicate a general trend of increasing heat flow with increasing heat production in Arizona and northwestern Mexico, but not in southern New Mexico. Edwards et al. (1978) note that the high heat flow in the southern Rio Grande rift is not associated with high radiogenic heat production, but is probably due to magmatic sources in the crust and upper mantle beneath the Rio Grande depression. The heat flow-heat production data suggest that similar conditions do not exist in the crust and upper mantle beneath southern Arizona and northwestern Mexico. The Arizona Basin and Range heat-flow data has both a mean and a standard deviation less than those for the Rio Grande rift data — 2.05 ± 0.45 HFU compared to 2.56 ± 0.65 HFU (Reiter et al., 1979b).

A heat-flow transition between the southern Basin and Range and the Colorado Plateau occurs within a lateral distance of 80 km in central Arizona. The data suggest a transi- from southern Basin and Range heat flow to a heat-flow value somewhat lower than that representative of the Colorado Plateau interior. Reiter et al. (1979a) report that the

regional heat flow for the interior of the Colorado Plateau is about 1.5 to 1.6 HFU. Thus, the 1.1 HFU measured at the northeast end of the heat-flow transition may be lowered 0.5 HFU by vertically downward ground-water movement resulting from the heavy snowfall in the mountains above the data site. The Pliocene to Holocene San Francisco volcanic field lies northeast of the heat-flow transition. Efforts to date to acquire heat-flow measurements in the area around the San Francisco volcanic field have been frustrated by the regional ground-water movement creating measured geothermal gradients close to zero.

Steady-state temperatures predicted for this transition from southern Basin and Range heat flow to Colorado Plateau heat flow suggest that the M-discontinuity is nearly coincident with an isotherm, an observation reasonable in light of the equivalent P_n velocities for the two provinces in central Arizona. This coincidence of the M-discontinuity with an isotherm, although interesting, is insufficient to simplify defining the M-discontinuity in terms of a phase change. The P_n velocity of 7.85 km/sec for central Arizona (Warren, 1969) suggests possibly garnet granulite (Condie, 1976). The sharpness of the M-discontinuity inferred from seismic data in central Arizona (Warren, 1969) is not compatible with the width of the garnet granulite pressure-temperature field (Ringwood, 1975).

In eastern Arizona, existing heat-flow data allow speculation about the heat-flow transition between the southern Basin and Range and the Colorado Plateau. High heat flows ($\geq$2.5 HFU) are reported in the Mogollon Slope of the southern Colorado Plateau, an area of extensive recent basaltic volcanism (Reiter and Shearer, in press). Thus a heat-flow transition in eastern Arizona from the southern Basin and Range to the Colorado Plateau would show an increase in heat flow, the reverse of the observations in central Arizona and in Utah. No heat-flow data are available for the structural Transition Zone in eastern Arizona.

The deeper data presented in this study suggest that the mean value for the Basin and Range heat flow in southern Arizona may be 1.9 to 2.0 HFU. Reiter et al. (1979a) report a heat flow of 1.5 to 1.6 HFU for the interior of the Colorado Plateau. Thus there may be as little as 0.3 HFU difference between the two provinces. A current study (Reiter et al., in prep.) indicates that the reduced heat flow for the Colorado Plateau may be about 1.1 ± 0.2 HFU. Reiter et al. (1979a) suggest that the western United States may have overridden hotter asthenosphere between 170 m.y. and 100 m.y. BP, and experienced lithospheric reheating. The Colorado Plateau has since maintained its structural integrity while being subjected to lithospheric reheating. In contrast, the Basin and Range has been subjected to extension at least during the last 17 m.y. and as such has been extensively

intruded by magmatic material as evidenced by the surface volcanics. The potential 0.3 HFU difference between the southern Basin and Range and the Colorado Plateau regional reduced heat flows could be due primarily to magmatic intrusion (Lachenbruch and Sass, 1978) and is possibly an indicator of the lithospheric responses of the two provinces to similar asthenospheric conditions.

APPENDIX I
THERMAL CONDUCTIVITIES, TEMPERATURE MEASUREMENTS, AND HEAT-FLOW VALUES

Thermal Conductivities

The thermal conductivities of both core and fragment lithologic samples are measured using an absolute, steady-state method described by Reiter and Hartman (1971). The steady-state heat conduction equation can be solved for K, the thermal conductivity, when written as

$$K = q \Big/ \frac{\Delta T}{\Delta Z} , \qquad \text{(I-1)}$$

where q is the heat flux into the sample and $\Delta T/\Delta Z$ is the temperature gradient across the sample.

The technique used to measure thermal conductivity involves placing a rock sample between a constant heat source and a heat sink (Figure I-1). The heat source is placed above the sample and the heat sink, a large aluminum block, is placed below the sample. This configuration avoids convective heat transport. The heat source consists of a resistor mounted on a copper disc. This heater assembly is molded in polyurethane so that virtually all of the heat is directed into the upper surface of the rock sample. Reiter and Hartman (1971) calculate that no more than 2.5% of the heat is lost through the insulation. Radial heat losses are minimized by insulating the rock sample with strips of foam rubber. Radial losses with this method are less than 2% (Reiter and Hartman, 1971).

Figure I-1. Schematic drawing of the thermal conductivity apparatus.

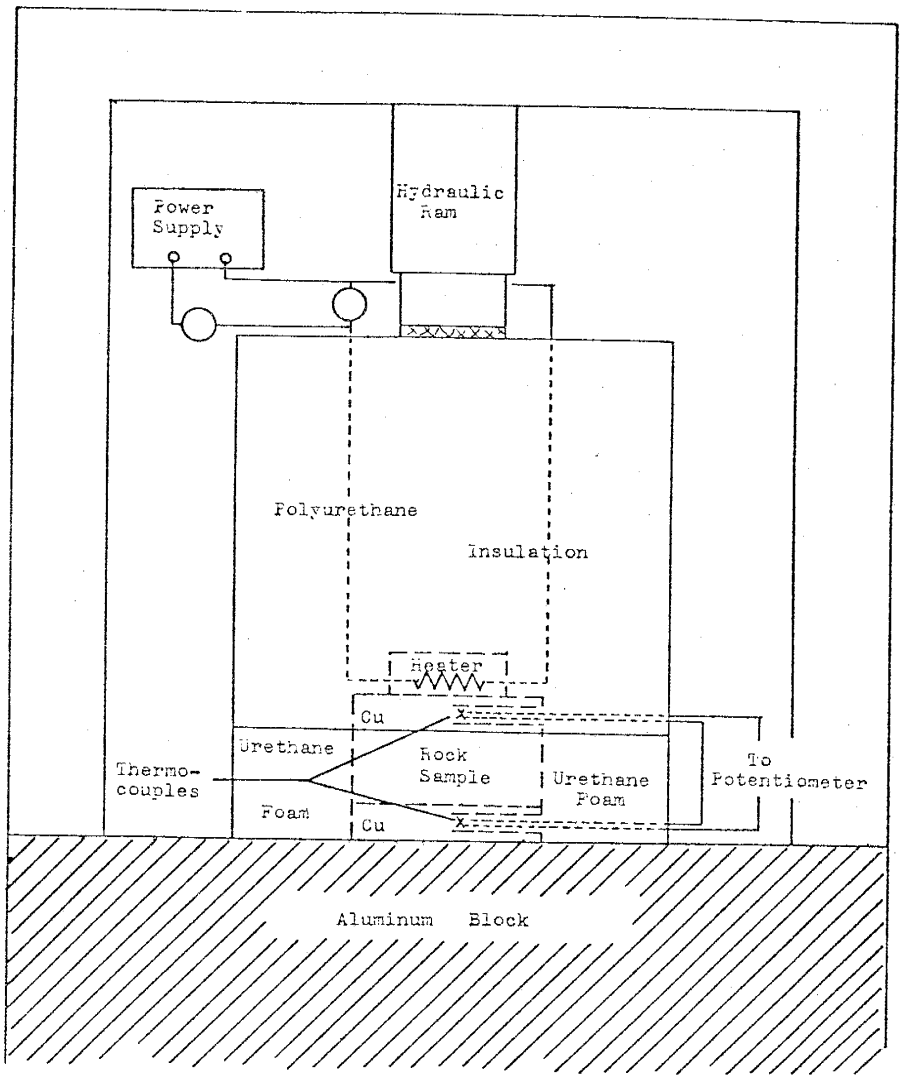

Assuming thermal equilibrium and no radial heat loss, the thermal conductivity of the sample can be determined from equation (I-1). The heat flux, q, is the product of the current through and the voltage across the heater resistor divided by the surface area of the sample. Copper-constantan thermocouples are used to measure the temperature difference, ΔT, across the sample. The thickness of the sample, ΔZ, is measured directly with a micrometer.

The measurement of the thermal conductivity of core samples is a direct application of equation (I-1). Prepared core samples are discs about 1.5 cm thick with faces ground flat and parallel to ± 0.005 cm. Usually, the water level in the drillhole is the only available indicator of depth to in-situ water-saturated conditions. Therefore, core samples from depths below the water level in the drillhole are vacuum flooded with distilled water to approximate in-situ saturated conditions. No attempt is made to re-create the in-situ water chemistry which is generally unknown.

An extension of this technique has been developed to allow measurements to be made on wafers prepared from split core samples. The prepared sample is vacuum flooded with distilled water and measured in the same manner as a full core disc. To investigate the applicability of this technique to measure split core samples, three samples have been prepared from a single, fine-grained, quartz monzonite whole core specimen. One sample has a cross-sectional area equal to that of the full core, one sample has a cross-sectional area

about 63% of that of the full core, and the third sample has a cross-sectional area about 37% of that of the full core. A series of thermal conductivity measurements yield values of 6.63 ± 0.03 mcal/cm-sec-^{o}C for the full core sample and 6.43 ± 0.15 mcal/cm-sec-^{o}C for the larger split core sample, indicating an error of 3% in measuring the split core. Measurements on the smaller split core sample yield widely varying results, reflecting the difficulty in obtaining good thermal contact between the heater assembly and the smaller rock sample. The measurement error for the larger split core sample is due to uncertainties in calculating the sample surface area, to heat loss from the upper copper disc which has a surface area greater than the sample, and to contact resistance. The estimation of the sample surface area may be in error as much as ± 5%. An over-estimation of this area by 5% will result in a 5% decrease in the measured thermal conductivity. The error due to heat loss has been modeled as the ratio of heat fluxes through two parallel conductors (the rock sample and the insulating foam rubber strips) between the upper and lower copper discs. The predicted error is less than 3% for a split core sample having a cross-sectional area only 60% of the area of the copper disc. The error due to contact resistance between the copper disc and the sample is present in all the thermal conductivity measurements and is discussed later in this section. Split core samples having a cross-sectional area 60% or more of a full core have been used in determining about 15% of the thermal

conductivity values presented in this study. These values are believed to be about 3% lower than the measured values that would have been obtained using full core samples.

This basic experimental technique and apparatus is also used to measure thermal conductivities of fragment samples in a manner described by Sass et al. (1971b). The fragments are packed into cylindrical cells which have dimensions about those of a typical core sample (3.8 cm diameter and 1.3 cm height). The cells have walls of plastic and faces of copper. A cell packed with fragments is vacuum flooded with distilled water and its composite thermal conductivity is measured as if it were a core sample. With the assumption that the thermal resistance of the cell assembly with its contents can be represented by the thermal resistances of the plastic cell wall and the aggregate of water and water-saturated rock fragments in parallel, the thermal conductivity of this aggregate of water and water-saturated fragments, K_a, is given by

$$K_a = \left(\frac{D^2}{d^2}\right) K_c - \left(\frac{D^2-d^2}{d^2}\right) K_p \qquad \text{(I-2)}$$

where D and d are, respectively, the outer and inner diameters of the plastic cell wall, K_c is the measured conductivity of the cell and its contents, and K_p is the thermal conductivity of the plastic cell wall. Also,

$$K_a = K_r^{\,1-\phi} K_w^{\,\phi} \qquad \text{(I-3)}$$

where K_r is the geometric mean conductivity of the solid fragments in the cell (the rock fragments with no porosity), K_w is the thermal conductivity of the water in the cell, and ϕ is the total volume fraction of water in the cell (both inter- and intra-fragment porosity). Combining equations (I-2) and (I-3) yields

$$K_r = K_w \left(\frac{D^2}{d^2} \frac{K_c}{K_w} - \frac{D^2-d^2}{d^2} \frac{K_p}{K_w} \right) \frac{1}{1-\phi} . \qquad \text{(I-4)}$$

Equation (I-4) represents the rock conductivity if the uncrushed rock has a negligible in-situ porosity. The conductivity of the uncrushed porous rock, K_{pr}, with porosity ϕ_o is given by

$$K_{pr} = K_w^{\phi_o} K_r^{1-\phi_o} . \qquad \text{(I-5)}$$

Substituting this equation into (I-4) yields

$$K_{pr} = K_w \left(\frac{D^2}{d^2} \frac{K_c}{K_w} - \frac{D^2-d^2}{d^2} \frac{K_p}{K_w} \right) \left(\frac{1-\phi_o}{1-\phi} \right) . \qquad \text{(I-6)}$$

The in-situ porosity, ϕ_o, is often not known, but it is especially important in determining the thermal conductivity of sedimentary rocks. Measurements of bulk density and matrix density can aid in estimating the in-situ porosity from the relation

$$\rho_B = \phi_o \rho_w + (1-\phi_o) \rho_m \qquad \text{(I-7)}$$

where ρ_B, ρ_w, and ρ_m are, respectively, the bulk, water, and matrix densities and ϕ_o is the in-situ porosity.

To calibrate the thermal conductivity measuring system, about one in every twenty measurements is made on one of the laboratory standards. Commercially prepared fused quartz cores are used as primary standards as are fused quartz fragments. Cores of both granite and amphibolite, prepared and measured by the U.S.G.S. laboratory, are used as secondary standards. Almandine fragments are also used as secondary standards. The thermal conductivities of fused quartz (3.29 mcal/cm-sec-^{o}C), of the granite and amphibolite (5.68 to 9.25 mcal/cm-sec-^{o}C), and of the almandine (8.07 mcal/cm-sec-^{o}C) allow calibration over the spectrum of thermal conductivity values typically measured for rocks.

Reproducibility of measurements on standards is 5% for both core and fragments. The mean measurement for each standard is about 3% below the true or accepted value. Beck (1976) notes that treating contact resistance as being in series with the thermal resistance of the sample yields the relation

$$\frac{D}{K_{app}} = \frac{2L}{K_f} + \frac{D+2L}{K_t} , \qquad (I-8)$$

where K_{app} is the apparent thermal conductivity, K_f is the contact film conductivity, K_t is the true sample conductivity, and D and L are, respectively, the thicknesses of the sample

and of the contact film on one sample face. For a fused quartz standard, K_t = 3.29 mcal/cm-sec-^oC, K_{app} = 3.19 mcal/cm-sec-^oC (3% error), and D = 1.27 cm. Assuming L = 0.0025 cm, K_f is found from (I-8) to be 0.481 mcal/cm-sec-^oC. A cell measurement of the thermal conductivity of the contact film (vaseline) yields 0.478 mcal/cm-sec-^oC. It is therefore likely that a systematic error of 3% is present in our measurements due to thermal contact resistance.

Thermal conductivity measurements in the laboratory are made at about 20 ^oC. The temperature range observed in the logged drillholes is about 25 ^oC to 60 ^oC. The temperature effect on the thermal conductivity is a decrease of about 1.5%/10 ^oC for granitic rocks (Clark, 1966). This indicates a maximum error of about 6%. Thermal conductivity increases with pressure such that a sample from 1 km depth has an actual conductivity value about 5% to 6% greater than the value measured in the laboratory at about 50 bars (Walsh and Decker, 1966). Therefore, errors in thermal conductivity measurements of core samples due to temperature and pressure effects are estimated to be less than about 1%.

Temperature Measurements

The temperature measurements presented in this study have been made by lowering a thermistor probe down a borehole, stopping the probe at specific depths and measuring the thermistor resistance with a Mueller bridge at each of those depths. The interval between depths is usually 10 m; in deeper boreholes, the interval is 20 m. A computer program is used to convert the measured resistances to temperatures by means of tables provided by the manufacturer of the thermistor probe. The resultant temperature-depth data are plotted and depth intervals having linear gradients are chosen by inspection of the plotted data. Linear gradient zones are believed to be most representative of conductive heat flux and to be least disturbed by such effects as ground-water movement. The temperature gradients of the chosen depth intervals are calculated by means of a computer program using the method of least squares.

Two types of thermistors have been used during this study, a 4 K ohm isocurve bead and a 100 K ohm isocurve bead. The beads are encased in needle-shaped, stainless steel housing 0.79 cm in length and 0.13 cm in diameter. These probes are periodically calibrated against a platinum temperature-sensing tool in an ice bath. Both the 4 K ohm and the 100 K ohm thermistor probes are accurate with respect to the platinum tool to better than 0.4 ^{o}C. The 4 K ohm probe has an ice point reproducibility of better than 0.02 ^{o}C and the 100 K ohm probe has an ice point reproducibility on the

order of 0.4 °C. Both thermistor probes have been calibrated against the platinum resistance thermometer at six temperatures ranging from about 17 °C to about 95 °C. These calibrations show that errors of less than 1% are introduced into measured temperature gradients by the inaccuracies of either thermistor probe with its associated logging cable and Mueller bridge.

The cable used to lower the thermistor probes down the drillholes is a rubber-jacketed, 4-conductor cable. The potential for stretching of this cable while making the temperature logs has been considered in two wells where the actual total depth is known to ± 1 m. The maximum indicated stretch of the cable is 3%, which would cause the observed temperature gradient to be 3% greater than the true gradient. It is believed, therefore, that a systematic error has increased the observed temperature gradients reported in this study to no more than 3% greater than the true temperature gradient.

Errors may result in the measured temperature gradients that are not due to the measuring equipment. A necessary consideration is whether the temperature disturbance due to drilling has dissipated and the drillhole has reached thermal equilibrium with the rock formations which it has penetrated. In this study, temperature measurements made in recently completed drillholes have been made in diamond-drilled, mineral exploration holes. Two such drillholes have been studied for possible temperature disturbances due to the drilling procedure.

At a location in the Hualpai Mountains in Mohave County, a drillhole completed on 16 Dec, 1976, to a total depth of 933 m has been logged to a depth of 810 m on 20 Dec, 1976, and 22 Dec, 1976. The difference in the observed temperature gradients in the bottom 200 m of the two logs is 4%. The difference in the upper part is less than 1%.

A drillhole in central Yavapai County, completed on 22 Dec, 1976, to a total depth of 914 m, has been logged to a depth of 430 m on 28 Dec, 1976, on 15 Jan, 1977, and on 1 Mar, 1977. The temperature gradient measured six days after completion is 1.5% greater than that measured seven weeks after completion.

These observations suggest that errors due to the temperature disturbance by the diamond-drilling of a borehole is probably only a few percent if the temperature log is made six days after completion of the borehole. From similar observations, Jaeger (1961) reports that temperature measurements made 1, 3, and 6 months after drilling had ceased are adequate to give values of the geothermal gradient without any correction. It should be noted, however, that the occurrence of any major circulation problems during the drilling would most likely be due to deep penetration of faults or rubble zones by the drilling fluid and would indicate that waiting considerably longer than six days might be necessary to obtain an undisturbed temperature log. Also, extrapolation

of these observations to rotary-drilled holes may be unwarranted because of the greater volume and flow rate of the drilling fluid.

Ground-water movement is another potential source of error in the observed temperature gradient. Mansure and Rieter (1979) have shown that downward ground-water movement of about 14 cm/yr over a vertical interval of less than 100 m can reduce the heat flow by a factor of 2. The temperature-depth plot of such a condition would be concave upward and can be observed if the rate of vertical ground-water movement is sufficiently great and if the temperature log was made over at least a major part of the depth interval in which the ground-water movement is occurring. The temperature-depth plots of some data acquired in the course of this study provide graphic examples of some effects of ground-water movement.

The Bisbee South drillhole, located in south central Cochise County, has indicated heat-flow values of 1.5 HFU for the depth interval 160 m to 200 m and 1.1 HFU for 630 m tO 650 m. The temperature-depth plot (Figure I-2) has a convex upward curve from 350 m to 580 m, indicating upward ground-water movement (Bredehoft and Papadopulos, 1965; Mansure and Reiter, 1979). Mansure and Reiter (1979) have developed a linear relationship between temperature gradient and temperature for the case of simultaneous heat flow and incompressible fluid flow. By plotting temperature gradient

Figure I-2. Temperature log for the Bisbee South drillhole.

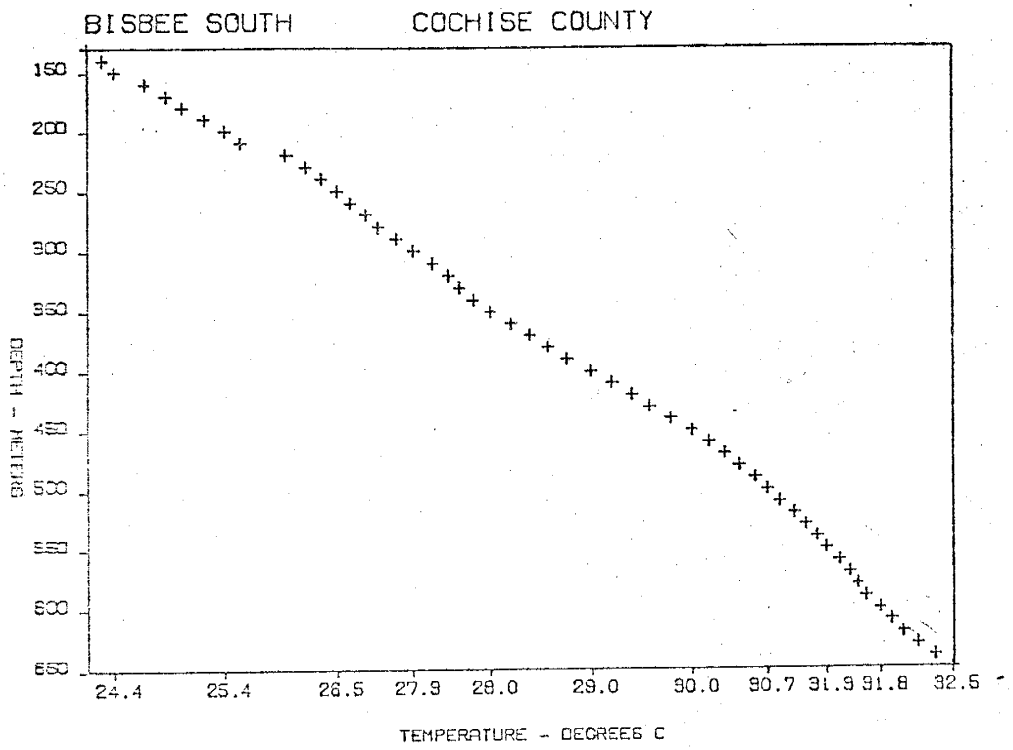

versus temperature and calculating the slope, which is proportional to the vertical fluid flux, one can estimate this vertical fluid flux. Application of the linear relationship developed by Mansure and Reiter (1979) to the data from Bisbee South indicates that vertical upward ground-water movement of about ½m/yr could result in a temperature distribution having the character exhibited in Figure I-2. A possible source for this upward ground-water movement might be a hydraulic head developed by downward ground-water movement along normal faults defining the mountain block adjacent to the Bisbee South location.

The Lake Mary drillhole (Figure I-3) penetrates Paleozoic formations at a location near Flagstaff, Arizona. The character of the temperature-depth plot indicates severe disturbances, possibly ground-water movement in both the drillhole and the formation. Furthermore, the indicated temperature gradient is about 1 ^{o}C/km, more than an order of magnitude less than what could be reasonably expected. This is also probably an indication of significant ground-water movement below the maximum depth of the temperature log.

Well #8 (Figure I-4) is an abandoned water well located west of Phoenix. The well casing is perforated at several different depths. The nearly isothermal section of the temperature-depth plot probably indicates flow between two aquifers by means of these perforations. High-volume pumps operating in other water wells in the area are likely stimulating this water movement in Well #8.

Figure I-3. Temperature log for the Lake Mary drillhole.

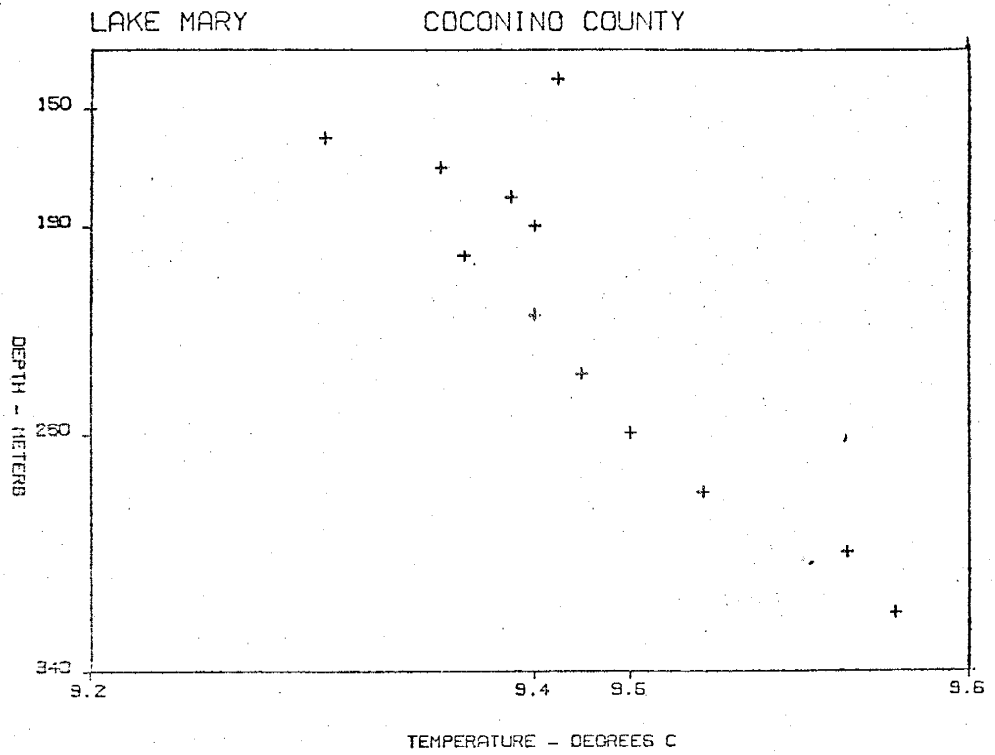

Figure I-4. Temperature log for Well #8.

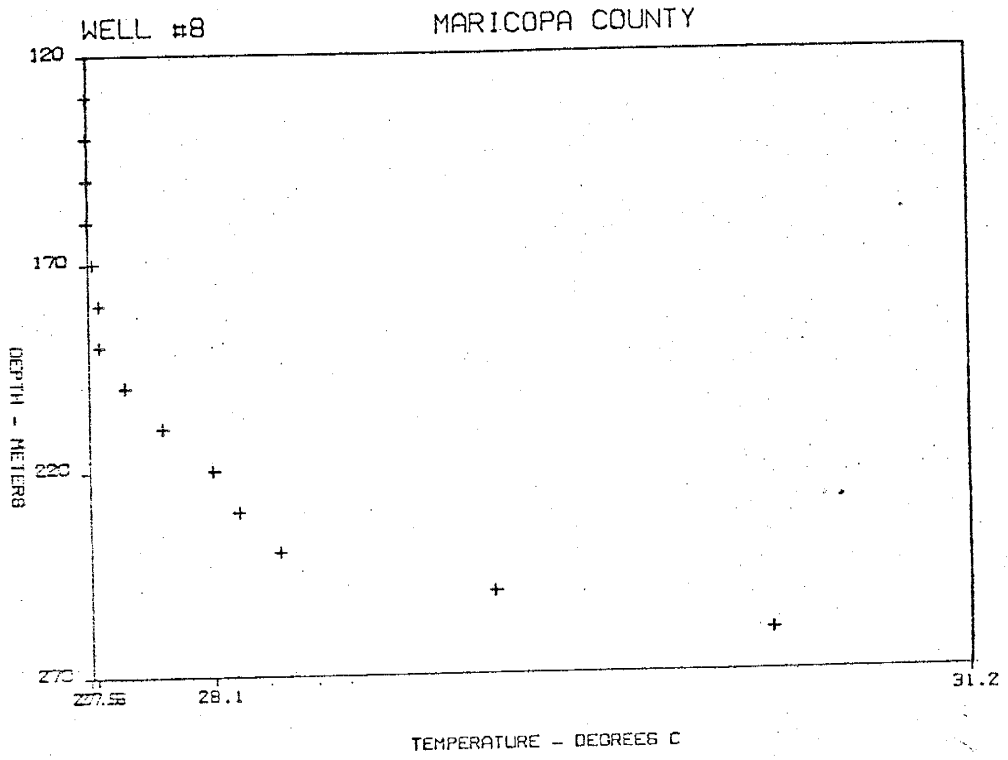

Figure I-5. Temperature log for the Dragoon #1 drillhole.

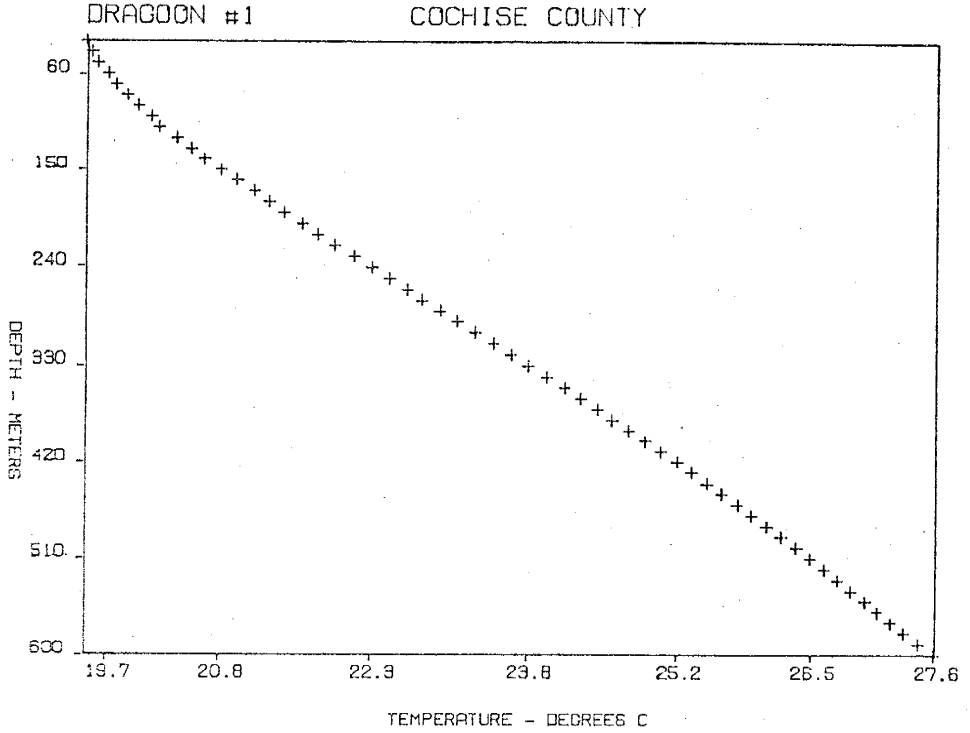

Figure I-6. Temperature log for the Dragoon #2 drillhole.

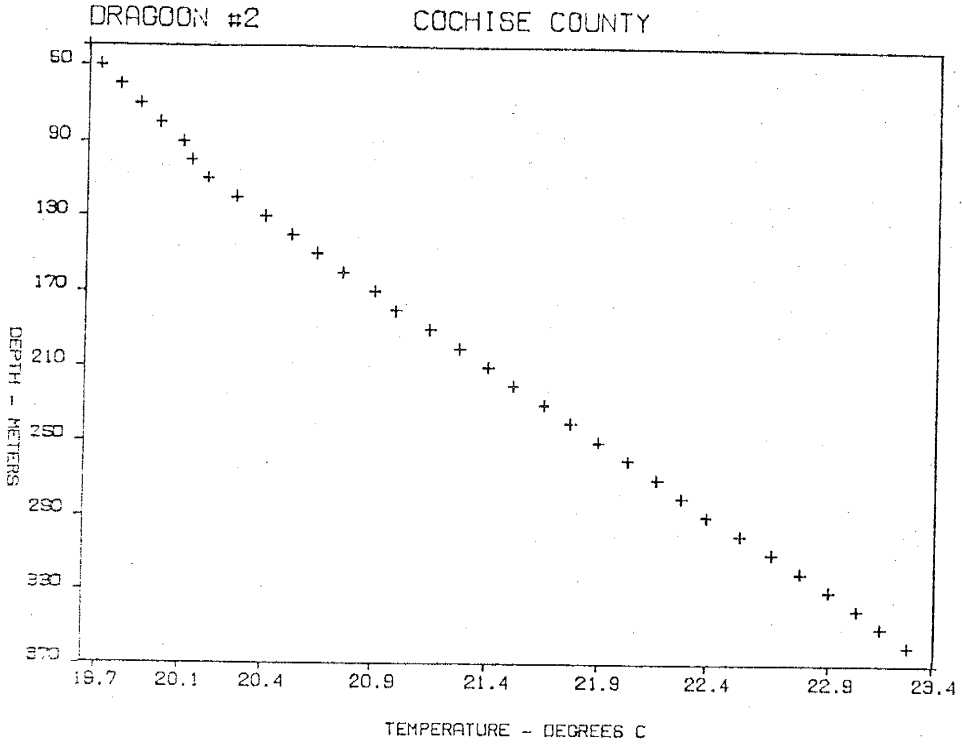

Temperature-depth plots for two drillholes, Dragoon #1 and Dragoon #2, which are about 400 m apart, demonstrate how the effects of hydrologic conditions can change over relatively short lateral distances. Figure I-5 shows a gentle S-shaped curve from 30 m to 600 m in Dragoon #1, while Figure I-6 indicates a generally linear gradient in Dragoon #2 below 110 m. Despite this apparent linearity, the data from Dragoon #2 are suspect because of the obvious disturbance in the deeper, nearby Dragoon #1.

Besides ground-water movement, there are other natural processes which affect the near-surface temperature distribution. These include diurnal and annual surface temperature variations, lateral variation in thermal conductivity, uplift, erosion, sedimentation, climatic changes and terrain irregularities.

The annual temperature oscillation can usually be neglected below 20 m depth. This can be seen by defining the temperature as $T_o \cos(\omega t)$ at the surface $z = 0$. Then, for a uniform earth (Carslaw and Jaeger, 1959),

$$T = T_o \exp(-\alpha z) \cos(\omega t - \alpha z), \qquad \text{(I-9)}$$

where $\alpha = (\omega/2k)^{\frac{1}{2}}$, $\omega = 2\pi/P$ where P is the period, and the wavelength is $\lambda = 2\pi/\alpha = (4\pi k P)^{\frac{1}{2}}$. For $k = 0.01$ cm^2/sec, the amplitude is reduced by a factor of $\exp(-2\pi) \cong 0.002$ at a depth of one wavelength. The wavelength of the diurnal

oscillation is 1 m and of the annual oscillation is 20 m. Therefore the effect of the annual temperature oscillation can generally be neglected below 20 m depth. As a general rule, temperature logs made in this study have started at a depth of at least 30 m.

Attempts to correct temperature measurements for effects of lateral variation in thermal conductivity, uplift, erosion, sedimentation, and climatic changes are subject to considerable uncertainties and are generally not carried out. Because these effects may be on the same order as the effect due to terrain irregularities, one can argue for a simple topographic correction.

Although different methods of topographic correction have been devised (e.g., Jeffreys, 1940; Bullard, 1940; Birch, 1950), perhaps the simplest to apply is that of Lees (1910). Lees (1910) shows that

$$v = V_o + \alpha z + \frac{A(z+a)}{x^2+(z+A)^2} \qquad \text{(I-10)}$$

is a solution for the diffusion equation for the region beneath a single mountain range which has a surface temperature defined by

$$(\alpha-\alpha')\ z + \frac{A(z+a)}{x^2+(z+A)^2} = 0 \ . \qquad \text{(I-11)}$$

The mountain range is symmetric about the x-axis, $z = 0$ at the foot of the range and is positive downward, α is the geo-

thermal gradient for $z \to \infty$, α' is the adiabatic lapse-rate of temperature along the surface, A and a are constants whose values depend on the maximum height of the range and the width of the range at half its maximum height, and V is the temperature at the foot of the range. The temperature perturbation has a maximum at $x = 0$, the crest of the range, and the temperature perturbation equals zero at $x = \pm\infty$ or $z = \infty$.

Lees' (1910) technique has been used to study the possible terrain effect on a temperature measurement made in drillhole DDH75-17 in Yavapai County. This drillhole is located on the steep flank of a range whose aspect ratio lends itself to Lees' (1910) two-dimensional model. Table I-1 lists the measured gradients and the terrain-corrected gradients for the drillhole. The table shows that the

Table I-1

Depth Interval (m)	Measured Temperature Gradient (^{o}C/km)	Gradient Corrected by Lees' Model (^{o}C/km)
210-230	12.9	12.9
240-260	13.1	13.1
270-290	18.8	18.9
290-330	13.9	13.9
340-370	16.7	16.8
380-430	15.5	15.6
440-470	15.8	15.9
470-510	20.3	20.4

terrain effect is negligible for the location of this drillhole. Lees' (1910) model indicates that the terrain effect is greatest for a temperature measurement at the crest of the range. A temperature log made in a drillhole at the crest of this same range would yield a temperature gradient lowered almost 20% by the terrain effect.

Heat-Flow Values

Heat-flow values are calculated by multiplying linear temperature gradients by their corresponding average thermal conductivites. In the ideal case for a single drillhole, two or more different linear temperature gradients and their correspondingly different average thermal conductivities yield the same heat-flow values. Therefore, a best heat-flow value is normally determined by averaging the heat flows of different depth intervals in the drillhole. In some instances, the heat flows in a drillhole will vary significantly. An attempt is then made to determine a heat-flow value based on consideration of the linearity of the temperature gradients, the lithology and thermal conductivity control, and the potential for ground-water movement and other disturbances. This last effect may include vertical water movement in the drillhole or regional ground-water movement through the rock.

The Kelvin #1 drillhole (Figure I-7) and drillhole #43 (Figure I-8) are two examples of locations where the calculated heat-flow values are thought to be most reliable. Kelvin #1 is in a single lithologic unit, a granite block, and has a linear temperature gradient of 27 ^{o}C/km between 50 m and 590 m with a heat flow of 2.3 HFU. Drillhole #43 has three depth intervals having linear temperature gradients of 36 ^{o}C/km between 370 m and 430 m, 41 ^{o}C/km between 430 m and 480 m, and 35 ^{o}C/km between 600 m and 650 m. The thermal conductivities vary correspondingly and the three respective heat

Figure I-7. Temperature log for the Kelvin #1 drillhole.

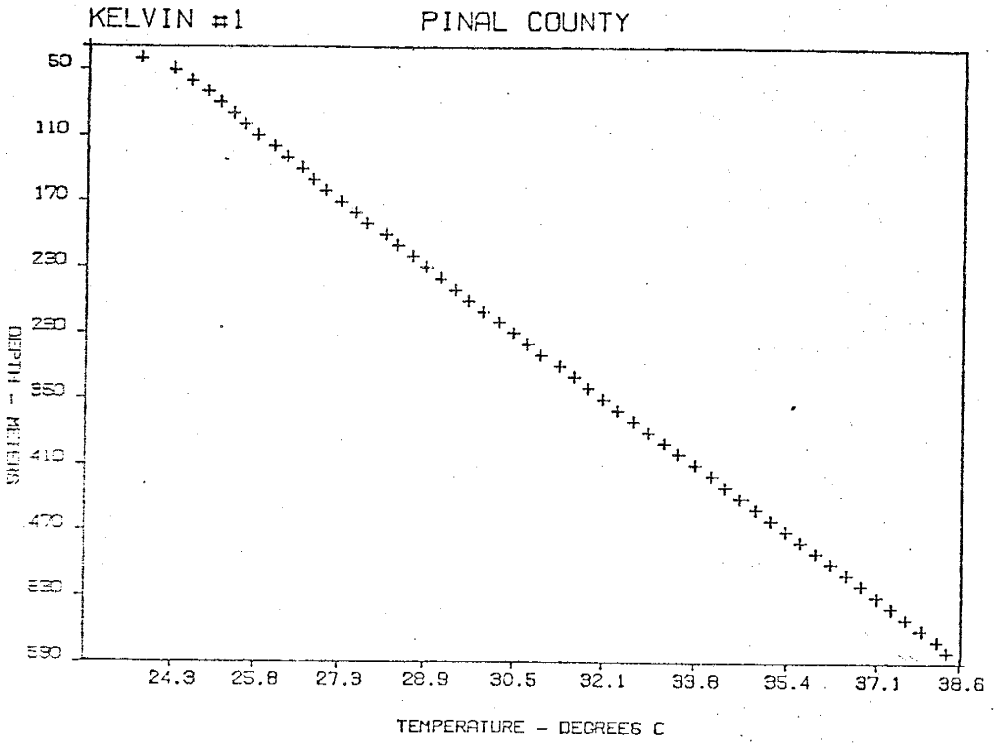

Figure I-8. Temperature log for the #43 drillhole.

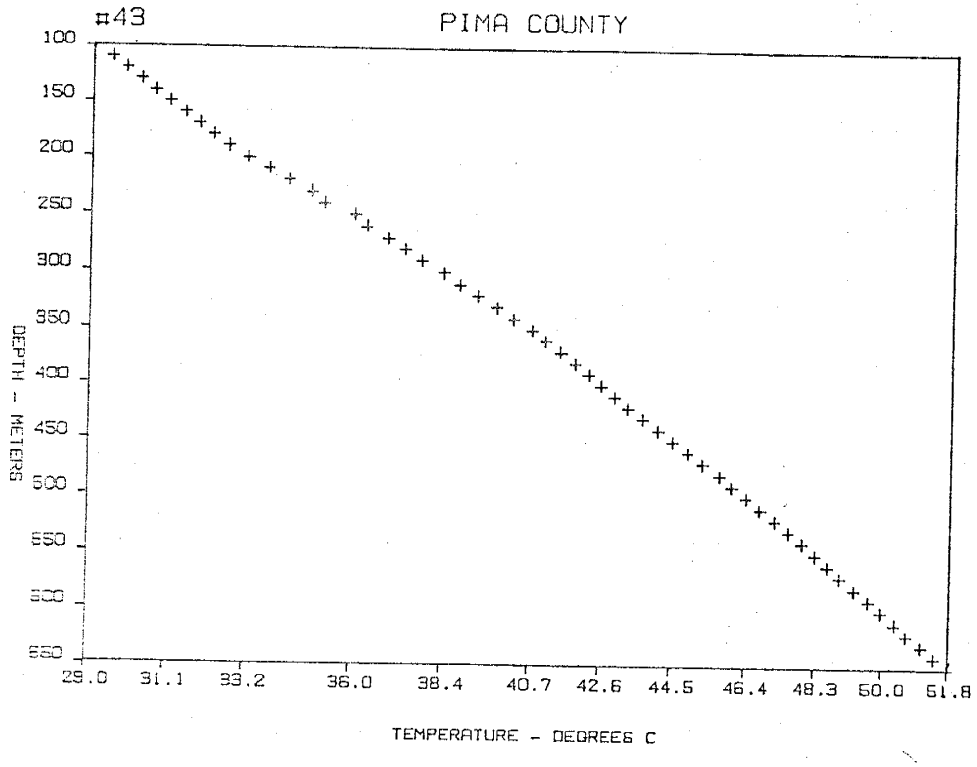

flows are 2.25 HFU, 2.25 HFU, and 2.25 HFU. Therefore 2.2 HFU is thought to be a reliable heat-flow value for the drillhole #43 location.

It has been noted in the previous sections of Appendix I that there are systematic errors in both the thermal conductivity measurements and the temperature measurements. The thermal conductivities are about 3% low and the temperature gradients are about 3% high due to these indicated systematic errors. The effect of these errors on the resultant heat-flow values has been considered for data from two locations, Kelvin #1 and H-1, and are summarized in Table I-2.

Table I-2

Kelvin #1

	Gradient (^{o}C/km)	Conductivity (mcal/cm-sec-^{o}C)	Heat Flow (HFU)
Measured	26.7 ± 0.07	8.43 ± 0.63	2.26 ± 0.17
Corrected	25.9 ± 0.07	8.69 ± 0.65	2.25 ± 0.17

H-1

	Gradient (^{o}C/km)	Conductivity (mcal/cm-sec-^{o}C)	Heat Flow (HFU)
Measured	29.4 ± 0.04	6.87 ± 0.59	2.02 ± 0.18
Corrected	28.5 ± 0.04	7.08 ± 0.61	2.02 ± 0.18

It can be seen from Table I-2 that the effect of the systematic errors in the thermal conductivities and in the temperature gradients on the calculated heat-flow values is negligible. Therefore, the corrections for these two systematic errors are not made in the calculation of heat-flow values.

Also, corrections are not generally made for terrain irregularities, uplift, erosion, sedimentation, climatic changes, lateral variation in thermal conductivity, or groundwater disturbances because the geologic and hydrologic data for these corrections are not generally available. Those temperature gradients which are recognized as perturbed in some manner are not used to determine heat-flow values.

APPENDIX II
DETERMINATION OF RADIOGENIC HEAT PRODUCTION

A heat-flow study should concern itself with regional variations in heat sources. Heat from the decay of radionuclides is such a source and is an important component of the observed surface heat flow.

Birch et al. (1968) describe a linear relation between heat flow and the radiogenic heat production of surface plutonic rocks. The relation can be written

$$q = q^* + DA(0), \qquad \text{(II-1)}$$

where q is the measured surface heat flow, A(0) is the radiogenic heat production of surface plutonic rocks, and q* and D are characteristic constants for major geologic provinces. Birch et al. (1968) and Roy et al. (1968b) consider A(z), the vertical distribution of radiogenic heat production, to be constant to depth D and q*, therefore, to be the heat flux into the base of the crustal layer of thickness D. Lachenbruch (1970) proposes

$$A(z) = A(0)e^{-z/D} \qquad \text{(II-2)}$$

whereby q* can be thought of as the heat flux from the mantle. In either model, the major radiogenic heat source concentration occurs in the upper 7 to 10 km of the crust. The exponential

model predicts slightly higher temperatures at depth than does the model having a constant heat source distribution, but the difference is about 1 ^{o}C at 3 km and less than a few tens of degrees at 10 km (Diment et al., 1975).

The component of the surface heat flow due to radioactive heat production in the upper crust, DA(0), can be estimated by multiplying the measured radiogenic heat generation of samples of crustal material by the value of D thought to be appropriate for the sample locations. A value of 10 km for D is used by Roy et al. (1968b) for the Basin and Range and is also used in heat-production calculations in this study.

As noted by Stacey (1969), more than 99% of the heat due to radioactive decay in rocks is generated by uranium, thorium, and potassium. For this study, borehole samples have been collected for twelve locations in Arizona in order to estimate the upper crustal concentration of uranium, thorium, and potassium for these locations. In ten instances, the samples come from the same borehole in which temperature measurements have been made. In the other two cases, the samples come from boreholes very near the holes in which the temperature logs have been made. The samples have been crushed and ground to 100 mesh and then sent to Atomic Energy of Canada Limited (AECL) in Ottawa, Ontario, Canada for analyses.

The procedure used by AECL for uranium analysis is a neutron activation/delayed neutron counting technique described

by Amiel (1962). Samples are placed in a reactor and irradiated by a pre-selected neutron flux of 10^{11}-10^{12} n/cm^2-sec, then transferred to a counting facility of six BF_3 neutron detectors embedded in paraffin. The standard sequence consists of a 60 sec irradiation, a 10 sec delay, and a 60 sec count. The analysis is a comparative procedure. The signal from an unknown is compared to that of a standard which has undergone an identical irradiation/counting history. The technique is specific for the determination of U^{235} because only U^{235} is fissioned by thermal neutrons. The uranium determination is then calculated assuming a normal isotopic abundance of 0.72% U^{235} in natural uranium. The important factors affecting the precision of the procedure are reproducibility of sample position in the reactor and stability of the neutron flux, variations in the time periods of the segments of the analysis sequence, and the statistics of the radioactivity measurements. AECL claims a precision of ± 20% at 1 ppm uranium and ± 15% at 10 ppm uranium. In the twelve instances where two or more samples have been prepared from a single borehole specimen, measurements by AECL show a reproducibility of better than 10% for the range of 1 ppm to 10 ppm uranium.

The procedure for thorium and potassium analysis is a neutron activation/delayed gamma ray count technique. The analytical sequences are a 4 hr irradiation, a 6-10 day delay and a 15 min count for the thorium and a 4 hr irradiation, a 2 day delay, and a 10 min count for the potassium. A

Ge(Li) detector is used to count the emitted gamma rays. Like the delayed neutron counting technique, this method is a comparative procedure and its precision is subject to the same factors.

The measured concentrations of uranium, thorium, and potassium received from AECL have been used to calculate heat generation values for the twelve sample locations. MacDonald (1959) gives the heat generation values for naturally occurring uranium, thorium, and potassium as 0.97, 0.26, and 3.55×10^{-5} erg/gm-sec, respectively. The borehole samples are of four different rock types-granite, granodiorite, gneiss, and quartz monzonite. The densities of several samples of each rock type have been measured and found to differ by no more than 2% from the means of the values given by Clark (1966). The density values used in the heat generation calculations are 2.667, 2.716, 2.68, and 2.645 gm/cm^3 for granite, granodiorite, gneiss, and quartz monzonite, respectively.

Table II-1 lists the concentration data received from AECL. Errors on the uranium values are not given by AECL, but have been calculated using their claimed precision per ppm. The errors on the thorium and potassium values are given by AECL. The calculated heat generation values are given in HGU's (10^{-13} cal/cm^3-sec).

Table II-1

Site	Sample	No. of Measure-ments	Uranium (ppm)	Thorium (ppm)	Potassium (%)	Heat Production (HGU)
C-4	C4AB	2	7.0±1.1	12.9±1.1	2.4±0.1	6.9±0.7
H-1	H1AB	2	4.3±0.6	2.0±0.1	2.9±0.1	3.6±0.3
	H1CD	2	1.6±0.2	4.5±0.3	2.4±0.07	2.3±0.1
	H1EF	2	2.6±0.4	15.0±0.9	4.1±0.1	5.0±0.4
H-2	H2AB	2	3.4±0.5	8.0±0.5	3.9±0.1	4.4±0.3
	H2CD	2	6.0±0.6	3.2±0.2	3.4±0.1	5.0±0.5
	H2EF	2	2.3±0.3	4.0±0.3	2.5±0.07	2.7±0.2
WA-5	AJ01	1	0.8±0.2	7.9±1.3	1.4±0.4	2.1±0.2
WA-7	AJ02	1	2.3±0.5	12.0±1.9	2.1±0.5	3.9±0.4
CBH-1	CBH1A	1	1.0±0.2	3.6±0.7	1.1±0.3	1.5±0.2
SD-702	DUQ3A	1	12.4±1.9	25.5±3.6	3.1±0.6	12.8±1.3
	DUQ4A	1	16.4±2.5	31.0±4.4	2.4±0.5	16.1±1.8
Kelvin #1	J-2	1	4.7±0.9	22.3±3.2	4.0±0.7	7.5±0.8
	NMB2	3	6.0±0.5	16.3±1.0	4.1±0.3	7.3±0.4
R-1	R1AA	1	1.7±0.3	4.4±0.8	2.6±0.5	2.3±0.2
	R12A	1	2.0±0.4	11.6±1.9	4.1±0.7	4.0±0.4
R-2	R2AA	1	1.5±0.3	3.2±0.7	3.0±0.7	2.1±0.3
	R2BA	1	3.2±0.6	14.4±2.3	3.3±0.7	5.1±0.6
761	TM3A	1	6.1±0.9	1.9±0.4	1.3±0.3	7.1±0.6
Sedona	BRAD1A	2	0.8±0.14	1.3±0.2	1.4±0.2	1.0±0.1
	BRAD2B	2	1.7±0.2	3.1±0.3	1.8±0.2	2.0±0.1

APPENDIX III
TEMPERATURE DATA PLOTS

The following sets of figures are plots of the temperature logs made in the course of this study. The plots on pages 96 to 154 are for the data sites listed in Table 1 and are in the same order. The plots on pages 155 to 171 are those temperature logs rejected as disturbed by water movement and are from those locations marked as X's on Figure 1. Both the horizontal and vertical scales are linear. The temperatures shown correspond to the indicated measurement depths.

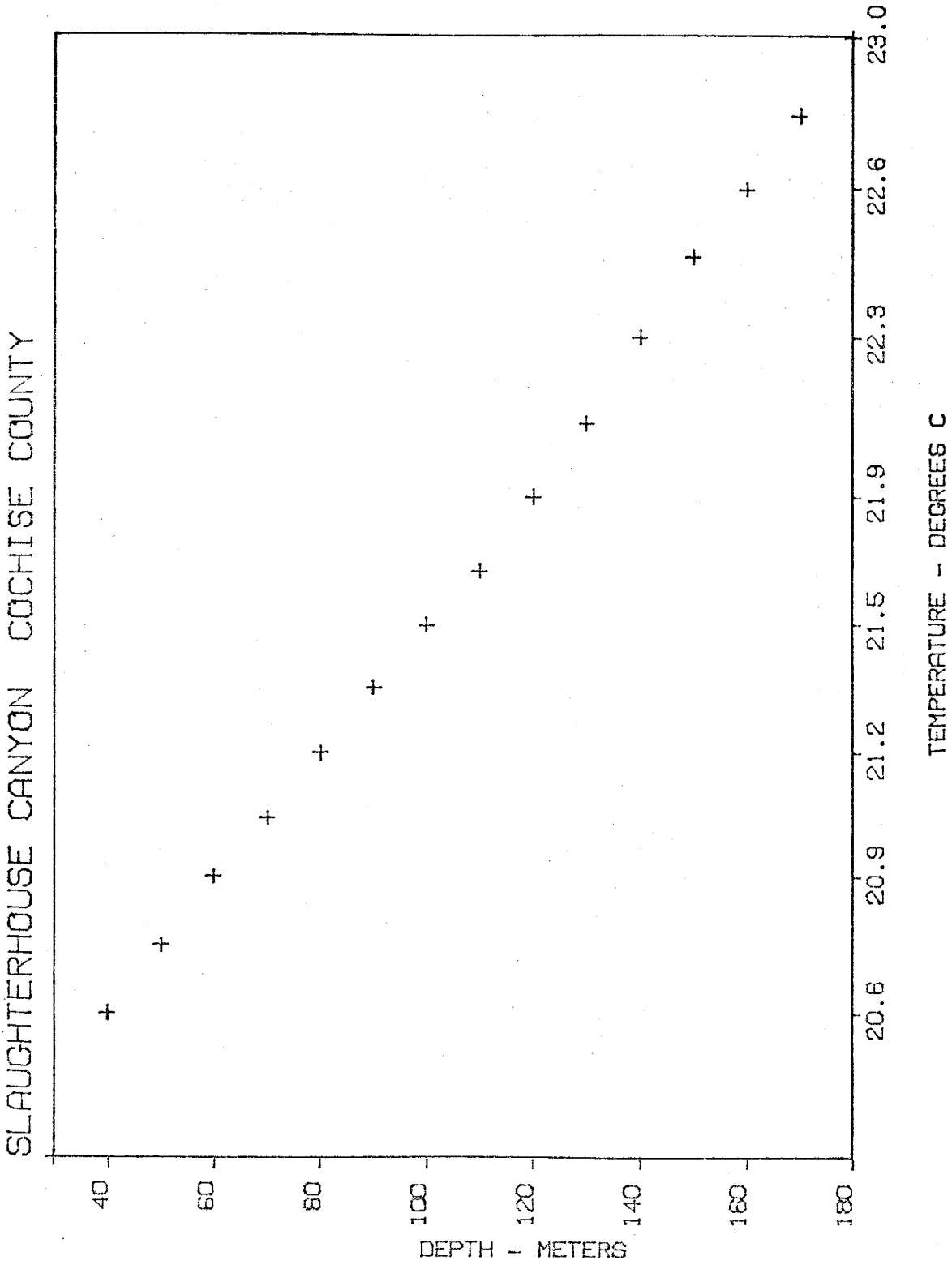
SLAUGHTERHOUSE CANYON COCHISE COUNTY
40
60
80
100
120
140
160
180
DEPTH - METERS
20.6
20.9
21.2
21.5
21.9
22.3
22.6
23.0
TEMPERATURE - DEGREES C

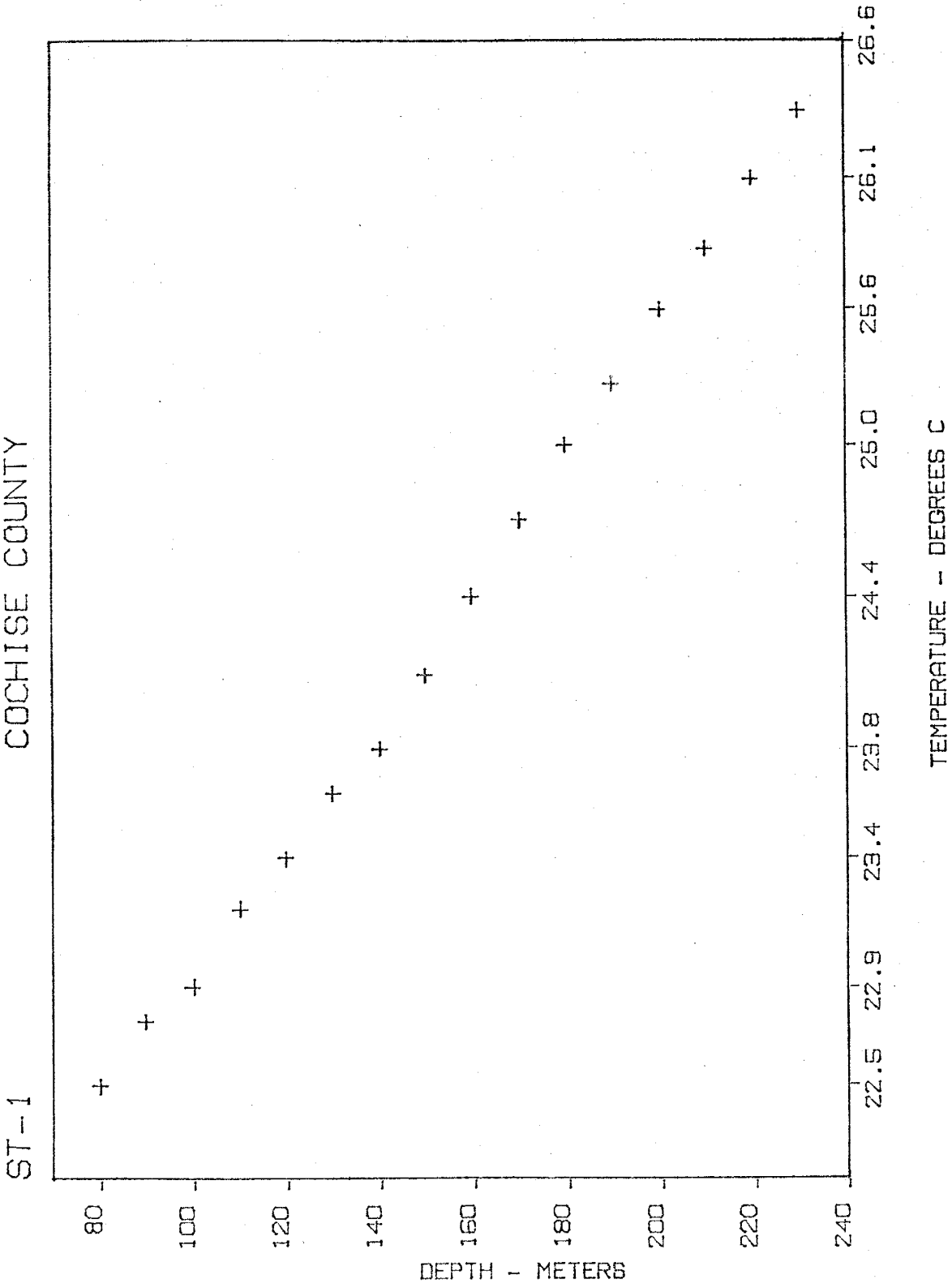
ST-1
COCHISE COUNTY
DEPTH - METERS
80
100
120
140
160
180
200
220
240
TEMPERATURE - DEGREES C
22.5
22.9
23.4
23.8
24.4
25.0
25.6
26.1
26.6

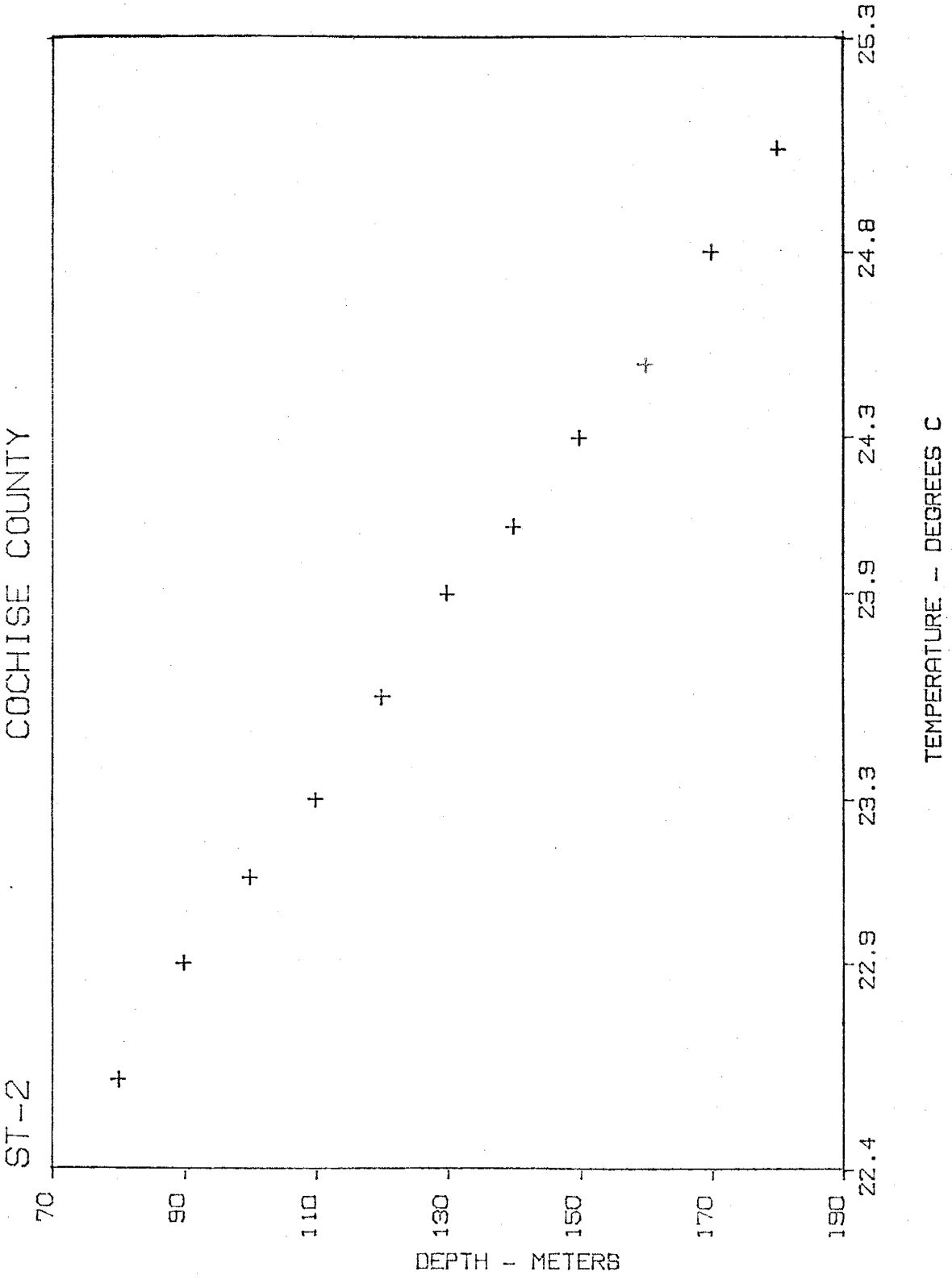
ST-2
COCHISE COUNTY
DEPTH - METERS
70
90
110
130
150
170
190
TEMPERATURE - DEGREES C
22.4
22.9
23.3
23.9
24.3
24.8
25.3

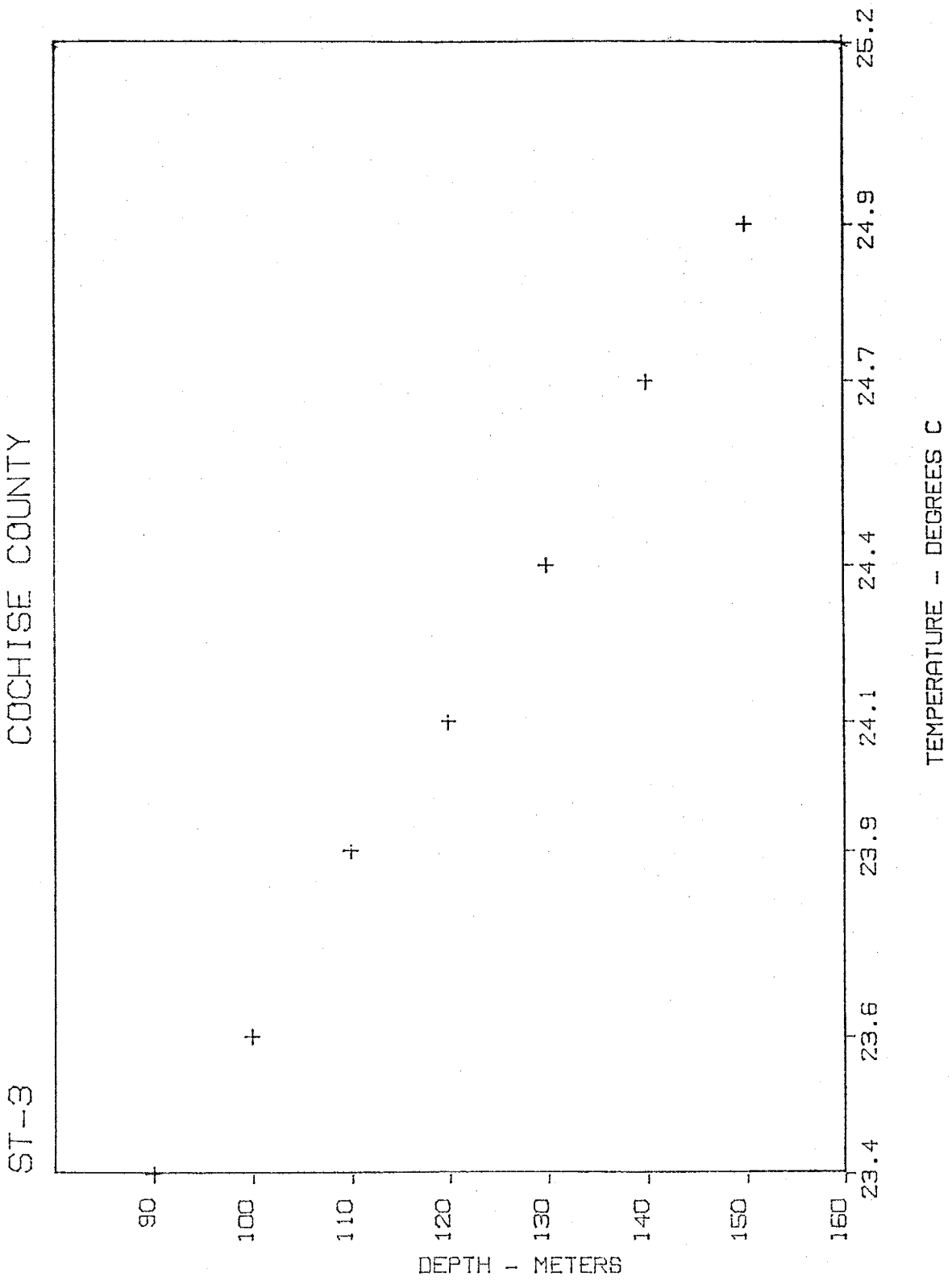
ST-3
COCHISE COUNTY
DEPTH - METERS
90
100
110
120
130
140
150
160
23.4
23.6
23.9
24.1
24.4
24.7
24.9
25.2
TEMPERATURE - DEGREES C

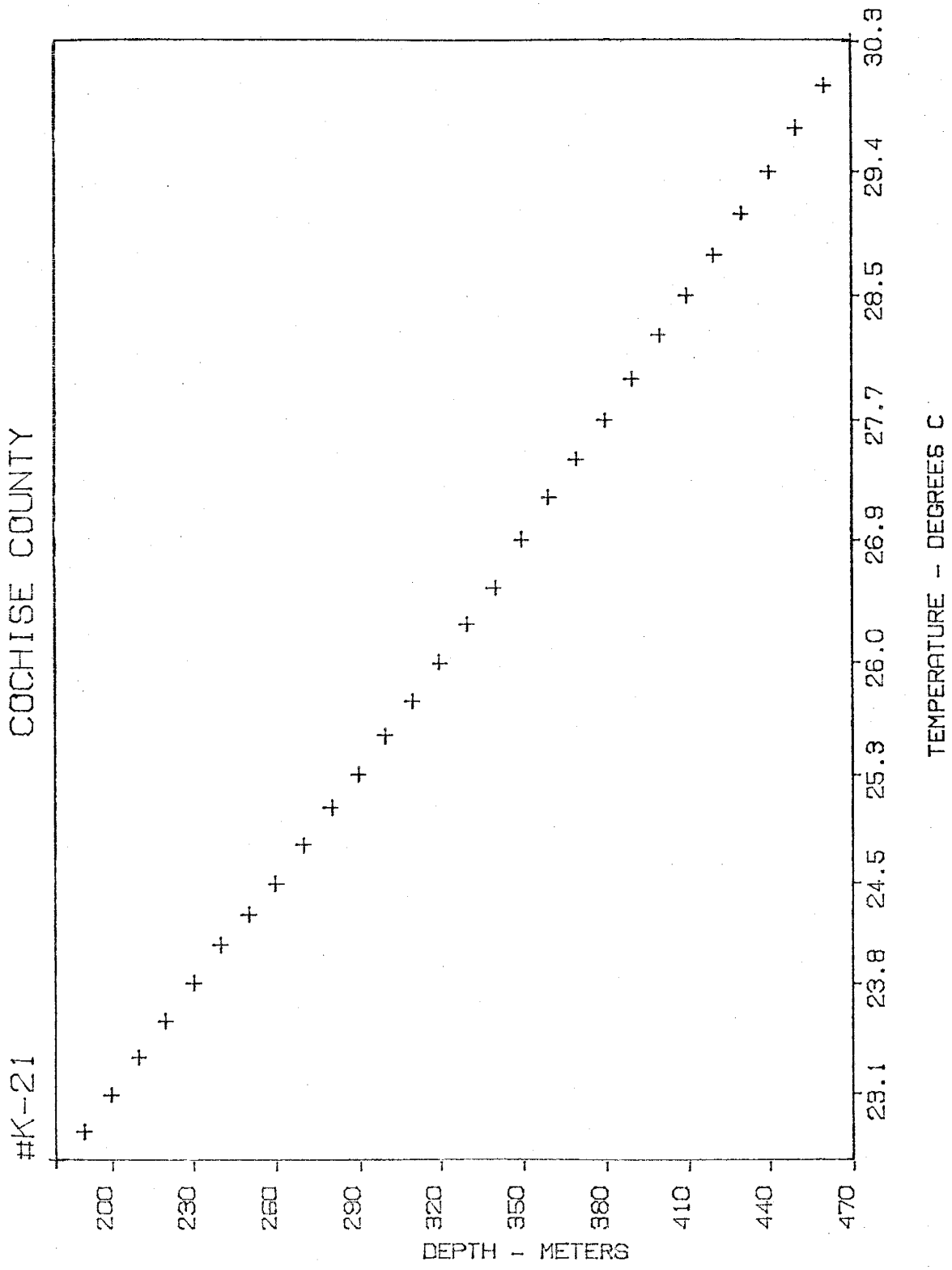
#K-21
COCHISE COUNTY
DEPTH - METERS
200
230
260
290
320
350
380
410
440
470
TEMPERATURE - DEGREES C
23.1
23.8
24.5
25.3
26.0
26.9
27.7
28.5
29.4
30.3

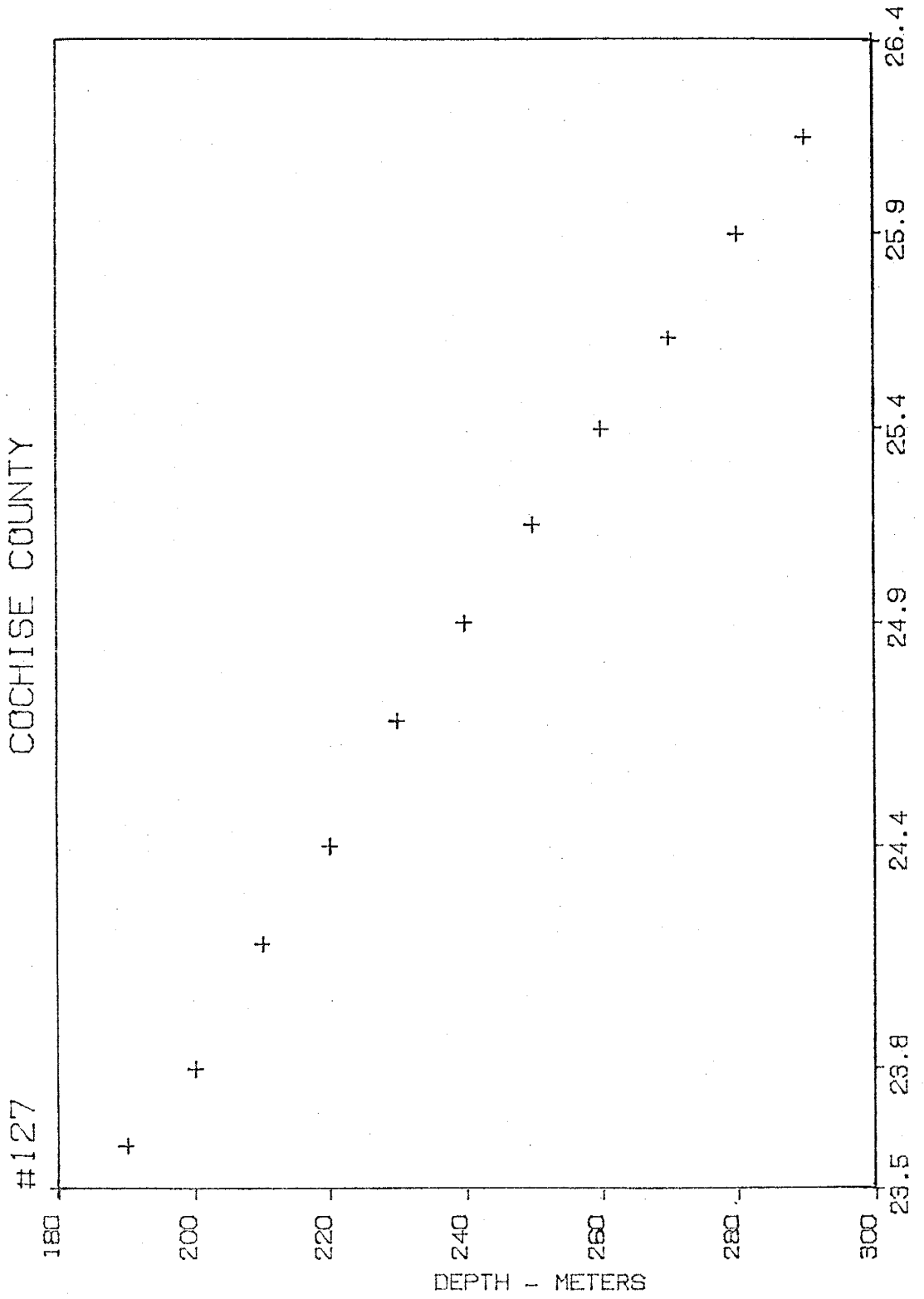
COCHISE COUNTY
#127
180
200
220
240
260
280
300
DEPTH - METERS
23.5
23.8
24.4
24.9
25.4
25.9
26.4
TEMPERATURE - DEGREES C

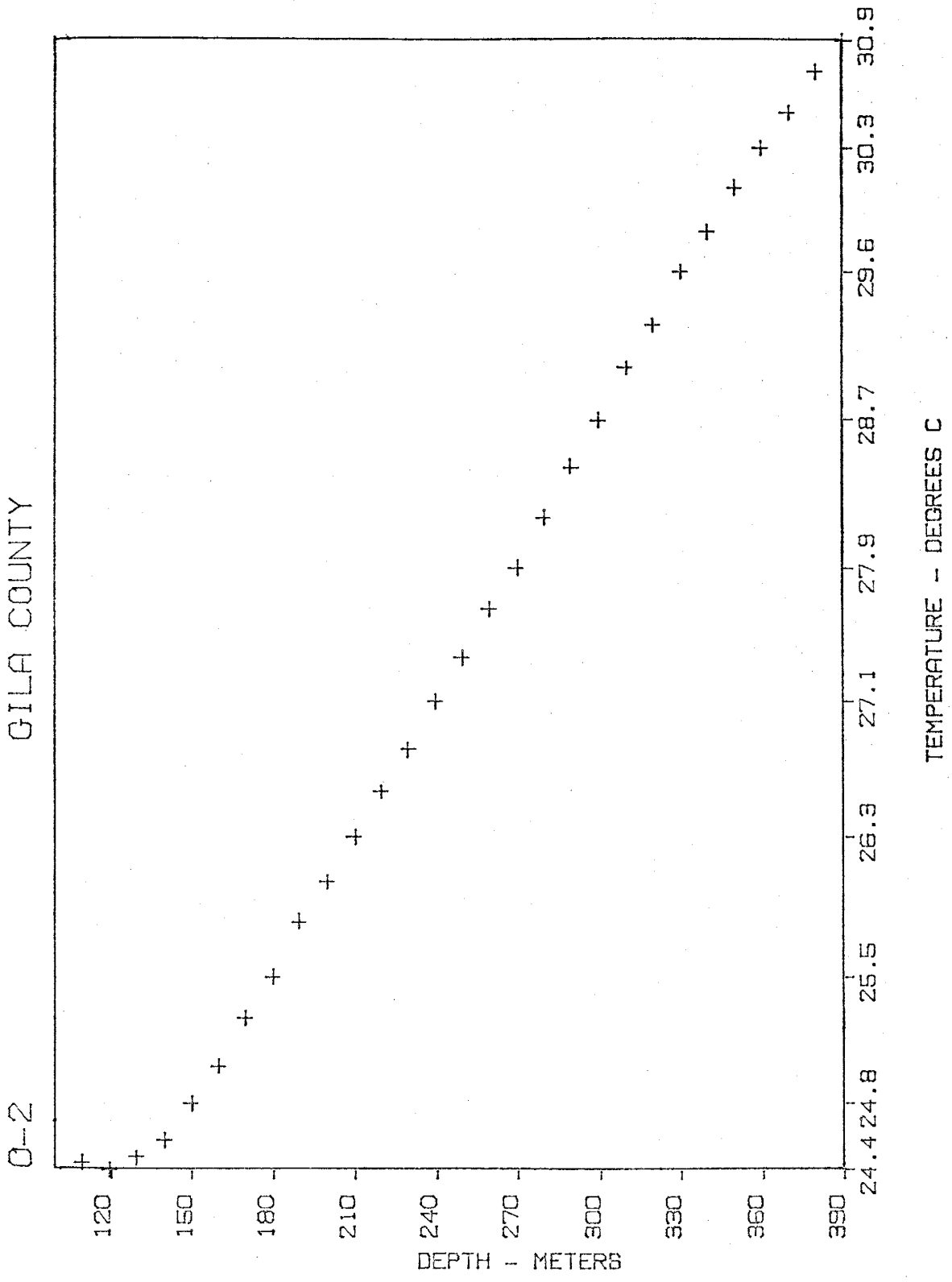
GILA COUNTY
0-2
DEPTH - METERS
120
150
180
210
240
270
300
330
360
390
TEMPERATURE - DEGREES C
24.4
24.8
25.5
26.3
27.1
27.9
28.7
29.6
30.3
30.9

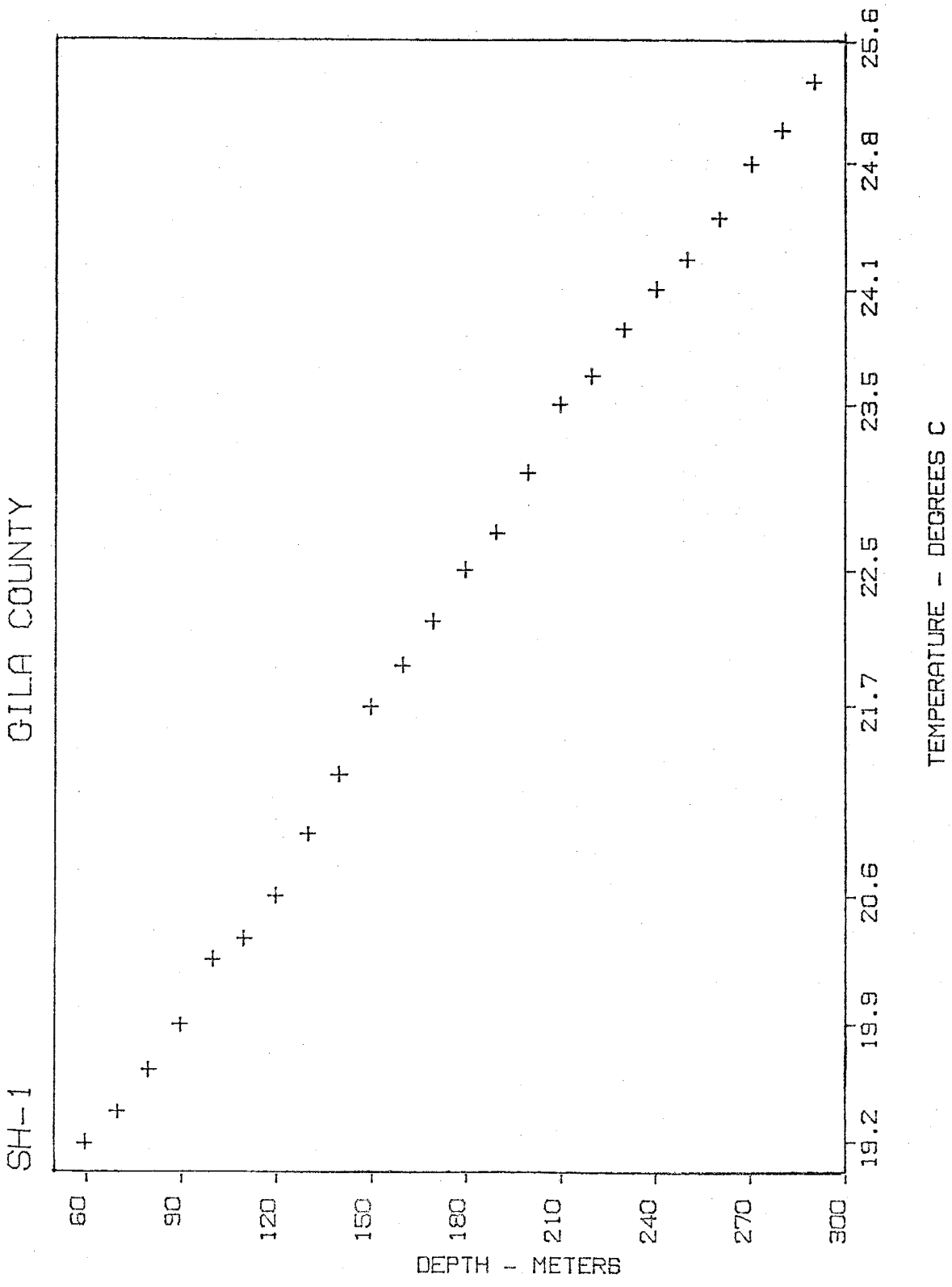
SH-1
GILA COUNTY
DEPTH - METERS
60
90
120
150
180
210
240
270
300
19.2
19.9
20.6
21.7
22.5
23.5
24.1
24.8
25.6
TEMPERATURE - DEGREES C

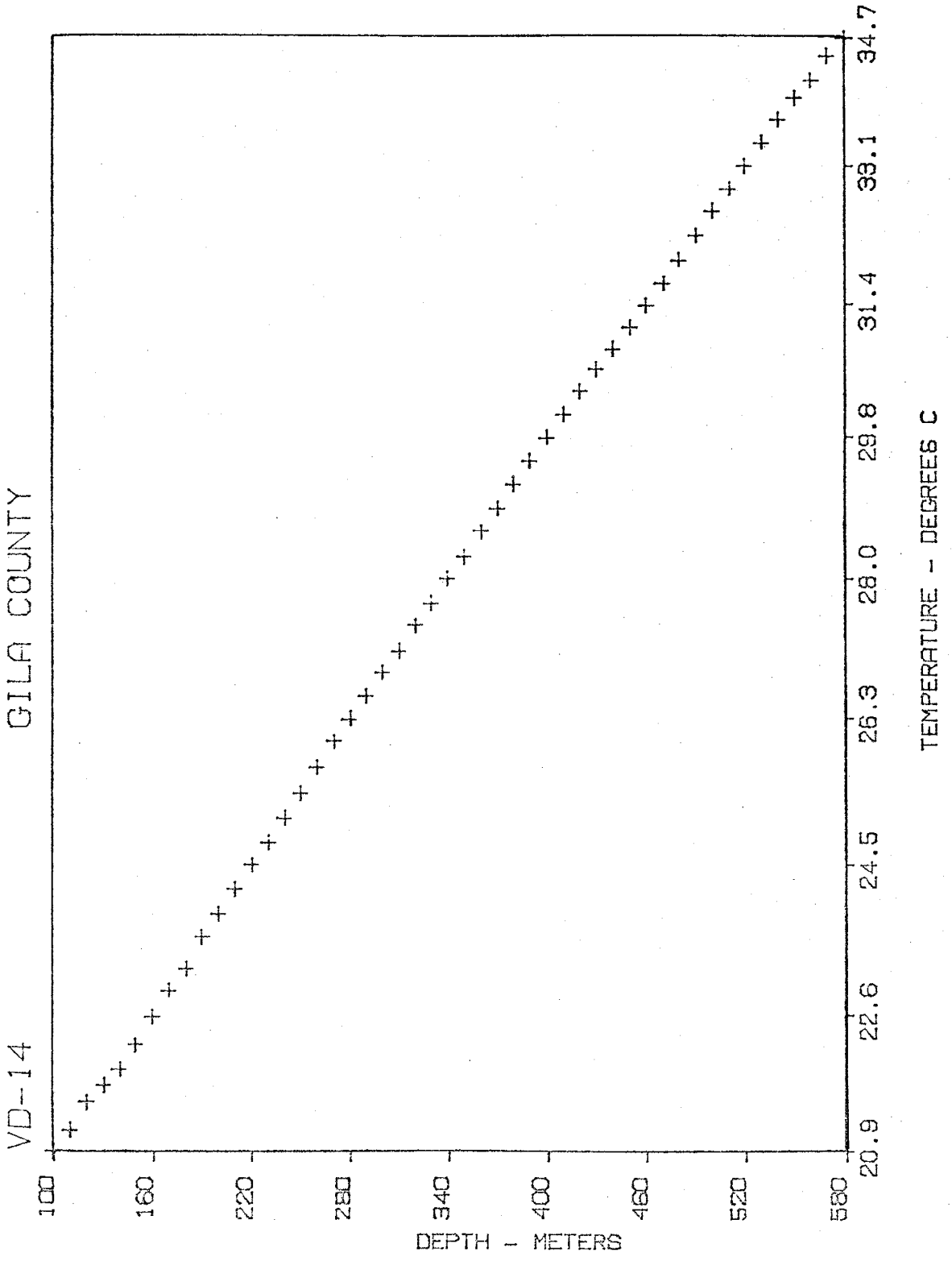
GILA COUNTY
VD-14
100
160
220
280
340
400
460
520
580
DEPTH - METERS
20.9
22.6
24.5
26.3
28.0
29.8
31.4
33.1
34.7
TEMPERATURE - DEGREES C

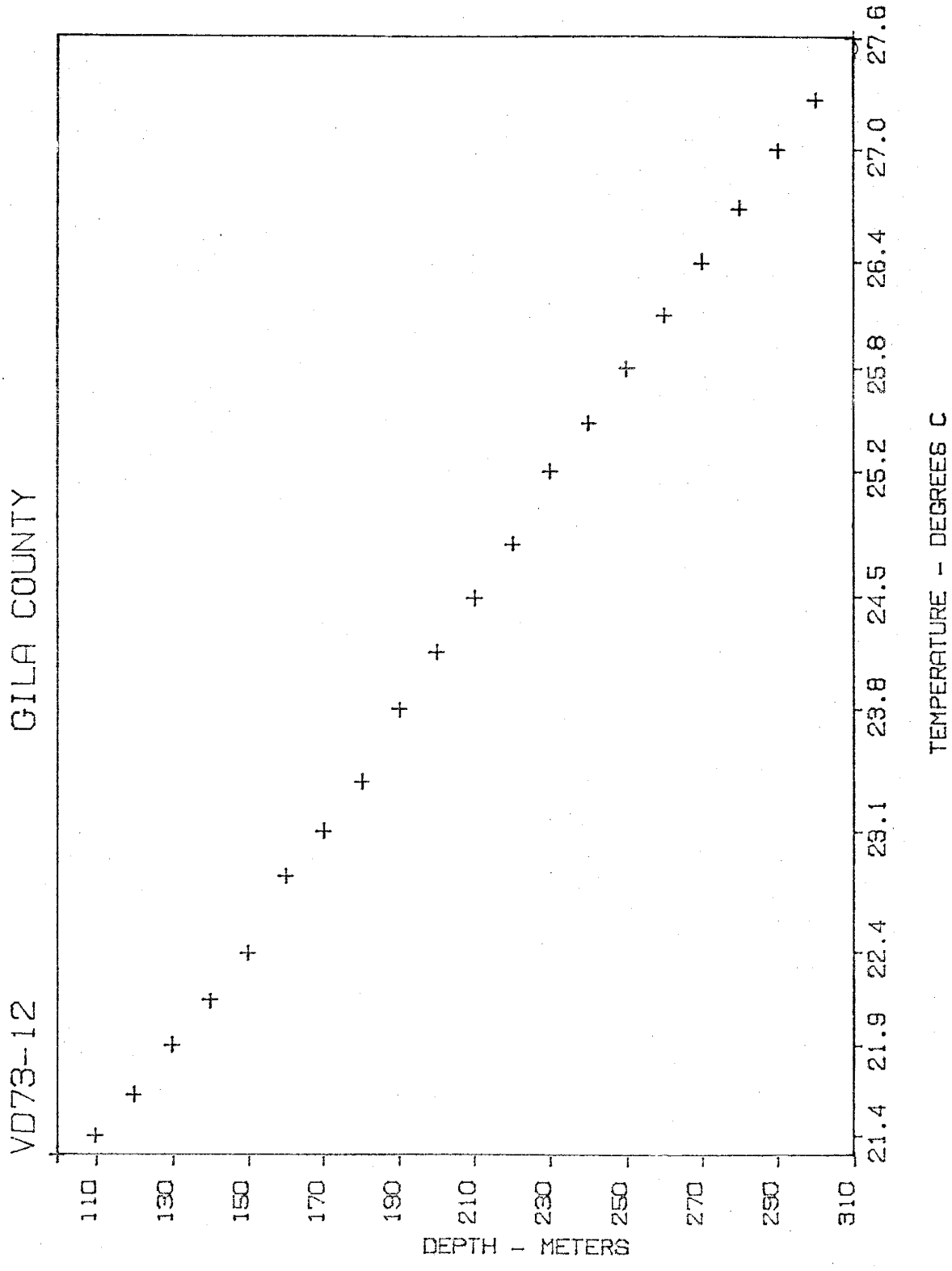
VD73-12
GILA COUNTY
DEPTH - METERS
110
130
150
170
190
210
230
250
270
290
310
TEMPERATURE - DEGREES C
21.4
21.9
22.4
23.1
23.8
24.5
25.2
25.8
26.4
27.0
27.6

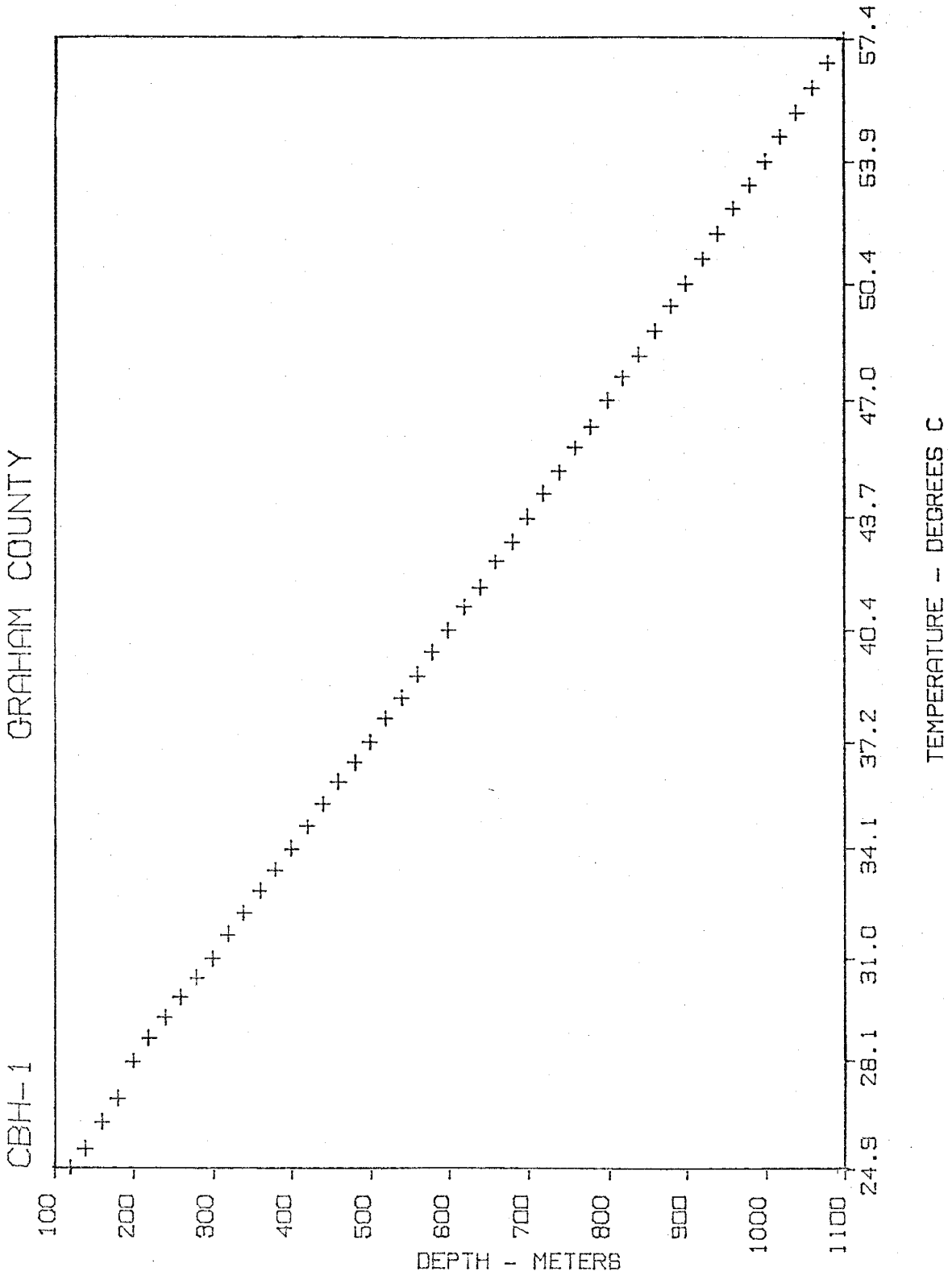
CBH-1
GRAHAM COUNTY
DEPTH - METERS
100
200
300
400
500
600
700
800
900
1000
1100
24.9
28.1
31.0
34.1
37.2
40.4
43.7
47.0
50.4
53.9
57.4
TEMPERATURE - DEGREES C

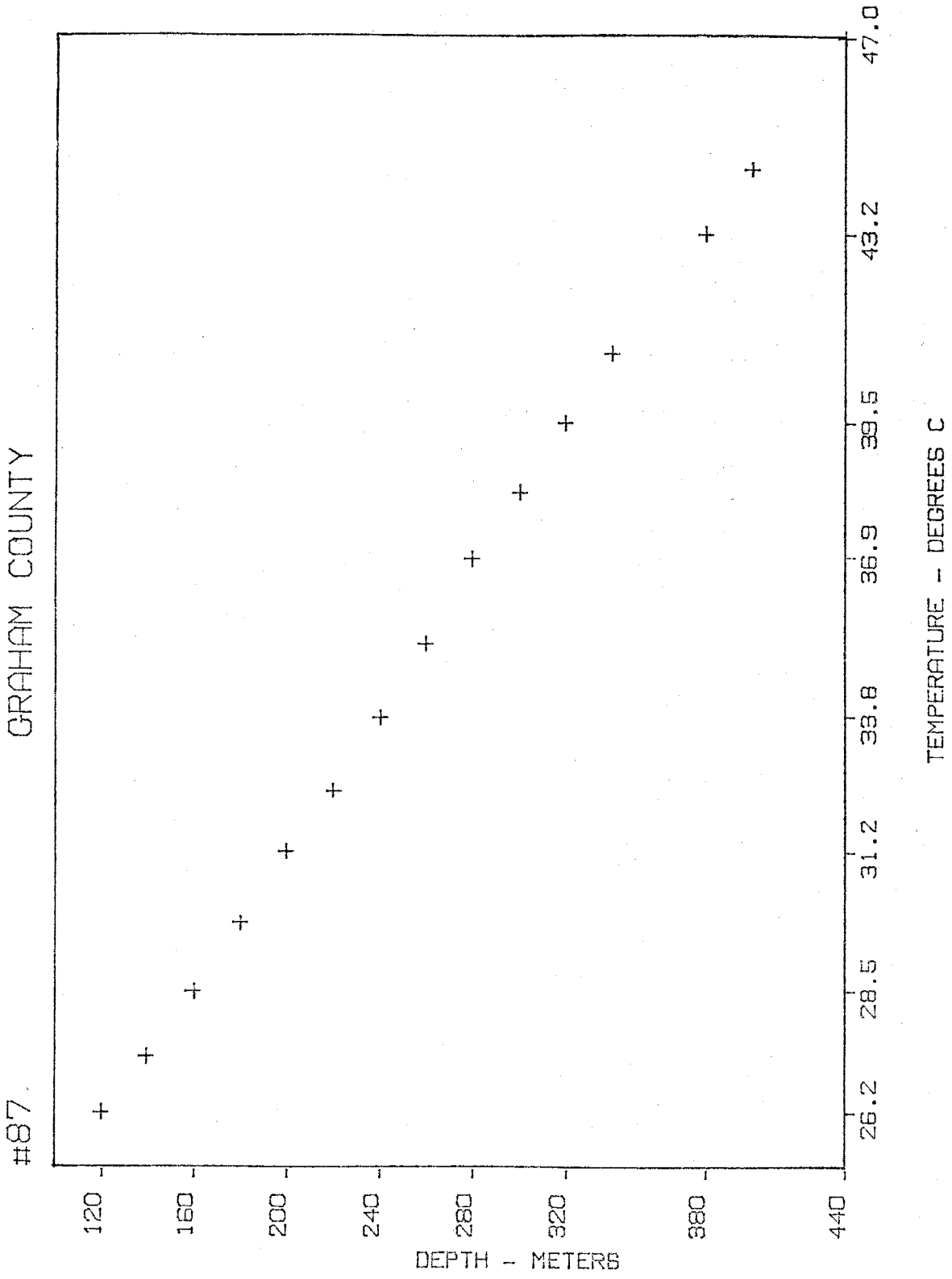
#87
GRAHAM COUNTY
120
160
200
240
280
320
380
440
DEPTH - METERS
26.2
28.5
31.2
33.8
36.9
39.5
43.2
47.0
TEMPERATURE - DEGREES C

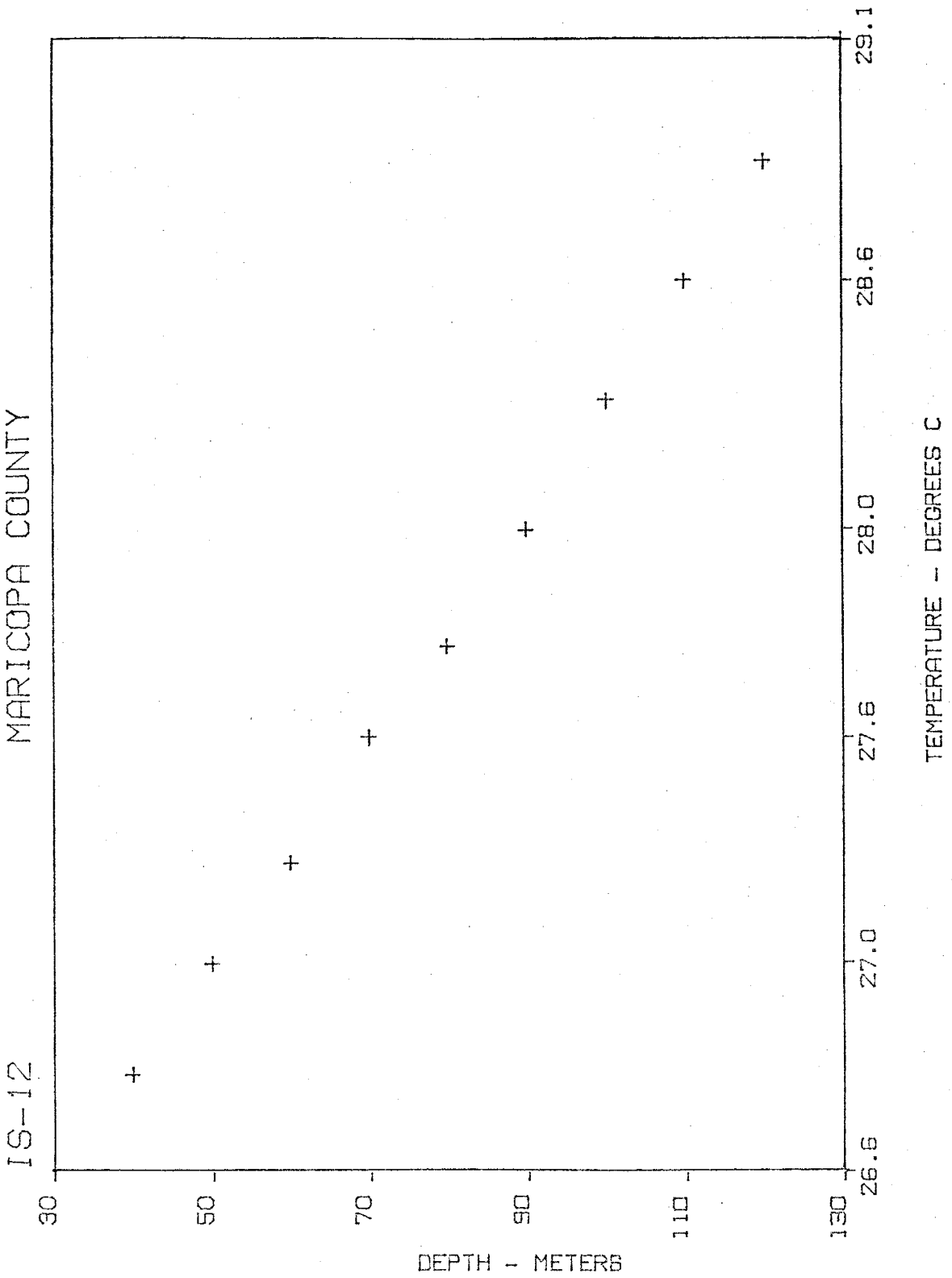
MARICOPA COUNTY
IS-12
30
50
70
90
110
130
DEPTH - METERS
26.6
27.0
27.6
28.0
28.6
29.1
TEMPERATURE - DEGREES C

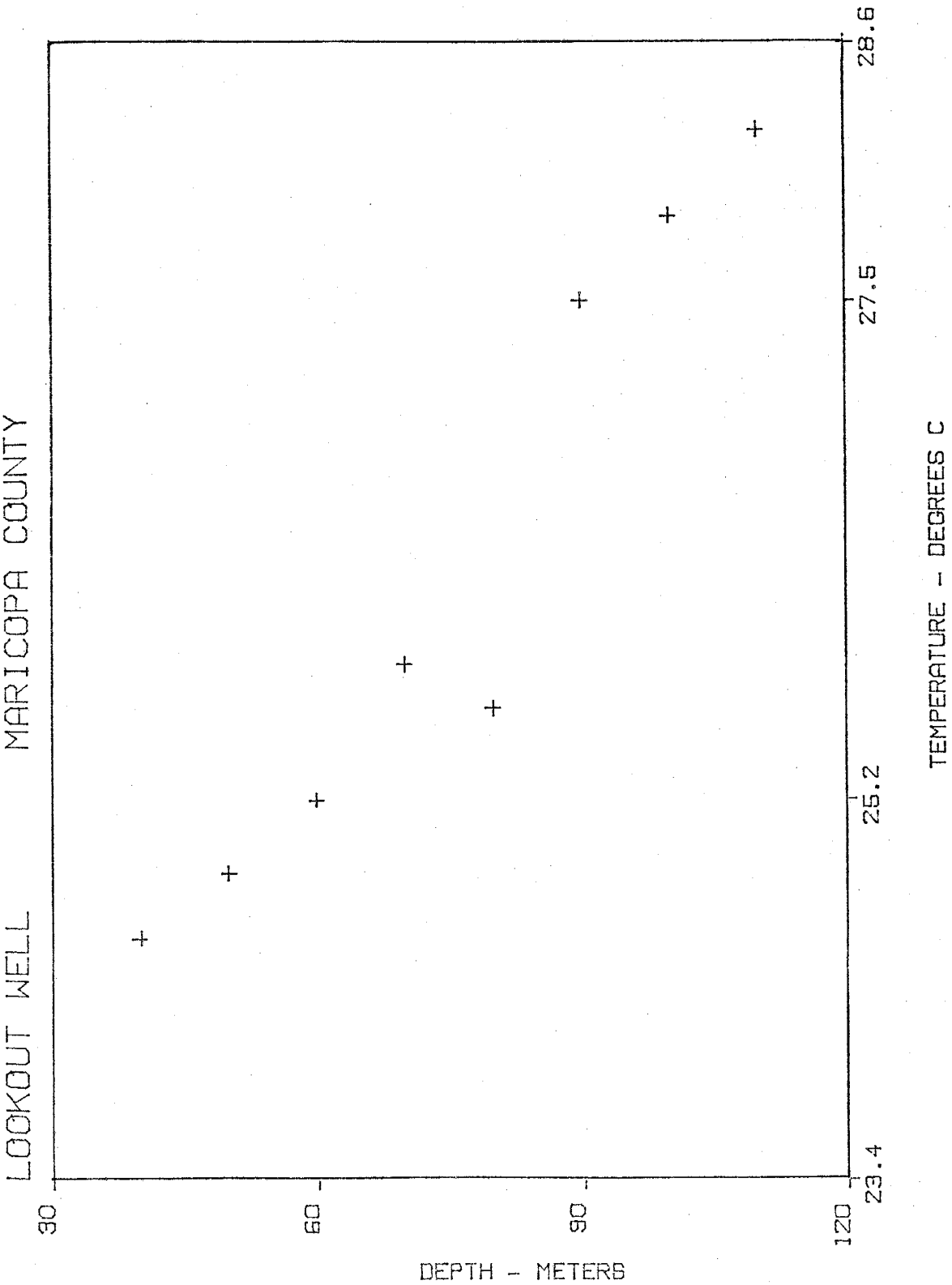
LOOKOUT WELL
MARICOPA COUNTY
30
60
90
120
DEPTH - METERS
23.4
25.2
27.5
28.6
TEMPERATURE - DEGREES C

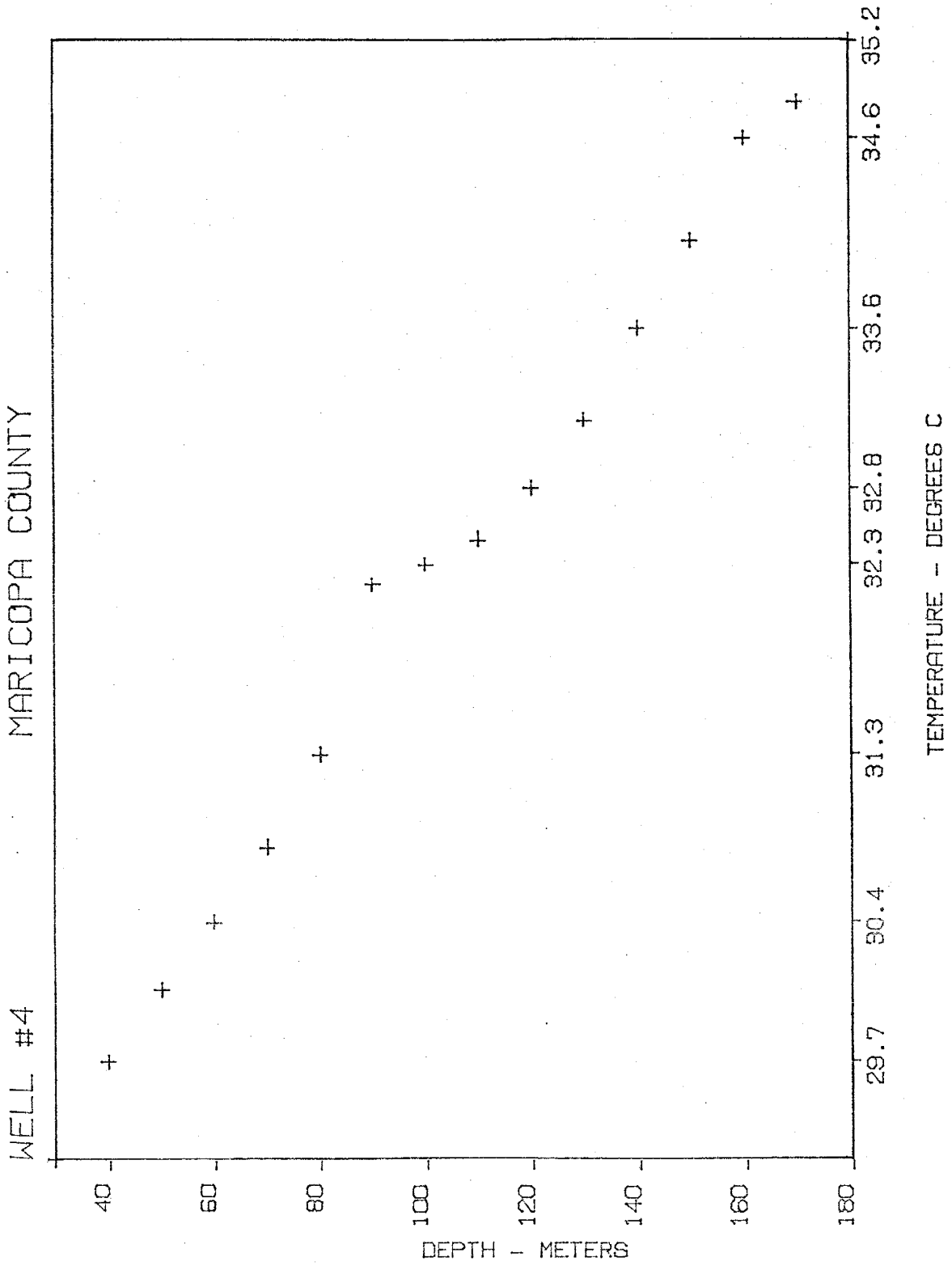
WELL #4
MARICOPA COUNTY
DEPTH - METERS
40
60
80
100
120
140
160
180
TEMPERATURE - DEGREES C
29.7
30.4
31.3
32.3
32.8
33.6
34.6
35.2

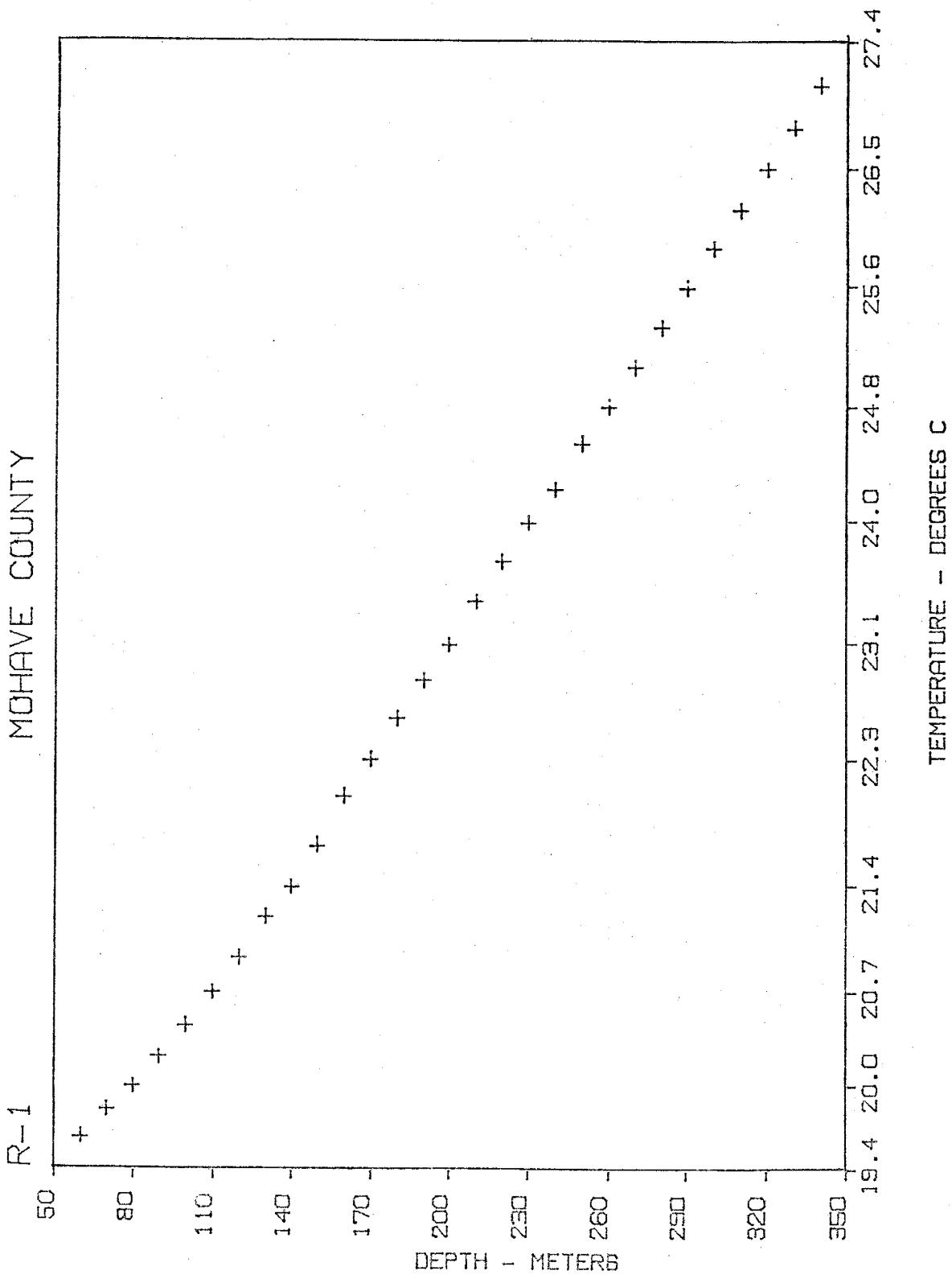
MOHAVE COUNTY
R-1
DEPTH - METERS
50
80
110
140
170
200
230
260
290
320
350
19.4
20.0
20.7
21.4
22.3
23.1
24.0
24.8
25.6
26.5
27.4
TEMPERATURE - DEGREES C

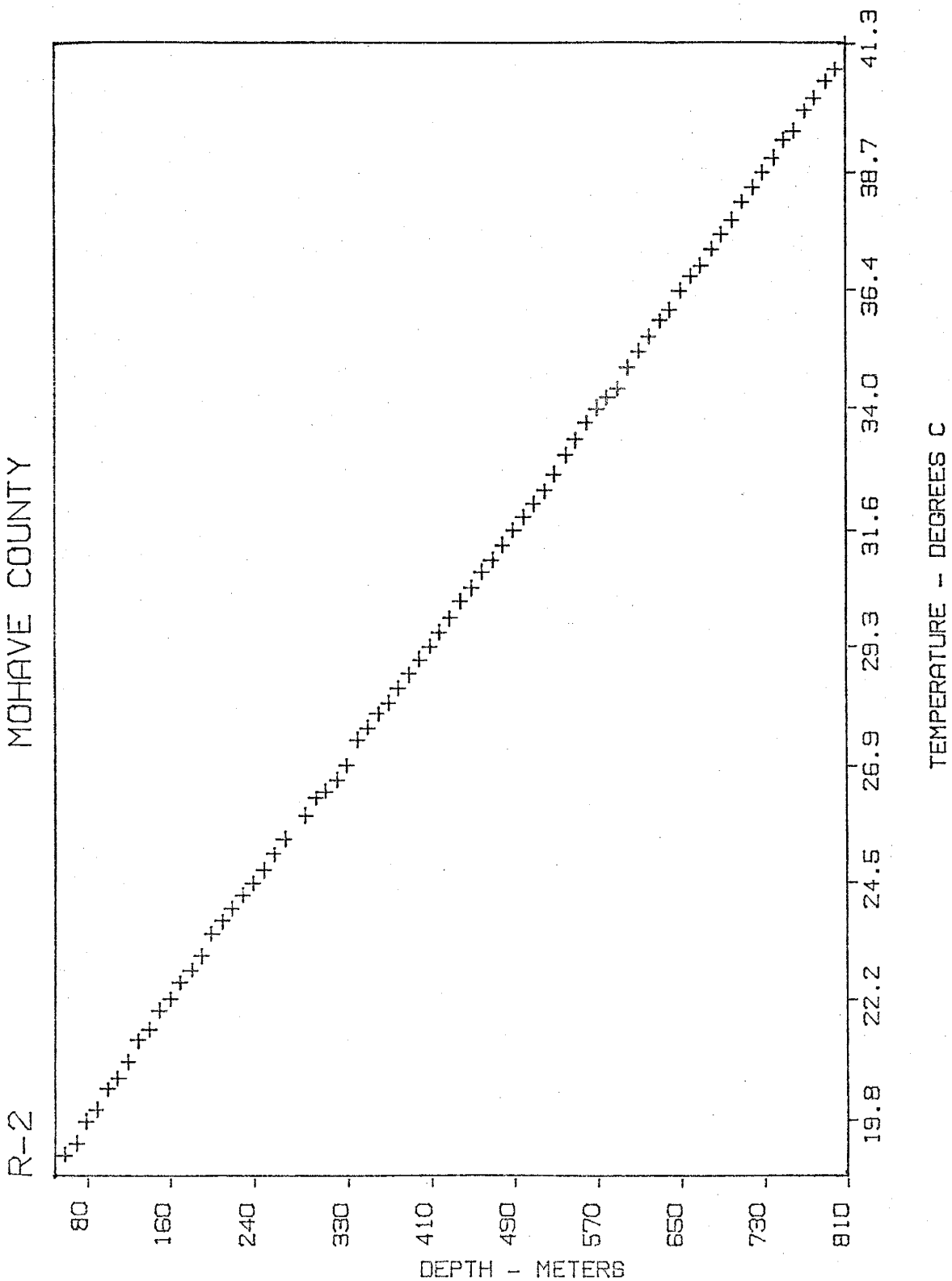
R-2
MOHAVE COUNTY
80
160
240
330
410
490
570
650
730
810
DEPTH - METERS
19.8
22.2
24.5
26.9
29.3
31.6
34.0
36.4
38.7
41.3
TEMPERATURE - DEGREES C

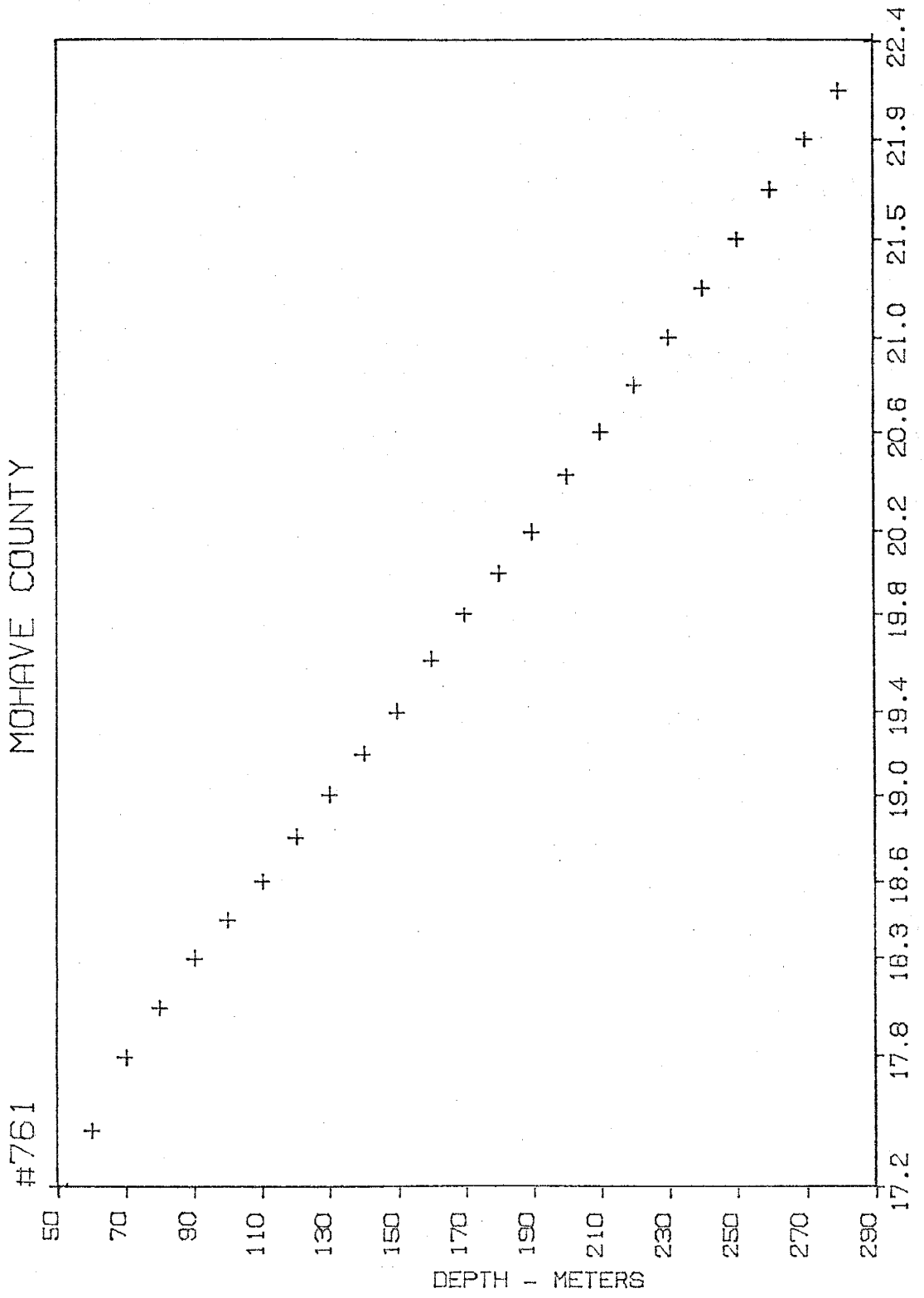
#761
MOHAVE COUNTY
DEPTH - METERS
50
70
90
110
130
150
170
190
210
230
250
270
290
TEMPERATURE - DEGREES C
17.2
17.8
18.3
18.6
19.0
19.4
19.8
20.2
20.6
21.0
21.5
21.9
22.4

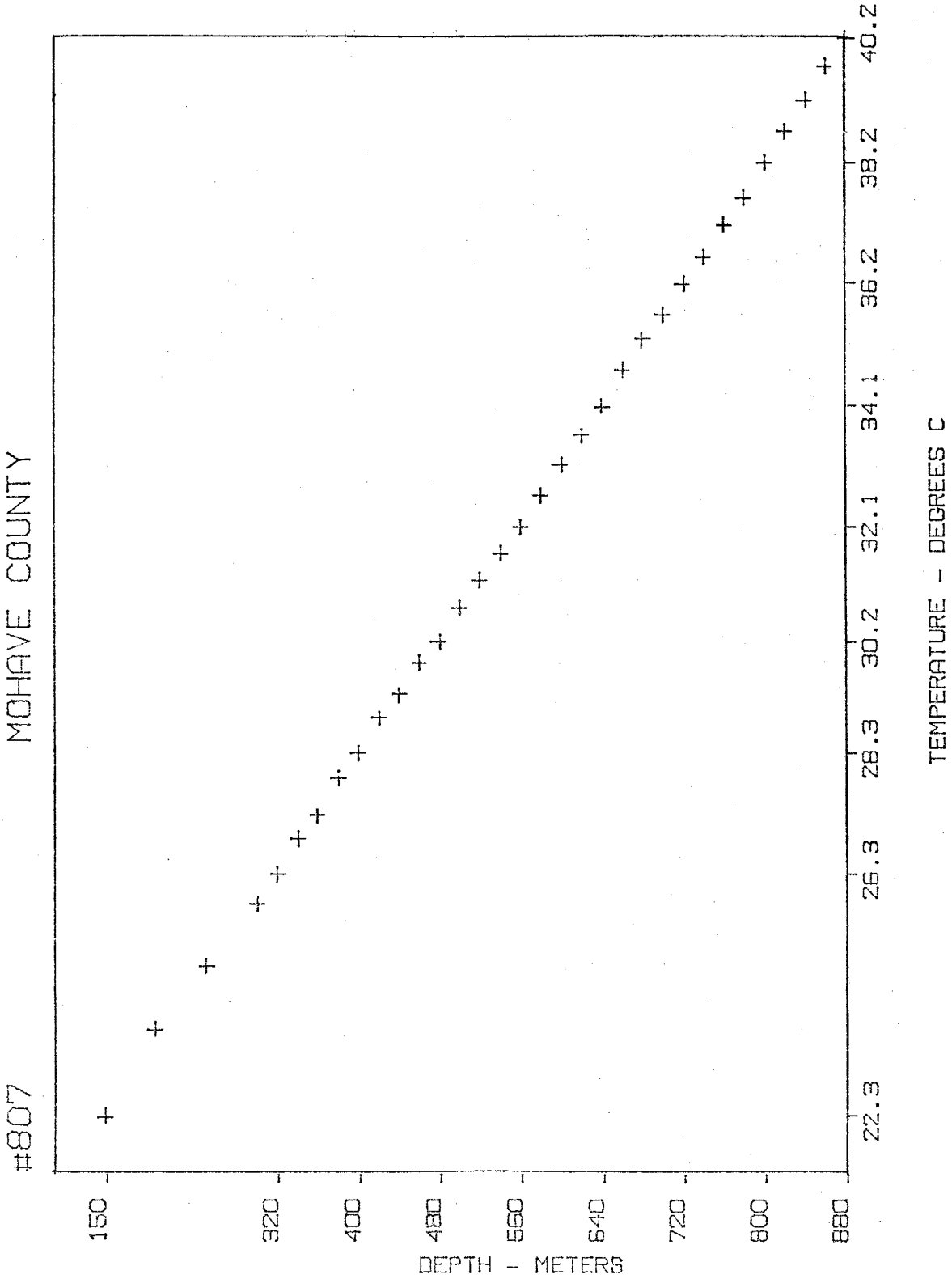
#807
MOHAVE COUNTY
150
320
400
480
560
640
720
800
880
DEPTH - METERS
22.3
26.3
28.3
30.2
32.1
34.1
36.2
38.2
40.2
TEMPERATURE - DEGREES C

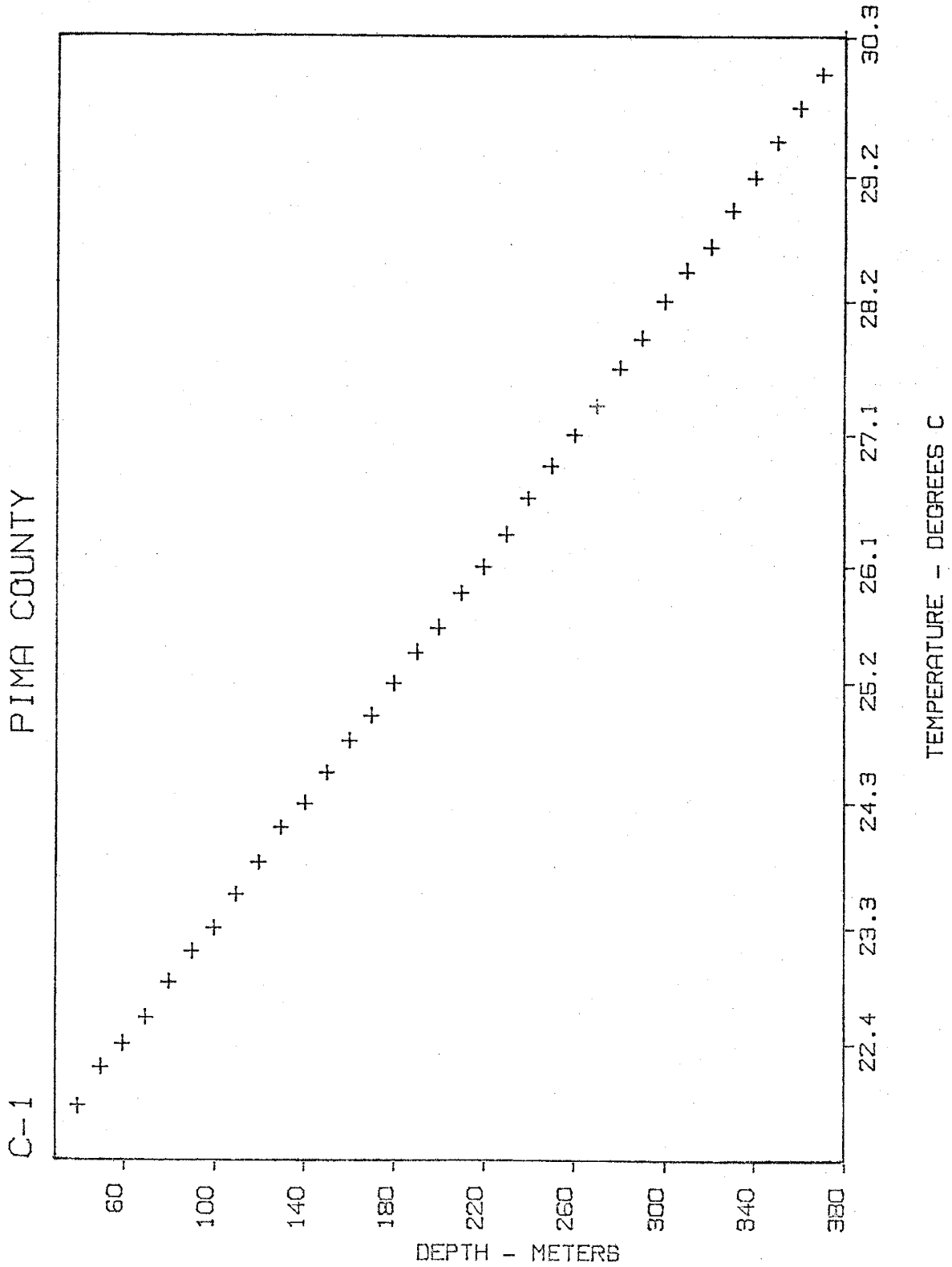
C-1
PIMA COUNTY
DEPTH - METERS
60
100
140
180
220
260
300
340
380
TEMPERATURE - DEGREES C
22.4
23.3
24.3
25.2
26.1
27.1
28.2
29.2
30.3

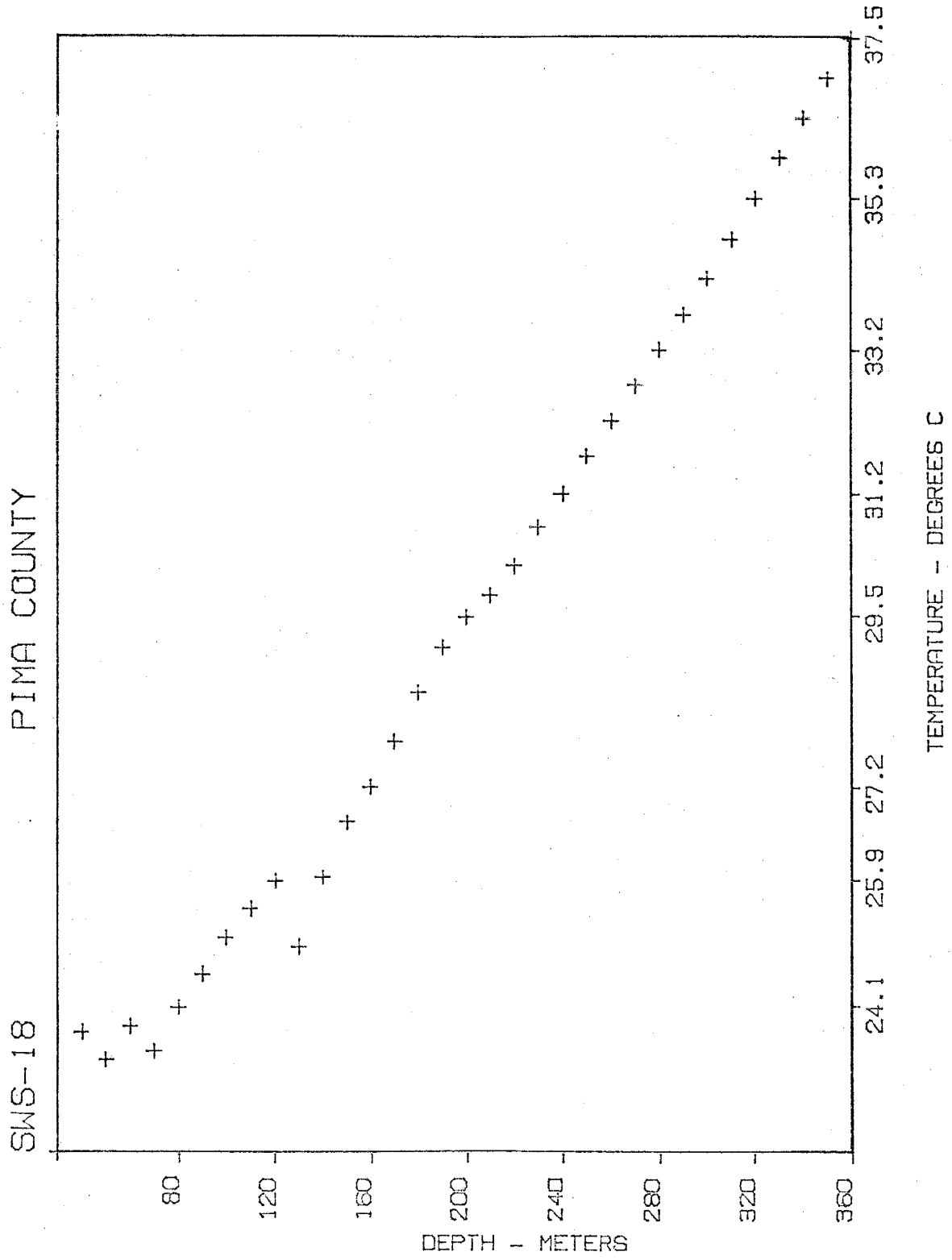
SWS-18
PIMA COUNTY
DEPTH - METERS
80
120
160
200
240
280
320
360
TEMPERATURE - DEGREES C
24.1
25.9
27.2
29.5
31.2
33.2
35.3
37.5

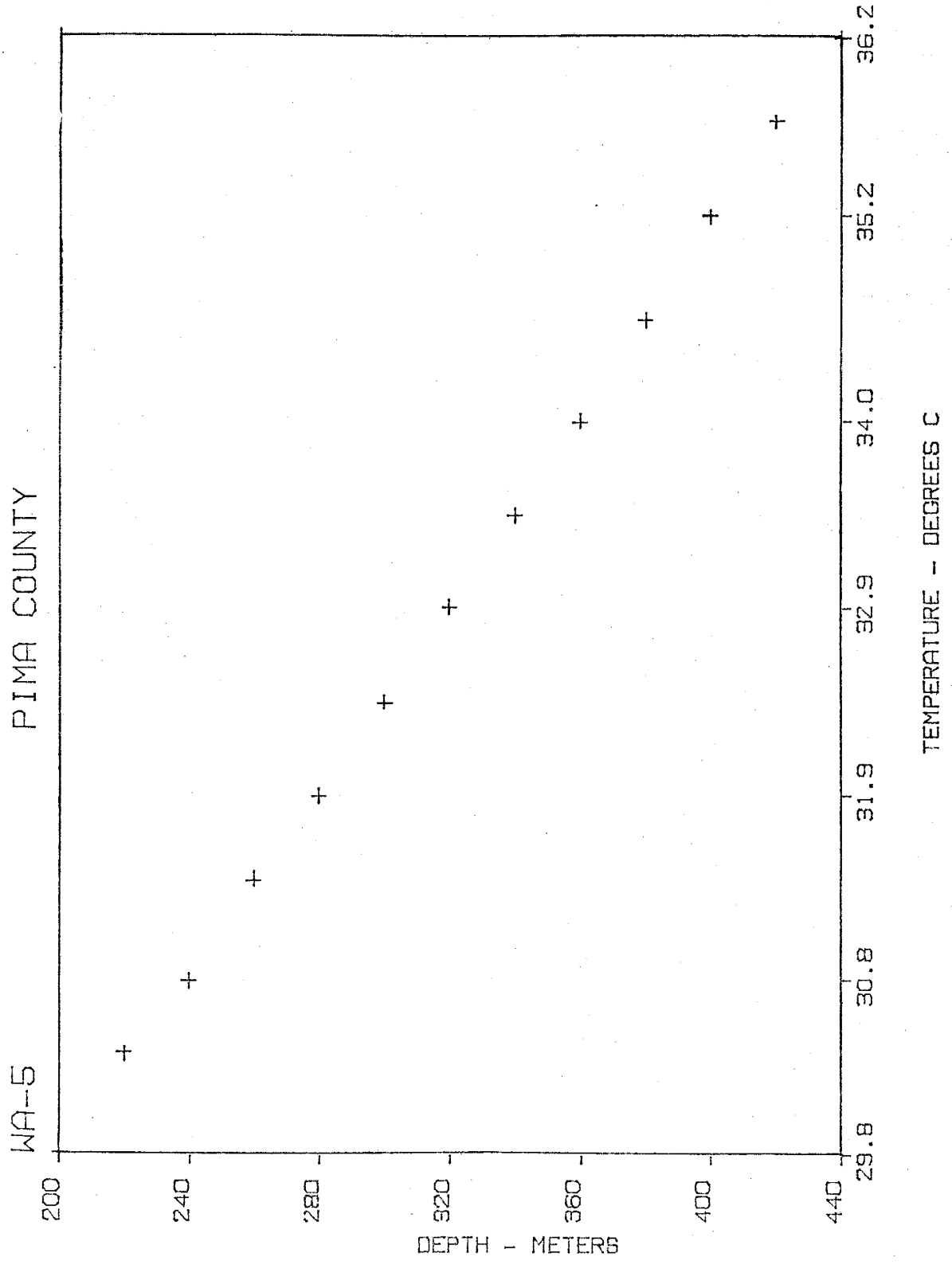
WA-5
PIMA COUNTY
200
240
280
320
360
400
440
DEPTH - METERS
29.8
30.8
31.9
32.9
34.0
35.2
36.2
TEMPERATURE - DEGREES C

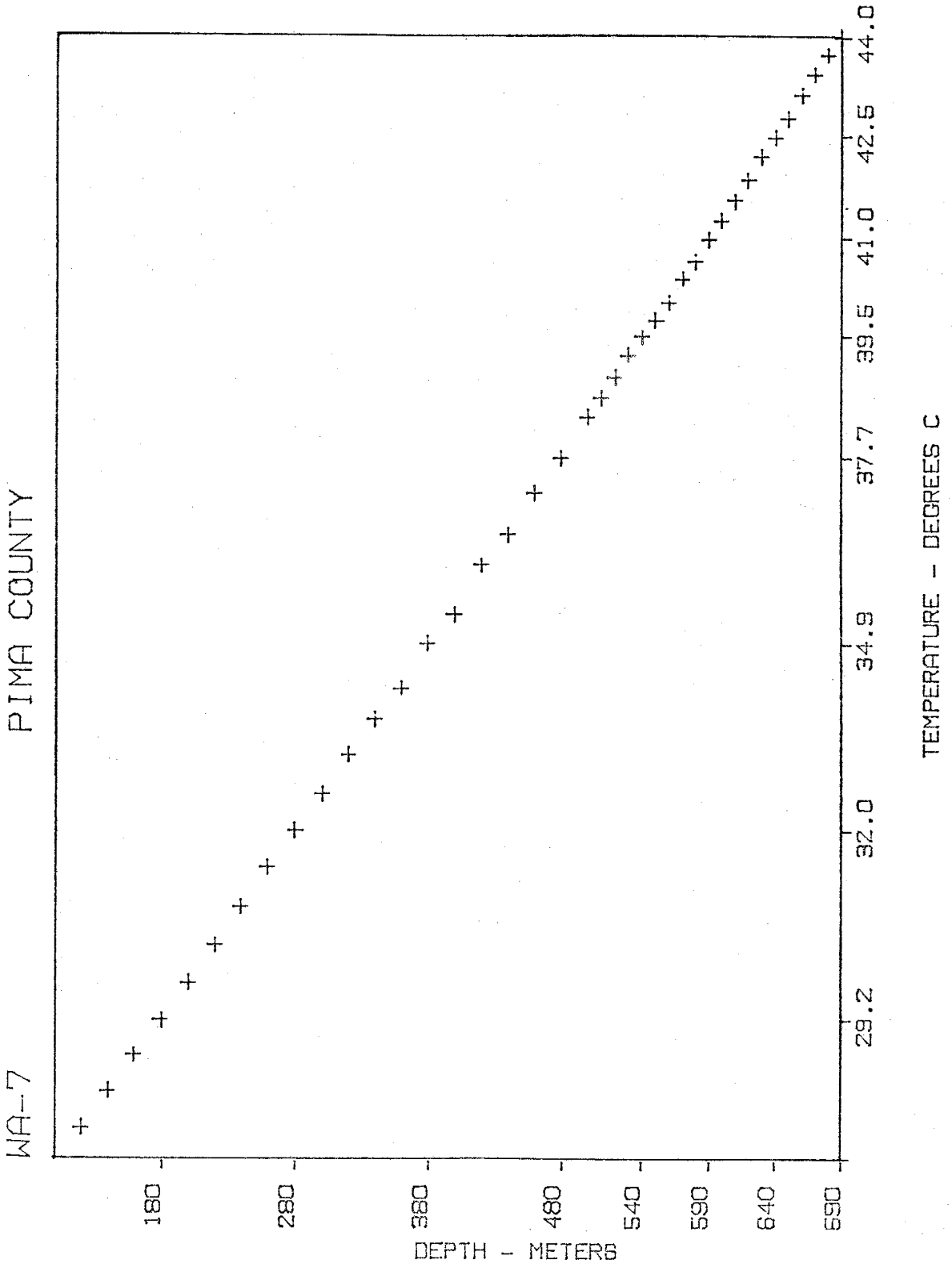
WA-7
PIMA COUNTY
DEPTH - METERS
180
280
380
480
540
590
640
690
29.2
32.0
34.9
37.7
39.5
41.0
42.5
44.0
TEMPERATURE - DEGREES C

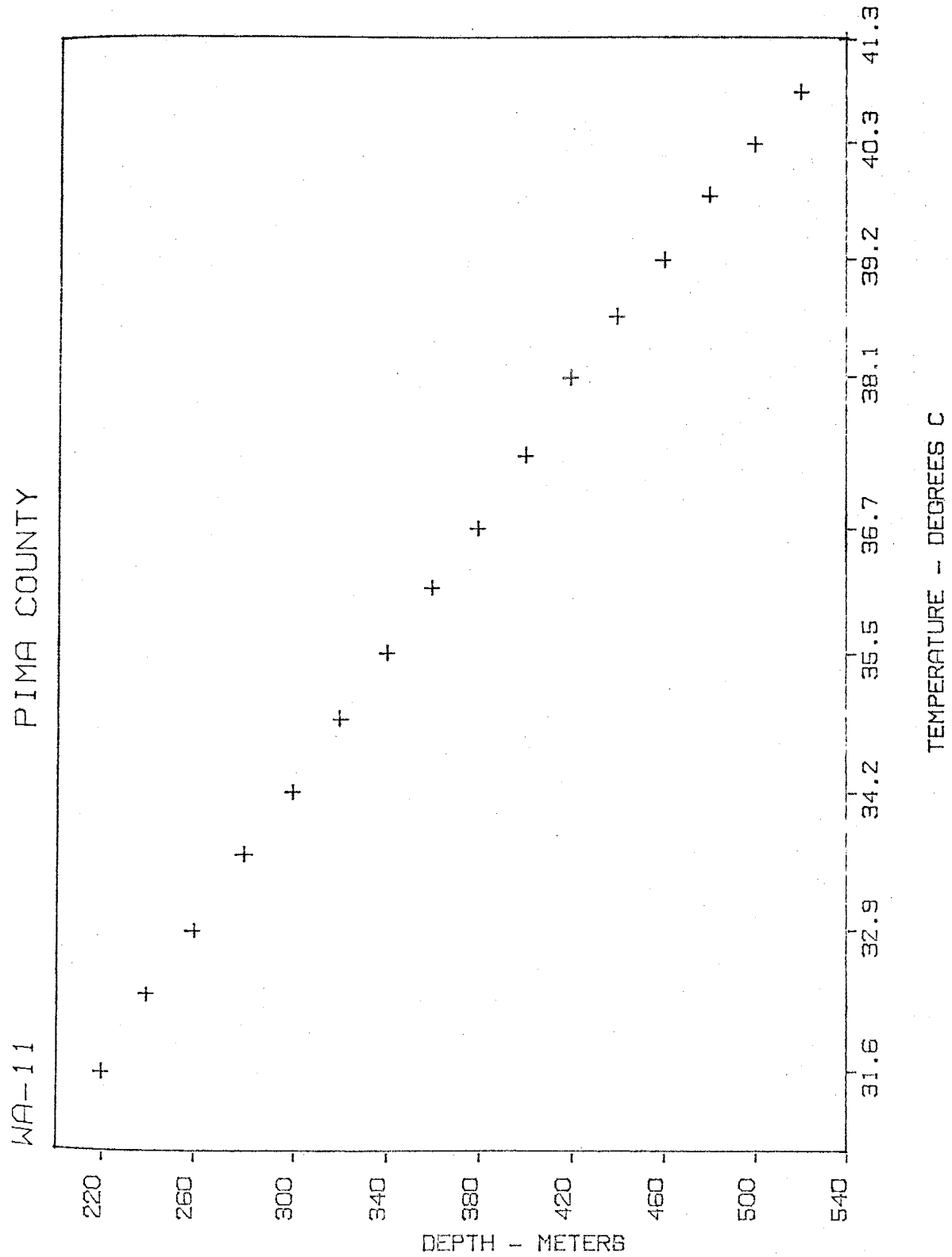
PIMA COUNTY
WA-11
DEPTH - METERS
220
260
300
340
380
420
460
500
540
TEMPERATURE - DEGREES C
31.6
32.9
34.2
35.5
36.7
38.1
39.2
40.3
41.3

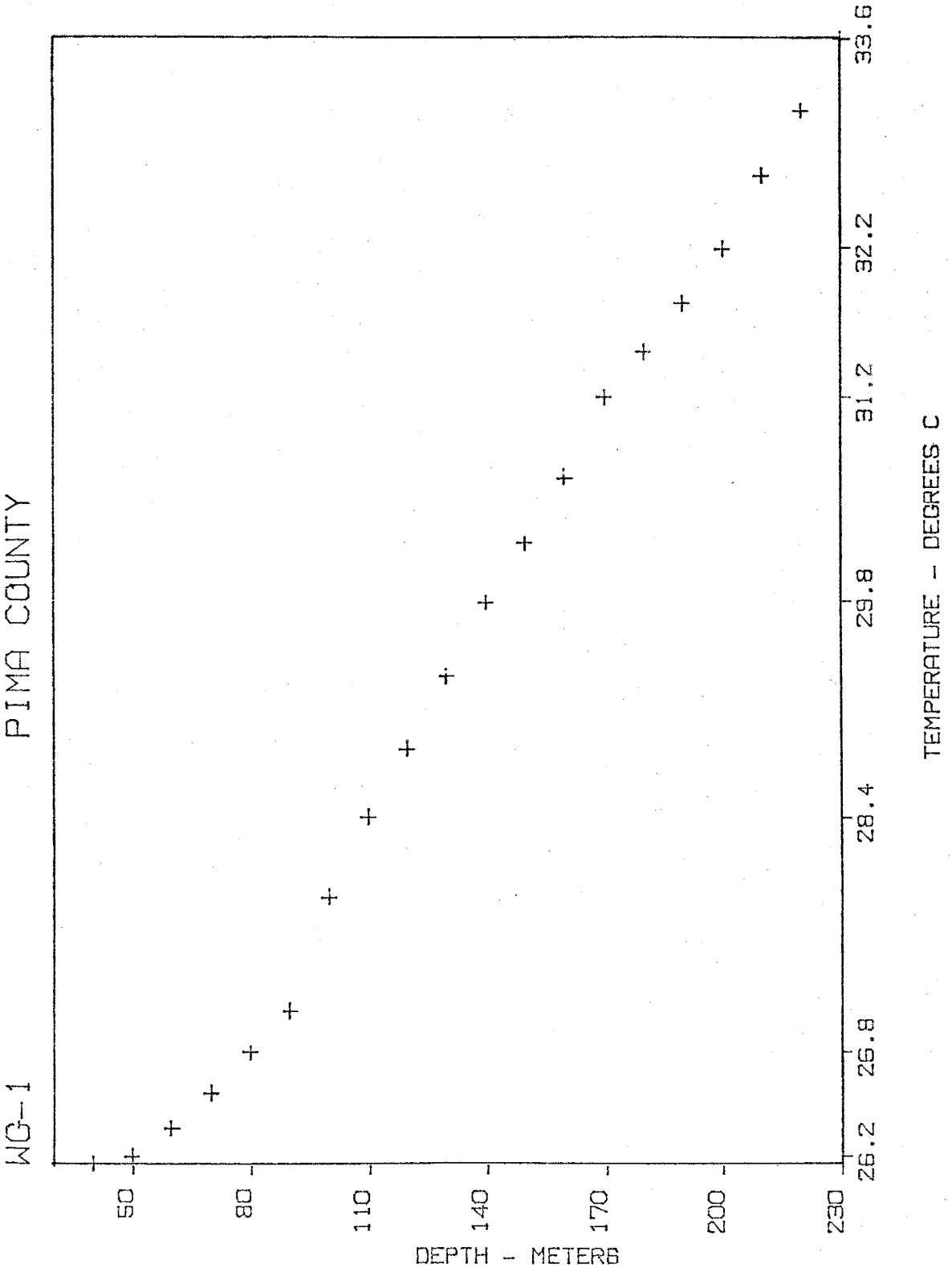
WG-1
PIMA COUNTY
DEPTH - METERS
50
80
110
140
170
200
230
26.2
26.8
28.4
29.8
31.2
32.2
33.6
TEMPERATURE - DEGREES C

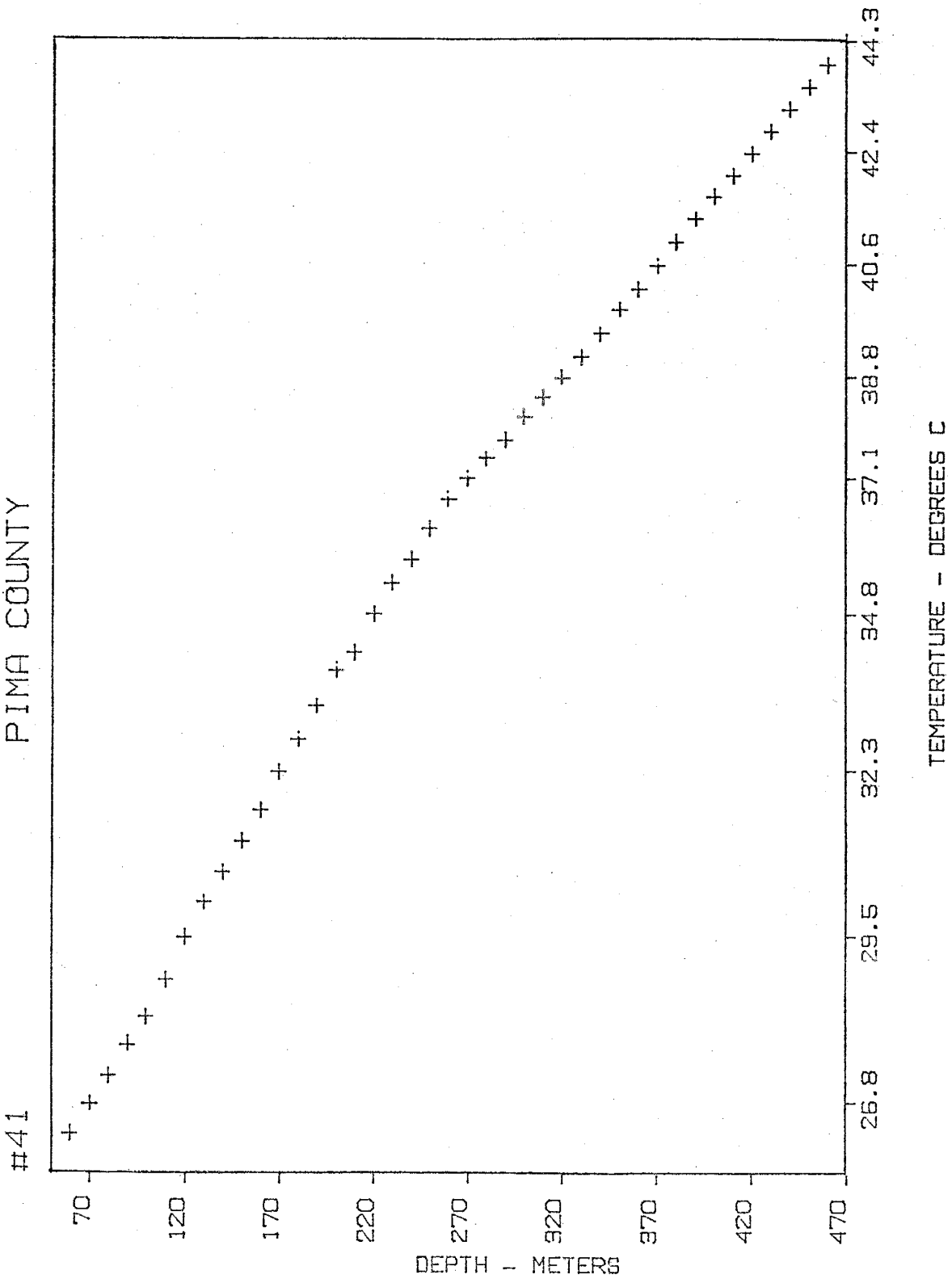
PIMA COUNTY
#41
DEPTH - METERS
70
120
170
220
270
320
370
420
470
TEMPERATURE - DEGREES C
26.8
29.5
32.3
34.8
37.1
38.8
40.6
42.4
44.3

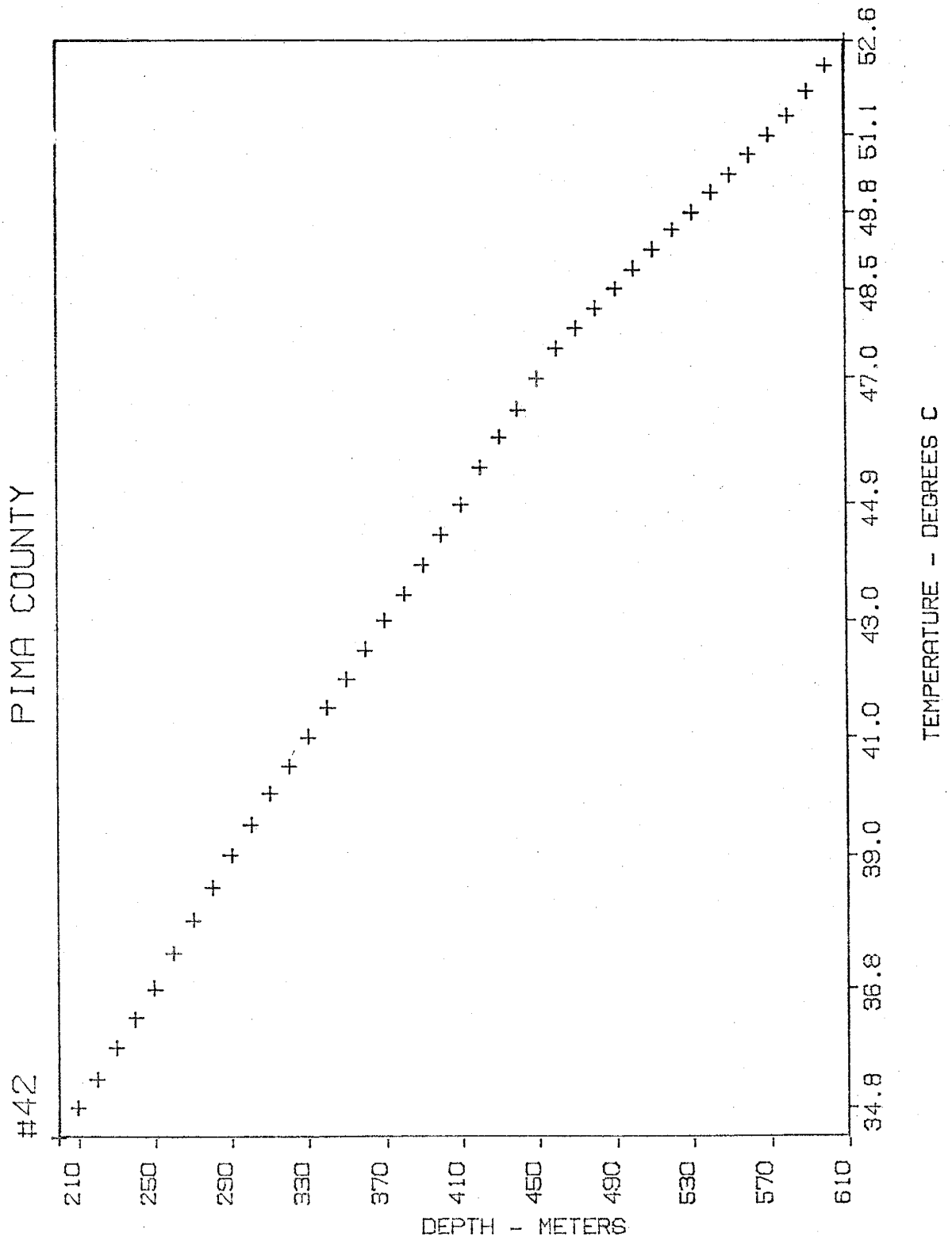
#42
PIMA COUNTY
DEPTH - METERS
210
250
290
330
370
410
450
490
530
570
610
TEMPERATURE - DEGREES C
34.8
36.8
39.0
41.0
43.0
44.9
47.0
48.5
49.8
51.1
52.6

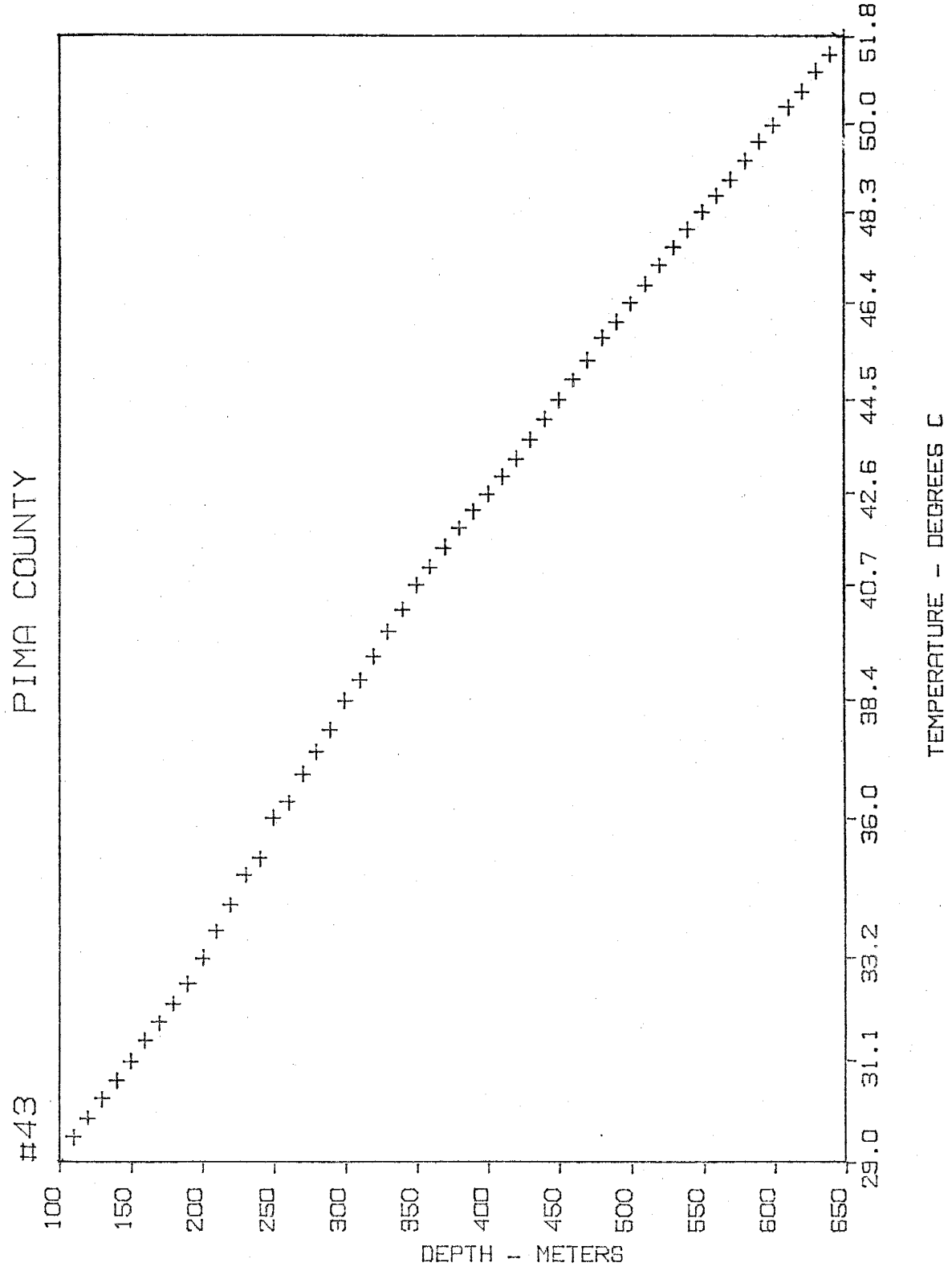
PIMA COUNTY
#43
DEPTH - METERS
100
150
200
250
300
350
400
450
500
550
600
650
29.0
31.1
33.2
36.0
38.4
40.7
42.6
44.5
46.4
48.3
50.0
51.8
TEMPERATURE - DEGREES C

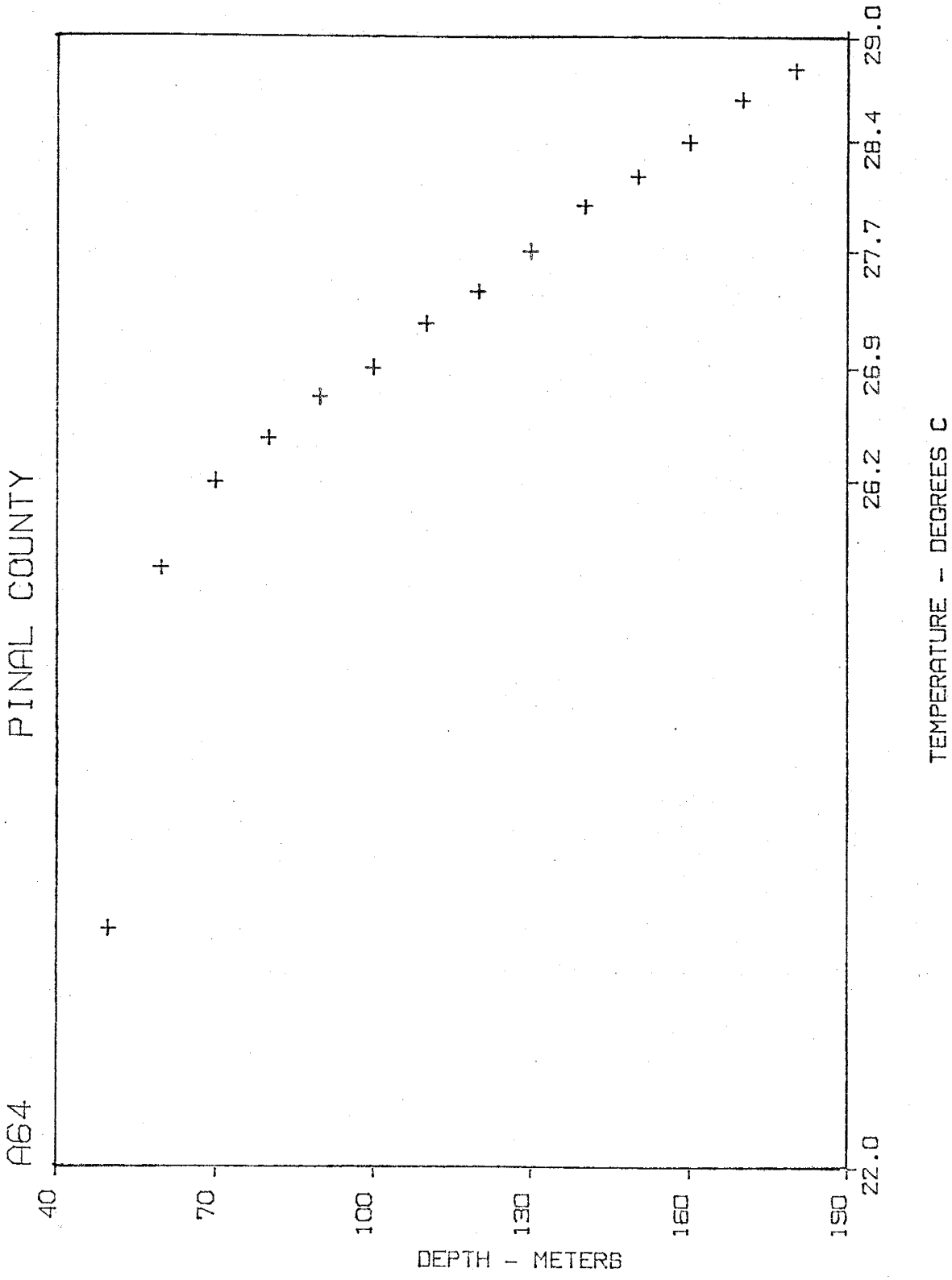
PINAL COUNTY
A64
40
70
100
130
160
190
DEPTH - METERS
22.0
26.2
26.9
27.7
28.4
29.0
TEMPERATURE - DEGREES C

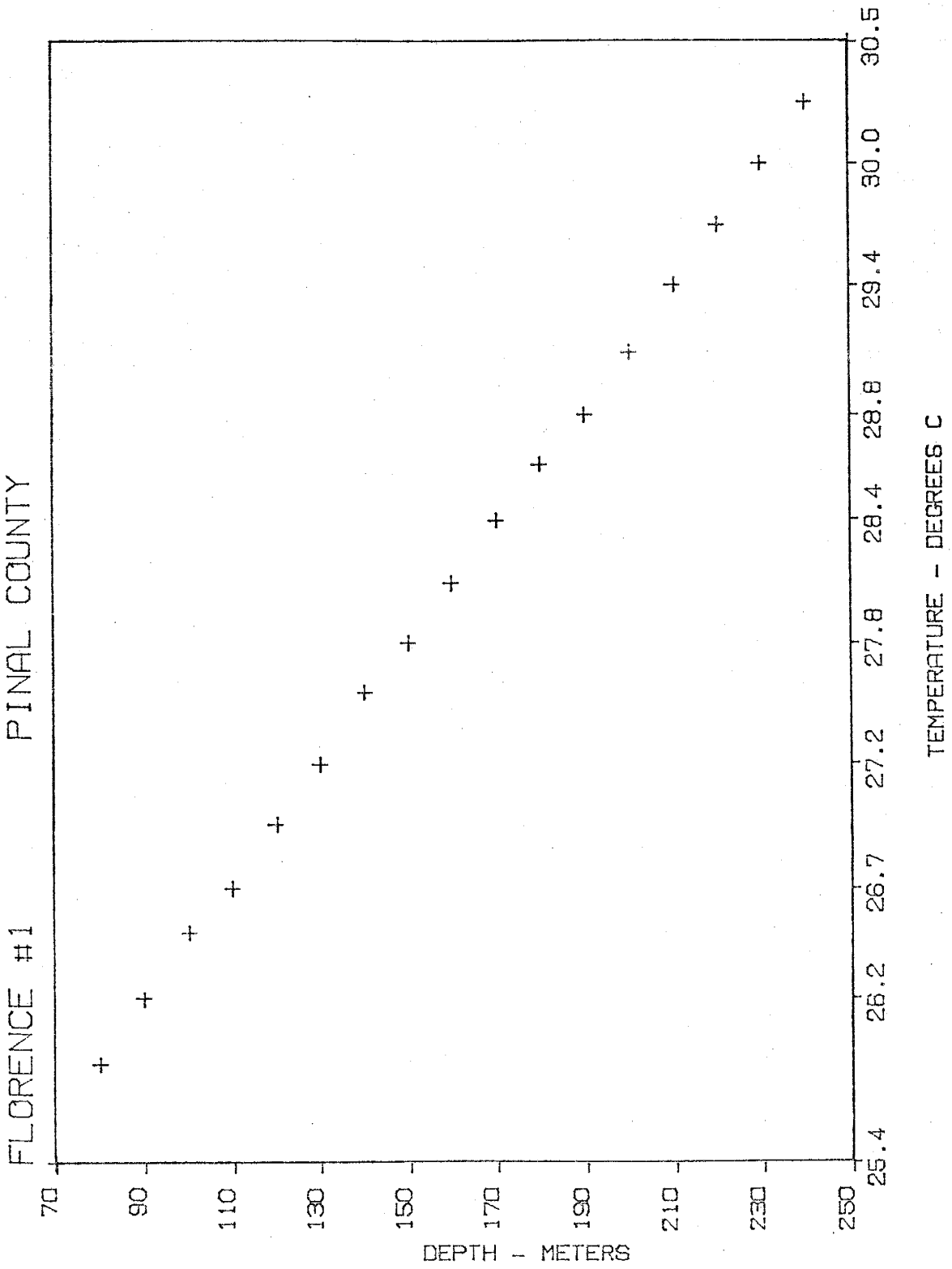
FLORENCE #1
PINAL COUNTY
DEPTH - METERS
70
90
110
130
150
170
190
210
230
250
TEMPERATURE - DEGREES C
25.4
26.2
26.7
27.2
27.8
28.4
28.8
29.4
30.0
30.5

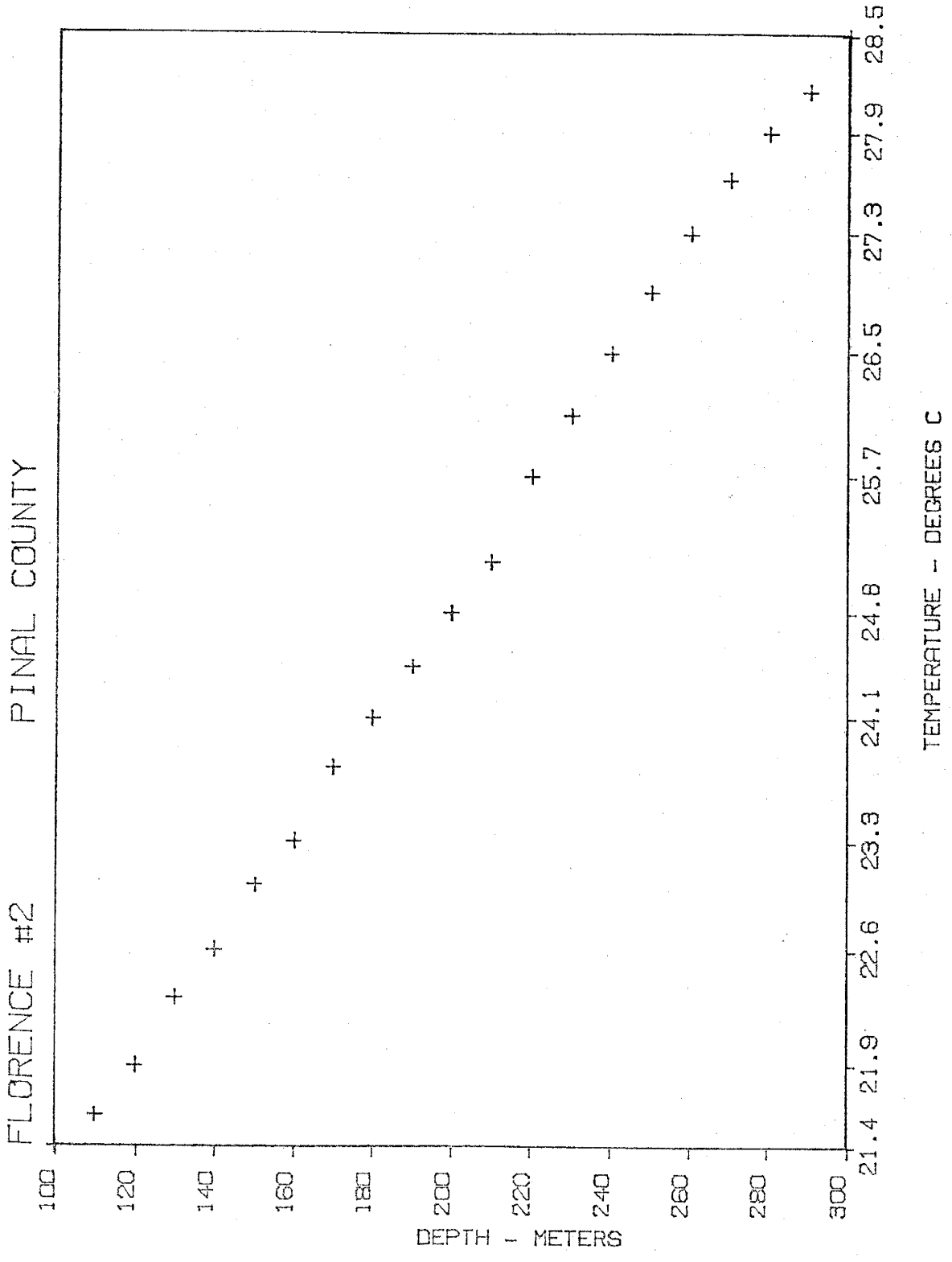
FLORENCE #2
PINAL COUNTY
DEPTH - METERS
100
120
140
160
180
200
220
240
260
280
300
TEMPERATURE - DEGREES C
21.4
21.9
22.6
23.3
24.1
24.8
25.7
26.5
27.3
27.9
28.5

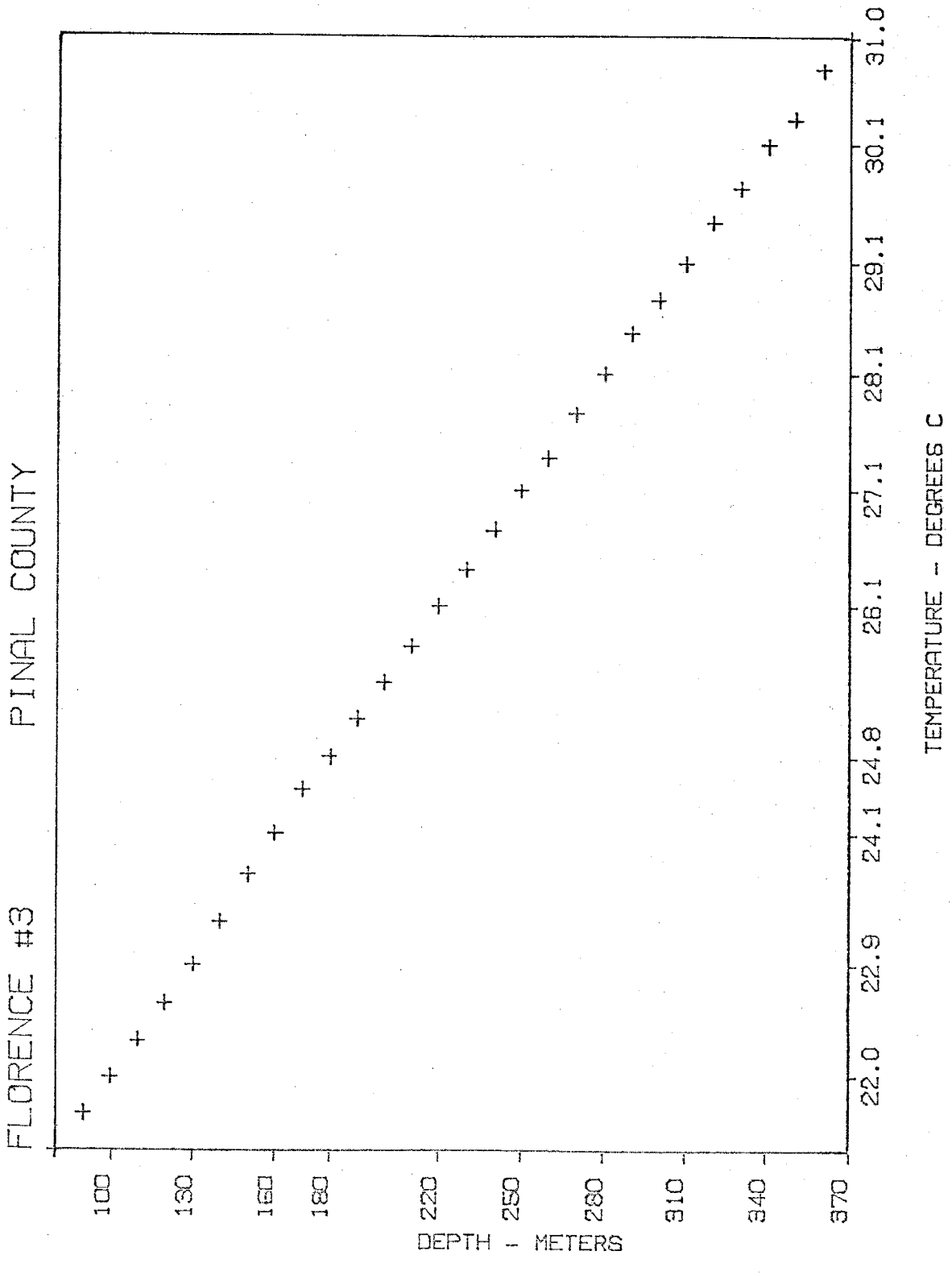
FLORENCE #3
PINAL COUNTY
DEPTH - METERS
100
130
160
190
220
250
280
310
340
370
TEMPERATURE - DEGREES C
22.0
22.9
24.1
24.8
26.1
27.1
28.1
29.1
30.1
31.0

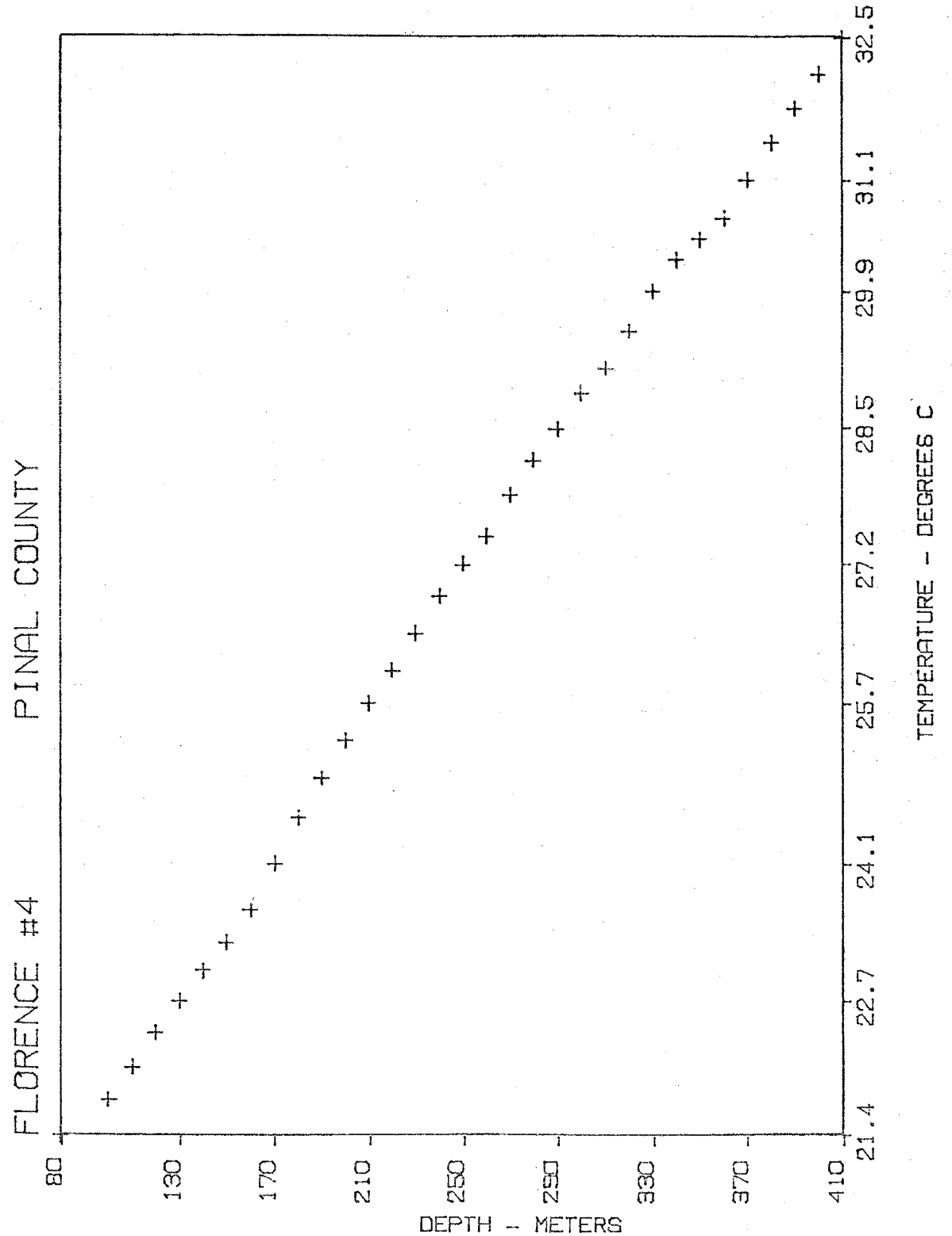
FLORENCE #4
PINAL COUNTY
80
130
170
210
250
290
330
370
410
DEPTH - METERS
21.4
22.7
24.1
25.7
27.2
28.5
29.9
31.1
32.5
TEMPERATURE - DEGREES C

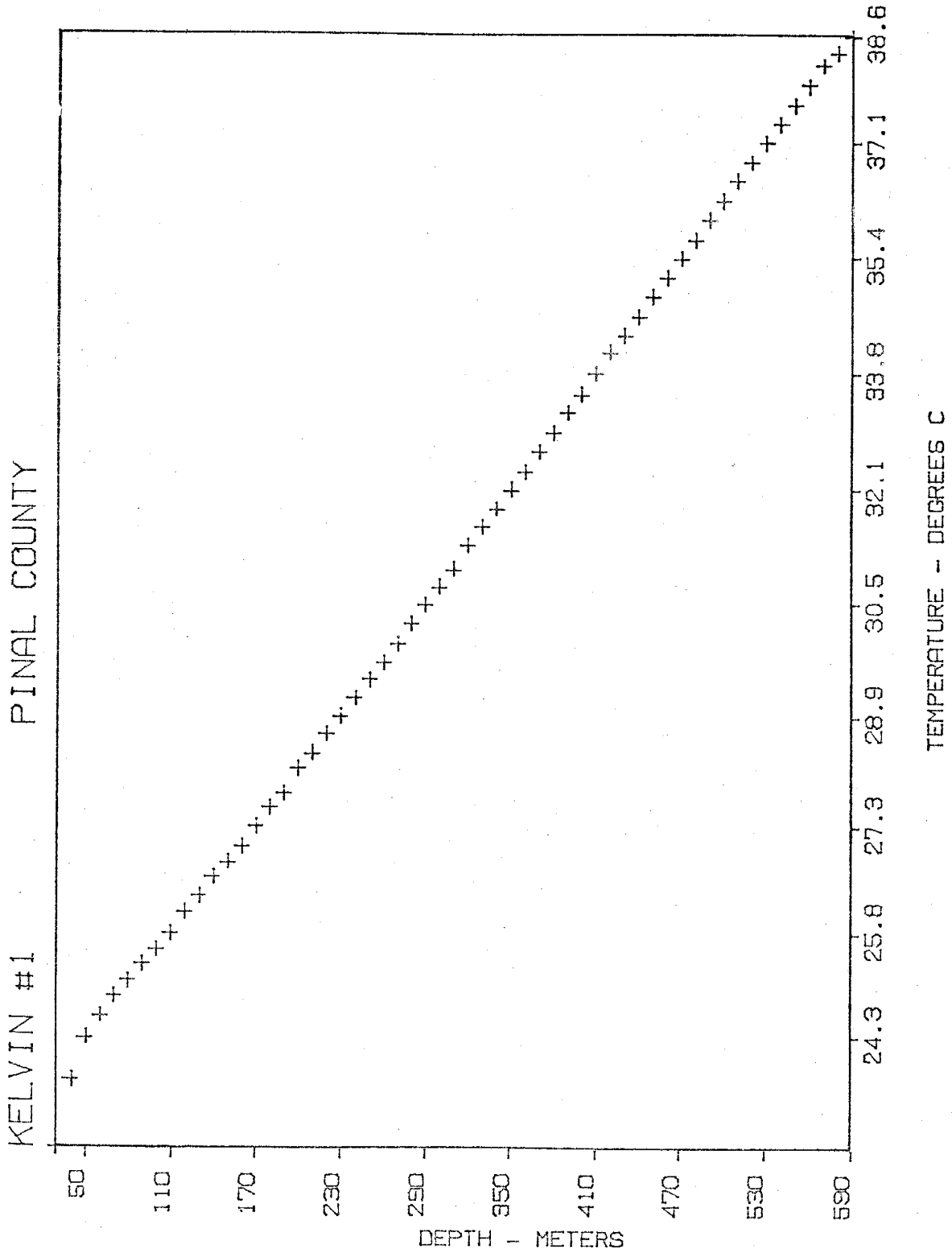
KELVIN #1
PINAL COUNTY
DEPTH - METERS
50
110
170
230
290
350
410
470
530
590
TEMPERATURE - DEGREES C
24.3
25.8
27.3
28.9
30.5
32.1
33.8
35.4
37.1
38.6

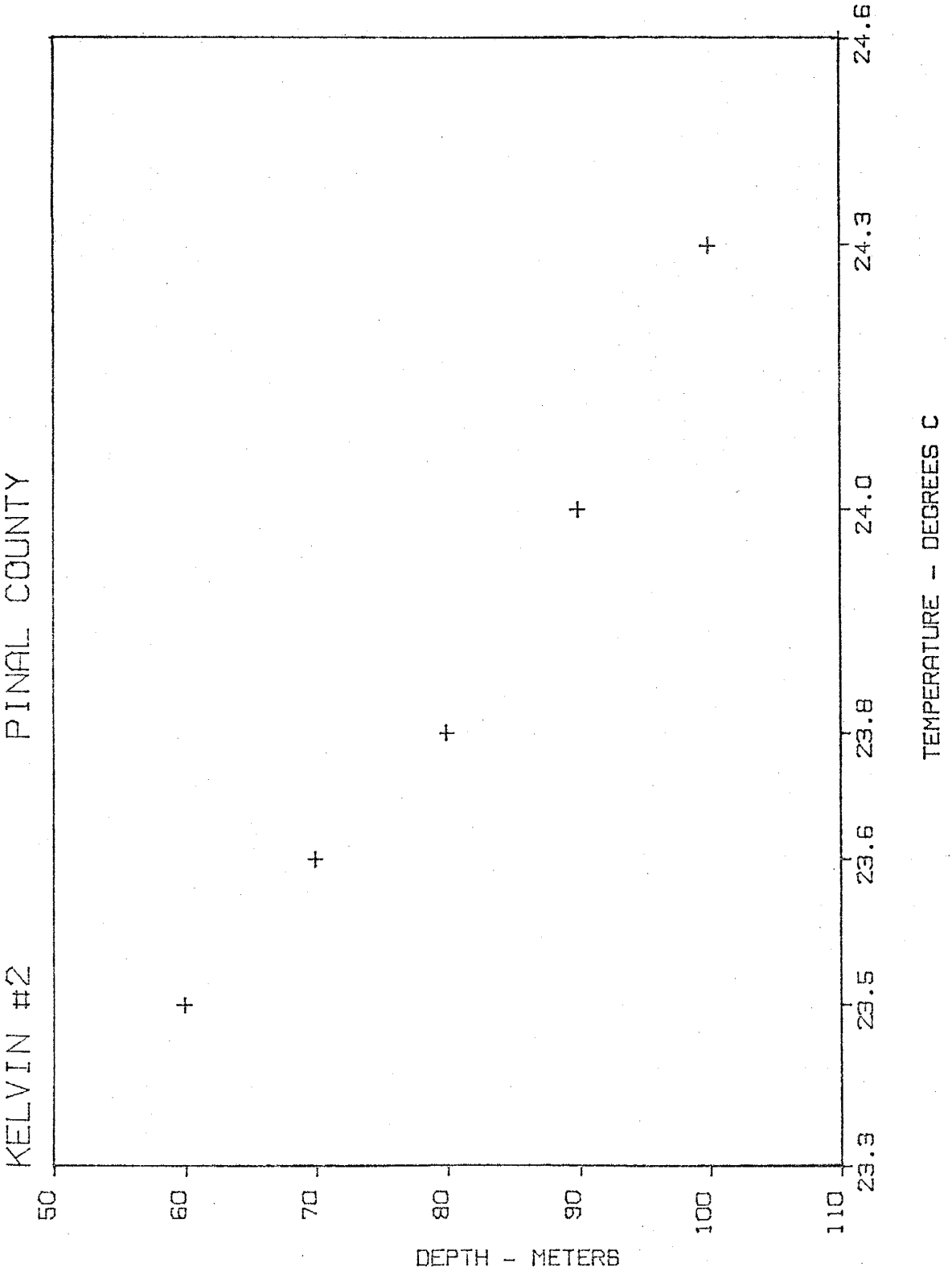
KELVIN #2
PINAL COUNTY
DEPTH - METERS
50
60
70
80
90
100
110
TEMPERATURE - DEGREES C
23.3
23.5
23.6
23.8
24.0
24.3
24.6

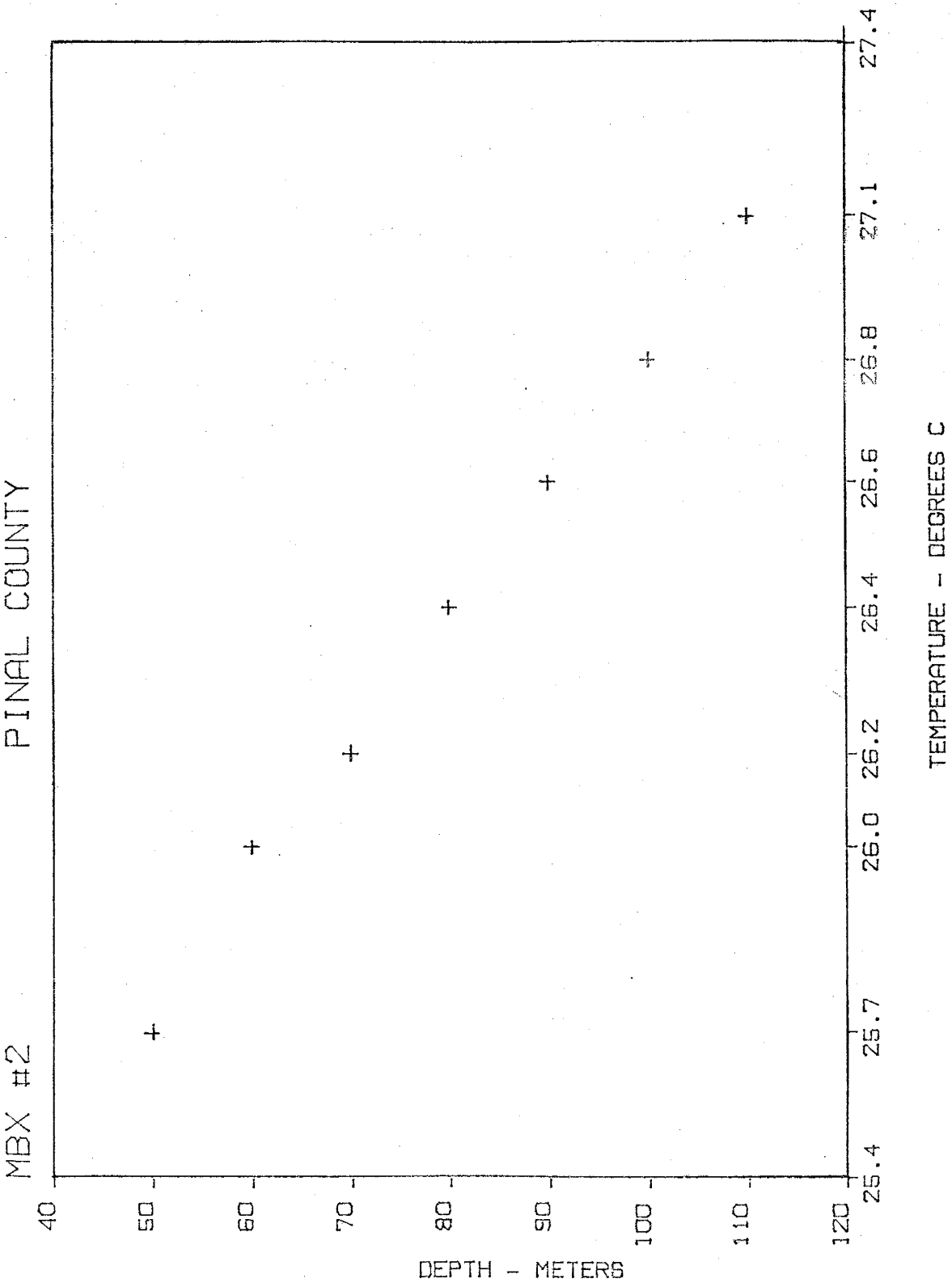
MBX #2
PINAL COUNTY
DEPTH - METERS
40
50
60
70
80
90
100
110
120
TEMPERATURE - DEGREES C
25.4
25.7
26.0
26.2
26.4
26.6
26.8
27.1
27.4

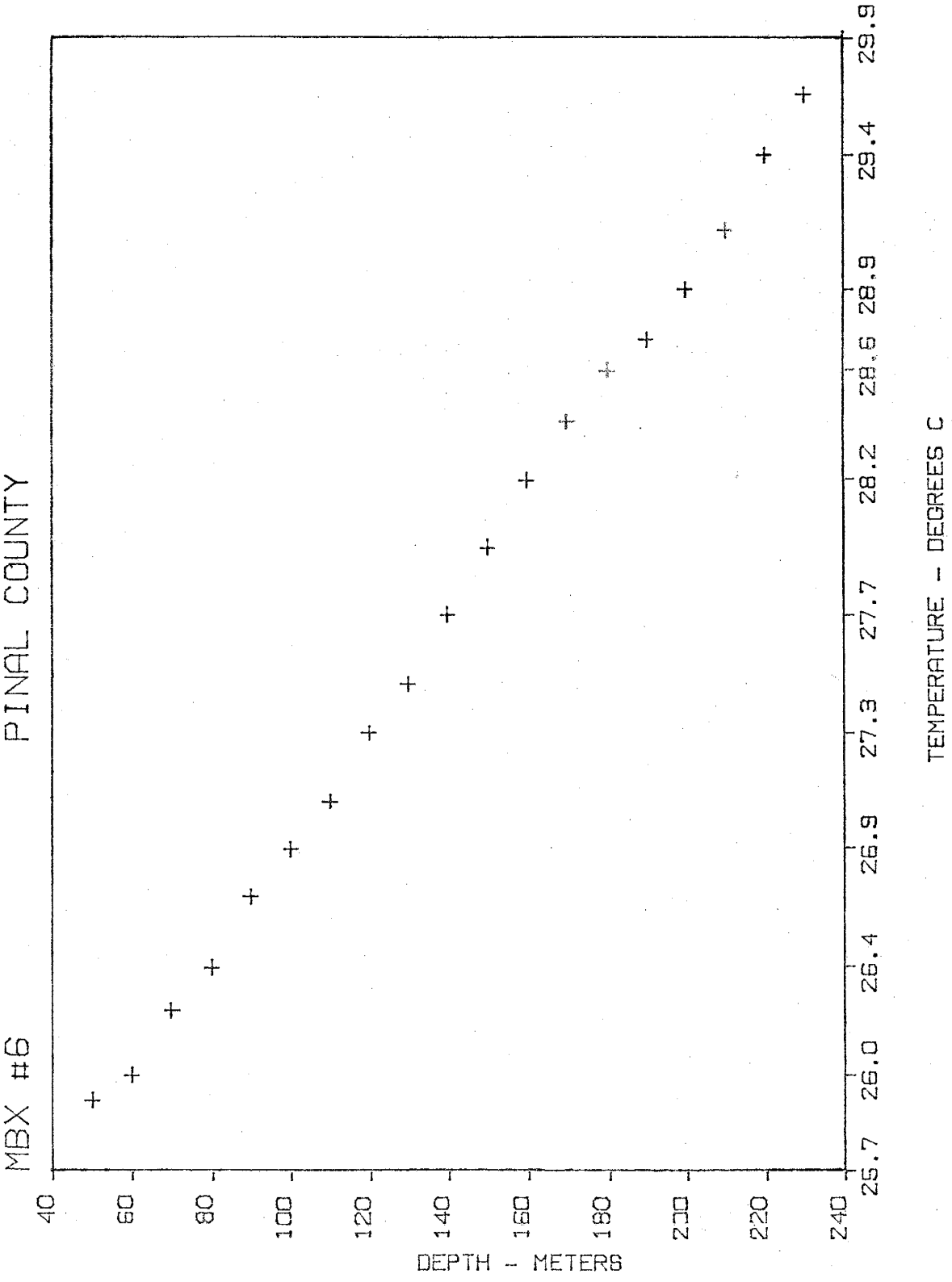
MBX #6
PINAL COUNTY
DEPTH - METERS
40
60
80
100
120
140
160
180
200
220
240
TEMPERATURE - DEGREES C
25.7
26.0
26.4
26.9
27.3
27.7
28.2
28.6
28.9
29.4
29.9

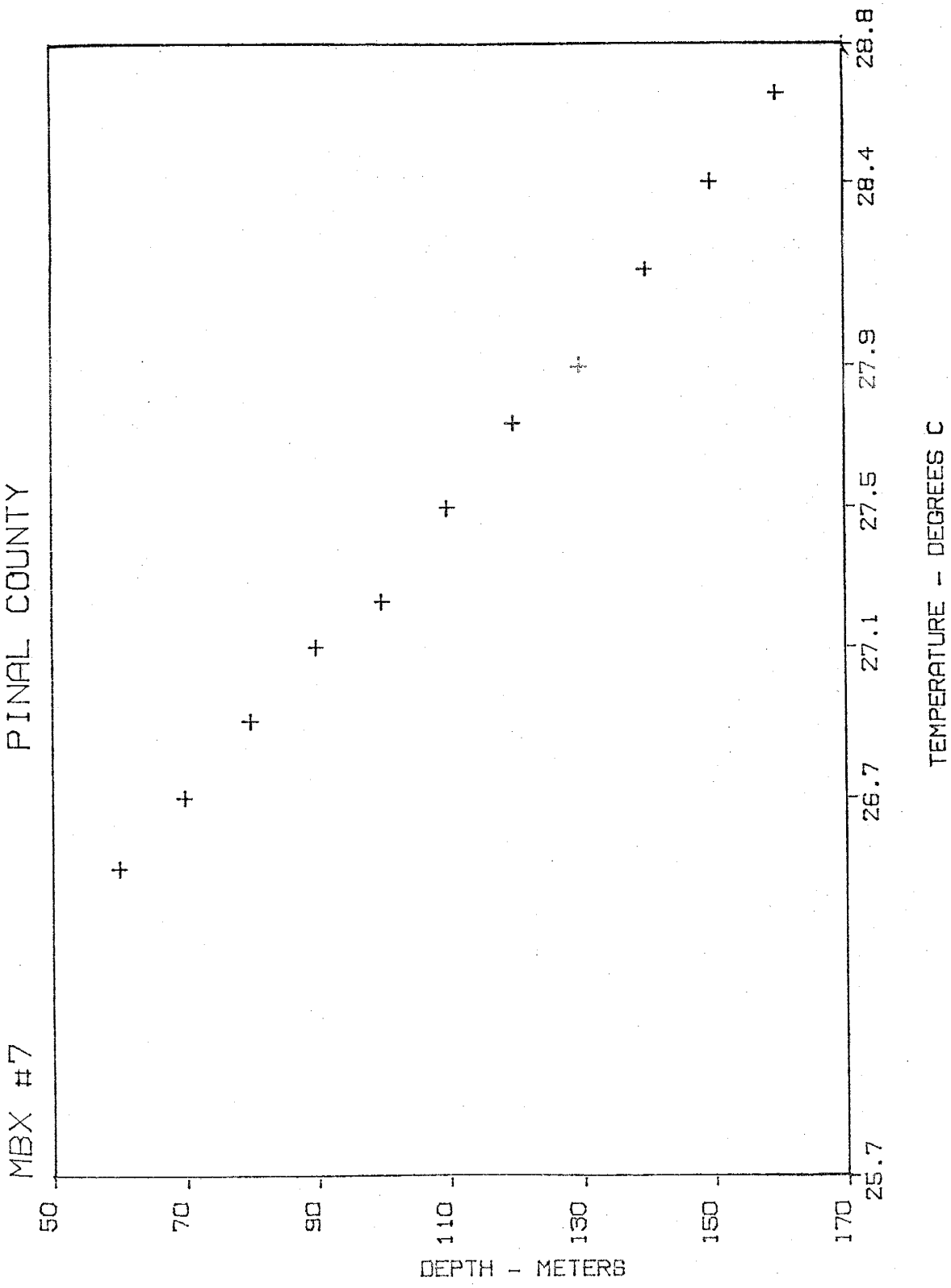
MBX #7
PINAL COUNTY
DEPTH - METERS
50
70
90
110
130
150
170
TEMPERATURE - DEGREES C
25.7
26.7
27.1
27.5
27.9
28.4
28.8

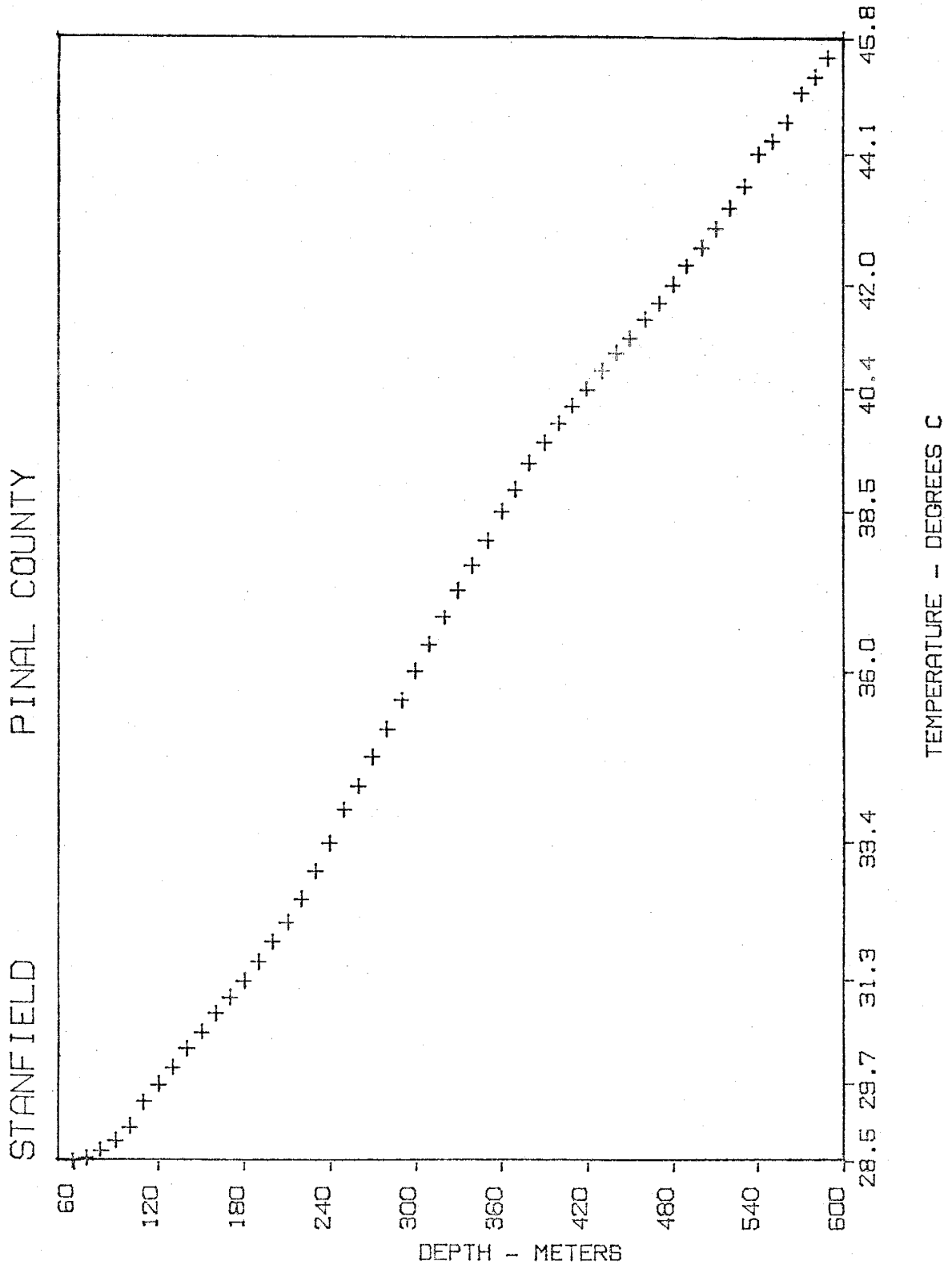
STANFIELD
PINAL COUNTY
DEPTH - METERS
60
120
180
240
300
360
420
480
540
600
28.5
29.7
31.3
33.4
36.0
38.5
40.4
42.0
44.1
45.8
TEMPERATURE - DEGREES C

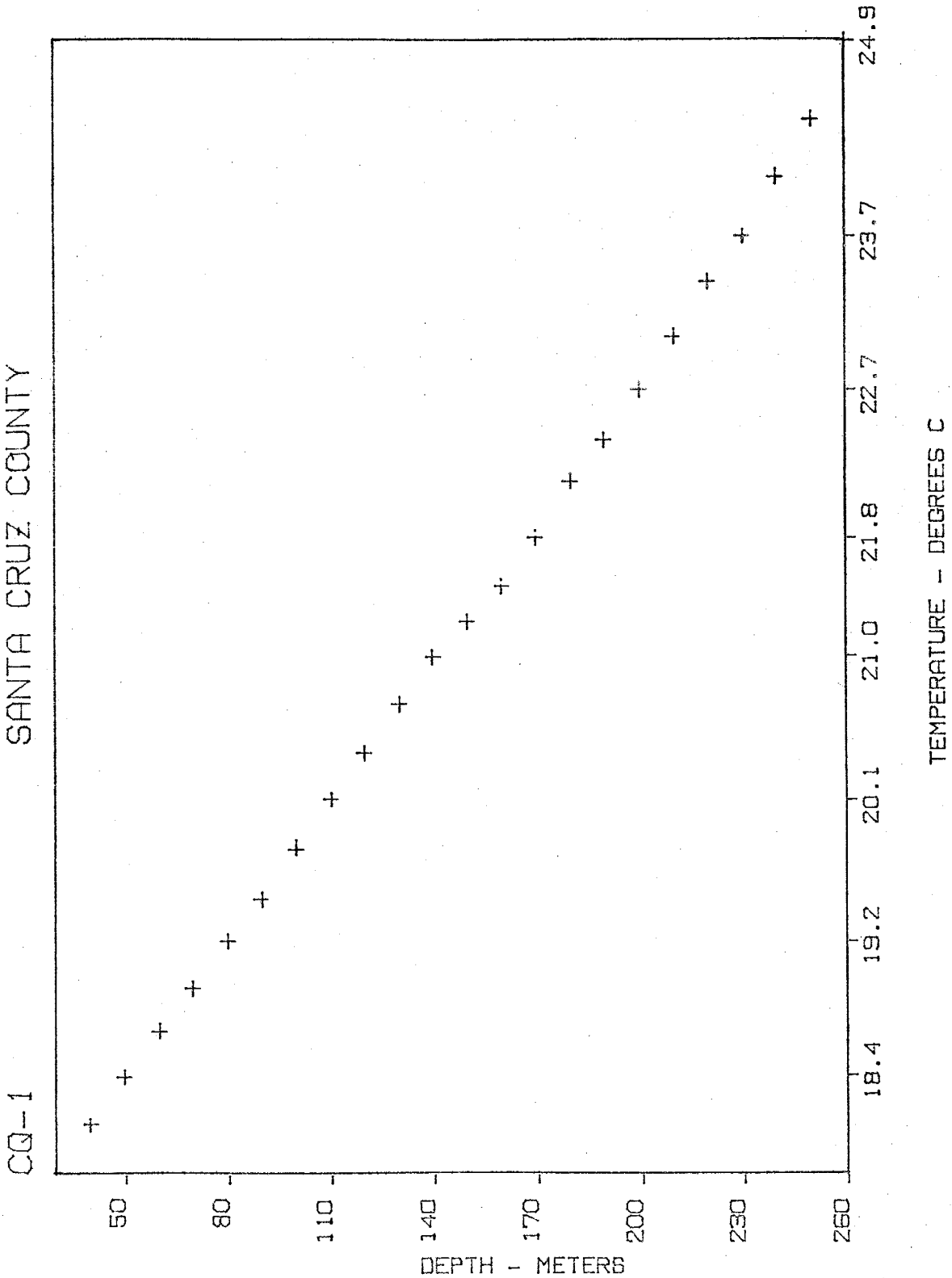
CQ-1
SANTA CRUZ COUNTY
DEPTH - METERS
50
80
110
140
170
200
230
260
18.4
19.2
20.1
21.0
21.8
22.7
23.7
24.9
TEMPERATURE - DEGREES C

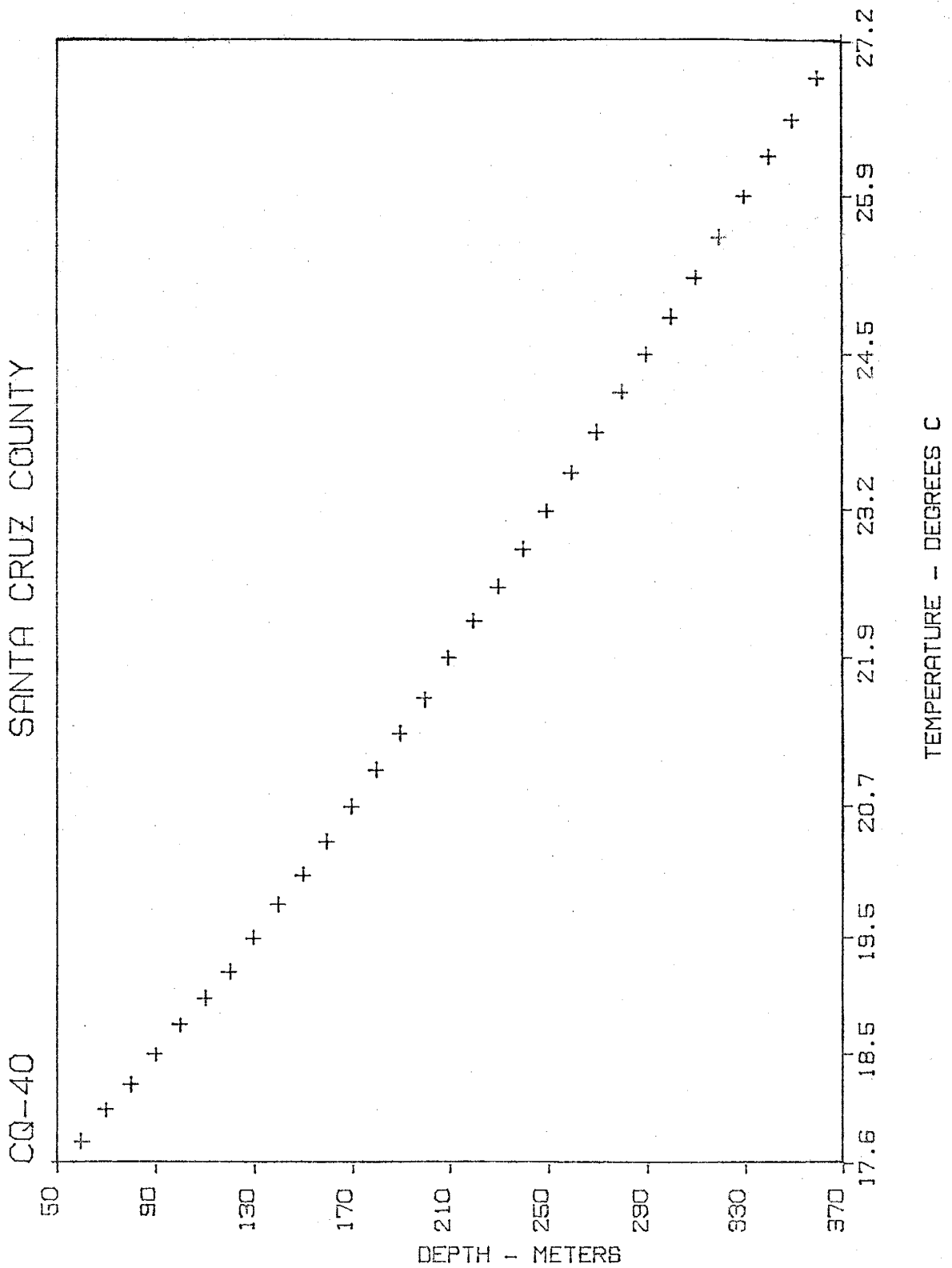
CQ-40
SANTA CRUZ COUNTY
50
90
130
170
210
250
290
330
370
DEPTH - METERS
17.6
18.5
19.5
20.7
21.9
23.2
24.5
25.9
27.2
TEMPERATURE - DEGREES C

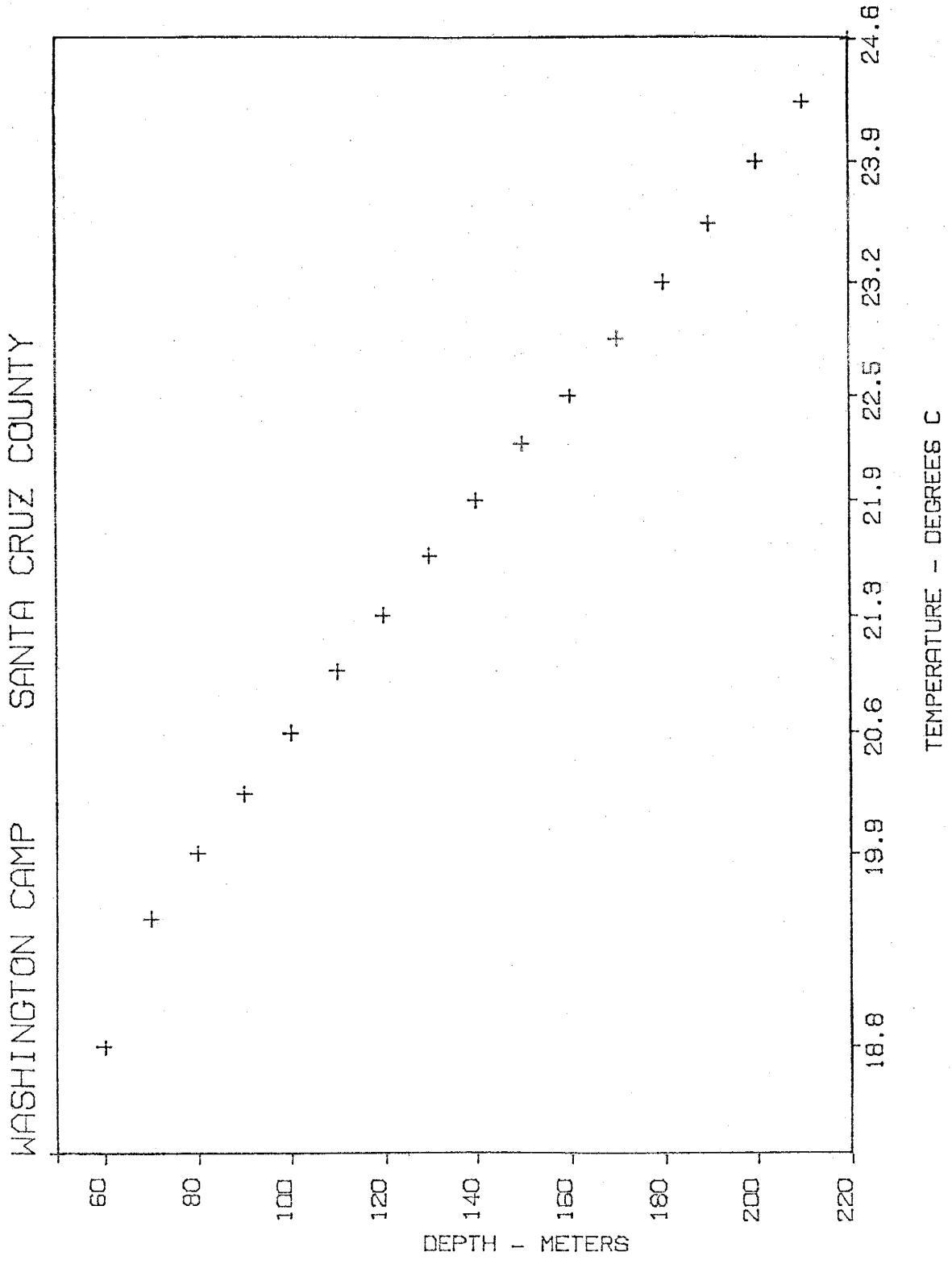
WASHINGTON CAMP SANTA CRUZ COUNTY
DEPTH - METERS
60
80
100
120
140
160
180
200
220
18.8
19.9
20.6
21.3
21.9
22.5
23.2
23.9
24.6
TEMPERATURE - DEGREES C

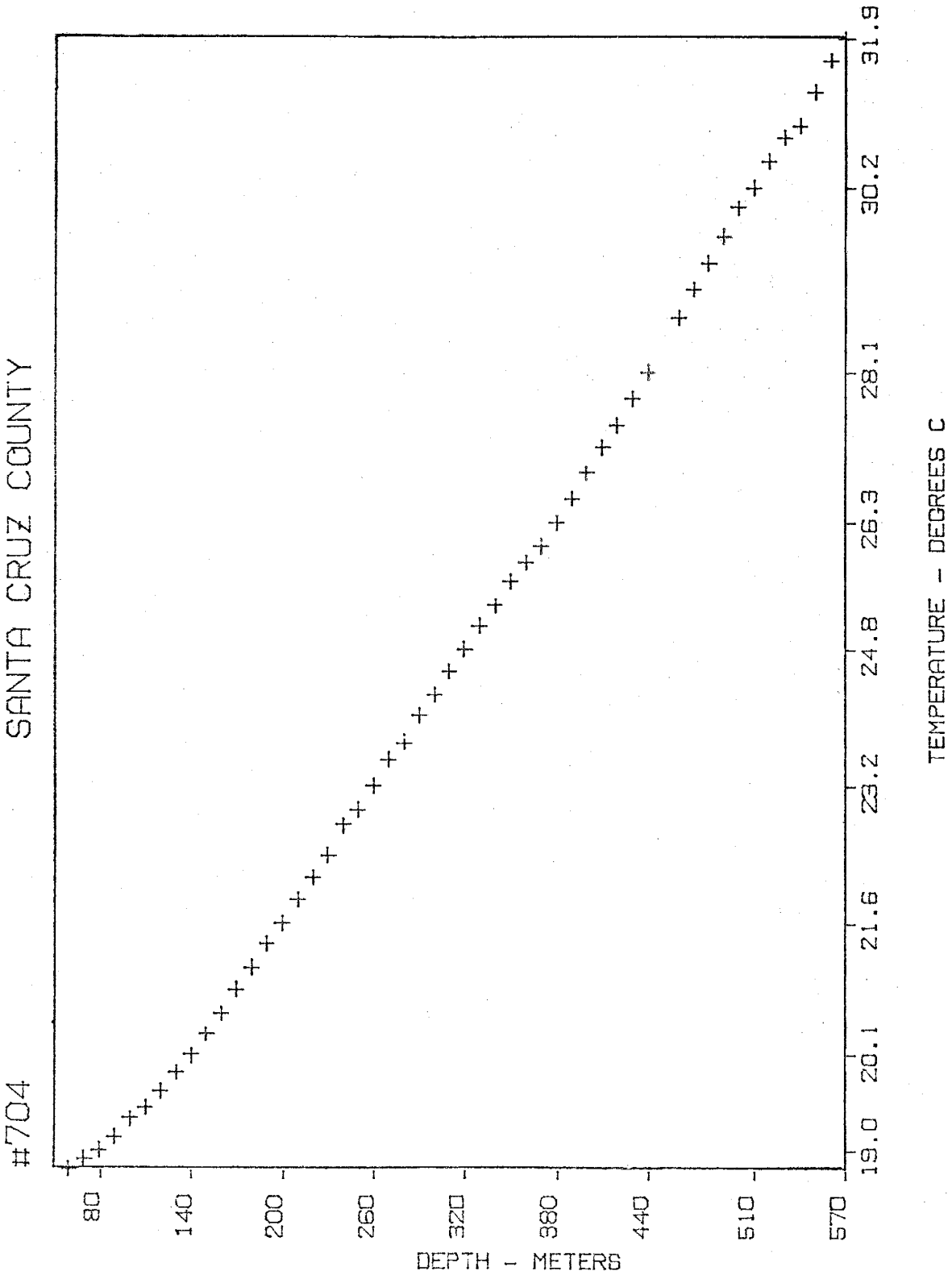
#704
SANTA CRUZ COUNTY
DEPTH - METERS
80
140
200
260
320
380
440
510
570
19.0
20.1
21.6
23.2
24.8
26.3
28.1
30.2
31.9
TEMPERATURE - DEGREES C

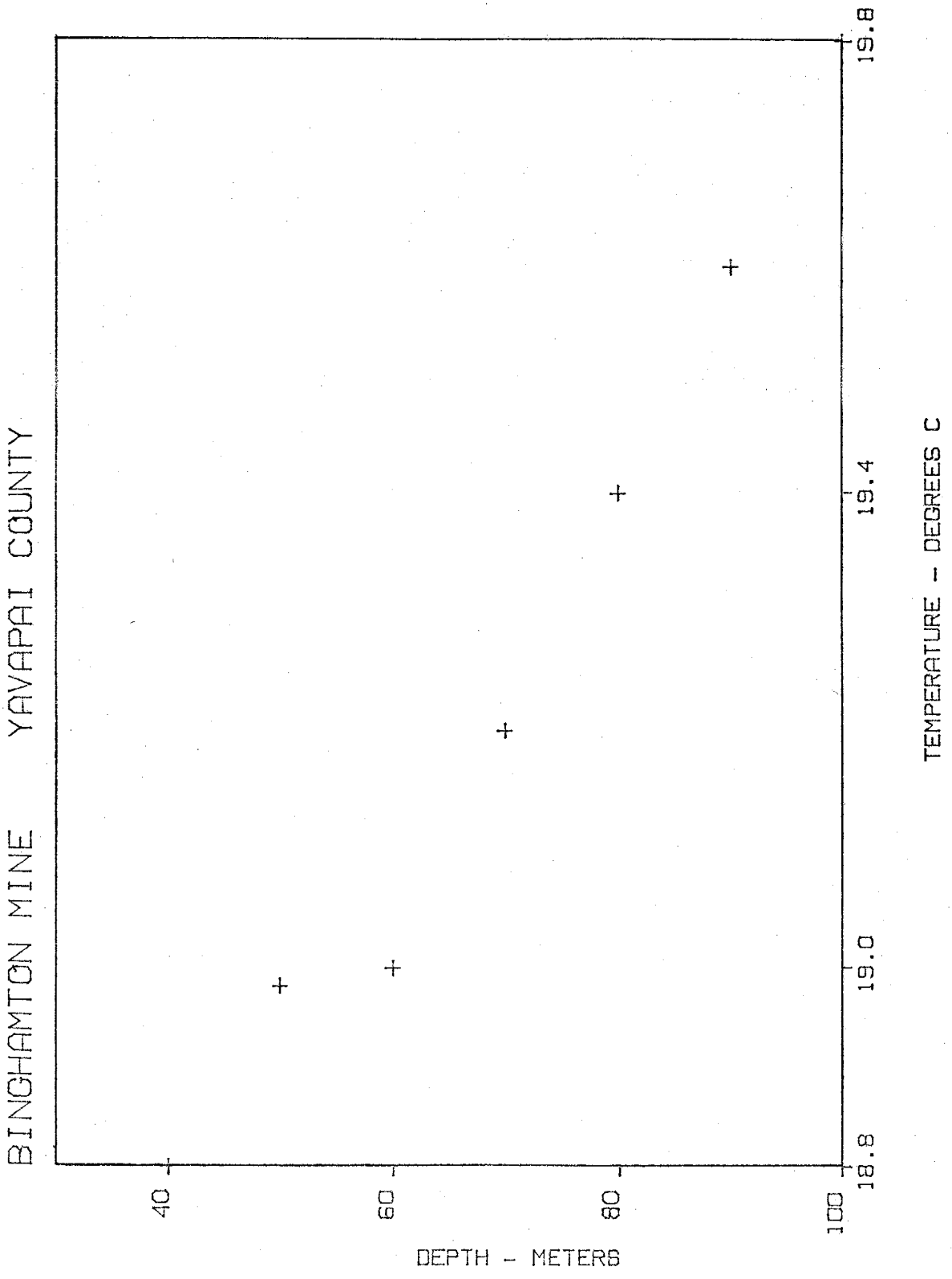
BINGHAMTON MINE YAVAPAI COUNTY
40
60
80
100
DEPTH - METERS
18.8
19.0
19.4
19.8
TEMPERATURE - DEGREES C

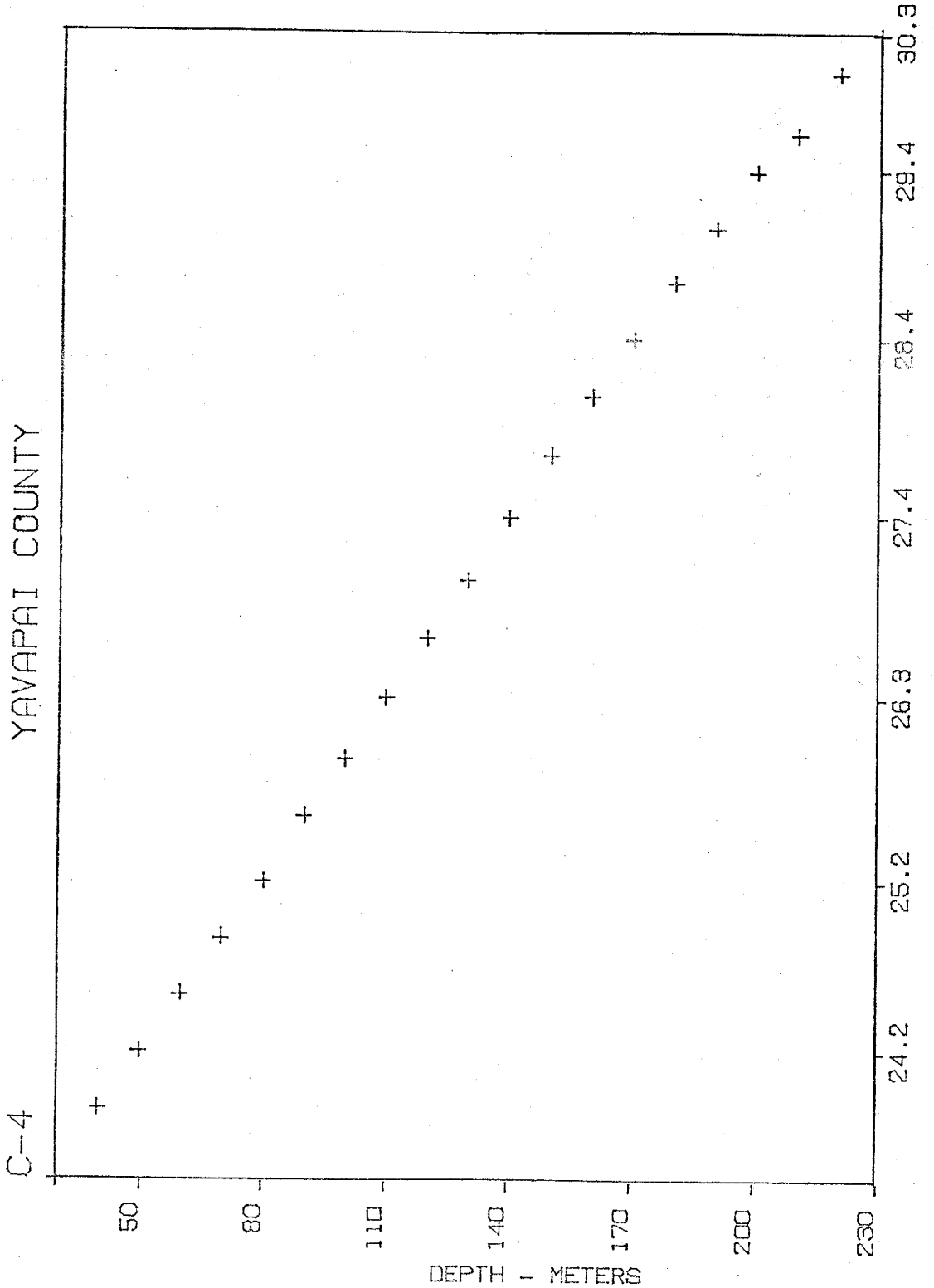
C-4
YAVAPAI COUNTY
DEPTH - METERS
50
80
110
140
170
200
230
TEMPERATURE - DEGREES C
24.2
25.2
26.3
27.4
28.4
29.4
30.3

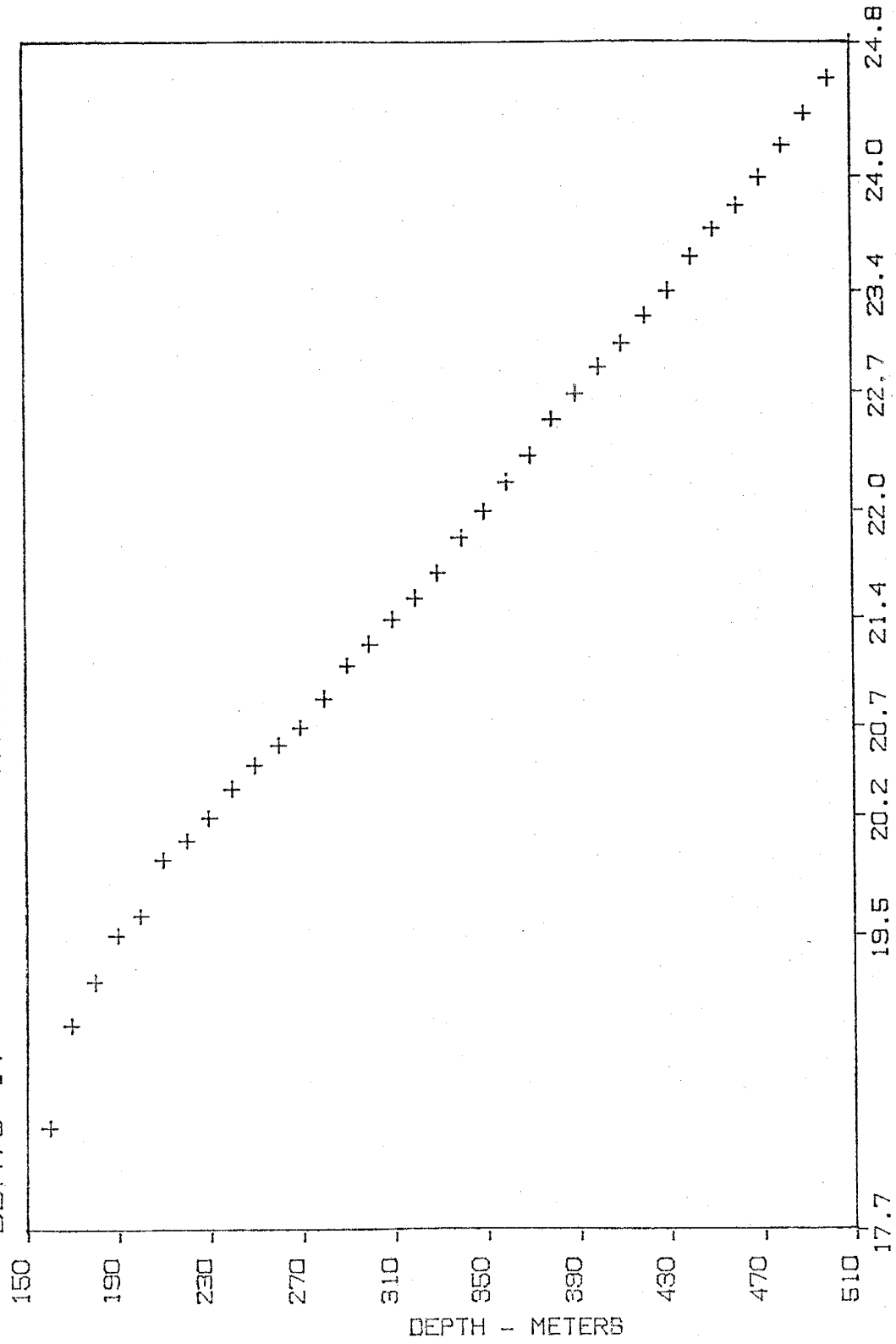
DDH75-17
YAVAPAI COUNTY
150
190
230
270
310
350
390
430
470
510
DEPTH - METERS
17.7
19.5
20.2
20.7
21.4
22.0
22.7
23.4
24.0
24.8
TEMPERATURE - DEGREES C

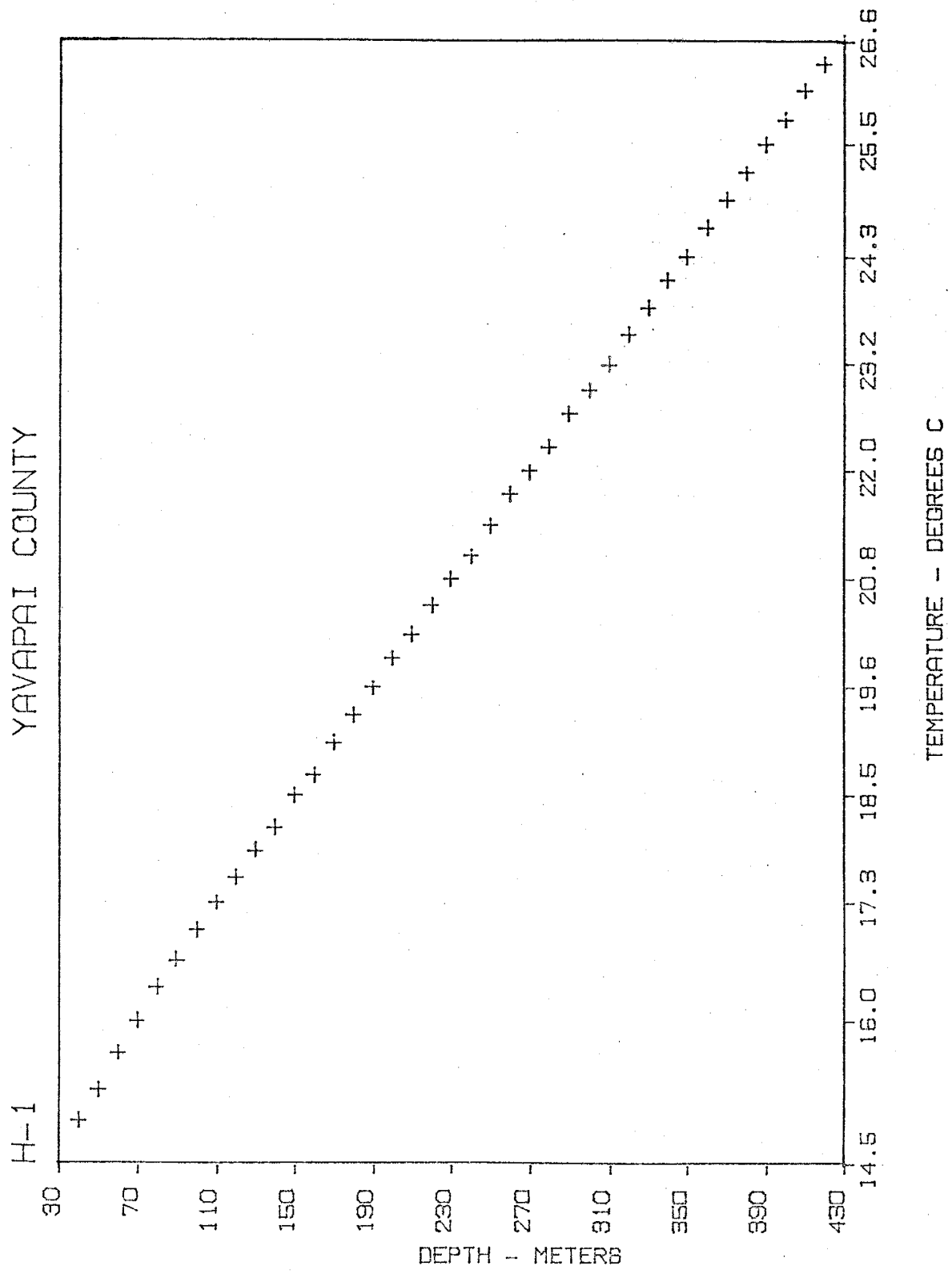
H-1
YAVAPAI COUNTY
DEPTH - METERS
30
70
110
150
190
230
270
310
350
390
430
TEMPERATURE - DEGREES C
14.5
16.0
17.3
18.5
19.6
20.8
22.0
23.2
24.3
25.5
26.6

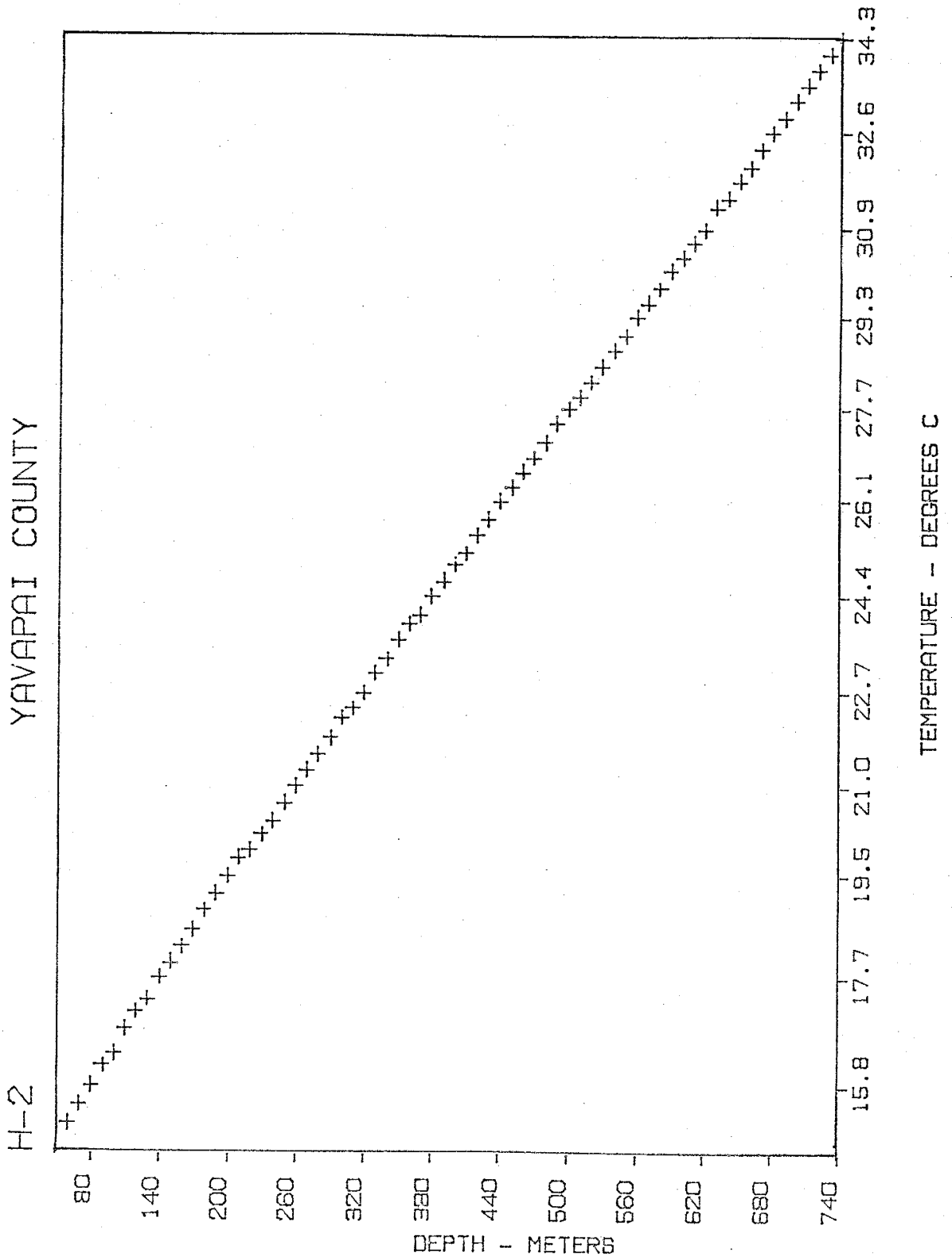
H-2
YAVAPAI COUNTY
80
140
200
260
320
380
440
500
560
620
680
740
DEPTH - METERS
15.8
17.7
19.5
21.0
22.7
24.4
26.1
27.7
29.3
30.9
32.6
34.3
TEMPERATURE - DEGREES C

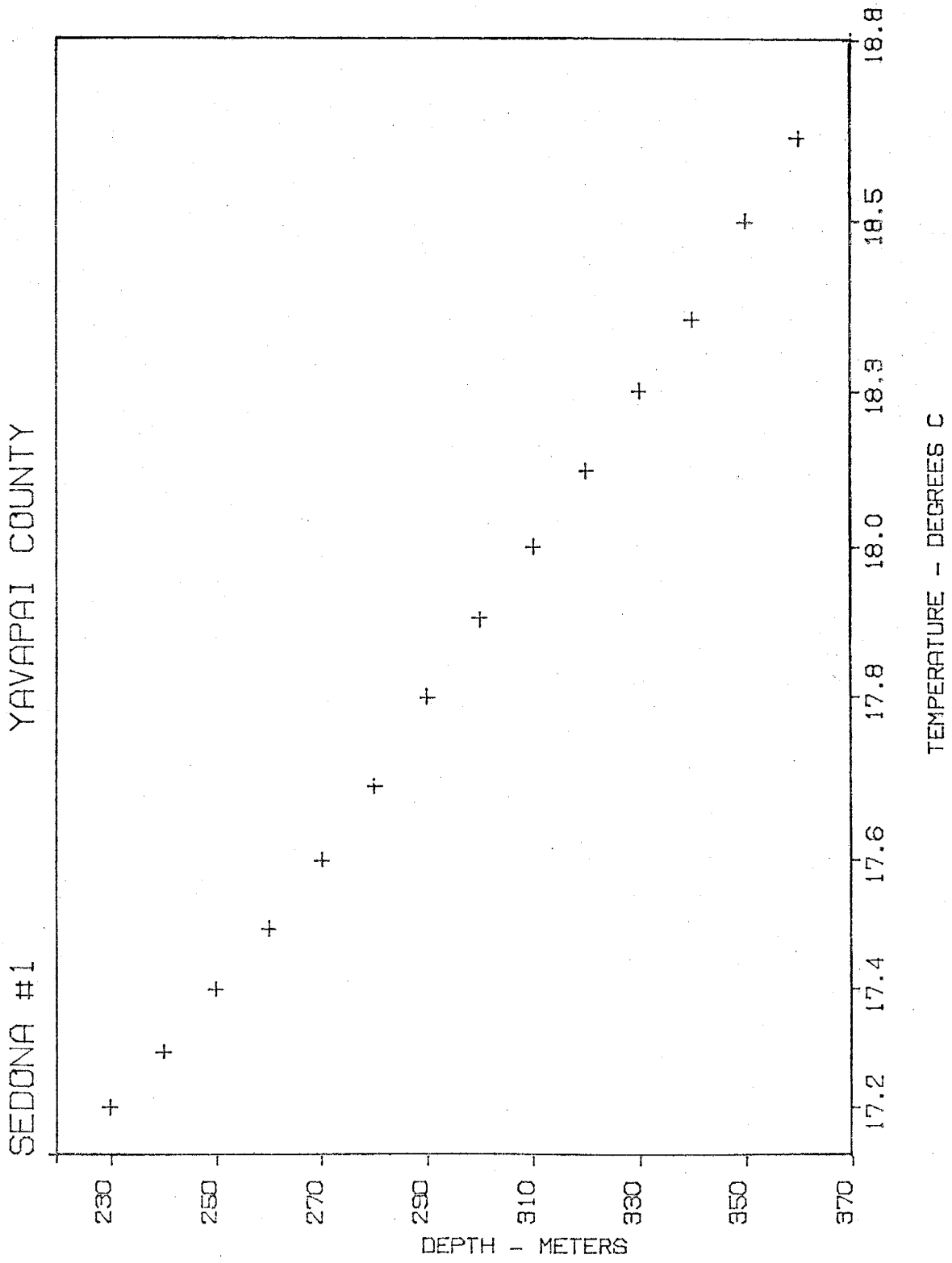
SEDONA #1
YAVAPAI COUNTY
DEPTH - METERS
230
250
270
290
310
330
350
370
TEMPERATURE - DEGREES C
17.2
17.4
17.6
17.8
18.0
18.3
18.5
18.8

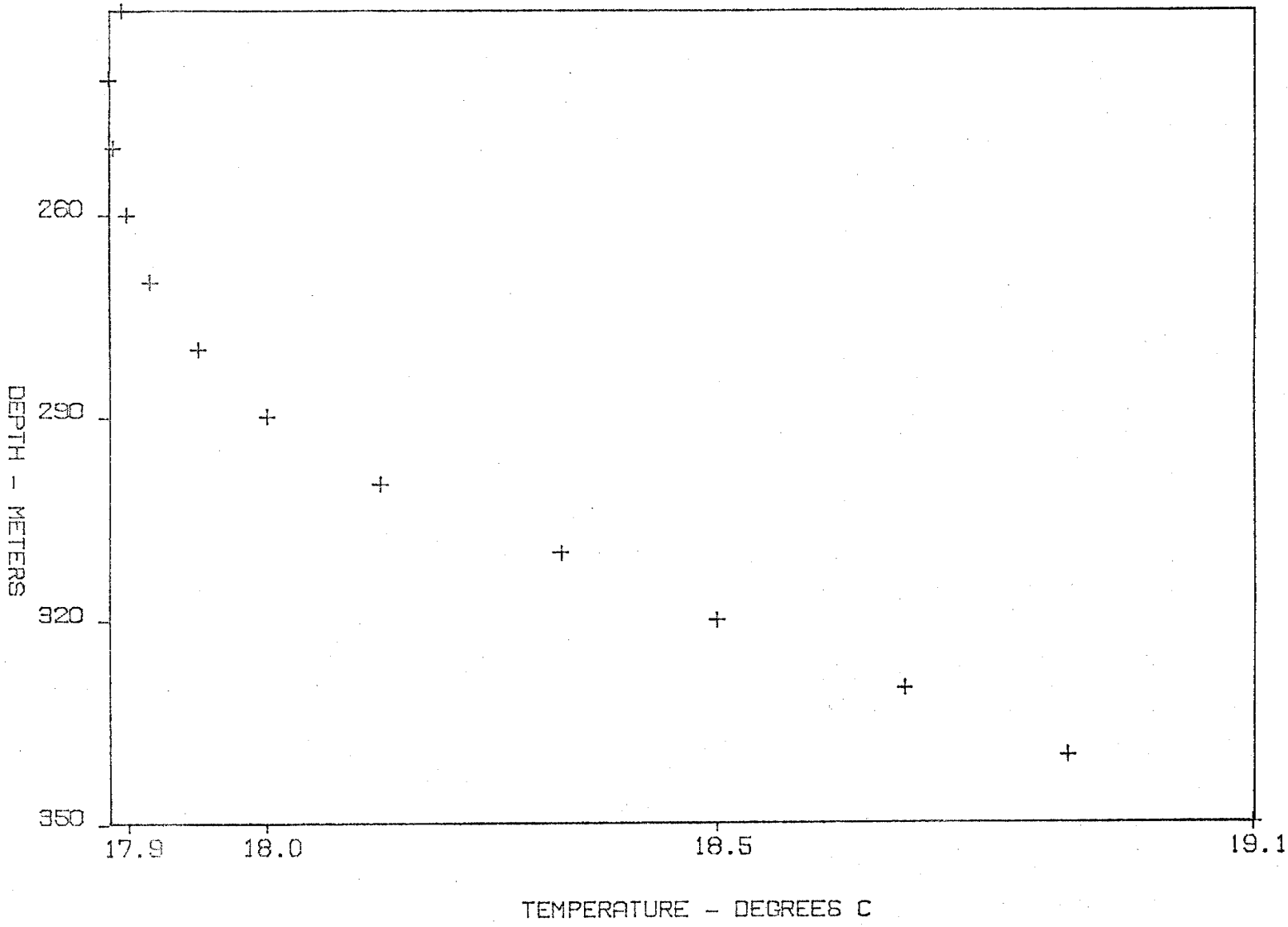
SEDONA #2
YAVAPAI COUNTY
260
290
320
350
DEPTH - METERS
17.9
18.0
18.5
19.1
TEMPERATURE - DEGREES C

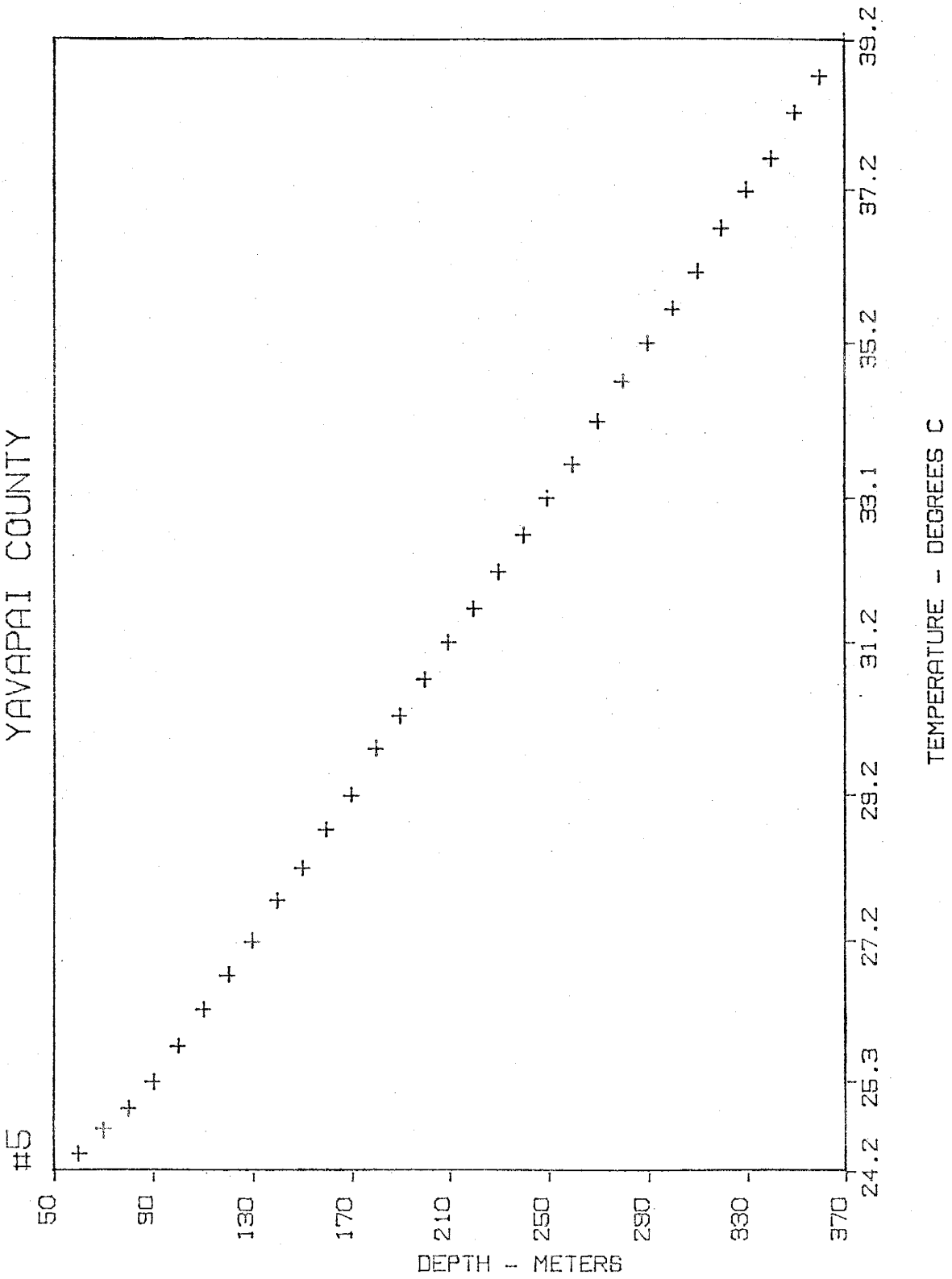
#5
YAVAPAI COUNTY
50
90
130
170
210
250
290
330
370
DEPTH - METERS
24.2
25.3
27.2
29.2
31.2
33.1
35.2
37.2
39.2
TEMPERATURE - DEGREES C

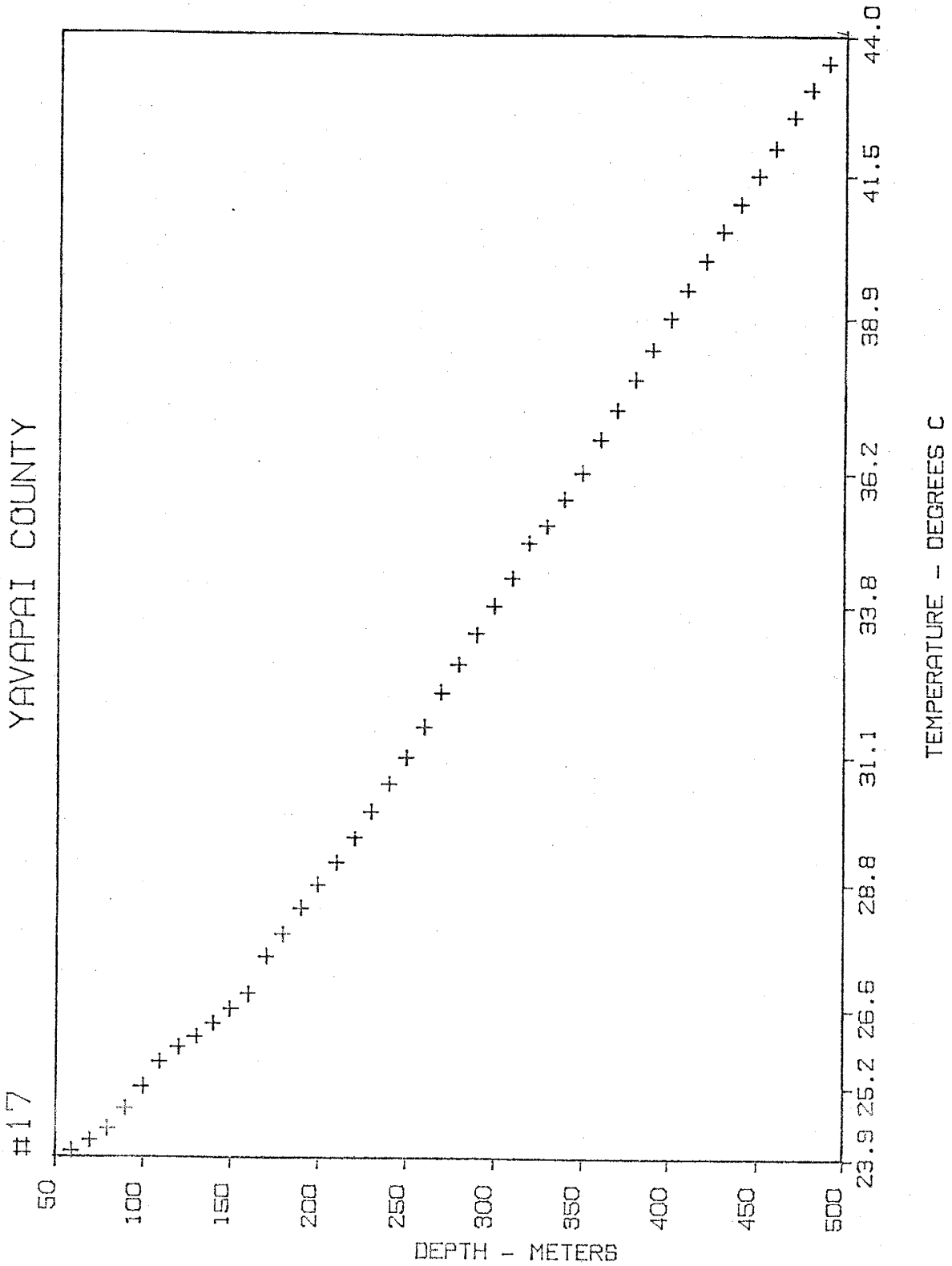
#17
YAVAPAI COUNTY
DEPTH - METERS
50
100
150
200
250
300
350
400
450
500
23.9 25.2 26.6 28.8 31.1 33.8 36.2 38.9 41.5 44.0
TEMPERATURE - DEGREES C

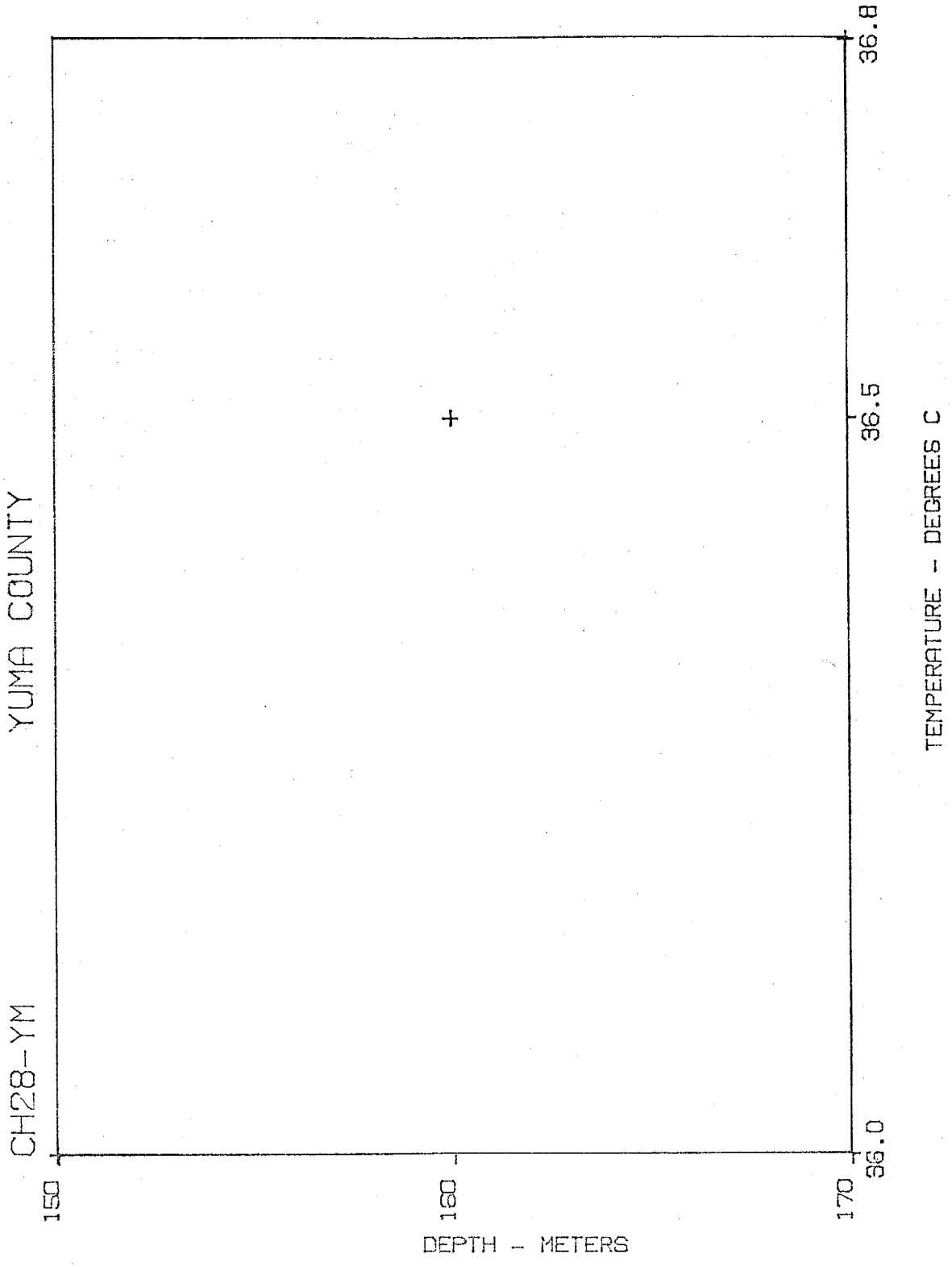
CH28-YM
YUMA COUNTY
150
160
170
DEPTH - METERS
36.0
36.5
36.8
TEMPERATURE - DEGREES C

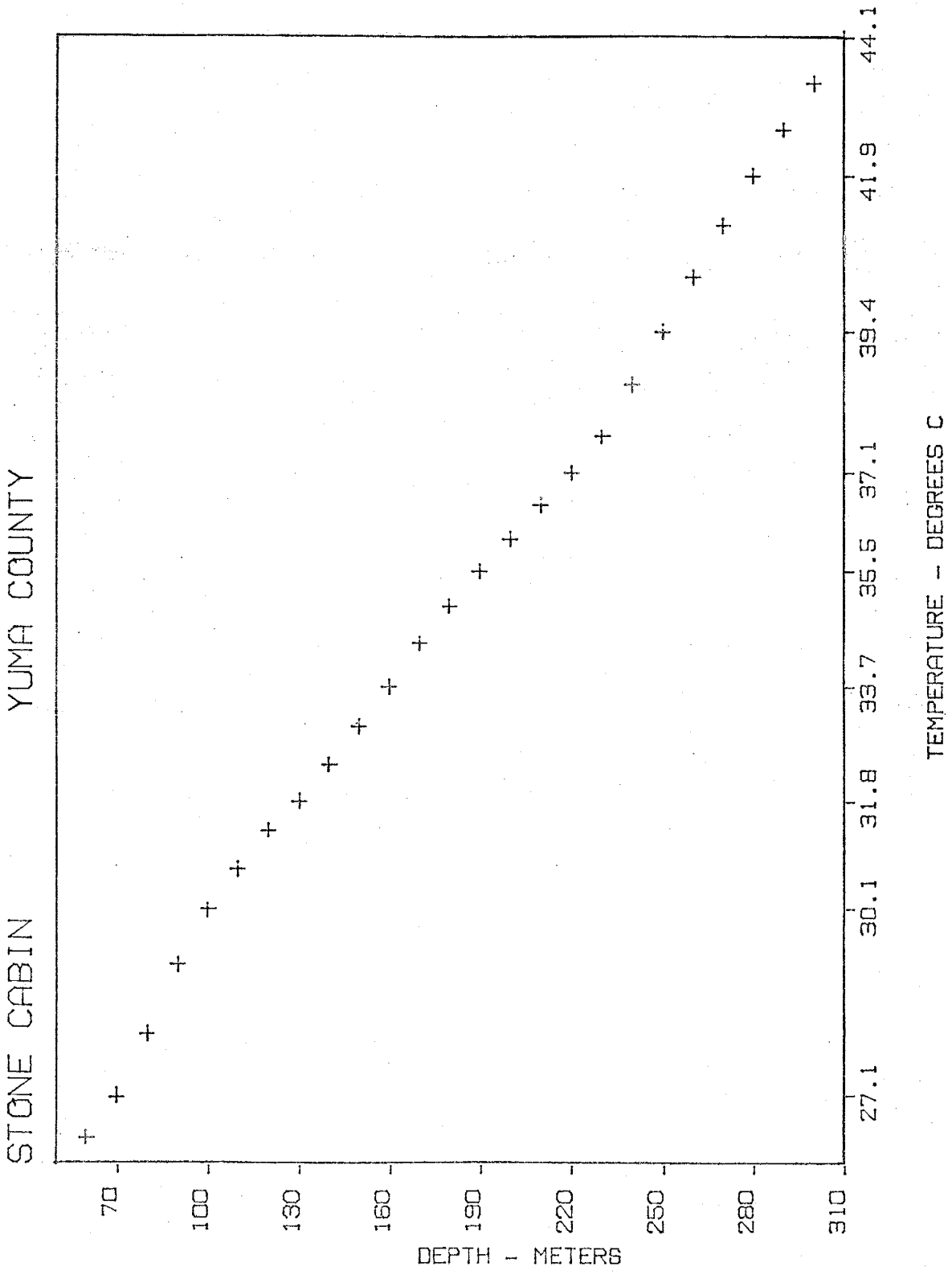
STONE CABIN YUMA COUNTY
DEPTH - METERS
70
100
130
160
190
220
250
280
310
TEMPERATURE - DEGREES C
27.1
30.1
31.8
33.7
35.5
37.1
39.4
41.9
44.1

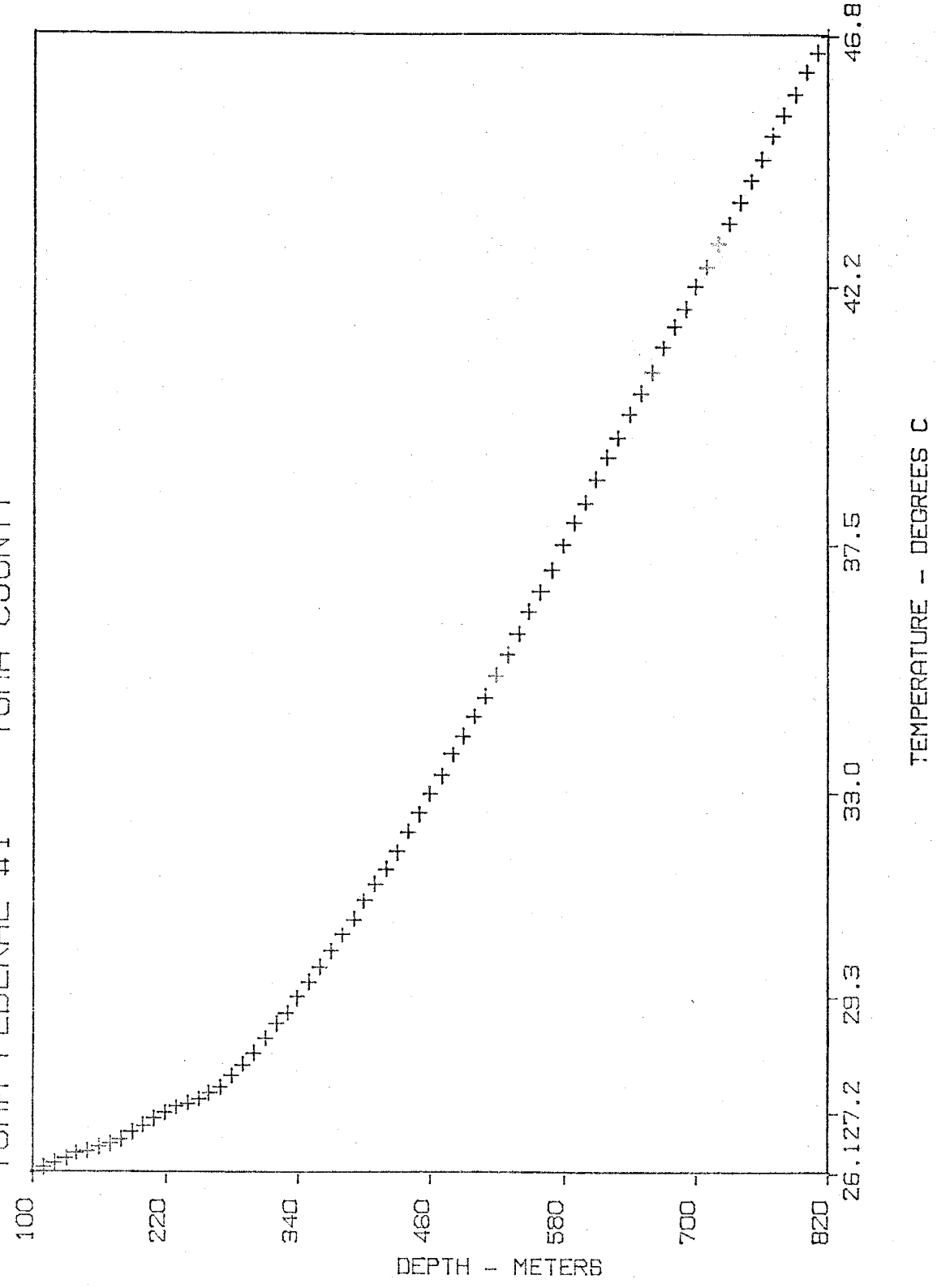
YUMA FEDERAL #1 YUMA COUNTY
100
220
340
460
580
700
820
DEPTH - METERS
26.1
27.2
29.3
33.0
37.5
42.2
46.8
TEMPERATURE - DEGREES C

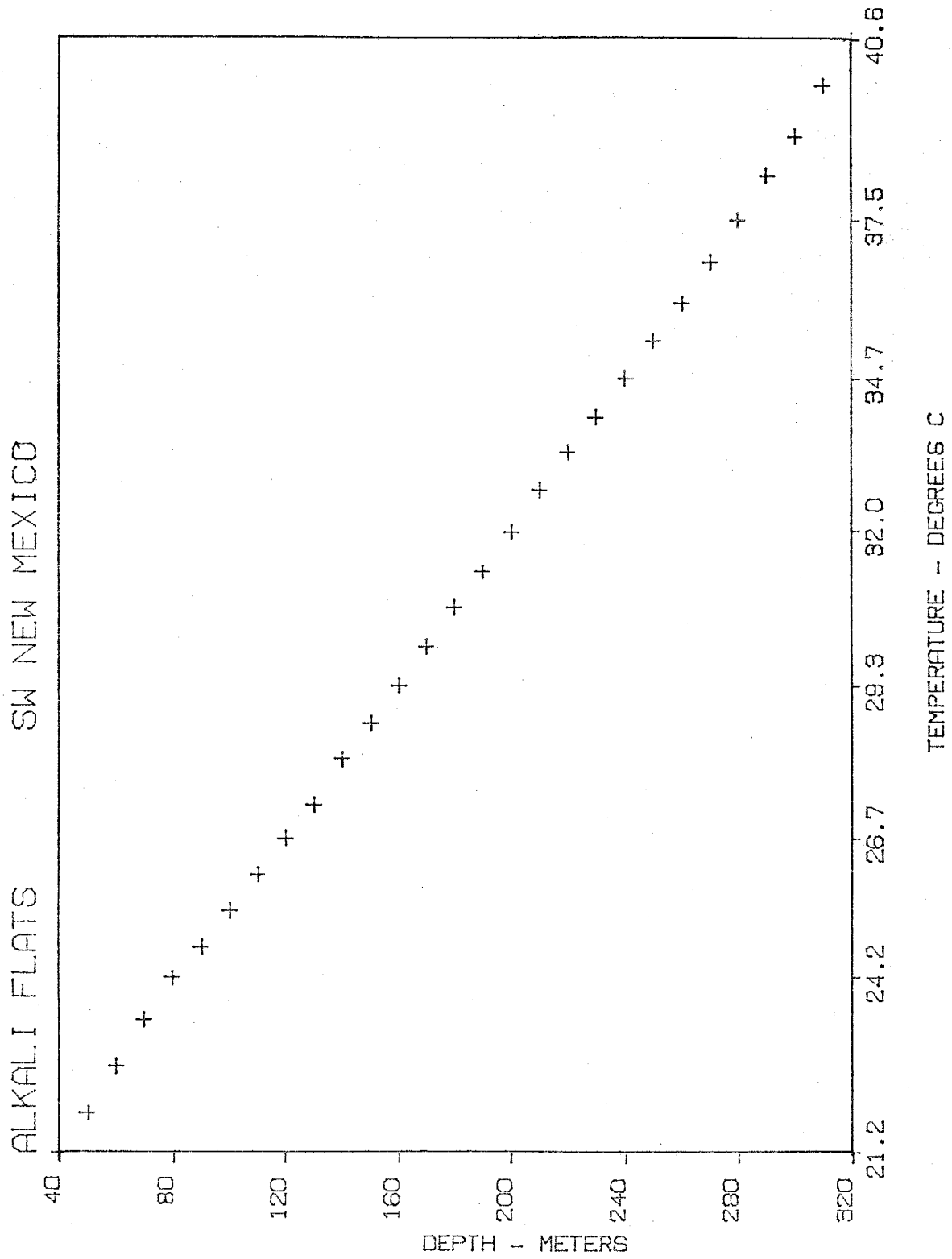
ALKALI FLATS SW NEW MEXICO
DEPTH - METERS
40
80
120
160
200
240
280
320
TEMPERATURE - DEGREES C
21.2
24.2
26.7
29.3
32.0
34.7
37.5
40.6

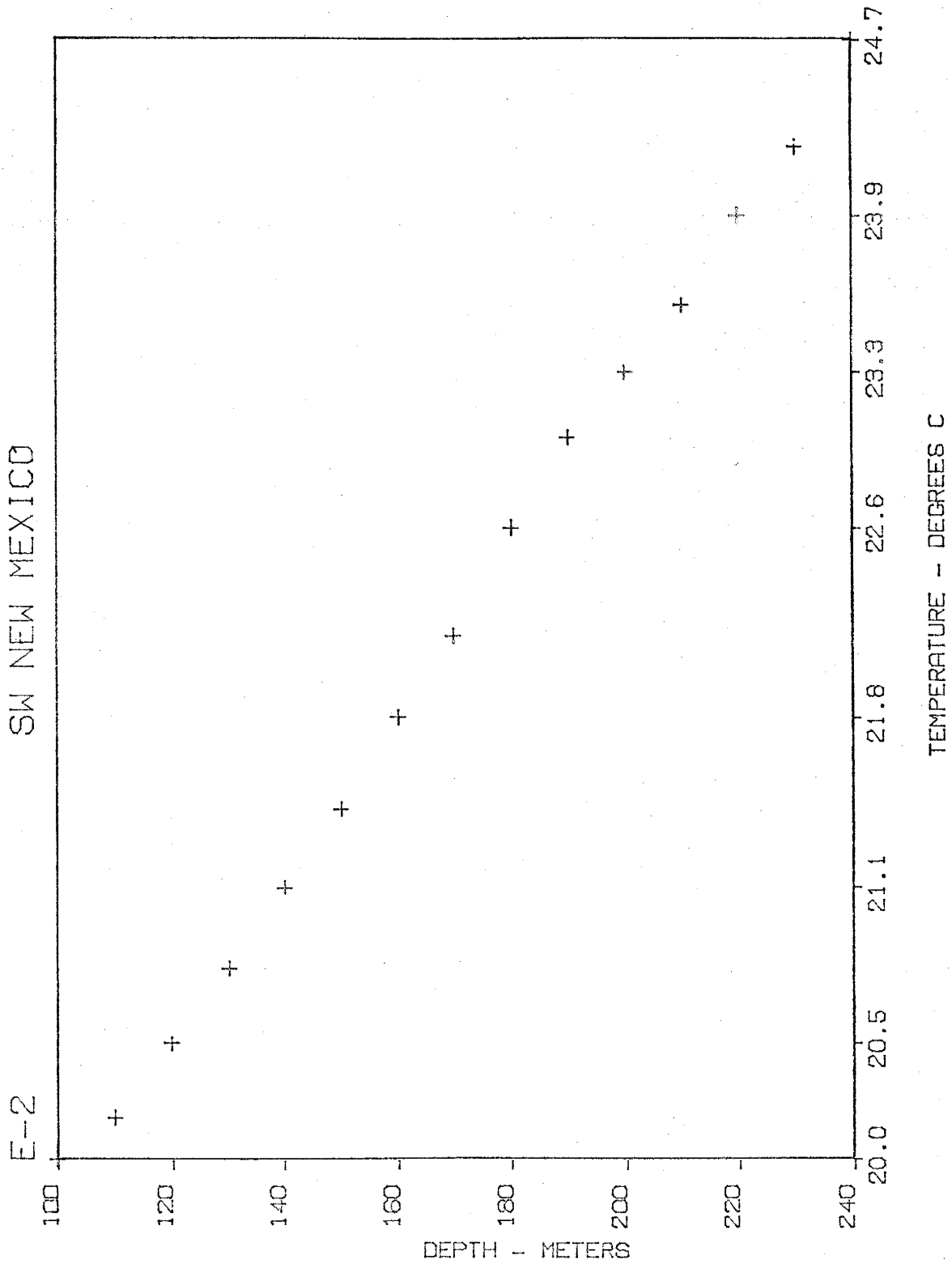
E-2
SW NEW MEXICO
100
120
140
160
180
200
220
240
DEPTH - METERS
20.0
20.5
21.1
21.8
22.6
23.3
23.9
24.7
TEMPERATURE - DEGREES C

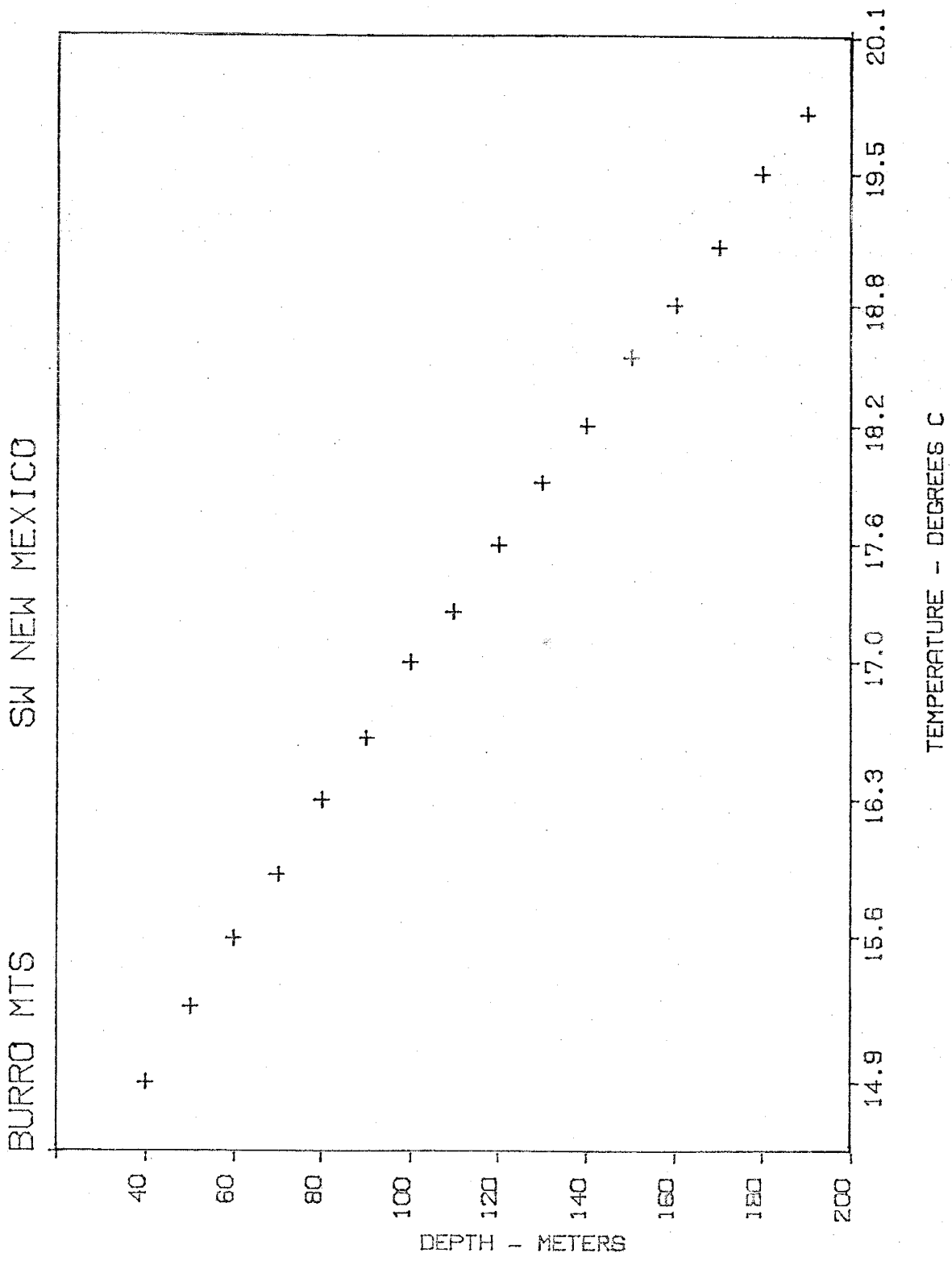
BURRO MTS
SW NEW MEXICO
DEPTH - METERS
40
60
80
100
120
140
160
180
200
TEMPERATURE - DEGREES C
14.9
15.6
16.3
17.0
17.6
18.2
18.8
19.5
20.1

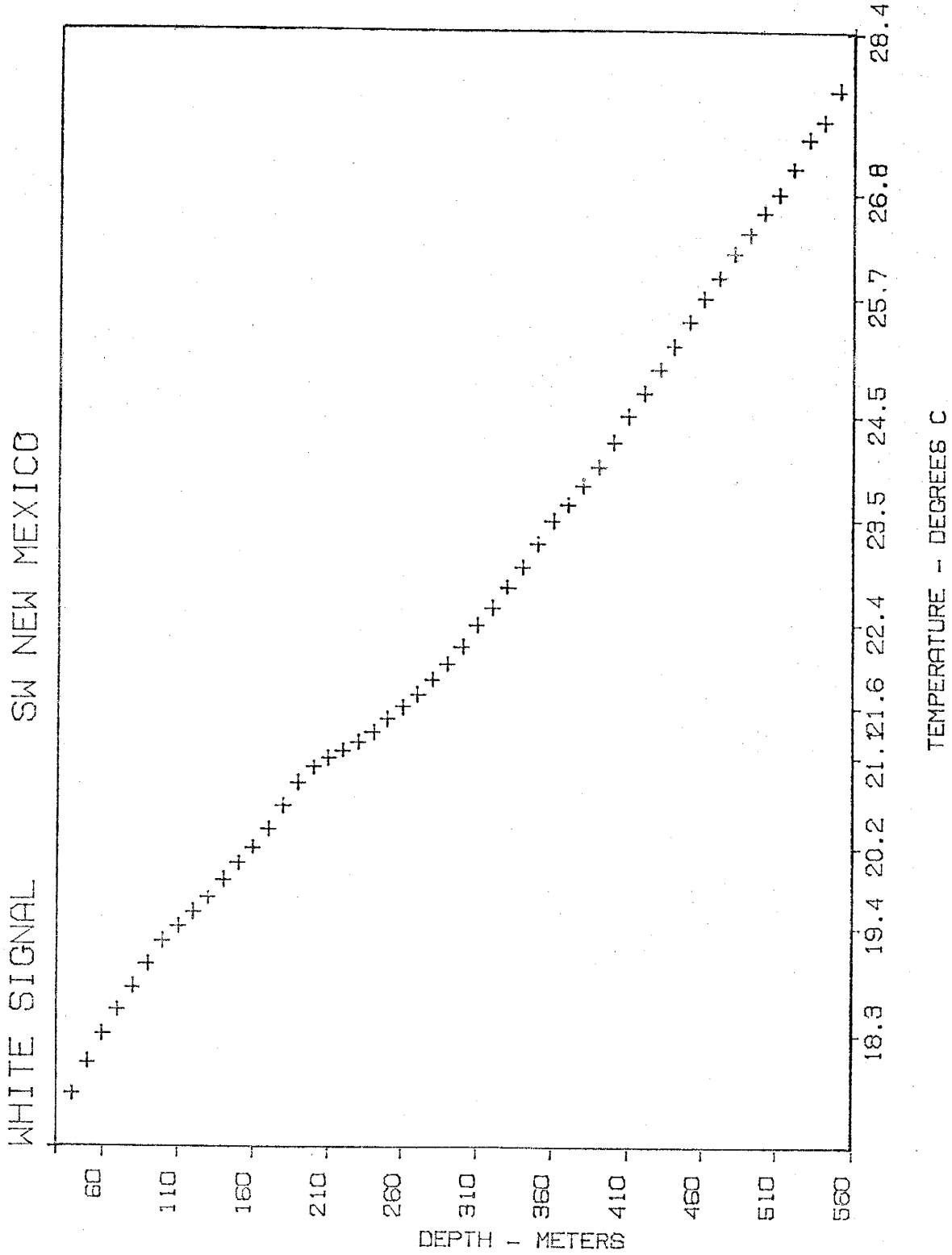
WHITE SIGNAL
SW NEW MEXICO
DEPTH - METERS
60
110
160
210
260
310
360
410
460
510
560
TEMPERATURE - DEGREES C
18.3
19.4
20.2
21.1
21.6
22.4
23.5
24.5
25.7
26.8
28.4

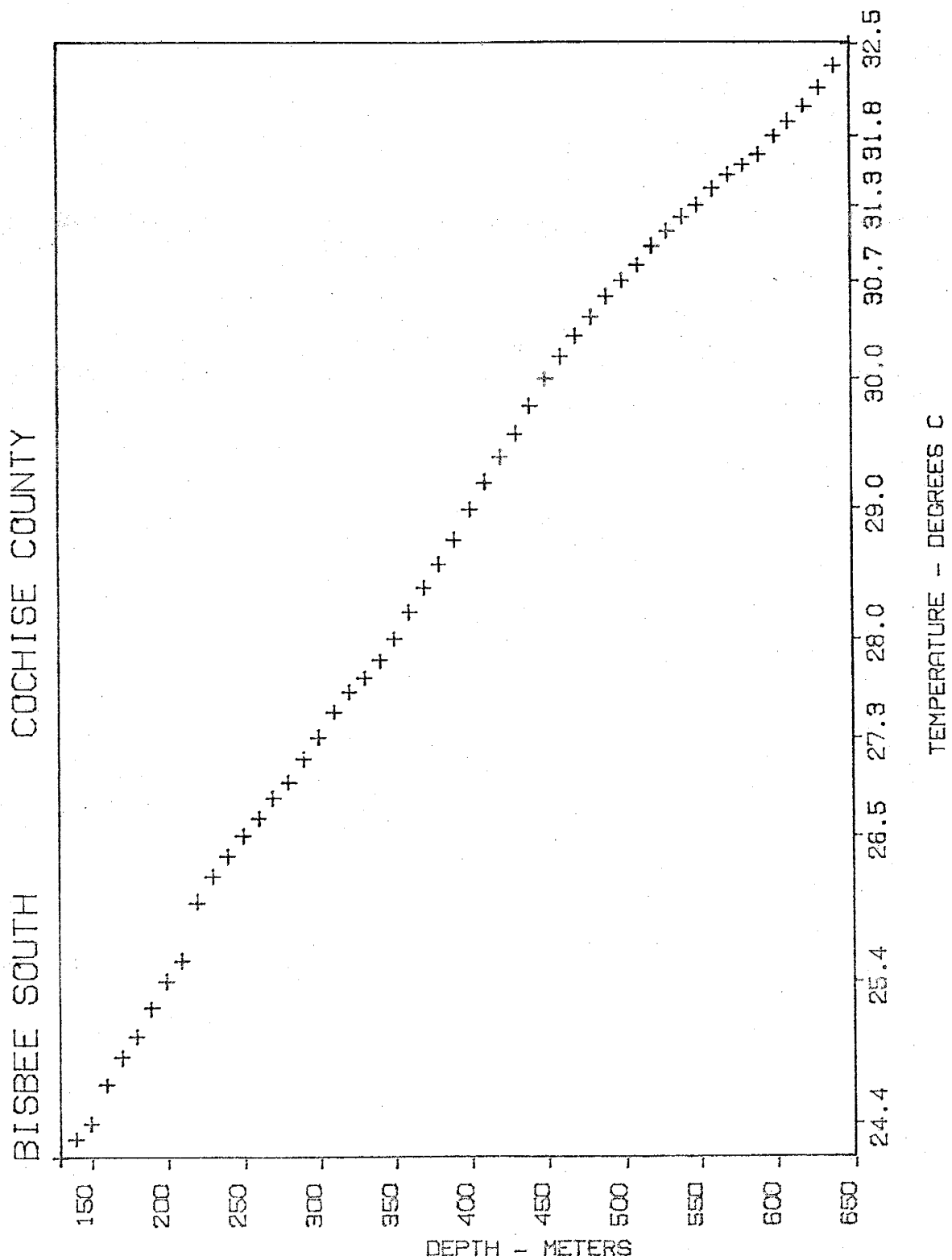
BISBEE SOUTH
COCHISE COUNTY
DEPTH - METERS
150
200
250
300
350
400
450
500
550
600
650
TEMPERATURE - DEGREES C
24.4
25.4
26.5
27.3
28.0
29.0
30.0
30.7
31.3
31.8
32.5

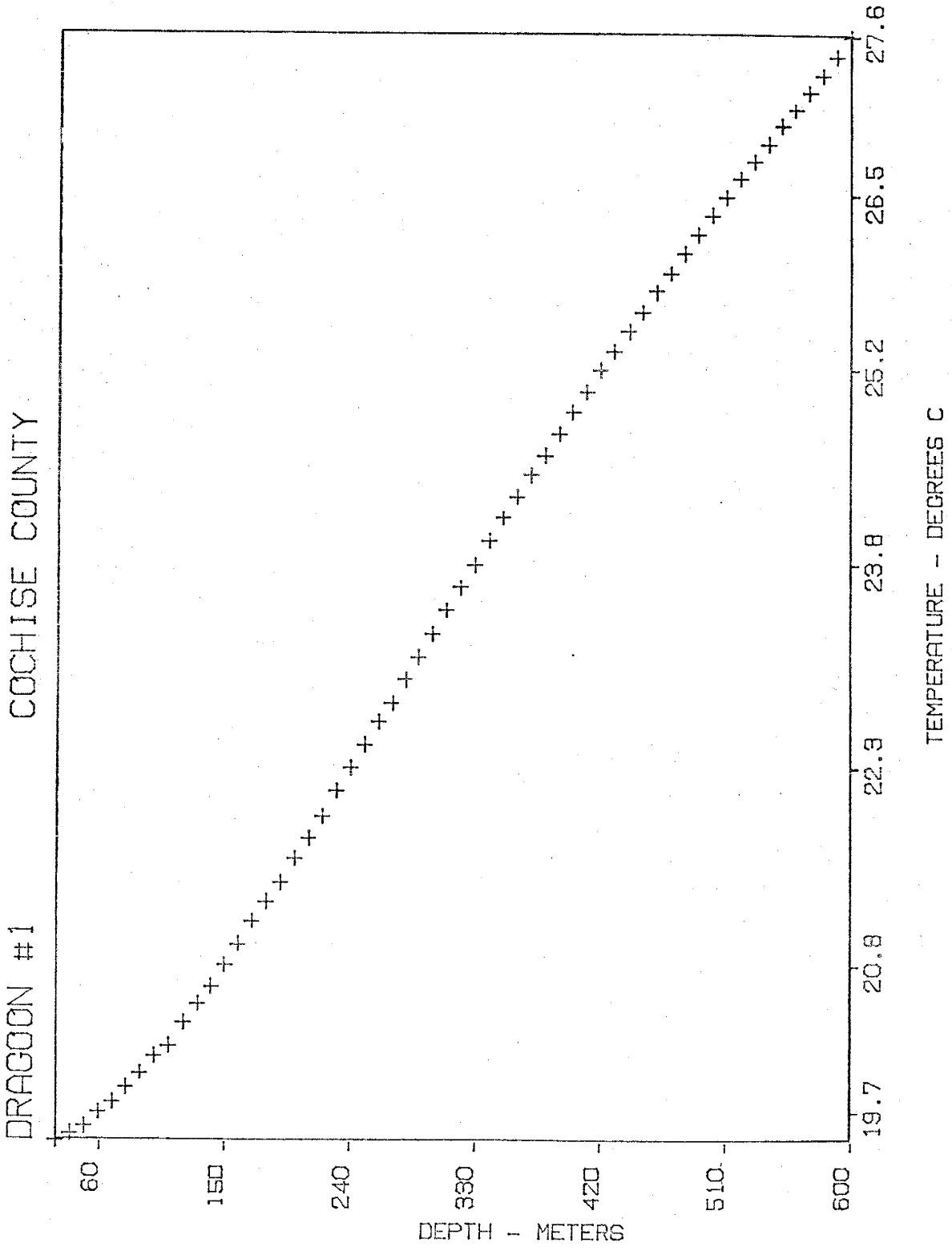
DRAGOON #1
COCHISE COUNTY
DEPTH - METERS
60
150
240
330
420
510
600
TEMPERATURE - DEGREES C
19.7
20.8
22.3
23.8
25.2
26.5
27.6

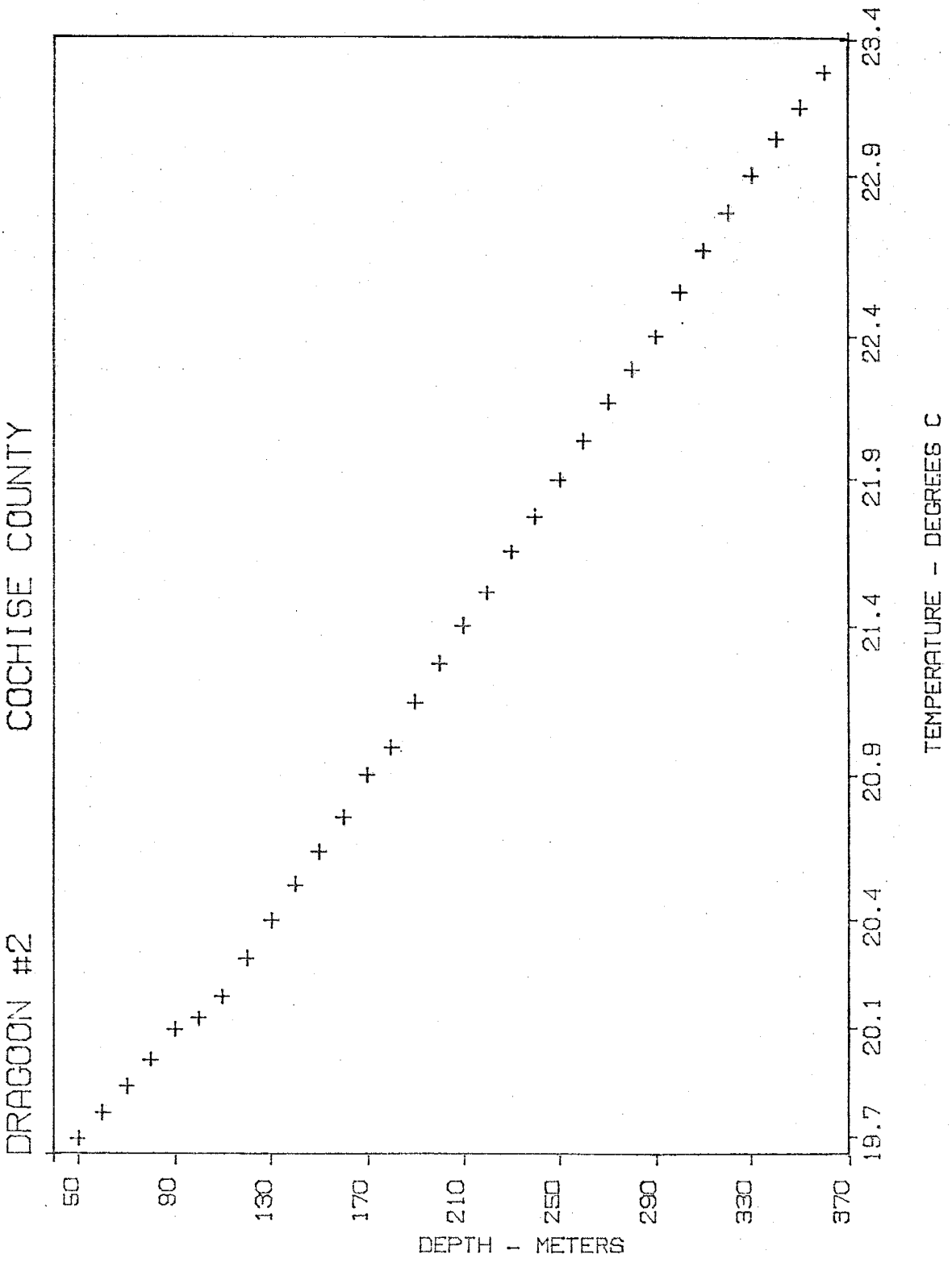
DRAGOON #2
COCHISE COUNTY
DEPTH - METERS
50
90
130
170
210
250
290
330
370
TEMPERATURE - DEGREES C
19.7
20.1
20.4
20.9
21.4
21.9
22.4
22.9
23.4

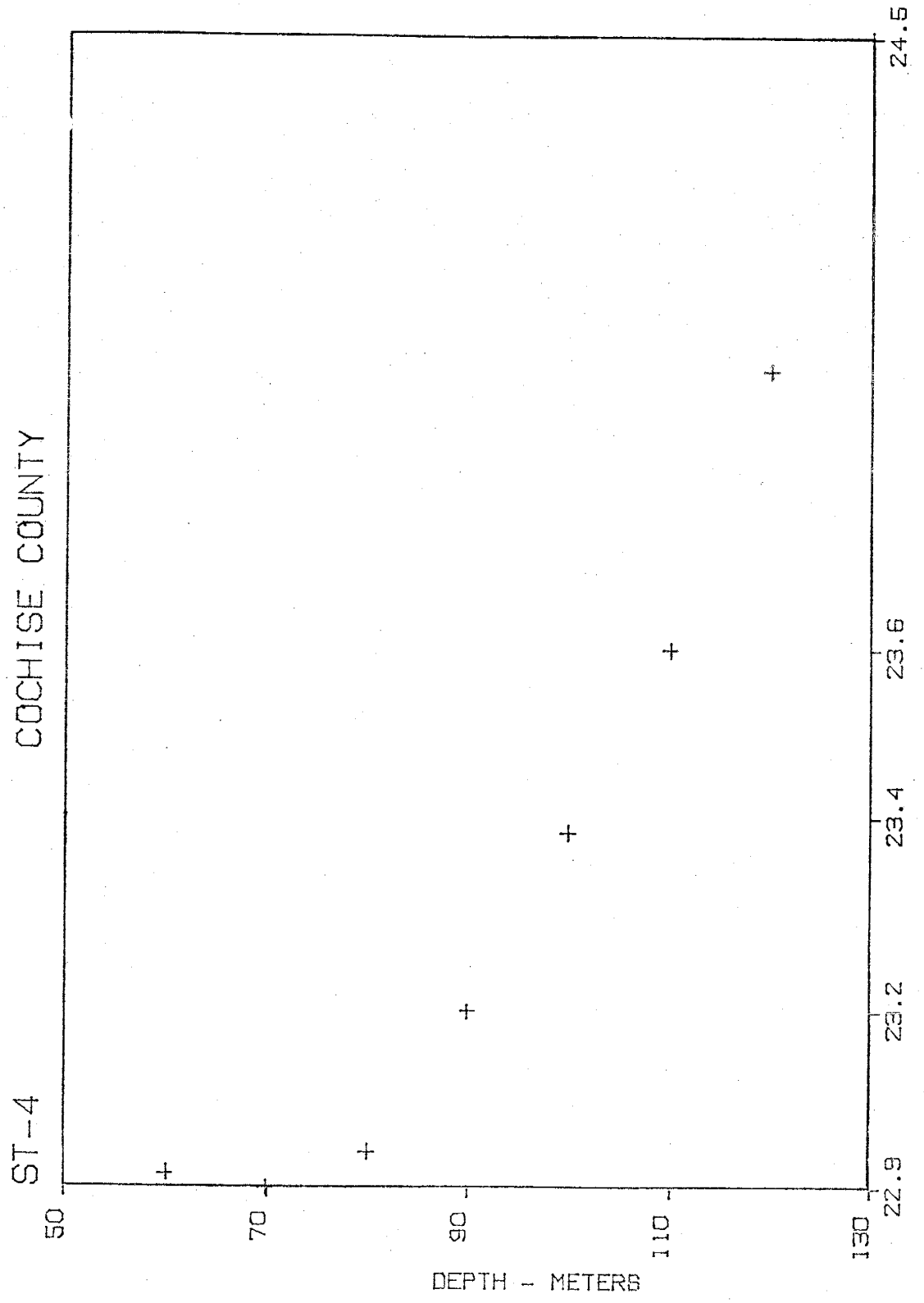
ST-4
COCHISE COUNTY
50
70
90
110
130
DEPTH - METERS
22.9
23.2
23.4
23.6
24.5
TEMPERATURE - DEGREES C

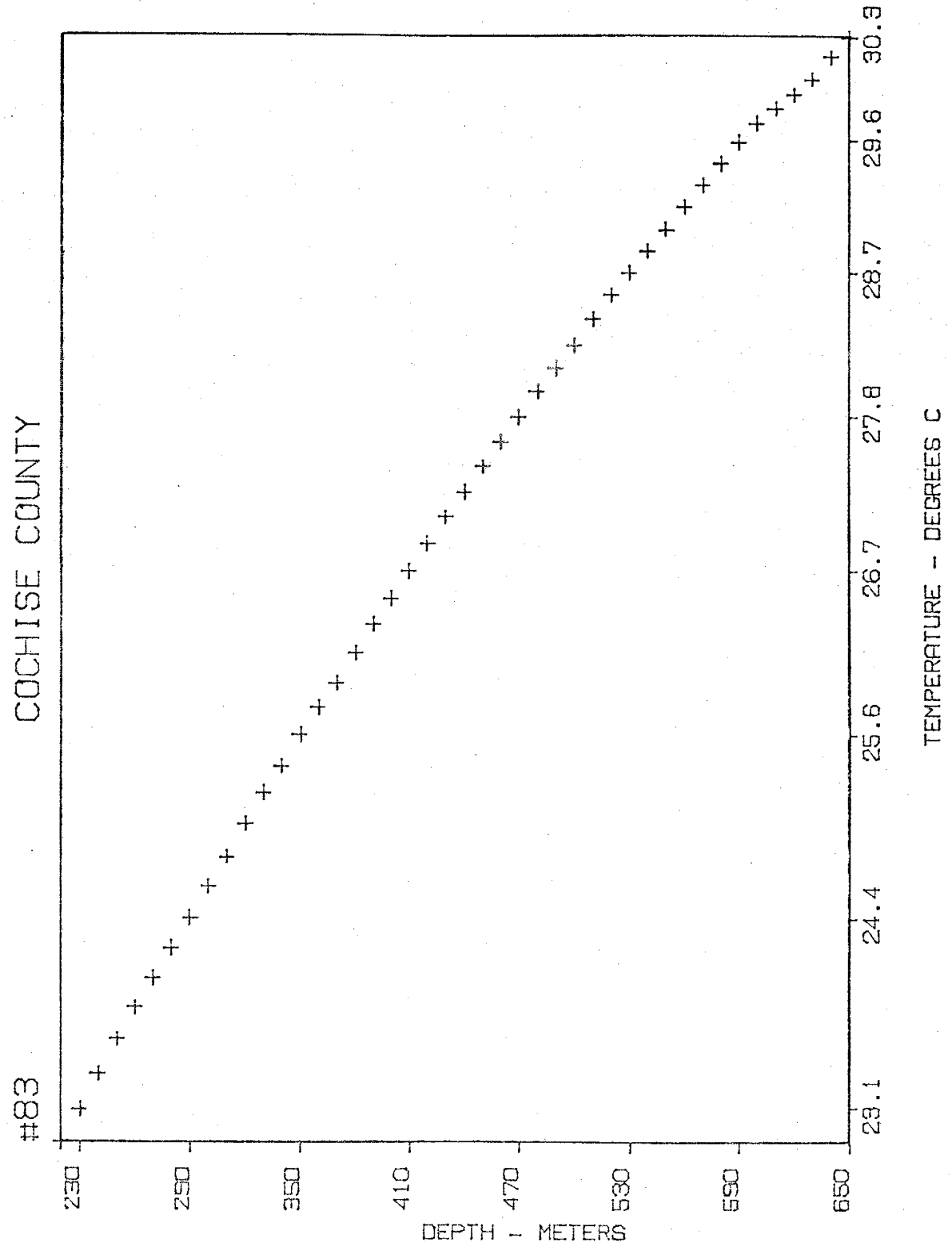
#83
COCHISE COUNTY
230
290
350
410
470
530
590
650
DEPTH - METERS
29.1
24.4
25.6
26.7
27.8
28.7
29.6
30.3
TEMPERATURE - DEGREES C

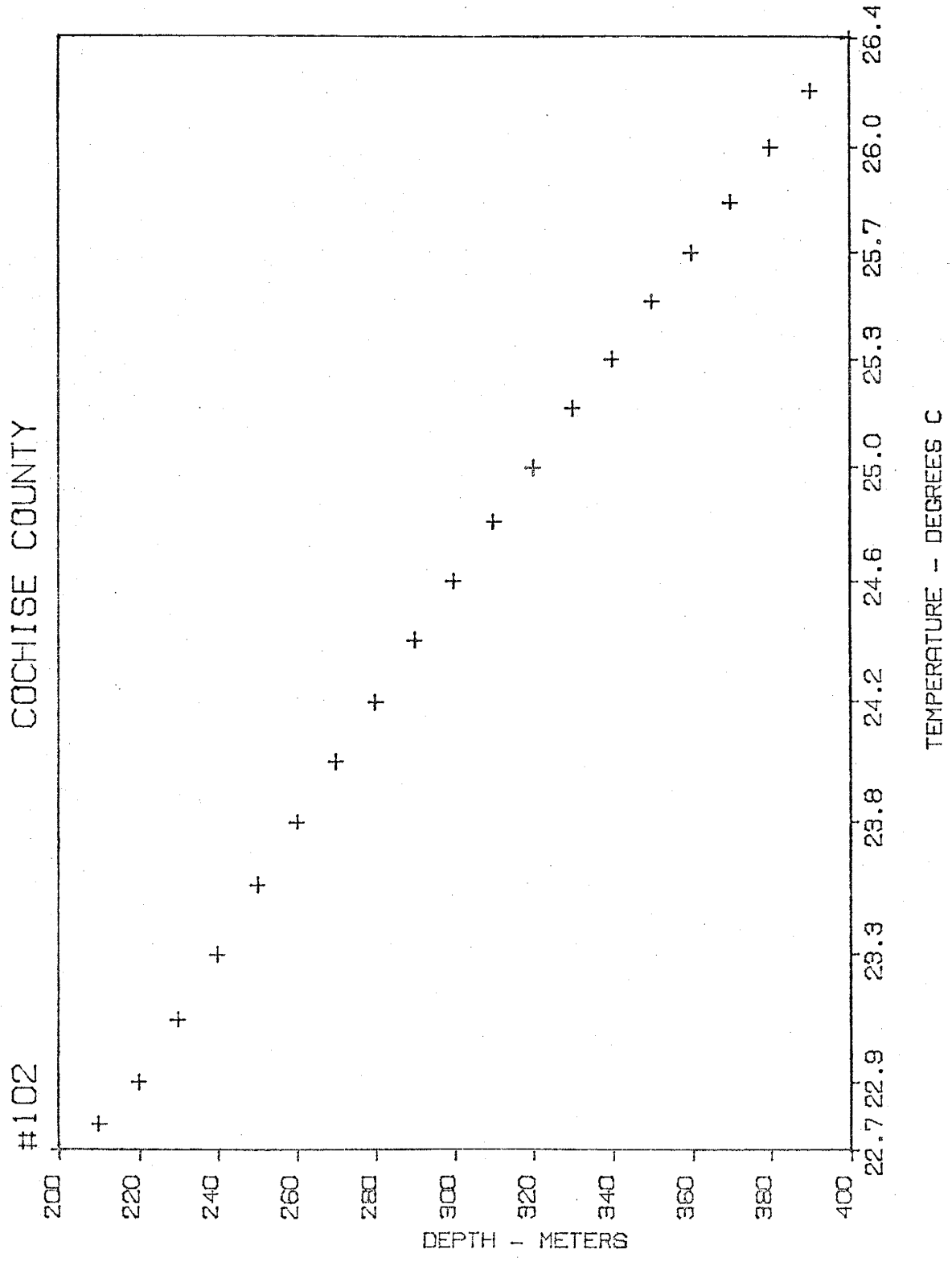
#102
COCHISE COUNTY
DEPTH - METERS
200
220
240
260
280
300
320
340
360
380
400
TEMPERATURE - DEGREES C
22.7
22.9
23.3
23.8
24.2
24.6
25.0
25.3
25.7
26.0
26.4

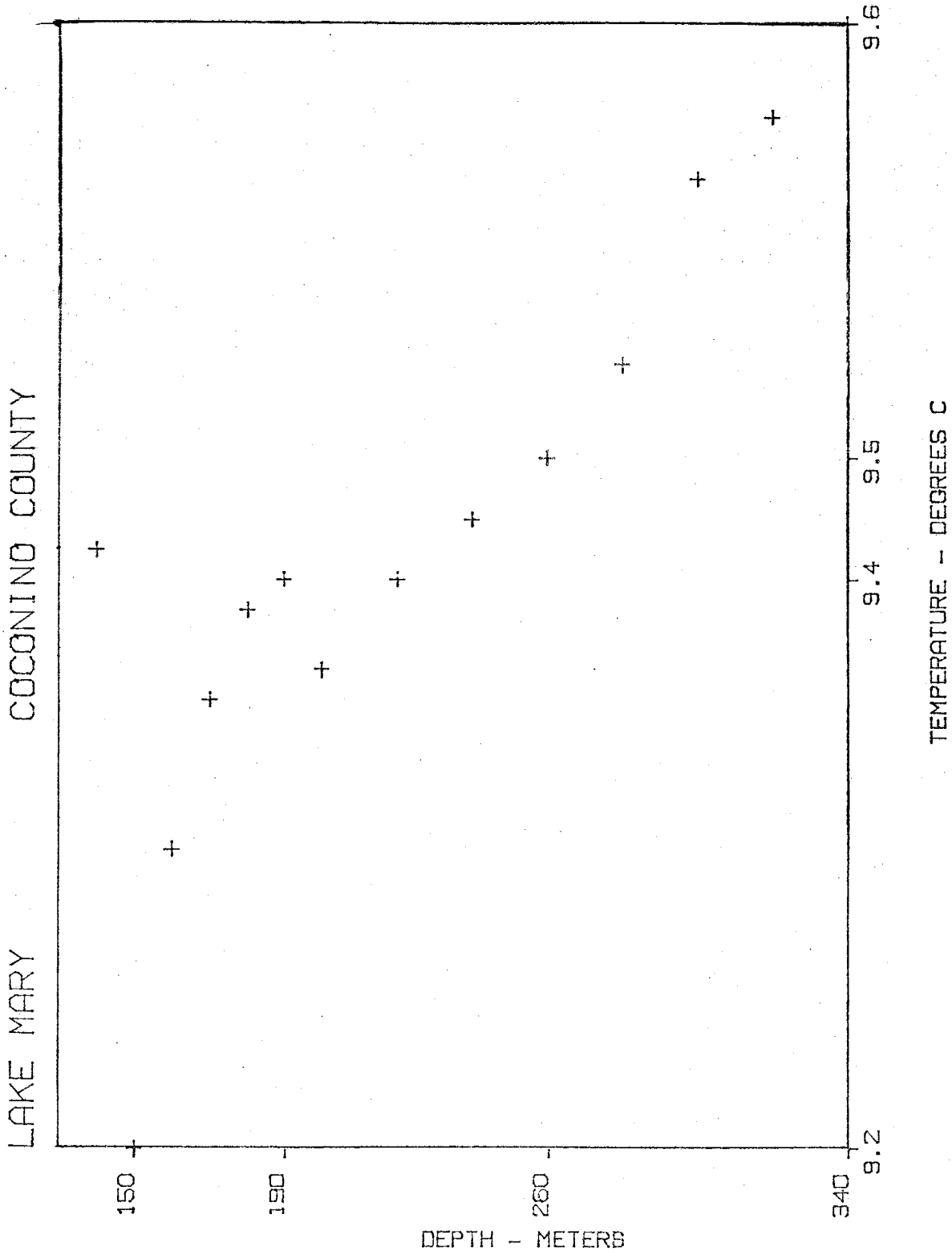
LAKE MARY
COCONINO COUNTY
150
190
260
340
DEPTH - METERS
9.2
9.4
9.5
9.6
TEMPERATURE - DEGREES C

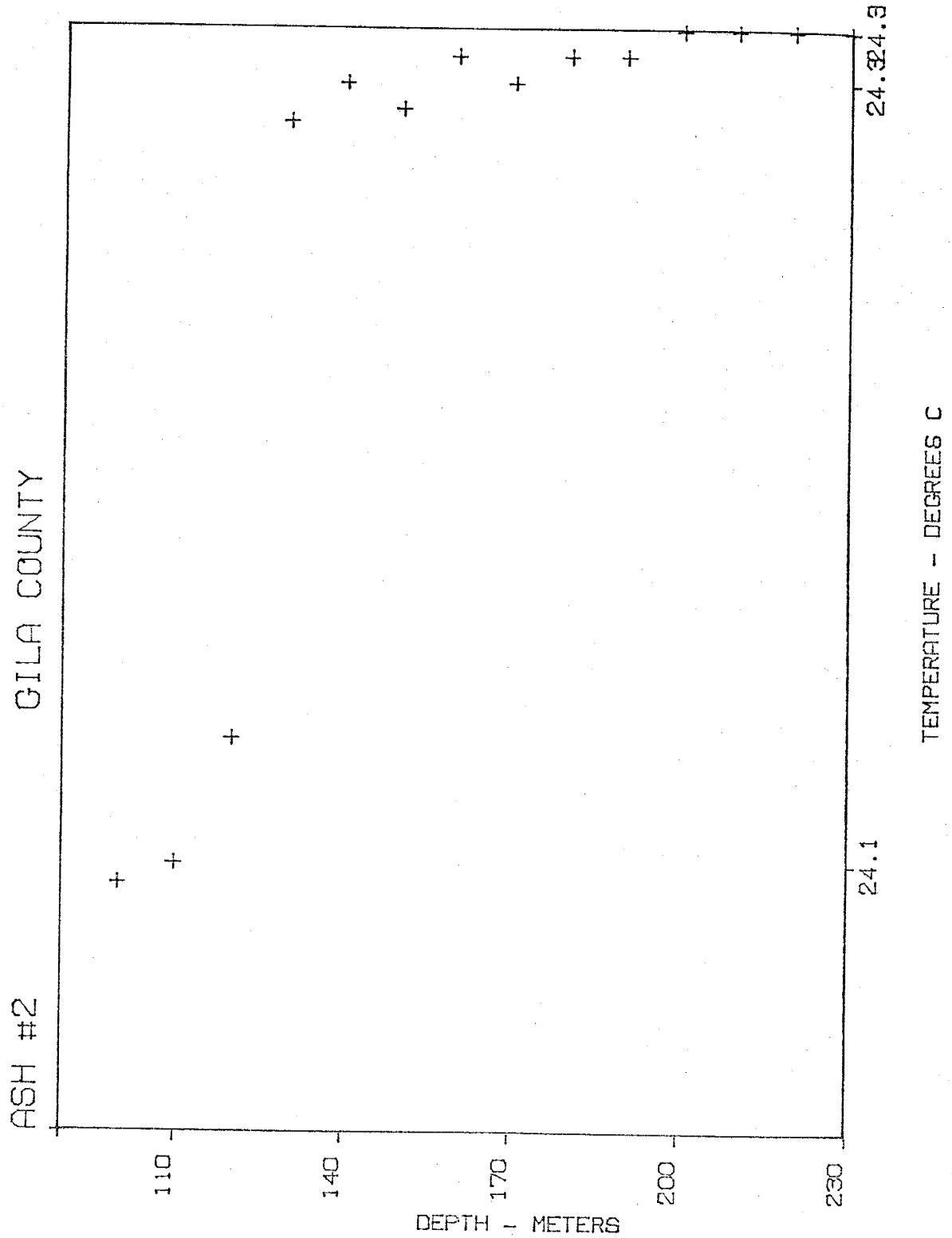
ASH #2
GILA COUNTY
110
140
170
200
230
DEPTH - METERS
24.1
24.3
24.5
TEMPERATURE - DEGREES C

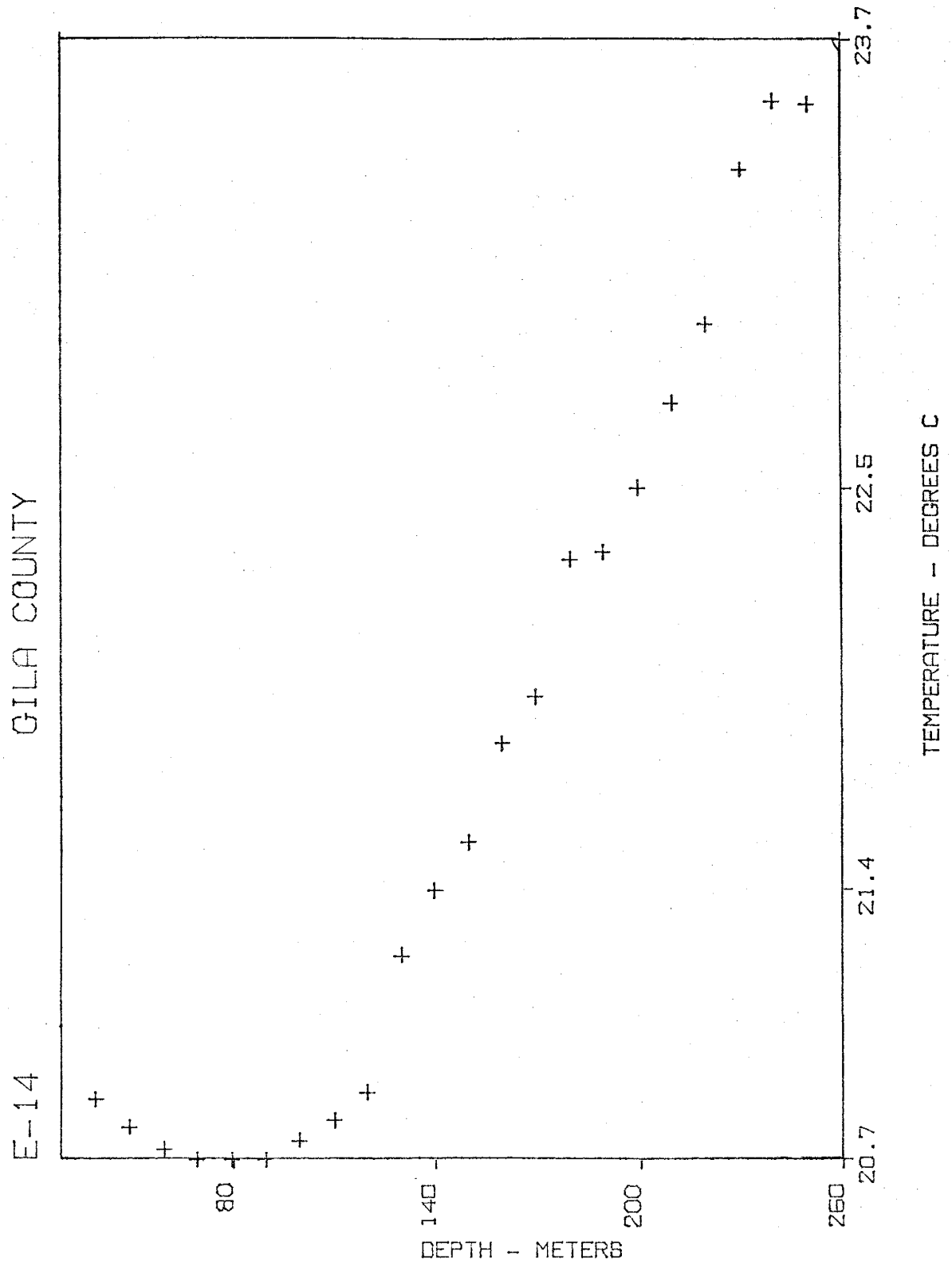
E-14
GILA COUNTY
80
140
200
260
DEPTH - METERS
20.7
21.4
22.5
23.7
TEMPERATURE - DEGREES C

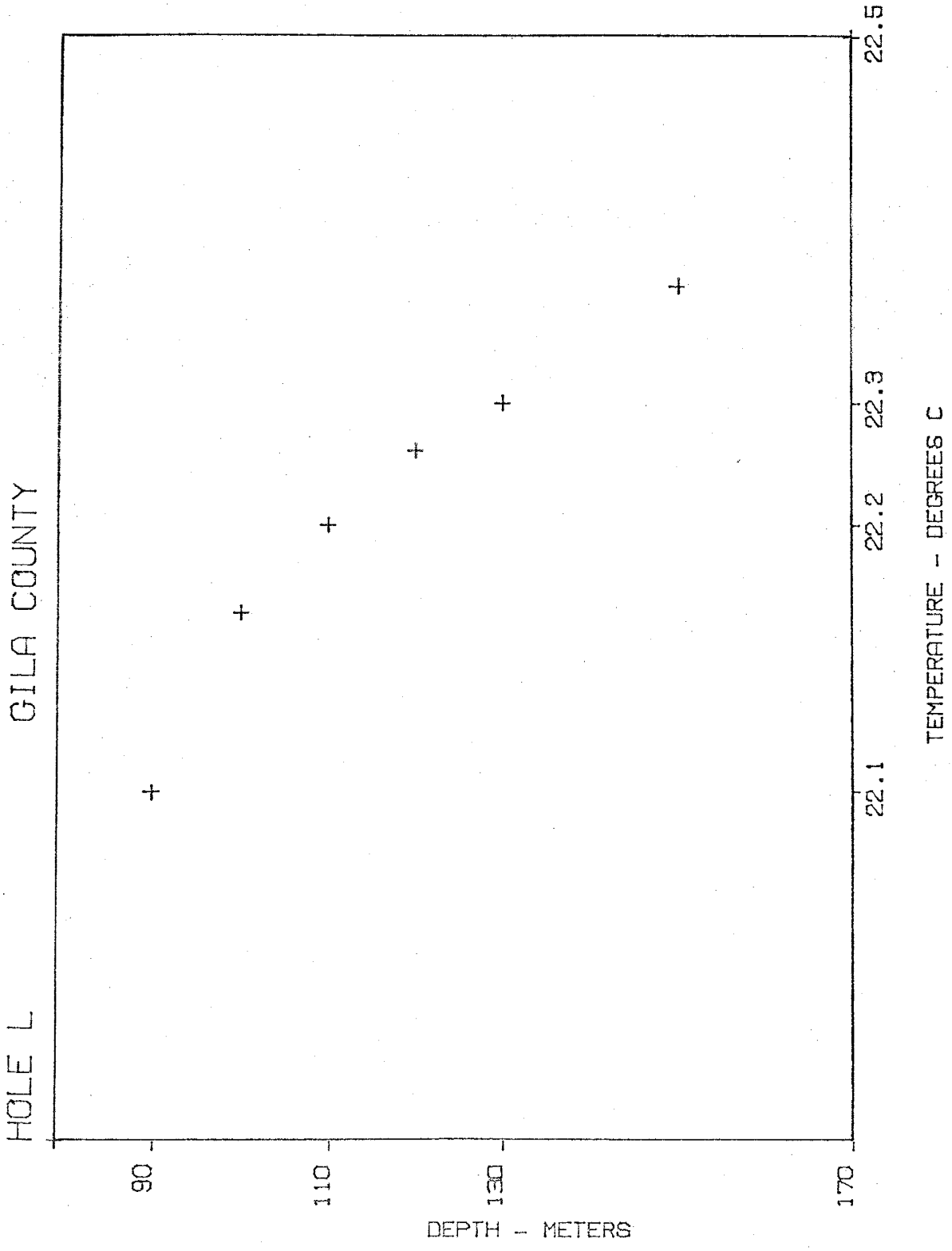
HOLE L
GILA COUNTY
90
110
130
170
DEPTH - METERS
22.1
22.2
22.3
22.5
TEMPERATURE - DEGREES C

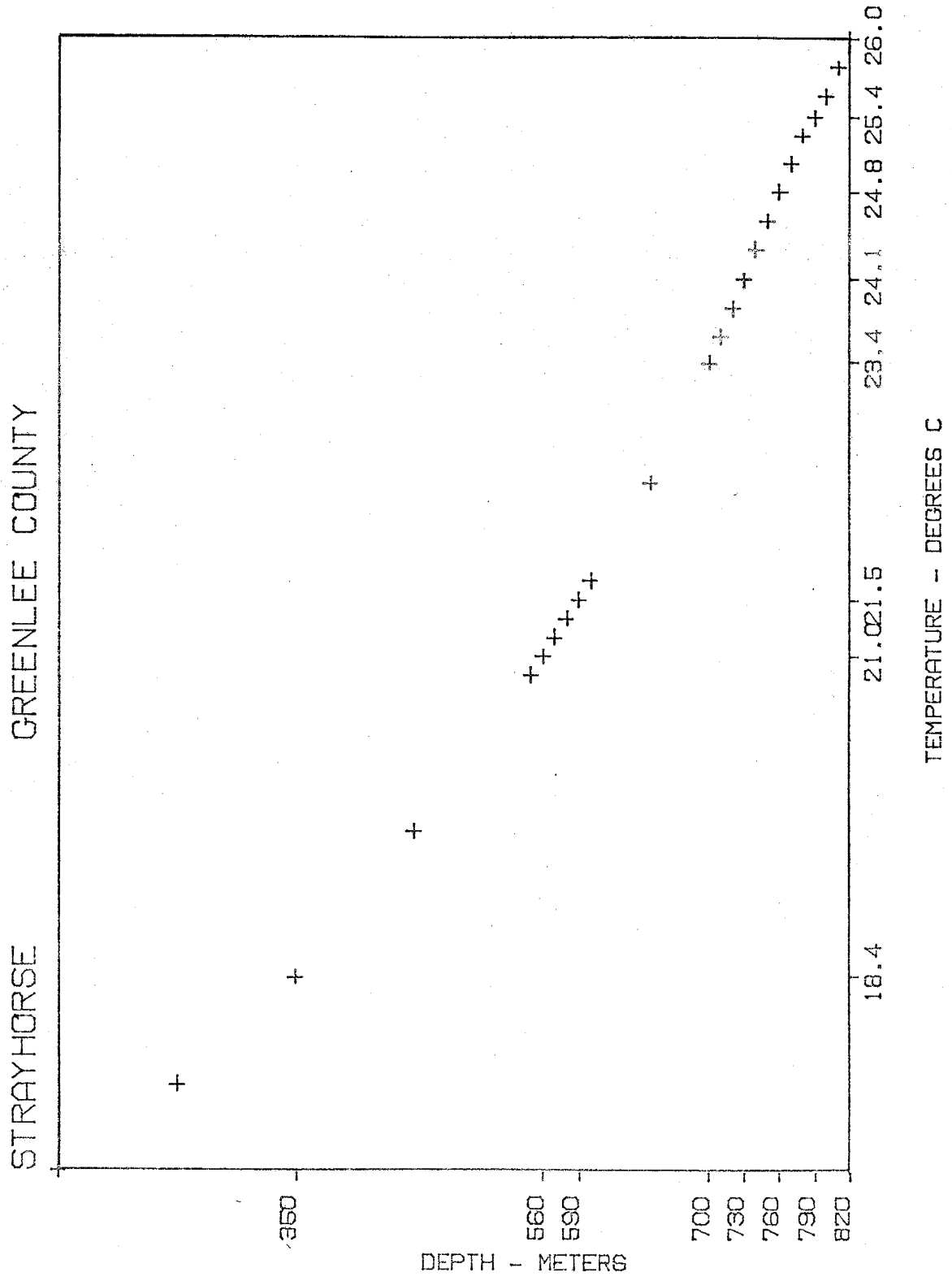
STRAYHORSE
GREENLEE COUNTY
350
560
590
700
730
760
790
820
DEPTH - METERS
18.4
21.0
21.5
23.4
24.1
24.8
25.4
26.0
TEMPERATURE - DEGREES C

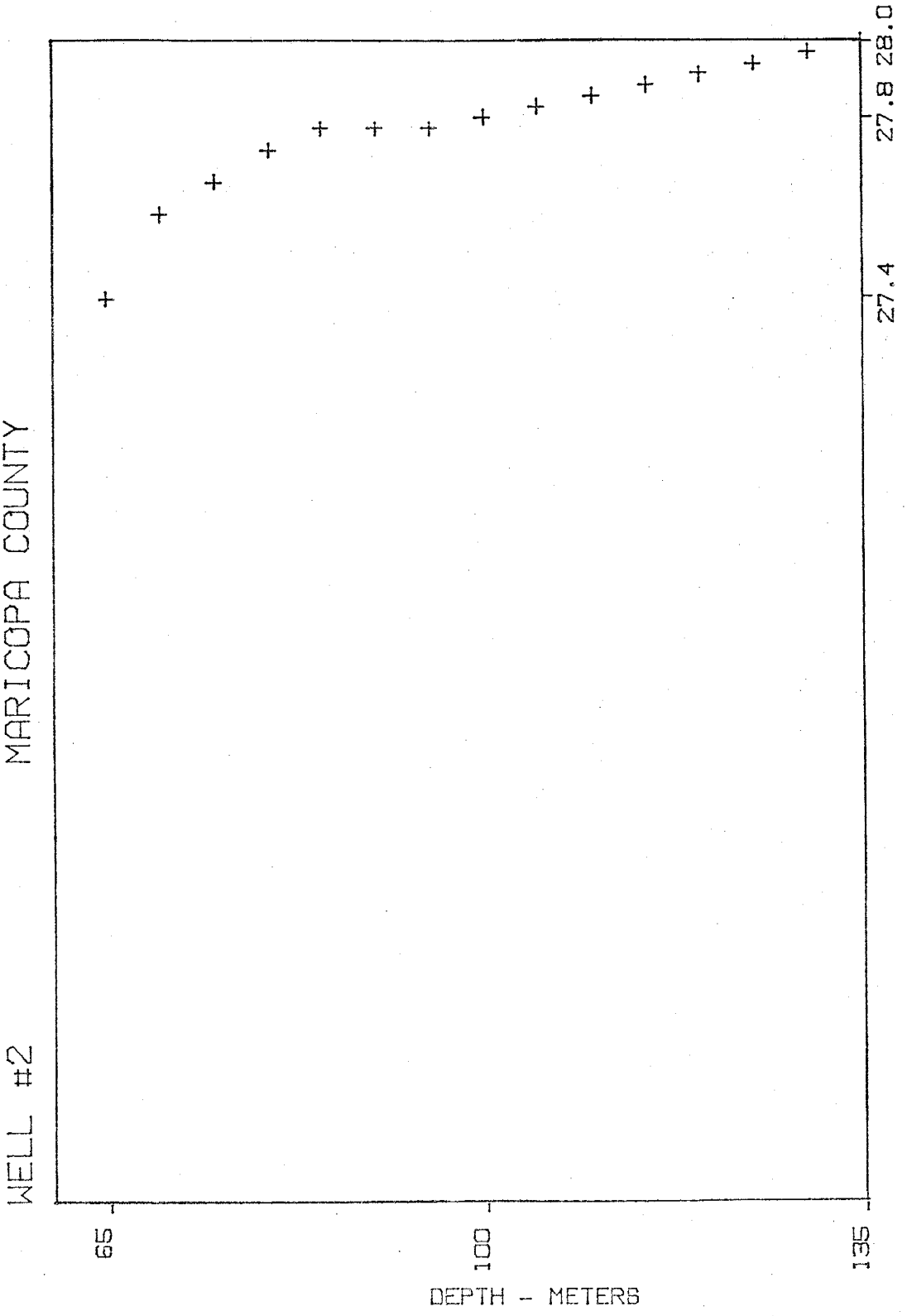
WELL #2
MARICOPA COUNTY
65
100
135
DEPTH - METERS
27.4
27.8
28.0
TEMPERATURE - DEGREES C

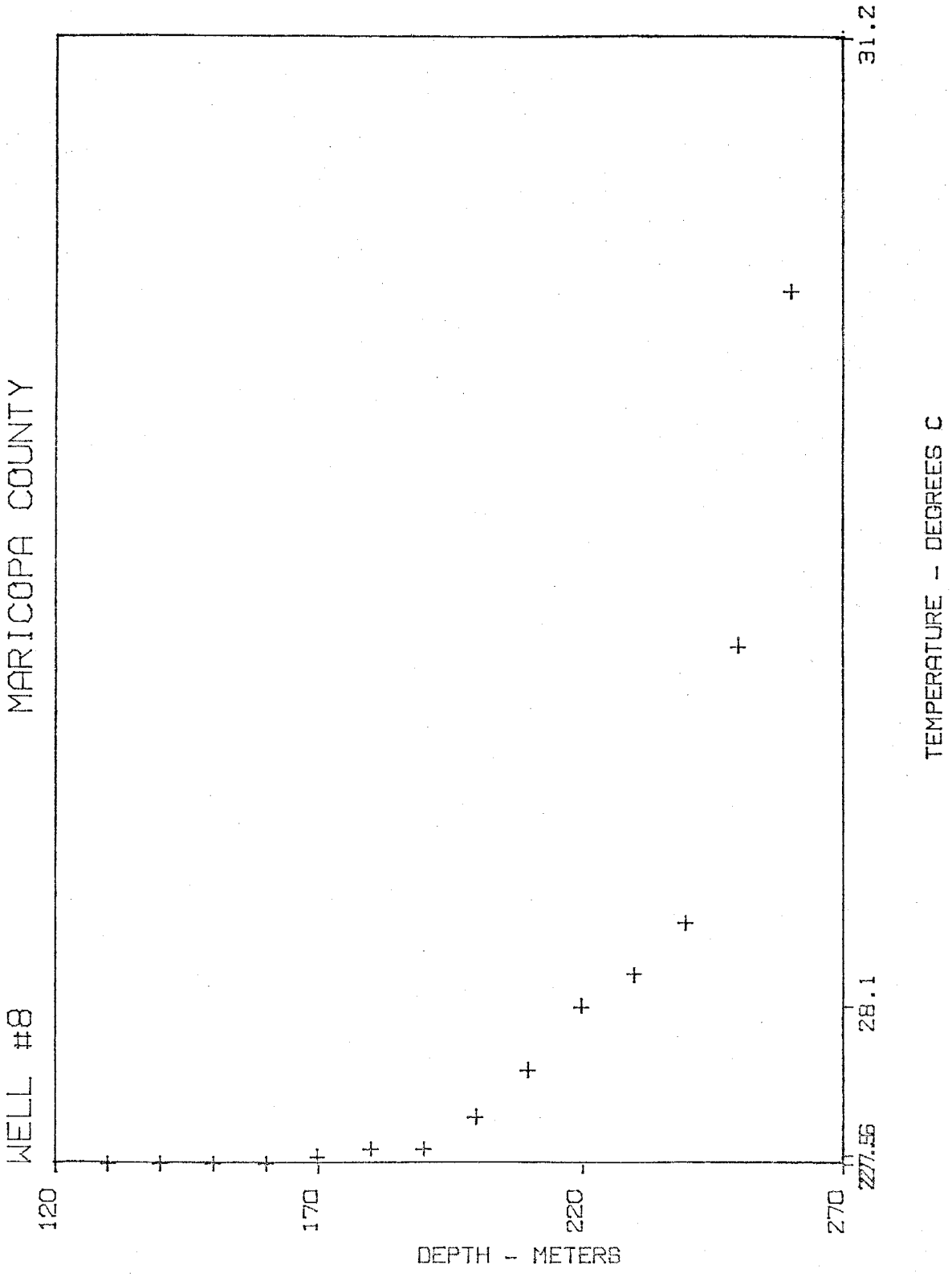
WELL #8
MARICOPA COUNTY
120
170
220
270
DEPTH - METERS
227.56
28.1
31.2
TEMPERATURE - DEGREES C

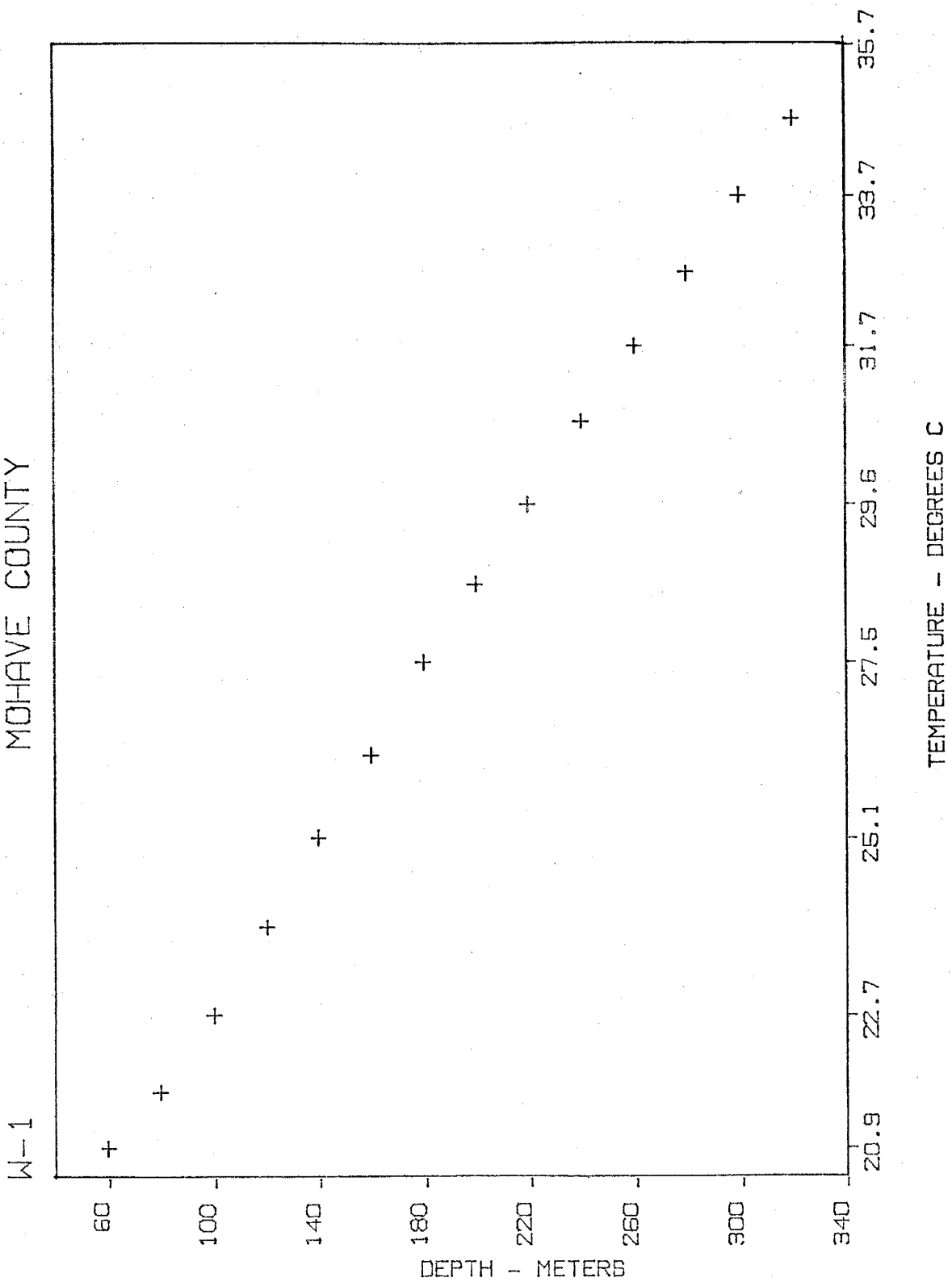
W-1
MOHAVE COUNTY
DEPTH - METERS
60
100
140
180
220
260
300
340
TEMPERATURE - DEGREES C
20.9
22.7
25.1
27.5
29.6
31.7
33.7
35.7

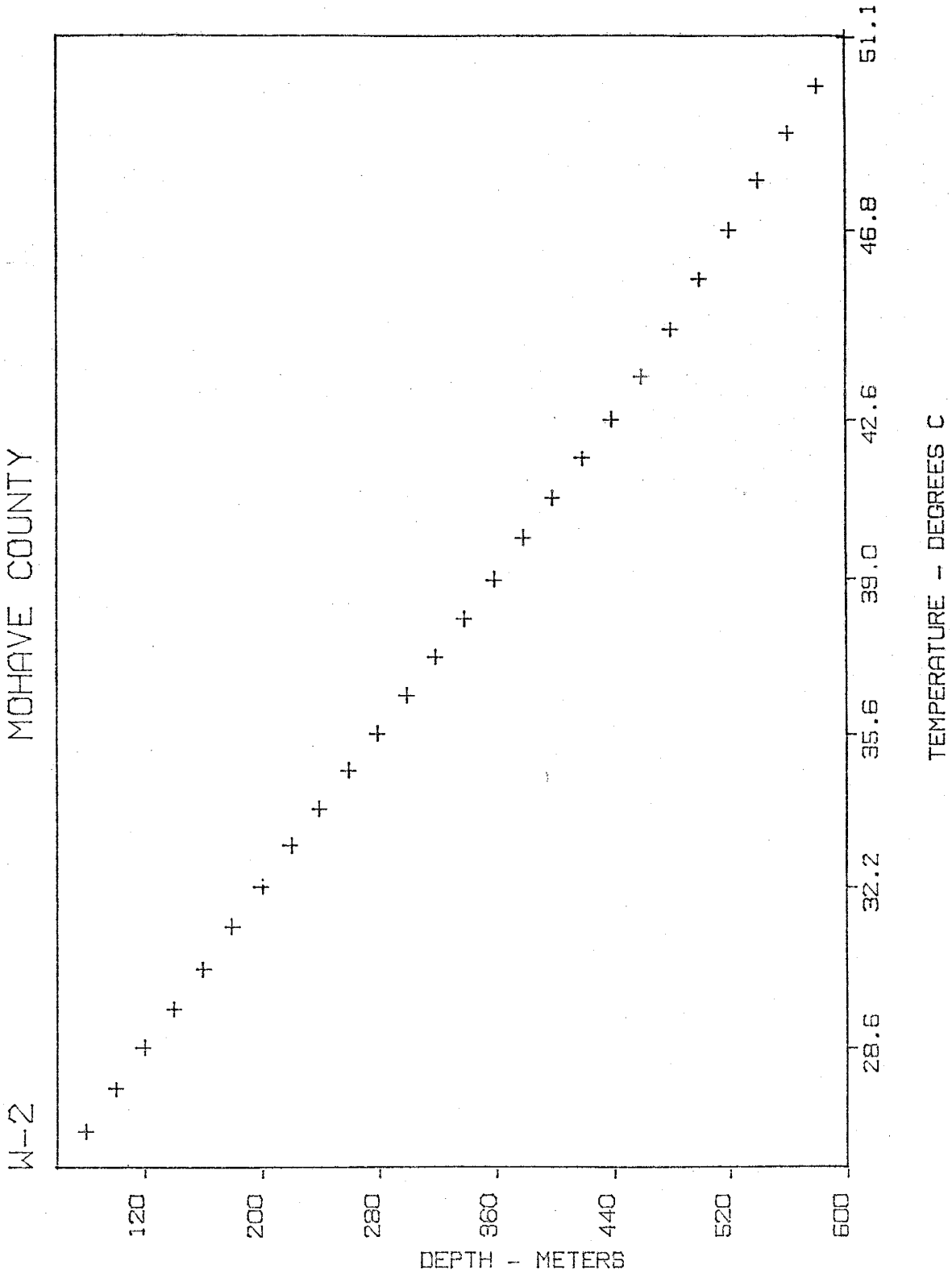
W-2
MOHAVE COUNTY
120
200
280
360
440
520
600
DEPTH - METERS
28.6
32.2
35.6
39.0
42.6
46.8
51.1
TEMPERATURE - DEGREES C

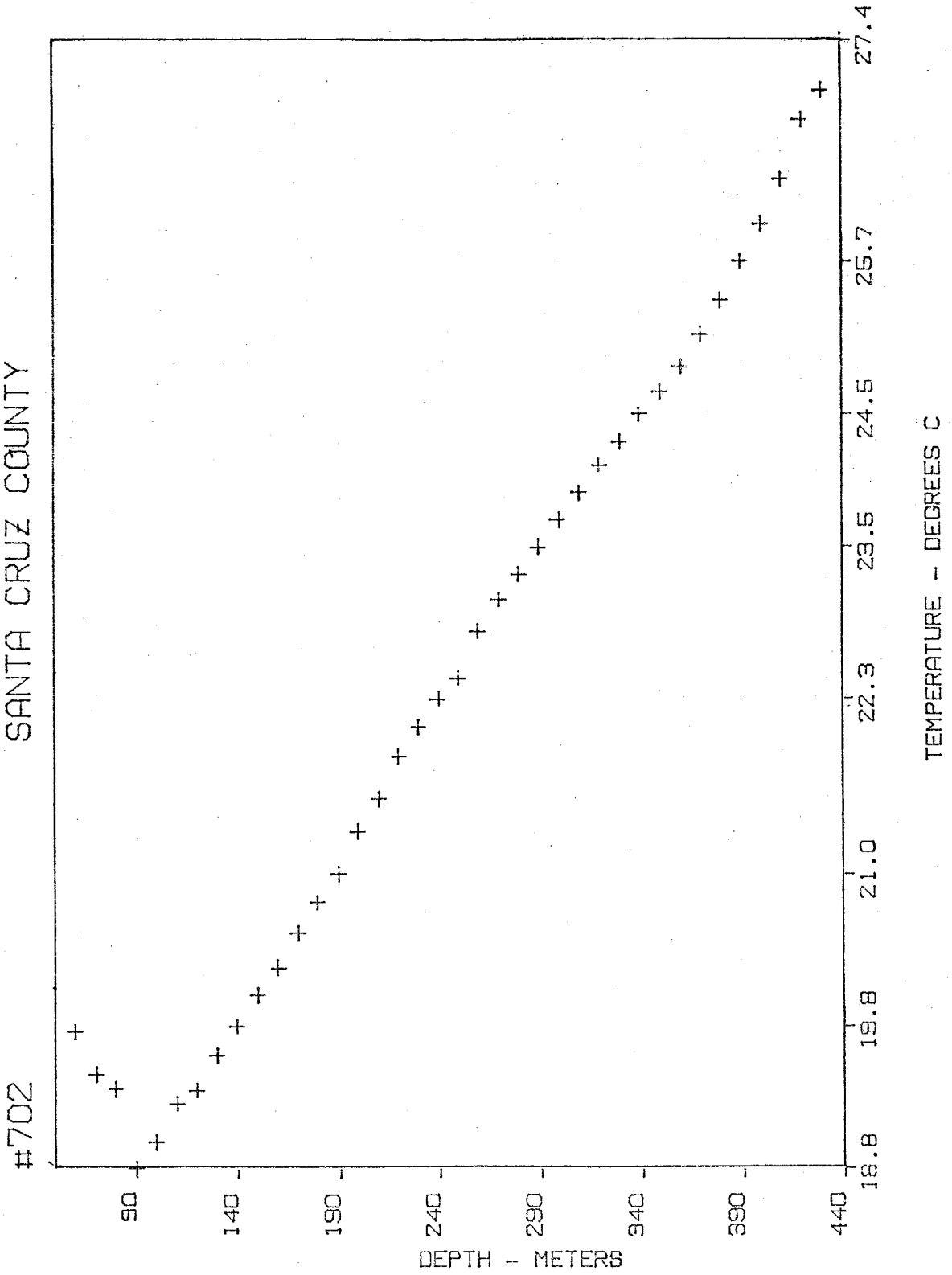
#702
SANTA CRUZ COUNTY
DEPTH - METERS
90
140
190
240
290
340
390
440
18.8
19.8
21.0
22.3
23.5
24.5
25.7
27.4
TEMPERATURE - DEGREES C

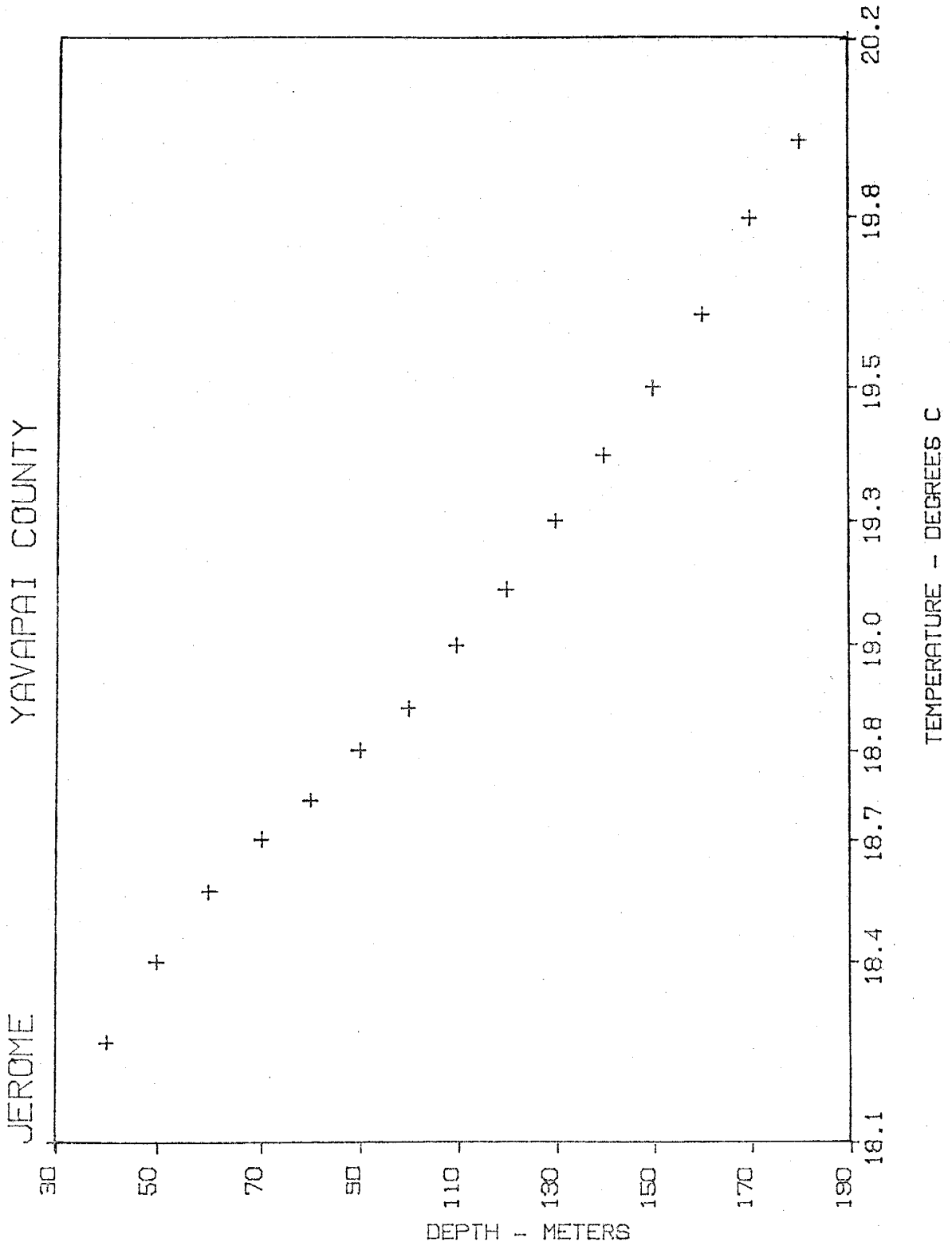
JEROME
YAVAPAI COUNTY
DEPTH - METERS
30
50
70
90
110
130
150
170
190
TEMPERATURE - DEGREES C
18.1
18.4
18.7
18.8
19.0
19.3
19.5
19.8
20.2

BIBLIOGRAPHY

Allis, R. G., A heat production model for stable continental crust, Tectonophysics, 57, 151-165, 1979.

Amiel, S., Analytical applications of delayed neutron emission in fissionable elements, Analytical Chemistry, 34, 1683-1692, 1962.

Anderson, C. A., and S. C. Creasey, Geology and ore deposits of the Jerome area, Yavapai County, Arizona, U.S. Geol. Surv. Prof. Pap., 308, 185, p. 1958.

Atwater, T., Implications of plate tectonics for the Cenozoic tectonic evolution of western North America, Geol. Soc. Amer. Bull., 81, 3513-3536, 1970.

Beck, A. E., An improved method of computing the thermal conductivity of fluid-filled sedimentary rocks, Geophysics, 41, 133-144, 1976.

Birch, F., Flow of heat in the Front Range, Colorado, Geol. Soc. Amer. Bull., 61, 567-630, 1950.

Birch, F., R. F. Roy, and E. R. Decker, Heat flow and thermal history in New England and New York, in Studies of Appalachian Geology: Northern and Maritime, edited by E. A. Zen, W. S. White, J. B. Hadley, and J. B. Thompson, pp. 437-451, Interscience, New York, 1968.

Bredehoeft, J. D., and I. S. Papadopulos, Rates of vertical groundwater movement estimated from the earth's thermal profile, Water Resources Research, 1, 325-328, 1965.

Bucher, R. L., and R. B. Smith, Crustal structures of the eastern Basin and Range province and the northern Colorado Plateau from phase velocities of Rayleigh waves, in The Structure and Physical Properties of the Earth's Crust, Geophys. Mongr. Ser., vol. 14, edited by J. G. Heacock, pp. 59-70, AGU, Washington, D.C., 1971.

Bullard, E. C., The disturbance of the temperature gradient in the earth's crust by inequalities of height, Monthly Notices Roy. Astron. Soc., Geophys. Suppl., 4, 360-362, 1940.

Carslaw, H. S., and J. C. Jaeger, Conduction of Heat in Solids, 2nd ed., Oxford University Press, New York, 510 p., 1959.

Chapin, C. E., and W. R. Seager, Evolution of the Rio Grande rift in the Socorro and Las Cruces areas, in Guidebook of the Las Cruces County, edited by W. R. Seager, R. E. Clemons, and J. F. Callender, pp. 297-321, New Mexico Geological Society, 1975.

Chapman, D. S., and H. N. Pollack, Regional geotherms and lithospheric thickness, Geology, 5, 265-268, 1977.

Christiansen, R. L., and P. W. Lipman, Cenozoic volcanism and plate tectonic evolution of western United States, II, Late Cenozoic, Phil. Trans. Roy. Soc. London, Ser. A, 271, 249-284, 1972.

Clark, S. P., Jr., Thermal Conductivity, in Handbook of Physical Constants, Geol. Soc. Amer. Mem., 97, edited by S. P. Clark Jr., pp. 459-482, Geol. Soc. Amer., Inc., Boulder, Colo., 1966.

Condie, K. C., Plate Tectonics and Crustal Evolution, Pergamon Press, New York, 288 p., 1976.

Coney, P. J., Mesozoic-Cenozoic Cordilleran plate tectonics, in Cenozoic Tectonics and Regional Geophysics of the Western Cordillera, Geol. Soc. Amer. Mem., 152, edited by R. B. Smith and G. P. Eaton, pp. 33-50, Geol. Soc. Amer., Inc., Boulder, Colo., 1978.

Costain, J. K., P. M. Wright, Heat flow at Spor Mountain, Jordan Valley, Bingham and La Sal, Utah, J. Geophys. Res., 78, 8687-8698, 1973.

Crowe, B. M., Cenozic volcanic geology and probable age of inception of basin-range faulting in the southeastern-most Chocolate Mountains, California, Geol. Soc. Amer. Bull., 89, 251-264, 1978.

Decker, E. R., Heat flow in Colorado and New Mexico, J. Geophys. Res., 75, 550-559, 1969.

Decker, E. R., and S. B. Smithson, Heat flow and gravity interpretation across the Rio Grande rift in southern New Mexico and west Texas, J. Geophys. Res., 80, 2542-2552, 1975.

Diment, W. H., T. C. Urban, J. H. Sass, B. V. Marshall, R. J. Monroe, and A. H. Lachenbruch, Temperatures and heat contents based on conductive transport of heat, in U.S. Geol. Surv. Circ., 726, pp. 84-103, 1975.

Donaldson, I. G., Temperature gradients in the upper layers of the earth's crust due to convective water flows, J. Geophys. Res., 67, 3449-3459, 1962.

Eardley, A. J., Structual Geology of North America, 2nd ed., Harper and Row, New York, 743 p., 1962.

Eaton, G. P., A plate-tectonic model for late Cenozoic crustal spreading in the western United States, in Rio Grande Rift: Tectonics and Magmatism, edited by R. E. Riecker, pp. 7-32, AGU, Washington, D.C., 1979.

Eaton, G. P., R. R. Wahl, H. J. Prostka, D. R. Mabey, and M. D. Kleinkopf, Regional gravity and tectonic patterns: Their relation to late Cenozoic epeirogeny and lateral spreading in the western Cordillera, in Cenozoic Tectonics and Regional Geophysics of the Western Cordillera, Geol. Soc. Amer. Mem., 152, edited by R. B. Smith and G. P. Eaton, pp. 51-91, Geol. Soc. Amer., Inc., Boulder, Colo., 1978.

Eberly, L. D., and T. B. Stanley, Jr., Cenozoic stratigraphy and geologic history of southwestern Arizona, Geol. Soc. Amer. Bull., 89, 921-940, 1978.

Edwards, C. L., M. Reiter, C. Shearer, and W. Young, Terrestrial heat flow and crustal radioactivity in northeastern New Mexico and southeastern Colorado, Geol. Soc. Amer. Bull., 89, 1341-1350, 1978.

Gillespie, J. B., and C. B. Bentley, Geohydrology of Hualpai and Sacramento Valleys, Mohave County, Arizona, U.S. Geol. Surv. Water Supply Pap., 1889-H, pp. H1-H37, 1971.

Gough, D. I., Electrical conductivity under western North America in relation to heat flow, seismology and structure, J. Geomag. Geoelectr., 26, 105-123, 1974.

Hunt, C. B., Cenozoic geology of the Colorado Plateau, U.S. Geol. Surv. Prof. Pap., 279, 99 p., 1956.

Ives, R., Recent vulcanism in northwestern Mexico, Pan Am. Geol., 63, 335-338, 1935.

Jaeger, J. C., The effect of the drilling fluid on temperatures measured in bore holes, J. Geophys. Res., 66, 563-569, 1961.

Jahns, R. H., Collapse depressions of the Pinacate Volcanic Field, Sonora, Mexico, in Southern Arizona Guidebook II, edited by L. A. Heindl, Arizona Geological Society, pp. 165-184, 1959.

Jeffreys, H., The disturbance of the temperature gradient in the earth's crust by inequalities of height, Monthly Notices Roy. Astron. Soc., Geophys. Suppl., 4, 309-312, 1940.

Keller, G. R., L. W. Braile, and P. Morgan, Regional crustal structure of the Colorado Plateau, in Papers presented to the conference on Plateau Uplift: Mode and Mechanism, Lunar Planet. Inst. Contr. 329, p. 26, 1978.

Kelley, V. C., Regional tectonics of the Colorado Plateau and relationship to the origin and distribution of uranium, Publ. in Geol. 5, Univ. of N. Mex., Albuquerque, 1955.

Lachenbruch, A. H., Crustral temperature and heat production: implications of the linear heat-flow relation, J. Geophys. Res., 75, 3291-3300, 1970.

Lachenbruch, A. H., and J. H. Sass, Heat flow in the United States and the thermal regime of the crust, in The Earth's Crust, Geophys. Monogr. Ser., vol. 20, edited by J. G. Heacock, pp. 626-675, AGU, Washington, D.C., 1977.

Lachenbruch, A. H., and J. H. Sass, Models of an extending lithosphere and heat flow in the Basin and Range province, in Cenozoic tectonics and regional geophysics of the western Cordillera, Geol. Soc. Amer. Mem., 152, 209-250, 1978.

Larson, R. L., H. W. Menard, and S. M. Smith, Gulf of California, a result of ocean-floor spreading and transform faulting, Science, 161, 781-784, 1968.

Lees, C. H., On the shapes of the isogeotherms under mountain ranges in radioactive districts, Proc. Roy. Soc. London, Ser. A, 83, 339-346, 1910.

Lubimova, E. A., R. P. Von Herzen, and G. B. Udintsev, On heat transfer through the ocean floor, in Terrestrial Heat Flow, Geophys. Monogr. Ser., vol. 8, edited by W. H. K. Lee, pp. 78-86, AGU, Washington, D.C., 1965.

Luchitta, I., Early history of the Colorado River in the Basin and Range province, Geol. Soc. Amer. Bull., 83, 1933, 1972.

MacDonald, G. J. F., Calculations on the thermal history of the earth, J. Geophys, Res., 64, 1967-2000, 1959.

Mansure, A. J. and M. Reiter, A vertical ground-water movement correction for heat flow, J. Geophys. Res., 84, 3490-3496, 1979.

McKee, E. D. and E. H. McKee, Pliocene uplift of the Grand Canyon region, time of drainage adjustment, Geol. Soc. Amer. Bull., 83, 1923-1932, 1972.

Moore, R. B., Cenozoic igneous rocks of the Colorado Plateau, in Papers presented to the conference on Plateau Uplift: Mode and Mechanism, Lunar Planet. Inst. Contr. 329, pp. 28-30, 1978.

Moore, R. B., and E. W. Wolfe, Geologic map of the eastern San Francisco Volcanic Field, Arizona, U.S. Geol. Surv. Misc. Invest. Ser., Map I-953, 1976.

Morrison, R. B., Ground-water resources of the Big Sandy Valley, Mohave County, Arizona, Ariz. State Water Commission, U.S. Geol. Surv. Mimeo Rep., 6 p., 1940.

Negi, J. G., and R. Narain Singh, On heat transfer in layered ocean sediments, Earth Planet. Sci. Lett., 2, 335-336, 1967.

Pakiser, L. C., Structure of the crust and upper mantle in the western United States, J. Geophys. Res., 68, 5747-5756, 1963.

Ratté, J. C., E. R. Landis, D. L. Gaskill, and R. G. Raabe, Mineral resources of the Blue Range Primitive Area, Greenlee County, Arizona, and Catron County, New Mexico, U.S. Geol. Surv. Bull., 1261-E, E1-E91, 1969.

Rehrig, W. A., and T. L. Heidrick, Regional tectonic stress during the Laramide and late Tertiary intrusive periods, Basin and Range province, Arizona, in Arizona Geol. Soc. Digest, vol. 10, edited by J. C. Wilt and J. P. Jenney, pp. 205-228, Tucson, 1976.

Reiter, M., C. L. Edwards, H. Hartman, and C. Weidman, Terrestrial heat flow along the Rio Grande rift, New Mexico and southern Colorado, Geol. Soc. Amer. Bull., 86, 811-818, 1975.

Reiter, M., and H. Hartman, A new steady-state method for determining thermal conductivity, J. Geophys. Res., 76, 7047-7051, 1971.

Reiter, M., A. J. Mansure, and C. Shearer, Geothermal characteristics of the Colorado Plateau, Tectonophysics, 61, 1979a.

Reiter, M., A. J. Mansure, and C. Shearer, Geothermal characteristics of the Rio Grande rift within the southern Rocky Mountain complex, in Rio Grande Rift: Tectonics and Magmatism, edited by R. E. Riecker, pp. 253-267, AGU, Washington, D.C., 1979b.

Reiter, M., C. Shearer, and C. L. Edwards, Geothermal anomalies along the Rio Grande rift in New Mexico, Geology, 6, 85-88, 1978.

Ringwood, A. E., Composition and Petrology of the Earth's Mantle, McGraw-Hill, New York, 618 p., 1975.

Roller, J. C., Crustral structure in the eastern Colorado Plateau Province from seismic-refraction measurements, Bull. Seismol. Soc. Amer., 55, 107-119, 1965.

Roy, R. F., D. D. Blackwell, and E. R. Decker, Continental heat flow, in The Nature of the Solid Earth, edited by E. C. Robertson, pp. 506-544, McGraw-Hill, New York, 1972.

Roy, R. F., E. R. Decker, D. D. Blackwell, and F. Birch, Heat flow in the United States, J. Geophys. Res., 72, 5207-5221, 1968a.

Roy, R. F., E. R. Decker, and D. D. Blackwell, Heat generation of plutonic rocks and continental heat flow provinces, Earth Planet. Sci. Lett., 5, 1-12, 1968b.

Sass, J. H., A. H. Lachenbruch, R. J. Monroe, G. W. Greene, and T. H. Moses, Heat flow in the western United States, J. Geophys. Res., 76, 6376-6413, 1971a.

Sass, J. H., A. H. Lachenbruch, and R. J. Monroe, Thermal conductivity of rocks from measurements on fragments and its application to heat flow determination, J. Geophys. Res., 76, 3391-3401, 1971b.

Shafiqullah, M., P. E. Damon, D. J. Lynch, P. H. Kuck, and W. A. Rehrig, Mid-Tertiary magmatism in southeastern Arizona, in Guidebook of the Land of Cochise, Southeastern Arizona, edited by J. F. Callender, J. C. Wilt, and R. E. Clemons, pp. 231-242, New Mexico Geological Society, 1978.

Smith, R. B., Seismicity, crustal structure, and intraplate tectonics of the interior of the western Cordillera, in Cenozoic Tectonics and Regional Geophysics of the Western Cordillera, Geol. Soc. Amer. Mem, 152, edited by R. B. Smith and G. P. Eaton, pp. 111-144, Geol. Soc. Amer. Inc., Boulder, Colo., 1978.

Smith, D. L., E. Nuckels III, R. L. Jones, and G. A. Cook, Distribution of heat flow and radioactive heat generation in northern Mexico, J. Geophys. Res. 84, 2371-2379, 1979.

Stacey, F. D., Physics of the Earth, Wiley and Sons, Inc., New York, 1324 p., 1969.

Stallman, R. W., Computation of ground-water velocity from temperature data, U.S. Geol. Surv. Water Supply Pap., 1544-H, pp. 36-46, 1963.

Stewart, J. H., Basin-range structure in western North America: A review, in Cenozoic Tectonics and Regional Geophysics of the Western Cordillera, Geol. Soc. Amer. Mem., 152, edited by R. B. Smith and G. P. Eaton, pp. 1-31, Geol. Soc. Amer., Inc., Boulder, Colo., 1978.

Stewart, J. H., and J. E. Carlson, Generalized maps showing distribution, lithology, and age of Cenozoic igneous rocks in the Western United States, in Cenozoic Tectonics and Regional Geophysics of the Western Cordillera, Geol. Soc. Amer. Mem., 152, edited by R. B. Smith and G. P. Eaton, pp. 263-264, Geol. Soc. Amer., Inc., Boulder, Colo., 1978.

Sumner, J. R., Tectonic significance of gravity and aeromagnetic investigations at the head of the Gulf of California, Geol. Soc. Amer. Bull., 83, 3103 - 3120, 1972.

Sumner, J. R., and G. A. Thompson, Estimates of strike-slip offset in southwestern Arizona, Geol. Soc. Amer. Bull., 85, 943-946, 1974.

Swanberg, C. A., P. Morgan, C. H. Stoyer, and J. C. Witcher, An appraisal study of the geothermal resources of Arizona and adjacent areas in New Mexico and Utah and their value for desalination and other uses, New Mexico Energy Institute, no. 006, New Mexico State University, Las Cruces, 1977.

Thompson, G. A., and D. B. Burke, Regional geophysics of the Basin and Range Province, in Ann. Rev. Earth Planet. Sci., edited by F. A. Donath, pp. 213-238, Annual Reviews, Inc., Palo Alto, Calif., 1974.

Tilling, R. I., and D. Gottfried, Distribution of thorium, uranium, and potassium in igneous rocks of the Boulder batholith region, Montana, and its bearing on radiogenic heat production and heat flow, U.S. Geol. Surv. Prof. Pap., 614-E, pp. E1-E29, 1969.

Toppozada, T. M. R., Seismic investigation of crustal structure and upper mantle velocity in the state of New Mexico and vicinity, Ph.D. thesis, New Mexico Institute of Mining and Technology, Socorro, New Mexico, 1974.

Walsh, J. B., and E. R. Decker, Effects of pressure and saturating fluid on the thermal conductivity of compact rock, J. Geophys. Res., 71, 3053-3061, 1966.

Warren, D. H., A seismic-refraction survey of crustal structure in central Arizona, Geol. Soc. Amer. Bull., 80, 257-282, 1969.

Warren, R. E., J. G. Sclater, V. Vacquier, and R. Roy, A comparison of terrestrial heat flow and transient geomagnetic fluctuations in the southwestern United States, Geophysics, 34, 463-478, 1969.

Williams, H., Pliocene volcanoes of the Navajo-Hopi country, Geol. Soc. Amer. Bull., 47, 111-172, 1936.

Wilson, E. D., and R. T. Moore, Structure of Basin and Range province in Arizona, in Arizona Geological Society Guidebook 2, 2nd Ann. Ariz. Geol. Soc. Digest, pp. 89-105, Arizona Geological Society, Tucson, 1959.

Wilson, E. D., R. T. Moore, and R. T. O'Haire, Geologic map of Navajo and Apache Counties, Arizona, scale 1:375,000, Arizona Bur. of Mines, Tucson, 1960.

Wyllie, P. J., Experimental limits for melting in the Earth's crust and upper mantle, in The Structure and Physical Properties of the Earth's Crust, Geophys. Monogr. Ser., vol. 14, edited by J. G. Heacock, pp. 279-301, AGU, Washington, D.C., 1971.

Yoder, H. S., Jr., and Tilley, C. E., Origin of basalt magmas: an experimental study of natural and synthetic rock systems, J. Petrol., 3, 342-532, 1962.

Young, R. A., and E. H. McKee, Early and middle Cenozoic drainage and erosion in west-central Arizona, Geol. Soc. Amer. Bull., 89, 1745-1750, 1978.

This thesis is accepted on behalf of the faculty of the Institute by the following committee:

Date 1 October 1979